UNIVERSITY OF SOUTHAMPTON

FACULTY OF ENGINEERING AND PHYSICAL SCIENCES

Fluid Structure Interactions Group

Volume I of I

Computationally Efficient Micromechanical Model-Aided Woven Fabric Composite Design based on Genetic Algorithms

by

Wang, Zhenzhou

BEng. MSc.(Hons)

Thesis for the degree of Doctor of Philosophy

Jan. 2020

UNIVERSITY OF SOUTHAMPTON

ABSTRACT

FACULTY OF ENGINEERING AND PHYSICAL SCIENCES

Thesis for the degree of Doctor of Philosophy

COMPUTATIONALLY EFFICIENT MICROMECHANICAL MODEL-AIDED WOVEN FABRIC COMPOSITE DESIGN BASED ON GENETIC ALGORITHMS

Wang, Zhenzhou

The manufacturing cost of woven fabric composites is low and this type of material exhibits high impact resistance and delamination resistance. Plain weave fabric composites are traditionally used on civil, offshore, marine and automobile structures but are increasingly utilised on aerospace structures in recent years. Triaxial weave fabric composites are new materials that are increasingly used in ultralight structures, such as the wings of unmanned aerial vehicles and deployable antenna on spacecraft. The need for better design of woven fabric composites is growing since having lower in-plane mechanical properties than unidirectional composite laminates becomes a problem which limits the use of woven fabric composites. However, the combination of modern manufacturing and optimisation techniques makes the wide use of bespoke high performance weave fabric composite become possible for aerospace applications. The yarn specification, including the undulation length, the width and the thickness of the yarn, significantly influences the mechanical properties and mass of these materials. Therefore, there is a chance to utilise optimisation techniques to search for the optimal design of these materials for a wide range of applications.

Optimisation techniques are widely used across many different disciplines. They are often used to provide innovative solutions or to gain insights into complex problems. The literature review highlights that Genetic Algorithms (GAs) are one of the most popular categories of optimisation techniques for solving engineering optimisation problems as they are able to robustly find the entire set of optimal solutions for single-, multi- and many-objective optimisation problems with large and complex search spaces. Genetic Algorithms are population, evolution and natural selection based optimisation tools inspired by Darwin's theory of evolution and Mendel's inheritance theory. The state-of-the-art Genetic Algorithms are developed and benchmarked with mathematical optimisation problems every year to find the best performing solvers for different types of problems. However, since the dominant characteristics of woven fabric composite optimisation problems are different from the

mathematical benchmarking problems in the evolutionary computational literature, it is difficult to select a suitable Genetic Algorithm for solving a weave fabric composite optimisation problem. Therefore, state-of-the-art Genetic Algorithms are benchmarked in this research to determine the dominant characteristics of weave fabric composite optimisation problems and which solvers perform best.

Using Genetic Algorithms is an effective method for solving weave fabric composite optimisation problems. However, it is obvious that using Genetic Algorithms requires high computational cost due to the large number of objective function evaluations, especially when the number of variables, objectives and constraints are increased. In addition, the computational time of evaluating each objective function significantly increases the total computational cost. Therefore, using computationally efficient methods to predict the mechanical properties of weave fabric composites becomes essential in the optimisation. This not only helps to reduce the computational cost, but also eliminates the limits on the optimisation techniques due to the difficulties of increasing the population size and generation number. The literature review of composite modelling methods highlights analytical methods as the most efficient methods when hundreds of thousands of different sets of weave patterns and yarn parameters are simulated to determine the optimal designs of weave fabric composites. However, the current available analytical methods are either imprecise or not robust when predicting the mechanical properties of woven fabric composites with different yarn specifications and material types. Therefore, two micromechanical models are developed in this work to achieve the computationally efficient predictions of the mechanical properties of weave fabric composites.

This research aims to develop a methodology to better design woven fabric composite materials with the aid of a computationally efficient micromechanics-based analytical model. This research aim is achieved by conducting a state-of-the-art literature review of composite structures/materials optimisation and genetic algorithms to determine the optimisation process used in the current research; comparing the advantages and disadvantages of each woven fabric composites modelling method to find out the most appropriate method to be used as the objective evaluation method in the optimisation; developing and validating novel analytical models to perform computationally efficient prediction of the mechanical properties of weave fabric composites; benchmarking state-of-the-art Genetic Algorithms in the optimisation of 2D weave fabric composites to find out the optimal designs and determine the dominant

characteristics of the optimisation problems for selecting the best practices of Genetic Algorithms.

Keywords: Woven fabric composites; State-of-the-art Genetic Algorithms; Comparative review; Analytical model; Mechanical properties; Multi- and many-objective optimisation; Benchmarking; Dominant characteristics.

Table of Contents

List of Tables

List of Figures

DECLARATION OF AUTHORSHIP

I, ZhenZhou Wang declare that this thesis and the work presented in it are my own and has been generated by me as the result of my own original research.

DEVELOPMENT OF MICROMECHANICAL MODELS FOR RAPID PREDICTION OF WOVEN FABRIC COMPOSITE MECHANICAL PROPERTIES, AND OPTIMISATION OF THE MECHANICAL PROPERTIES USING GENETIC ALGORITHMS

I confirm that:

1. This work was done entirely or mainly while in candidature for a research degree at this University;

2. Where any part of this thesis has previously been submitted for a degree or any other qualification at this University or any other institution, this has been clearly stated;

3. Where I have consulted the published work of others, this is always clearly attributed;

4. Where I have quoted from the work of others, the source is always given. Except for such quotations, this thesis is entirely my own work.

5. I have acknowledged all main sources of help;

6. Where the thesis is based on work done by myself jointly with others, I have made clear exactly what was done by others and what I have contributed;

7. Parts of this work have been published as:

Wang, Z.*, Sobey, A.J. Optimising the damage resistance of 2D woven composite structures with Genetic Algorithms. *20th International Conference on Composite Structures*, (2017).

Wang, Z., Bai, J.*, Sobey, A.J., Xiong, J., Shenoi, R.A. Optimal design of triaxial weave fabric composites under tension. *Composite Structures*, 201 (2018) 616-624. doi:10.1016/j.compstruct.2018.06.090

Wang, Z.*, Sobey, A.J. Optimal design of triaxial weave fabric composites for specific strength and stiffness under tension. *18th European Conference on Composite Materials*, (2018).

Bai, J., Wang, Z.*, Sobey, A.J., Shenoi, R.A. Micromechanical model for rapid prediction of plain weave fabric composite strengths under biaxial tension. *Composite Structures*. (2020). (Under review).

Wang, Z.*, Sobey, A.J. A comparative review of Genetic Algorithms use in composite optimisation and the state-of-the-art in evolutionary computation. *Composite Structures*. (2019). doi:10.1016/j.compstruct.2019.111739

Wang, Z.*, Sobey, A.J. A micromechanical model for computationally efficient prediction of plain weave fabric composite shear moduli and strengths. Under Preparation for *Composite Structures*. (2020).

Wang, Z.*, Sobey, A.J. Determination of best Genetic Algorithms and dominant characteristics for many-objective optimal design of plain weave fabric composites through benchmarking. Under Preparation for *Composite Structures*. (2020).

Signed: Zhenzhou Wang 王振舟 …….

Date: 31/March/2020 ……..

Dedicated to my parents, MingWei Wang and Xi Chen, and my parents-in-law, ZhiCai Lu and ShuZhen Zhai, who have always loved me unconditionally and whose good examples have taught me to work hard for the things that I aspire to achieve.

Dedicated to my wife, Dr. SiYao Lu, who have always loved me, supported me and helped me unconditionally.

Dedicated to my gorgeous and adorable dog, Nemo, who have always loved me, supported me and brought happy to my life.

Acknowledgements

Firstly, I would like to express my deep sense of gratitude to my supervisors, Dr. Adam Sobey and Prof. Ajit Shenoi, for their continuous interest, encouragement, inspirational guidance, valuable suggestions, unselfish help and support through this research. With their helps, I completed this report and all works done in this report.

Secondly, I would like to thank Lloyd's Register Foundation (LRF) and China Scholarship Council (CSC) who provide me tuition fee and living expenses to support my PhD study.

Thirdly, I am thankful to Dr. JiangBo Bai. He gave me a large amount of supports and shared his research experience and methods to help me solve some problems. We did enjoy the collaborations.

Fourthly, I would like to say thanks to my internal examiners, Dr. David Toal and Dr. Scott Walker. They gave me valuable advice in my 18 months transfer viva. I learned a lot from them.

Fifthly, I would like to say thanks to my colleagues and friends: Dr. XiaoYu Zhang, Dr. CaoYang Yu, Dr. YanXiang Wan, Dr. YiKun Wang, Dr. Wei Wang, to-be-Dr. Ugur Mutlu, Dr. JunYi Liu, Miss Qiu Jin, to-be-Dr. Prezemyslaw Grudniewski, Dr. Mehmet Cihan, to-be-Dr. Yu Cao, Dr. David Bossens and Dr. Jeanne Blanchard *etc.* Thank you for your help in my PhD study.

Sixthly, I would like to thank University of Southampton, Faculty of Engineering and Physical Science and Fluid Structure Interactions Group where I obtained all resources and facilities to achieve my final thesis.

The last but not the least, I have to thank my family. I would say thanks to my parents for their love and support throughout my life. I would say thanks to my parents-in-law for their love, support and concern.

I would say thanks to my wife, Dr. SiYao Lu. She gave me valuable advice; encouraged me and helped me. Thanks to her for giving me support to chase my dreams and giving me help to reach the stars. I cannot successfully finish my PhD study without her encouragements.

I would say thanks to my lovely dog, Nemo. He is intelligent and sensitive to my emotions; he comforts me, relieves my stress and brings me happy.

Nomenclature

GA – Genetic Algorithm

PSO – Particle Swarm Optimisation

AC – Ant Colony

SA – Simulated Annealing

DE – Differential Evolution

IA – Immune Algorithm

ABC – Artificial Bee Colony

FA – Firefly Algorithm

FEM – Finite Element Method

ANN – Artificial Neural Network

PWF – Plain Weave Fabric

TWF – Triaxial Weave Fabric

RVE – Representative Volume Element

LSS – Laminated Stacking Sequence

SO – Shape Optimisation

MP – Mechanical Property

NF – Natural Frequency

VF – Vibration Frequency

MAP – Microwave Absorption Performance

WFC – Woven Fabric Composite

PF – Progressive Failure; Pareto Front

CEC – Congress on Evolutionary Computation

VEGA – Vector Evaluated Genetic Algorithm

WBGA – Weight-Based Genetic Algorithm

MOGA – Multi-Objective Genetic Algorithm

AGA – Adaptive Genetic Algorithm

SAGA – Self-Adaptive Genetic Algorithm

SPEA – Strength Pareto Evolutionary Algorithm

NCGA – Neighbourhood Cultivation Genetic Algorithm

AMGA – Adaptive Micro-GA

IBEA – Indicator-Based Evolutionary Algorithm

BCE – Bi-Criterion Evolution

HEIA – Hybrid Evolutionary Immune Algorithm

MOEA/D – Multi-Objective Evolutionary Algorithm based on Decomposition

PSF – Penalty Scalarizing Function

MSF – Multiplicative Scalarizing Function

NSGA-II – Non-dominated Sorting Genetic Algorithm II

NSGAIILS - Non-dominated Sorting Genetic Algorithm II with Local Search

NSGA-III - Non-dominated Sorting Genetic Algorithm for many-objective optimisation

U-NSGA-III – Unifies NSGA-III for mono-, multi- and many-objective optimisation

COEA – Competitive-cooperative Evolutionary Algorithm

DMOEA-DD – Dynamic Multi-Objective Evolutionary Algorithm with Domain Decomposition technique

MLSGA – Multi-Level Selection Genetic Algorithm

cMLSGA – co-evolutionary Multi-Level Selection Genetic Algorithm

MLS1 – Multi-Level Selection method 1

MLS2 – Multi-Level Selection method 2

MLS2R – Multi-Level Selection method 2 Reverse

MLSU – a combination of MLS1, MLS2 and MLS2R

MTS – Multiple Trajectory Search

LiuLi – an evolutionary algorithm developed by Hailin Liu and Xueqiang Li

IGD – Inverted Generational Distance

mIGD – mimicked Inverted Generational Distance

HV – Hyper Volume

mHV – mimicked Hyper Volume

UAV – Unmanned Aerial Vehicle

SBX – Simulated Binary Crossover

SVM – Support Vector Machine

CST – Composite Science and Technology

CPA – Composites Part A: Applied Science and Manufacturing

CPB – Composites Part B: Engineering

CS – Composite Structures

AppCM – Applied Composite Materials

IJSS – International Journal of Solids and Structures

JCM – Journal of Composite Materials

JSSM – Journal of Sandwich Structures & Materials

TWS – Thin-Walled Structures

CMAME – Computer Methods in Applied Mechanics and Engineering

IJMS – International Journal of Mechanical Sciences

AIAA – American Institute of Aeronautics and Astronautics journal

SCS – Steel and Composite Structures

JCC – Journal of Composite for Construction

MS – Marine Structures

MD – Materials and Design

SMO – Structural and Multidisciplinary Optimisation

List of Symbols

A_i the cross-sectional area of the tow

AD the areal density of a EW220/5284 plain weave fabric composite ply

B_i the transformation variables referred in Chapter 6

$C_i\ (i=1,2,3)$ the transformation variables referred in Chapter 6

$C_i\ (i=1,2,3.\ldots.18)$ the transformation variables listed in the Appendix I-A

$d(v,O)$ the minimum Euclidean distance between *v* and the points in *O*

D_i the determinants listed in the Appendix I-B

D_n the determinants listed in the Appendix II-C

E the elastic modulus of a yarn in the longitudinal direction

E_f the Young's modulus of the fibre

E_m the Young's modulus of the matrix

E_{t2} the elastic modulus of the tow

E_T the tensile modulus of the triaxial weave fabric composites

$F_n(x)$ the internal forces on any cross-section of the warp and weft tows

F_1 the decomposed shear forces applied to the weft yarns

F_2 the decomposed tensile forces on the weft yarns

F_3 the decomposed shear forces applied to the warp yarns

F_4 the decomposed tensile forces on the warp yarns

G the in-plane shear modulus of the tows

G_f the fibre shear modulus

G_m the resin shear modulus

G_{f12} the shear modulus of the plain weave fabrics

G_{12} the shear modulus of the plain weave fabric composite

h_i the yarn thickness

H the plain weave fabric composite ply thickness

I_{yi} the moment of inertia along the transverse direction of the tow

I_{zi} the moment of inertia along the through-thickness directions of the tow

I_{pi} the polar inertia moment of the tow

$J_n\ (n=1,2,3,.....,8)$ the transformation variables listed in the Appendix II-A

$K_n\ (n=1,2,3,.....,72)$ the transformation variables listed in the Appendix II-B

L_i one quarter of the undulation length of the tow

l_i the coefficient for calculating one quarter of yarn undulation length

$M_n(x)$ the bending moments on the warp and weft tows for each cross-section

$M_{yi}(x)$ the y axis bending moments at each cross-section for the warp and weft tows

$M_{zi}(x)$ the z axis bending moments at each cross-section for the warp and weft tows

M_1 warp tensile loading induced bending moment (Chapter 4); shear force induced bending moment (Chapter 5)

M_2 weft tensile loading induced bending moment (Chapter 4 and 5)

M_3 shear force induced bending moment

M_4 warp tensile loading induced bending moment

M_v the M_1 and the M_3 are replaced by the M_v since they are equal

$mIGD(O,M^*)$ the mimicked inverted generational distance

M^* A set of points along the mimicked Pareto front

N_1 the internal force along the through-thickness direction at the interaction area between the weft and warp yarns

N_2 the in-plane internal forces induced by the rotation of the yarns

N_3 the in-plane internal forces induced by the rotation of the yarns

O A set of points on the currently obtained Pareto front

P_1 the tensile forces along the warp direction (Chapter 4); the virtual tension (Chapter 5)

P_2 the tensile forces along the weft direction (Chapter 4); the actual tension (Chapter 5)

P_f the critical external biaxial tensile forces at each crest and trough location

P_{tf1} the internal tensile loading along the 0 degree yarns of the triaxial weave fabric composites

P_{tf2} the internal tensile loading along the $\pm$ 60 degrees yarns of the triaxial weave fabric composites

P_{resin} the external force distributed on the resin

P_c the critical equivalent external force on the plain weave fabric composite

Q the interaction force between the warp and weft tows at the interlacing surface

$Q_n\left(n=1,2,3,.....,58\right)$ the transformation variables listed in the Appendix II-A

S the in-plane shear strength of the lamina (Chapter 4); the in-plane shear strength of the plain weave fabric composites (Chapter 5)

$T_{xi}\left(x\right)$ the torque moments on the warp and weft tows for each cross-section

T_1 the internal torques on the weft tows

T_2 the internal torques on the warp tows

T_{in} the internal torque moment between the weft and warp tows' interlacing surfaces

U_i^* the complementary potential energies of the warp and weft tows in the unit cells

V_f^0 the fibre volume fraction (Chapter 4)

V_{f0} the fibre volume fraction (Chapter 5 and 7)

V_f^y the fibre volume fraction in a single yarn (Chapter 5)

V_f the fibre volume fraction in a single yarn (Chapter 4, 6 and 7)

V_m the volume fraction of the matrix in a single yarn

V_y the yarn volume fraction of a unit cell

v Each point in the set M^*

w_i the yarn width

w_l the yarn having larger width between the weft and warp tows

w_s the yarn having smaller width between the weft and warp tows

X_{t0} the tensile strength of the tows in the longitudinal direction

X_t the fibre tensile strength in the longitudinal direction (Chapter 4); the tensile strength of a triaxial weave fabric composite (Chapter 6)

X the longitudinal tensile strength of the plain weave fabric composite lamina

Y the transverse tensile strength of the plain weave fabric composite lamina

z_i the undulated neutral axis of the yarns

z_0 the maximum normal stress location

α a coefficient table related to the torque moment

γ the ratio of F_1 over F_3

$\delta_{P_1(\lambda=0)}$ the displacement along P_1 direction (Chapter 5)

$\delta_{P_2(\lambda=0)}$ the displacement along P_2 direction (Chapter 5)

ε_{P_1} the tensile strain along P_1 direction

ε_{P_2} the tensile strain along P_2 direction

ε_{ft}^{u} the ultimate tensile strain of the fibre

ε_{mt}^{u} the ultimate tensile strain of the matrix

$\varepsilon_{\text{Shear}}$ the shear strain of the plain weave fabric composite

θ the off-axial angle of the undulated yarns

λ the ratio between the two tensile loadings

$\prod^{*}$ the total complementary potential energy of the unit cell

ρ_f the density of the T300 carbon fibre

ρ_{fibre} the density of the EW220 glass fibre

ρ_m the density of the Hexcel 8552 resin

ρ_{resin} the density of the 5284 resin

ρ_c the density of the T300/Hexcel 8552 fibre tow

ρ_{tow} the density of the EW220/5284 fibre tow

ρ the surface density of a T300/Hexcel 8552 triaxial weave fabric composite ply

σ_{P_2} the tensile loading stress along the P_2 direction

$\sigma_{1\max}$ the maximum normal stresses at the crest and trough of the warp tow

$\sigma_{2\max}$ the maximum normal stresses at the crest and trough of the weft tow

σ_1 the tensile stress in longitudinal direction for the plain weave fabric composite lamina

σ_2 the tensile stress in transverse direction for the plain weave fabric composite lamina

σ_m^{*} the average longitudinal matrix stress when ultimate fibre strain is reached

τ the shear stress of the plain weave fabric composite

τ_{max} the maximum shear stress

τ_{12} the in-plane shear stress

Chapter 1. Introduction

1.1 Motivation

Textile composites are increasingly utilised in industry, where the global textile composites market was $4.8 billion in 2015 and it is estimated to reach $6.6 billion by 2020 [1]. They are a potential alternative to unidirectional composites since the capability of automatically producing complex structures reduces the overall manufacturing costs. The use of textile composite materials is widely found in the aerospace industry, automotive industry and marine industry. A review of textile composites utilised in transportation [2] points out that textile composites are found on civilian aircraft, helicopters, unmanned aerial vehicles, military jets, radome and wing structures [3,4] since using textile composites helps to reduce fuel consumption and production costs and improve fatigue and impact resistance and radar transparency. Moulded woven fabric composite materials are applied in the automotive marketplace in car bumpers due to their low weight and high impact resistance [5–7]. Furthermore, the review states that using high performance textile composites on seat structures, door and side panels and thermal and sound insulation enhances the comfort and safety of cars [2]. In shipbuilding, woven fabric composites are used to produce sandwich construction parts due to the low manufacturing cost. In addition, they are widely found on power boats, racing yachts and naval vessels in order to resist wave impacts when under maximum speed [2]. Woven fabric composites are one typical type of textile composite, where the textiles are formed from interlacing fibre tows; typical 2D woven fabrics are shown in Figure 1-1. Woven fabric composites not only have advantages like high strength-to-weight ratio and low manufacturing costs, but also exhibit the advantages over traditional unidirectional composite laminates, such as improved delamination and fatigue resistance, reduced impact failures and increased damage tolerance [8]. Unidirectional composite laminates may have invisible delamination when working under impact loadings, which results in a potential structural safety hazard. Although the potential hazard could be eliminated by improving resin properties and non-destructive testing, it results in further inevitable increase in costs and is accompanied by manufacturing moulding problems. However, using woven fabric composites can significantly reduce the chance of having this potential hazard while maintaining low manufacturing costs [8]. In addition, due to the ease of draping, using woven fabric composites rather than using unidirectional composite laminates could avoid having wrinkle and discontinuous fibres, which avoiding reduced mechanical properties when produce complex structures such as composite

‘T’ or ‘Π’ sections, where the connections at junctions can be woven together rather than using adhesives.

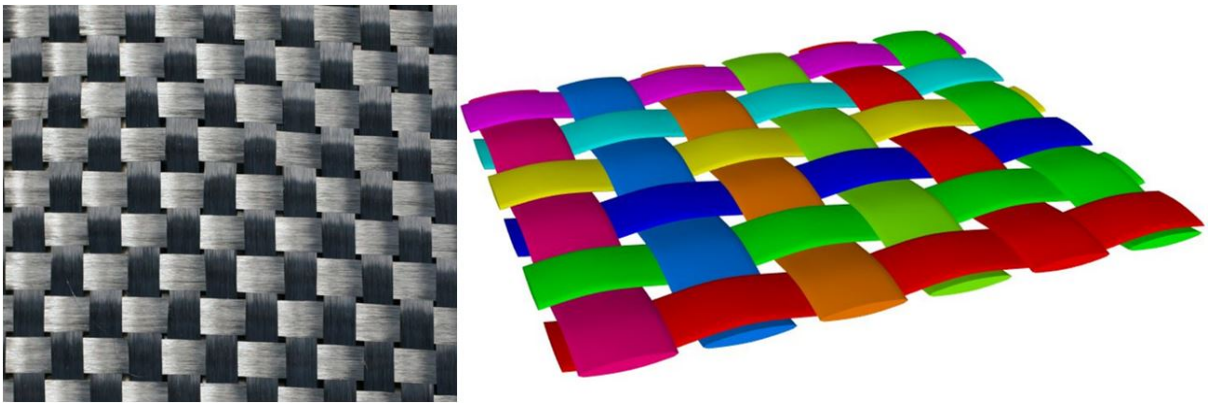

Figure 1- 1. Typical 2D woven fabric

The need for better design of woven fabric composites is growing since having lower in-plane mechanical properties than unidirectional composite laminates becomes a problem which limits the use of woven fabric composites. If the improved properties are achieved, more industry will use woven fabric composites because of the overall low manufacturing costs and the capability of producing complex structures. The mechanical properties of woven fabric composites are significantly influenced by the specifications and architecture of the fibre tow, where the weave pattern and yarn geometrical parameters change the mechanical performance. Due to the number of parameters and weave patterns a woven fabric composite structural optimisation problem forms a complex design variable space. Furthermore, it is difficult to determine the relationship between the objective space and variable space through parametric studies. Therefore, it is complicated to achieve optimal designs of woven fabric composites without the help of optimisation techniques.

The optimisation of woven fabric composites aims to reduce cost, weight and improve the mechanical performance to achieve better designs of woven fabric composites. Evolutionary algorithms are one of the most popular categories of optimisation technique, especially in engineering design, as they are able to find optimal solutions in large and complicated search spaces. According to the results of a recent review, Genetic Algorithms (GAs), are the most popular method utilised for solving a wide range of engineering optimisation problems, which occupies 56% of applications comparing against all the other evolutionary algorithms [9]. It has shown continued popularity despite the increasing competition from other evolutionary algorithms. Therefore, the current research utilises Genetic Algorithms to solve composite optimisation problems. Genetic Algorithms use natural

evolutionary-like mechanisms, such as inheritance, crossover, mutation and selection, to generate optimal solutions to problems. Several types of Genetic Algorithms have been utilised to solve composite optimisation problems. However, most state-of-the-art Genetic Algorithms are not seen in the current literature. In addition, since engineering optimisation problems are not categorised using the terms found in the optimisation literature, such as constrained/unconstrained problem, connected/disconnected objective space and convex/concave Pareto front, it is not easy to select a suitable genetic algorithm. Additionally, the current literature just picks one of the popular optimisation algorithms with a bias towards the simple or outdated Genetic Algorithm and assumes it will solve the problem. However, optimisation algorithms follow the 'no free lunch' theorem which states that if an algorithm is improved for a category of problems, it inevitably degrades its performance when solving other types of problem. No optimisation algorithm can perform the best across all problem types. There are a limited number of benchmarking studies in the current composite optimisation literature, which makes it difficult to determine the most appropriate solver for each composite optimisation problem. Furthermore, it is difficult to obtain the optimal designs of woven fabric composites for many-objectives since there are only four single-objective optimisation studies [10–13] investigating the influences of yarn parameters and weave patterns on the mechanical properties of woven fabric composites. Therefore, making a comprehensive investigation into the design space and finding the dominant characteristics for composite optimisation problems are necessary to select the most appropriate Genetic Algorithm before solving a composite optimisation problem.

1.2 Aim and objectives

This research is about the optimisation of woven fabric composites using Genetic Algorithms. Finite element methods are accurate, robust and can be easily utilised as the fitness evaluation within an optimisation process. However, they are computationally expensive when called by a Genetic Algorithm since hundreds of thousands of fitness evaluations are performed in each independent run cycle. Each Genetic Algorithm requires several independent run cycles to obtain the entire statistical distribution of the solutions as they are stochastic solvers. Even if a computationally efficient finite element method is able to obtain results within a minute, it is still thousands of times more costly than an analytical method which solves the problem within a few milliseconds. Compared with finite element methods, analytical methods compromise the accuracy of prediction. However, gaining significant computational efficiency enables Genetic Algorithms to search all possible optimal solutions when analytical methods

are used as the fitness evaluation method. Therefore, analytical models are proposed and utilised in this research as the objective evaluation methods to search optimal designs of woven fabric composites.

This research aim is to develop a methodology to better design woven fabric composite materials with the aid of a computationally efficient micromechanics-based analytical model. The aim is achieved through a series of objectives:

1. Conduct a state-of-the-art literature review of composite structures/materials optimisation and genetic algorithms to determine the optimisation process used in the current research. Compare the advantages and disadvantages of each woven fabric composites modelling method to find out the most appropriate method to be used as the objective evaluation method in the optimisation.
2. Using analytical methods is the best choice to be the objective evaluation method according to the review result, but they are not available in the current literature. Therefore, the current work proposes novel micromechanical models of woven fabric composites for rapid prediction of mechanical properties.
3. Benchmark state-of-the-art Genetic Algorithms in the optimisation of 2D weave fabric composites to find out the optimal designs and determine the dominant characteristics of the optimisation problems for selecting the best practice of Genetic Algorithms.

1.3 Research novelty

Since the current woven fabric composites optimisation works show the limitation of increasing the population size and generation number when uses finite element method models as the fitness function in Genetic Algorithms, it is suggested that utilising analytical models instead of using finite element method models may be the solution for the issue. Therefore, the micromechanical models for rapid prediction of the woven fabric composite mechanical properties are proposed in this research.

The novelty of this research is developing a methodology to determine the dominant characteristics of woven fabric composite optimisation problems for better selection of the best practice of the state-of-the-art Genetic Algorithm and improving the capability of the selected Genetic Algorithms on searching optimal solutions.

1.4 The scope of work

The proposed micromechanical models are derivation and computation based only, and the experiments are executed by the co-author of the published papers. The prediction results from other finite element methods are used to verify the proposed micromechanical models thus these finite element models are not recreated in the current research. The optimisation processes are based on Genetic Algorithms, thus other evolutionary algorithms will not be extensively studied. The optimisation works will be computation based without verification experiments.

1.5 Outline of the study

Chapter 2 demonstrates a comparative review of textile composites modelling methods and a comparative review between Genetic Algorithm use in composite optimisation and the state-of-the-art in evolutionary computation. Chapter 3 explains the methodology of the research works and illustrates the relationship between each research works. Chapter 4 demonstrates a novel micromechanical model for rapid prediction of plain weave fabric composite strengths under biaxial tension. Chapter 5 demonstrates a novel micromechanical model for rapid prediction of plain weave fabric composite shear modulus and strength. Chapter 6 demonstrates the optimal designs of triaxial weave fabric composites under tension, including tensile strength, modulus and material areal density. Chapter 7 demonstrates a five-objective optimal designs of the plain weave fabric composite under tension and shear, including tensile modulus and strength, shear modulus and strength and the material areal density. The benefits and the limitations of this work and the future works are demonstrated in Chapter 8. Finally, the entire work is concluded in Chapter 9.

1.6 List of publications

Wang, Z.*, Sobey, A. Optimising the damage resistance of 2D woven composite structures with Genetic Algorithms. *20th International Conference on Composite Structures*, (2017).

Wang, Z., Bai, J.*, Sobey, A.J., Xiong, J., Shenoi, R.A. Optimal design of triaxial weave fabric composites under tension. *Composite Structures*, 201 (2018) 616-624. doi:10.1016/j.compstruct.2018.06.090

Wang, Z.*, Sobey, A.J. Optimal design of triaxial weave fabric composites for specific strength and stiffness under tension. *18th European Conference on Composite Materials*, (2018).

Bai, J., Wang, Z.*, Sobey, A.J., Xiong, J., Shenoi, R.A. Micromechanical model for rapid prediction of plain weave fabric composite strengths under biaxial tension. *Composite Structures*. (2020). (Under review).

Wang, Z.*, Sobey, A.J. A comparative review between Genetic Algorithm use in composite optimisation and the state-of-the-art in evolutionary computation. *Composite Structures*. (2019). doi:10.1016/j.compstruct.2019.111739

Wang, Z.*, Sobey, A.J. A micromechanical model for computationally efficient prediction of plain weave fabric composite shear moduli and strengths. *Composite Structures*. (2020). (Under Preparation).

Wang, Z.*, Sobey, A.J. Determination of best Genetic Algorithms and dominant characteristics for many-objective optimal design of plain weave fabric composites through benchmarking. *Composite Structures*. (2020). (Under Preparation).

Chapter 2. Literature review

Since the need of bespoke design of woven fabric composite is growing as mentioned in the Chapter 1, this research is going to obtain improved mechanical properties of woven fabric composite materials with the help of computationally efficient mechanical properties prediction methods and the state-of-the-art Genetic Algorithms. In order to achieve the objective, the literature reviews of state-of-the-art woven fabric composite modelling methods, the mechanisms of state-of-the-art Genetic Algorithms and the optimisation of composite materials and structures are conducted to obtain the computationally efficient model and the best practice of Genetic Algorithms for solving composite optimisation problems.

2.1 Comparative review of woven fabric composite modelling methods

2.1.1 Modelling methods of woven fabric composites

The methods to model textile composites are mainly divided into two categories: finite element methods (FEMs) and analytical methods. The finite element methods are the most commonly utilised method in woven fabric composite modelling. Many of the literature utilise unit cell modelling methods for woven fabric composites modelling due to the repetition of weave pattern in a woven fabric composite. For textile composites, the unit cells can be considered as small repeated building blocks for assembling the woven fabric composites in all three dimensions [14,15]. Sankar & Marrey [16] provide a unit cell model for predicting the elastic properties of plain weave fabric composite using 2D beam elements. The model analyses the stiffness properties by assuming homogeneous strain state in the material. The unit cell defined in the model is the cross-section area along the loading direction. Since the accuracy of the model is not verified against any experiments, it is difficult to evaluate the validity of the model. Hahn & Pandey [17] generate a plain weave fabric composite by using representative volume elements. The model can predict the linear thermal expansion coefficient and the effective elastic moduli. Kwon & Roach [18] also use a unit-cell model for modelling plane weave fabric composites. Compared to the method proposed by Hahn & Pandey [17], they both present good accuracy, where the stress-strain plots obtained from both models coincide with those from experiments. However, the method developed by Kwon & Roach [18] has better extendibility since it can be combined with multi-scale techniques to predict the strength and stiffness of composite structures in the progressive damage.

Naik & Ganesh [19] suggest two methods for modelling woven composites: a slice array model and an element array model. The slice array model method discretises unit cells into

slices along the loading direction and each slice is individually analysed, which is similar the method proposed by Sankar & Marrey [16]. The element array model method discretises the unit cells into slices with either along or across loading direction and slices will be divided into elements to evaluate the slice elastic constants. Both methods can provide good predictions of elastic properties compared with experimental results, which is evaluated by comparing the stress-strain plots obtained from both predictions and experiments. Furthermore, the same authors [20] utilise the same slice array and element array models to predict the thermal expansion coefficient of plain weave fabric composites. However, this method seems not to be widely used with unknown reason according to the low number of citation after 2010. Adumitroaie & Barbero [21] present a repetitive unit cell modelling method to predict tensile stiffness and strength of plain weave fabric composites. It has good accuracy when compared to experimental data. This method improves the traditional unit cell modelling method and achieves accuracy in modelling the complexity of geometry and material behaviour with a relatively simple formulation. However, if detailed geometry is not required to be modelled, this method is not recommended because of the high computational cost.

Karkkainen & Sankar [22] apply a quick and efficient finite element method, 'The Binary Model', which is first used by Cox et al. [23], to analyse plain weave composites. Fibres are simply modelled as 1-D line elements and embedded within the homogenous solid element that is represented as the matrix [22]. In the binary model, axial tow properties are only represented by 'tow' elements (1D line elements) and other mechanical properties are accounted by 'effective medium elements' which are solid homogenous elements [23]. This method can be used in both 2D plane weave composites modelling and 3D textile composites modelling. Additionally, this method is able to be extended for analysing the strength of different types of woven fabric composite materials. Flores et al. [24] use the binary model to simulate tensile failure tests on woven fabric ceramic matrix composites. The numerical simulations are well matched with the experimental measurements on the stress-strain plots. Yang & Cox [25] predict strains of graphite/epoxy woven fabric composites using binary model with spatially averaged method but their numerical results are not validated with experimental results. The same authors [26] later use the method to predict the mechanical properties of carbon fibre/epoxy matrix composites and validated the simulated results with the test data. This method is fast and effective in analysing woven fabric composites. Therefore, the binary model is used and improved by other researchers.

Since the binary model is a mesoscopic method for analysing textile composite structures, it cannot represent a lot of details during the analysis, such as the stress distribution on the transverse direction of the yarn, the stress distribution between the yarns at the intersection. Therefore, some authors implement a microscopic method to model textile composites to obtain more detailed results that are more accurate. Lomov et al. [27] present a textile geometry pre-processor, which is a geometric model, to model detailed complex textile composites. They compare model predictions with experimental data and state that this method gives a good prediction of mechanical properties of composites and provides an opportunity to use manufacturing data of fibres and yarns to model composite materials. Verpoest & Lomov [28] also use a micro-mechanical method to perform a structural analysis with assistance of 'WiseTex' geometric model software. They compare simulated results with experimental data to prove that 'WiseTex' textile composites software provides an integrated description of the internal geometry and properties of textile fabrics and composites on unit cell level and can be used for multi-scale analysis. 'TexGen' [29] is a widely utilised textile composites geometry pre-processing software as well. Both are useful for understanding the weave geometry and creating customised weave fabric composites. However, since the detailed model is built and transferred to the FEM analysis, the computational efforts are inevitably increased.

Among the above FEM models, WiseTex [28] and TexGen [29] are the most convenient two software to be used for modelling 2D woven fabric composites but they are computationally expensive. The binary model [23] is the most efficient model for the predictions of mechanical properties of 2D woven fabric composites. However, the binary model is still computationally expensive when used in the industrial design and optimisation. The industrial design requires many repetitions of virtual experiments to determine a suitable type of material for their structural design and optimisation needs hundreds of thousands sets of material parameters to determine the optimal design [30,31]. Therefore, there is an interest to develop analytical methods for the predictions of the mechanical properties of woven fabric composites.

Cheng and Xiong [32] propose an analytical model based on the minimum total complementary potential energy principle to predict the compressive modulus of PWF composites. A mean error of ~10% in both warp and weft direction predictions indicates the practical use of the model. However, the robustness and extendibility of the model are unknown since they have not verified the model for different material types and yarn specifications. Naik et al. [33] propose an analytical model based on curved beams to predict the compressive

strength of PWF composites. The model is validated with the experimental data and predictions from other micromechanical models. A mean error of 15.79% in both warp and weft direction predictions indicates the accuracy of the model is acceptable. However, it has the same problem as the model proposed by Cheng and Xiong [32], where the robustness and extendibility of the model are unknown.

Scida et al. [34] develop an analytical model based on classical thin laminate theory to predict the tensile strength of plain weave, twill weave and satin weave fabric composites. The model divides the undulated tows into straightened segmented tows to represent the peaks and troughs of the undulated tow. This makes the accuracy of the prediction low, which are between 17%-21% for plain, twill and satin weave fabric composites when compared to the experimental results, since the influences of the fibre tow undulation and interactions between the interlaced tows are not considered. Ishikawa & Chou [35] propose three methods of modelling plane weave fabric composites in one published paper. The first one is mosaic model, where a woven fabric after impregnation with resin is idealized as an assemblage of asymmetrical cross-ply laminates, can effectively predict the elastic properties of woven fabric composites. However, fibre continuity and undulation are omitted in this method, which is similar as the model proposed by Scida et al. [34]. This can significantly influence the prediction accuracy because the weave fibres are considered as unidirectional fibres. The second one is an undulation model, which takes into account fibre continuity and undulation, is used to analyse elastic behaviour of plain weave fabric composites. Zhang & Harding [36] also use this undulation model to analyse the mechanical properties of plane weave composites and they add the strain energy equivalency method to obtain a mean error of 15.2% on the elastic properties predictions of a plain weave composite but the model is only verified through one case. This method has much better predictability than mosaic model and is faster than finite element method with an acceptable level of accuracy. However, this model is only suitable for predicting the elastic properties of plain weave fabric composites [35]. The third modelling method they stated is a bridging model which is developed to evaluate the load transfer among the interlaced regions in satin weave fabric composites. This model is focusing on a specific area of a fixed type of weave fabric composite, which is not suitable for a large range of applications. Xiong et al. [37] propose an analytical model to predict the tensile modulus of 2D woven fabric composites. Their model is validated against experimental measurements and other proposed models with a mean error of 13.77%. However, all of the above analytical models are only able to predict the elastic properties and strengths of 2D woven fabric

composites under uniaxial tension and none of them is able to predict the elastic properties, strengths and failure location under multi-direction loadings. It is worth to investigate the mechanical properties and failure mechanisms of 2D woven fabric composites under biaxial loadings since these properties better represent the performance of these materials under complex loading conditions. Escárpita and David [38] propose a model to calculate the strength under equal biaxial tension according to a given uniaxial strength. However, the failure location and the strength under different biaxial loading ratios are not predictable from the model. Therefore, additional improvements are required to accurately and rapidly model 2D woven fabric composites under biaxial tension. Bai et al. [39,40] propose two analytical models based on the minimum total complementary potential energy principle for the predictions of modulus and strength of plain weave fabric composites under biaxial tension. The two models are combined together and uploaded to open access platform for easy access [41]. The two models are able to predict the tensile modulus and strength under different biaxial loading ratios. Furthermore, they are able to predict the tensile modulus and strength under uniaxial tension by setting the biaxial loading ratios to zero or infinites. Additionally, the biaxial strength analytical model [40] is able to predict the failure location under different loading conditions. The two analytical models are both validated against several experimental measurements with different types of materials. The two analytical models are proved to be robust and effectiveness for usage with a mean error of 5.50% for moduli predictions and a mean error of 11.22% for strength predictions. Although the two analytical models are developed for plain weave fabric composites, they are able to be extended to predict the mechanical properties of twill and satin weave fabric composites. The method has been stated in [40].

For the shear properties of 2D woven fabric composites, Nguyen et al. [42] develop an analytical method for predicting the shear modulus of plain weave dry fabrics and pre-preg fabrics but the model is not applicable for stiffer plain weave fabric composites where the resin are infused into the fibre tows. Furthermore, the minimum prediction error validated against experiments is 26.3% for two types of carbon fabrics. Sun and Pan [43] propose a model based on the model proposed by Nguyen et al. [42] and have achieved improved accuracy where the minimum error is 22.2% validated against the experiments. However, this model is still not able to predict the shear performance of stiff plain weave fabric composites. Cheng et al. [44] propose an analytical model to predict the shear moduli of the stiff plain weave fabric composites. They achieve a mean error of 15.56% on accuracy and 8.86 on the standard deviation of the prediction errors when verifying the model with two types of materials in three

cases. However, the model is not able to predict the shear strength of plain woven fabric composites. Naik and Ganesh [45,46] propose two analytical models for the predictions of shear modulus and shear strength of plain weave fabric composites respectively. Their model is able to be utilised for a range of material types. However, the shear modulus prediction model is not robust since the prediction accuracy for the carbon fibre plain weave fabric composites, which is over 30%, is much lower than the accuracy for the glass fibre plain weave fabric composites, which is 16.37% on average. Furthermore, their model for the prediction of shear strengths of glass fibre plain weave fabric composites is around 22.55% by comparing the experimental data with the prediction results captured in the figure shown in the literature. Due to the successful implementation of the minimum total complementary potential energy principle on the predictions of biaxial tensile moduli and strengths of plain weave fabric composites, Wang and Sobey [47] propose an analytical model based on the same principle to predict the shear modulus and strength of plain weave fabric composites. Their model is inspired by one type of experimental method, called bias extension experiments, of plain weave fabric composites and the analytical model for the prediction of biaxial tensile strengths of plain weave fabric composites. Their model is validated against experimental measurements with three types of material and it is verified with seven fabric specifications. A mean error of 15.24% for shear modulus predictions, a mean error of 3.60% for shear strength predictions and a standard deviation of 4.10 among seven-case prediction errors demonstrate the robustness and practical use of the model.

In addition, a few analytical models are proposed to predict the mechanical properties of triaxial weave fabric composites (TWF) composites. Kueh et al. [48–50] develop a straight beam based semi-analytical model to evaluate the linear elastic response of triaxial weave fabric (TWF) composites using Kirchhoff plate theory and finite element analysis. The tension, compression and shear properties are deduced through the equivalent stiffness matrix. The predicted stress-strain plots are matched with the plots from experiments. Bai et al. [51,52] propose an analytical model to predict the tensile and shear behaviours of triaxial weave fabric composites but using the minimum complementary potential energy principle based on micromechanics. Compared with Kueh's et al. [48–50] methods, Bai et al.'s analytical models don't require the help of finite element analysis thus the computational effort is much lower than Kueh's et al. methods. Additionally, Bai et al.'s method is more convenient to be utilised and has better extendibility, where the method can be used to obtain the mechanical properties of both triaxial and plain weave fabric composites. Furthermore, Bai's et al. method has good

accuracy when verified using experimental results of three types of materials where the mean errors are 10.29% for the tensile modulus predictions and 2.97% for the tensile strength predictions.

According to the consideration of prediction accuracy, efficiency, robustness and extendibility, Bai et al.'s [39,40,51,52] and Wang and Sobey's [47] analytical models are the most appropriate methods to be used in the optimisation among the above analytical methods. All of these models are based on the same principle, which is the minimum total complementary potential energy principle. The reason of using this principle is that the minimum total complementary potential energy principle states that the solution of the unknown variables is the one that minimises the total complementary potential energy in all possible statically admissible stress fields [53]. There are several undetermined internal forces and moments that need to be solved after the micromechanical analysis of the unit cell. According to this definition the undetermined internal forces can be determined by the minimum total complementary potential energy and establish the relationship with the known external loadings. There is a potential to utilise this methodology to propose new analytical models for the predictions of mechanical properties of 2D woven fabric composites, such as the compressive modulus and strength.

2.1.2 Summary

Woven fabric composite modelling methods have been comparatively reviewed in this section. The current research aims to obtain the optimal designs of 2D woven fabric composites by optimising the fibre tow specifications and weave patterns. These reviewed finite element methods are able to more accurately predict the mechanical properties than analytical methods. However, the finite element methods are computationally expensive when compared with analytical methods, especially when they are used in the optimisation where hundreds of thousands of fibre specifications and weave patterns are evaluated. In order to feasibly implement the optimisation, analytical methods with the best prediction accuracy are selected. According to the prediction accuracy of the reviewed analytical methods, the analytical models developed by this research, which are Wang and Sobey [47] and Bai et al. [40], and by Bai et al. [39,51,52] are chosen as the fitness evaluation methods in the optimisation.

2.2 A comparative review of Genetic Algorithms in composite materials and structural optimisation

2.2.1 A brief timeline of major Genetic Algorithm developments

A brief timeline of the major developments in Genetic Algorithms is summarised in Figure 2-1. The frequently utilised Genetic Algorithms in composite optimisation literature are highlighted in red, those that are less common in this literature are highlighted in green and those missing from the literature are in black. To support this review the reader is referred to [54] for an excellent introduction and clear explanation of the standard Genetic Algorithm mechanisms and Konak et al. [55] for a detailed and clear explanation of the mechanics for most of the main multi-objective Genetic Algorithms developed before 2006.

Genetic Algorithms are inspired by Darwin's theory of evolution and Mendel's inheritance theory. The idea is that by mating the fittest individuals in a population the children of the next generation are fitter, on average, than the last. The initial inspiration was provided by Turing in 1950 [56] who outlines the potential for a biologically inspired learning machine including the ability to mutate and exhibiting survival of the fittest. In the 1960s early group selection theories were developed in an attempt to simulate and study natural selection. The first successful implementation of a Genetic Algorithm was performed by Holland and is summarised in 1969 [57]. These initial studies inspired others to develop algorithms for use in optimisation, or implement additional mechanisms, often moving away from the initial biological inspiration. Elitism [58], which was developed in 1975, is one of the most important mechanisms as it is used to retain the best solutions between generations, substantially improving the performance of these algorithms. This increases the search speed as the best solution in each generation is guaranteed to survive but is also a core strategy in multi-objective solvers to keep non-dominated solutions.

The first multi-objective Genetic Algorithm, Vector Evaluated Genetic Algorithm (VEGA) [59] was developed in 1985, which utilises a single objective Genetic Algorithm to approximate the Pareto-optimal set, where the population is divided into K subpopulations for K objectives with each subpopulation corresponding to one objective. All of the subpopulations are then combined to perform fitness-proportional selection, crossover and mutation using a single objective to determine the fitness before creating a new population which is then randomly sorted into subpopulations. These different processes were combined by Goldberg [60] who developed what can be considered to be the algorithm closest to a standard version of a multi-objective Genetic Algorithm utilising classical mechanisms. This was developed

alongside the first Pareto ranking approach proposed for multi-objective optimisation in 1989, which is at the core of many modern Genetic Algorithms, the niching algorithms, and this process is based on Pareto optimality.

In 1993 Hajela and Lin [61] find a simple method to find the Pareto optimal front using a Weight-Based Genetic Algorithm (WBGA) to automate the process of changing weights to find the Pareto front in multi-objective optimisation. Fonseca and Fleming [62] later develop the first Genetic Algorithm utilising Pareto ranking and niching techniques to solve multi-objective optimisation problems, called multi-objective Genetic Algorithm (MOGA), in 1993. This is integrated into MATLAB through the popular MATLAB GA Toolbox by Chipperfield and Fleming [63] in 1994, which is still currently in many optimisation problems. In the same year, an adaptive Genetic Algorithm (AGA) [64] is developed to reduce the influence of crossover and mutation probability settings. The AGA is the implementation of the suggestions from Grefenstette [65], where the Genetic Algorithm changes the parameters itself to adapt the optimisation problem. It achieves much higher performance in solving multimodal problems when benchmarked with the standard GA in a series of cases. Another Genetic Algorithm with self-tuning, self-adaptive Genetic Algorithm (SAGA) [66], is developed in 1996. However, both AGA and SAGA need extra internal parameters, such as the frequency of tuning for crossover and mutation probability, which are sensitive to the performance of both algorithms. Extending the ideas from Goldberg, the non-dominated sorting method [67] and simulated binary crossover [68] are first developed in 1994 as NSGA. These improve the Pareto ranking technique and create a shift from binary encoding to real value encoding. In 1998, the island model Genetic Algorithm [69] is developed that divides the population into sub-population islands and allows the migration of individuals between islands, improving the diversity of the solutions and is among the first hierarchical algorithms. An effective Genetic Algorithm which combines the characteristics from several previous multi-objective evolutionary algorithms is developed in 1999, which provides leading performance in the 1990s, called Strength Pareto Evolutionary Algorithm (SPEA) [70]. It is upgraded to SPEA2 [71], which is still used in the composite optimisation literature, and updated to the Neighbourhood Cultivation Genetic Algorithm (NCGA) [72]. To reduce the number of function calls, micro-GA [73] is introduced in 2001, which is based on small population sizes with an external population for updating and re-initialisation. The micro-GA is improved in 2008 as the Adaptive Micro-GA (AMGA) [74].

Modern Genetic Algorithms are considered here to be from NSGA-II, as the oldest currently competitive algorithm. NSGA-II [75] is an improvement of the non-dominated

method, a more efficient non-dominated sorting Genetic Algorithm, which is developed in 2002. Multi-island Genetic Algorithm [76], developed in 2004, extends the concepts from the island model Genetic Algorithm. It is frequently used in the composite optimisation literature since there is a commercial optimisation software based on this algorithm produced by SIMULIA, Isight, which easily links to ABAQUS, though the software contains a number of other Genetic Algorithms. In 2004, the indicator-based selection approach is first developed in Indicator-based Evolutionary Algorithm (IBEA) [77], which improves the efficiency of finding the final Pareto front. Rather than using dominance to evaluate the achieved solutions, the indicator is used to reflect the diversity and quality of current Pareto front in each generation and pushes the solutions to the true Pareto front. The indicator-based selection approach is increasingly investigated in recent years, and is included in the top performing algorithms Bi-Criterion Evolution (BCE) [78] and Hybrid Evolutionary Immune Algorithm (HEIA) [79].

Multi-Objective Evolutionary Algorithm based on Decomposition (MOEA/D) is developed by Zhang and Li [80] in 2007 based on the Tchebycheff decomposition approach [81]. This algorithm has demonstrated top performance on unconstrained optimisation problems at the Congress on Evolutionary Computation 2009 benchmarking competition [82], on a set of problems developed by the same authors, and a number of subsequent benchmarking exercises. Various groups around the world are working on upgrading these mechanisms leading to a range of top performing algorithms based on these mechanisms for specific characteristics such as MOEA/D-M2M [83], which improves the diversity of the population by decomposing multi-objective problems into a number of simple multi-objective sub-problems which performs well on solving multimodal problems. Two other approaches are MOEA/D-PSF and MOEA/D-MSF [84] that propose two improved scalarizing functions: penalty scalarizing function (PSF) and multiplicative scalarizing function (MSF), to replace the Tchebycheff scalarizing approach in MOEA/D to improve the balance between the convergence and diversity of the algorithm. In 2017, a Genetic Algorithm based on Multi-Level Selection theory first proposed in 1999 [85], which uses individual and collective evolution mechanisms is developed by Sobey and Grudniewski [86]. The algorithm is hybridised with a range of top performing algorithms to achieve top performance across a wide range of test problems including constrained, unconstrained and discontinuous problems and importantly is one of a limited number of diversity first convergence second Genetic Algorithms [87]. The addition of a co-evolutionary inspired mechanisms lead it to being benchmarked as the top performing general solver [88].

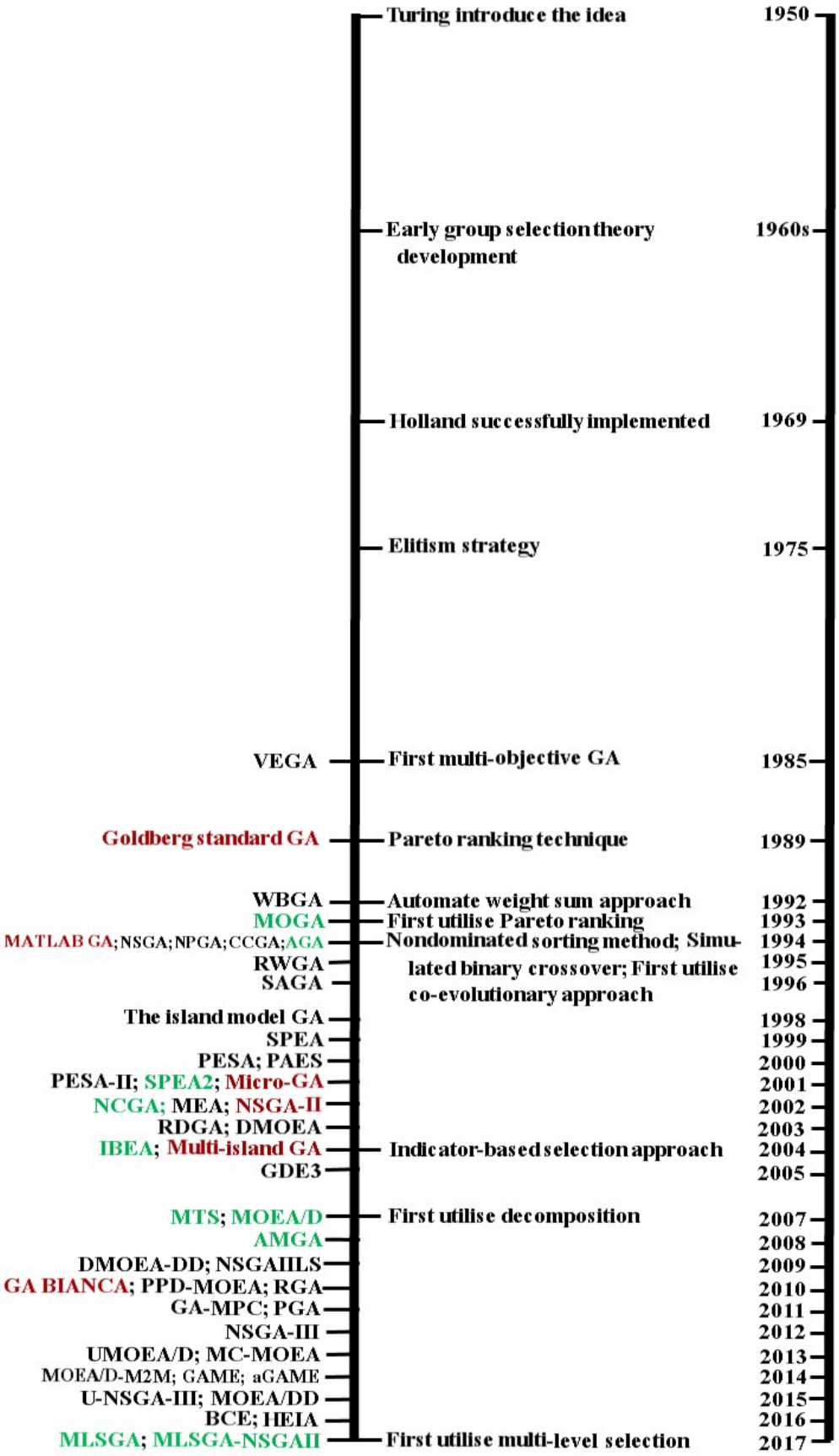

Figure 2- 1. Timeline of the main Genetic Algorithm developments with Algorithms on the left and methods on the right

2.2.2 Categorisation and description of mechanisms for the leading Genetic Algorithm methodologies

Of the frequently used Genetic Algorithms in the composite optimisation literature some of those considered to be state-of-the-art in various benchmarking exercises in evolutionary computation are not visible. Therefore a brief review of the current state-of-the-art in evolutionary computation is performed to encourage further benchmarking of these algorithms. These are performed by splitting the algorithms into 4 broad categories: niching, decomposition, co-evolutionary and multi-level selection algorithms. Codes for: cMLSGA, HEIA, NSGA-II, U-NSGA-III, MOEA/D, MOEA/D-MSF, MOEA/D-PSF, MOEA/D-M2M, BCE, IBEA and MTS are available for benchmarking in C++ and python from multiple sources including[1].

2.2.2.1 Niching algorithms

In ecology a niche is defined as the fit of a species living under specific environmental conditions. In Genetic Algorithms, niching describes the formulation of sub-populations in a population, where each sub-population responds to a sub-task of the optimisation problem. The introduction of niching techniques increases the diversity of the population and helps the Genetic Algorithms to improve the ability to solve multi-peak optimisation problems.

The niching technique was first proposed by Cavicchio [89] in 1970, where this method is based on the preselection mechanism meaning that the parent individuals can only be replaced when the newly created offspring individuals are higher in terms of fitness than the parent individuals, otherwise the parent individuals are retained. De Jong [90] further develops this preselection mechanism and proposes a niching technique based on the crowding mechanism. In this method 1/CF individuals, where CF is the Crowding Factor, are randomly selected to expel the individuals that are similar to the newly generated members. The similarity is calculated according to the Hamming distance, which is the number of different symbols at corresponding positions between the encoded strings of the two individuals. In 1987, Goldberg and Richardson propose a fitness sharing based niching technique [91]. The fitness of the individuals is adjusted in the population by using a sharing function that reflects the similarity between individuals to maintain the diversity of the population. The algorithm performs selection operations by adjusting the fitness in the later generations. This method is one of the most widely utilised niching techniques. Sequential niching [92] is developed to improve the performance of searching all of the optimal solutions since the technique is able to be included

[1] https://www.bitbucket.org/Pag1c18/cmlsga

in any kind of GA. It is more efficient than the fitness sharing based niching technique and capable of locating all of the maxima in multimodal problems, requiring fewer function evaluations. Clearing based niching technique [93] is beneficial where there are significantly complex search spaces since the technique has a reduced complexity, meaning more efficiency, than the fitness sharing technique and can achieve significant improvements in the probability of finding all of the peaks over the fitness sharing technique, and is used to solve complex multimodal problems with several million local maxima.

NSGA-II is the most popular Genetic Algorithm using niching as it is a robust general solver with few hyperparameters and good diversity of population based on the fast non-dominated ranking. There have been a number of updates to this algorithm and the most recent, currently version 1.1.6 [94], should be used to ensure the best performance. Simple Genetic Algorithms face difficulties in solving optimisation problems with multiple peaks since fitness proportional selection methods are utilised which reduce the diversity of the solutions. This is because competition between individuals allows the best individual to rapidly dominate the entire population. However, the focus is at one global or local optimum which can lead to some optimal solutions being missed.

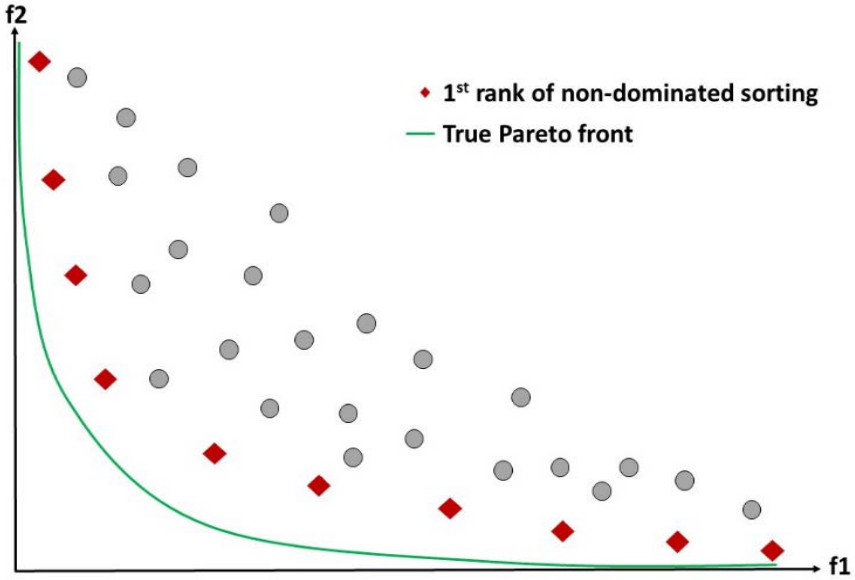

Figure 2- 2. Mechanism of NSGA-II [75]*: non-dominated sorting*

In the fast non-domination of solutions, the parent and offspring population are combined together and sorted by the fast non-dominated sorting procedure. The solutions that are not dominated by each other are categorised into the same non-domination rank. All individuals are classified into different non-domination ranks, where the previous ranks are temporarily discounted when formulating a new rank. The best half ranks are reserved in each generation,

where the best rank of non-dominated solutions are shown in Figure 2-2. However the total number of individuals in the reserved best half is often larger than the population size. Therefore, the crowding distance niching technique is implemented in the reserved rank to eliminate the individuals in the crowded area and maintain the same number of individuals. The crowding distance is evaluated on each individual in the rank. The objective functions are normalised and the crowding distance of the *i*th solution is the sum of the distances of two individuals on either side of the individual along each of the objectives, which is shown in Figure 2-3. These procedures are continued until the termination criterion is achieved. This algorithm has been upgraded to a variety of versions, such as Local Search based NSGA-II (NSGAIILS) [95] that effectively and accurately converges to the Pareto front by hybridising local search methods, NSGA-III [96] for solving many-objective optimisation problems and U-NSGA-III [97] that unifies NSGA-III to be suitable for mono-objective, multi-objective and many-objective problems.

.

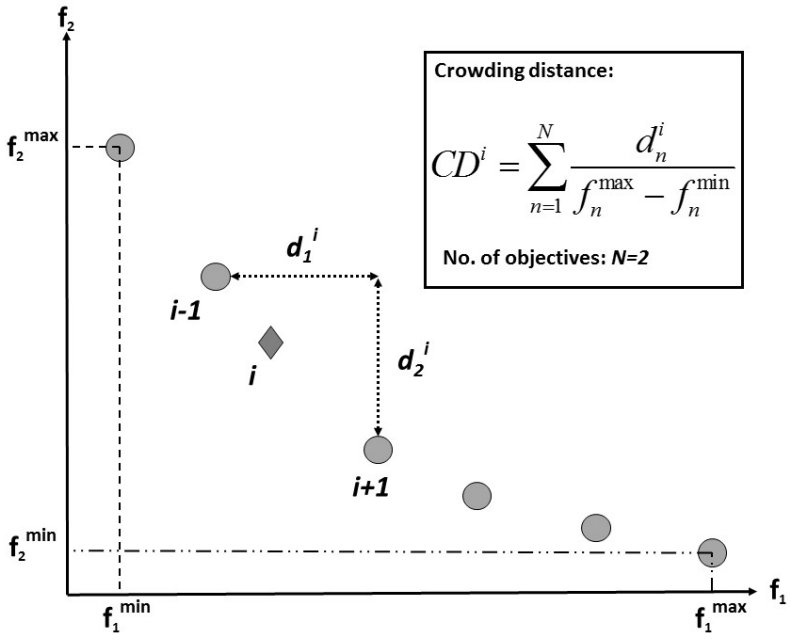

Figure 2- 3. Mechanism of NSGA-II [75]*: crowding-distance calculation*

2.2.2.2 Decomposition algorithms

In decomposition algorithms, the population is divided into sub-groups that search different sub-regions of the entire search space. Decomposition methods are a popular approach in the recent evolutionary computation literature dominating the benchmarking of unconstrained problems; examples include: MOEA/D [80], MOEA/D-M2M [83], CS-NSGA-II [98], DMOEA-DD [99] and LiuLi [100]. These algorithms require additional setting

parameters, such as the weight vectors in MOEA/D. These parameters influence the ability of the algorithm to find the optimal solutions and it is important to determine the optimal settings of these hyperparameters, or the performance is extremely poor.

MOEA/D is the original decomposition method and still shows top performance on unconstrained benchmarking problems. It works by initially creating a set of homogeneous distributed weight vectors and an empty external population for keeping and updating the non-dominated solutions. The multi-objective optimisation problem is divided into N weighted multi-objective optimisation sub-problems. These sub-problems are synchronously optimised in the algorithm. The Euclidean distances between any two weight vectors are calculated and the closest M weight vectors of the weight vector, γ, are defined as its neighbourhood. The neighbourhood can overlap and each weight vector has its neighbourhood. An initial population of solutions can then be randomly generated. Two individuals in the neighbourhood of weight vector γ are randomly selected to generate the offspring solutions through crossover and mutation. The offspring solutions are compared with their parents and neighbourhood of parents. If the newly generated solutions are better than their parents and neighbourhood of parents, they replace the previous solutions and the reference points of the weight vector and neighbouring solutions are updated. The non-dominated solutions of each sub-problem are combined to achieve the Pareto front. The mechanism of MOEA/D is illustrated in Figure 2-4.

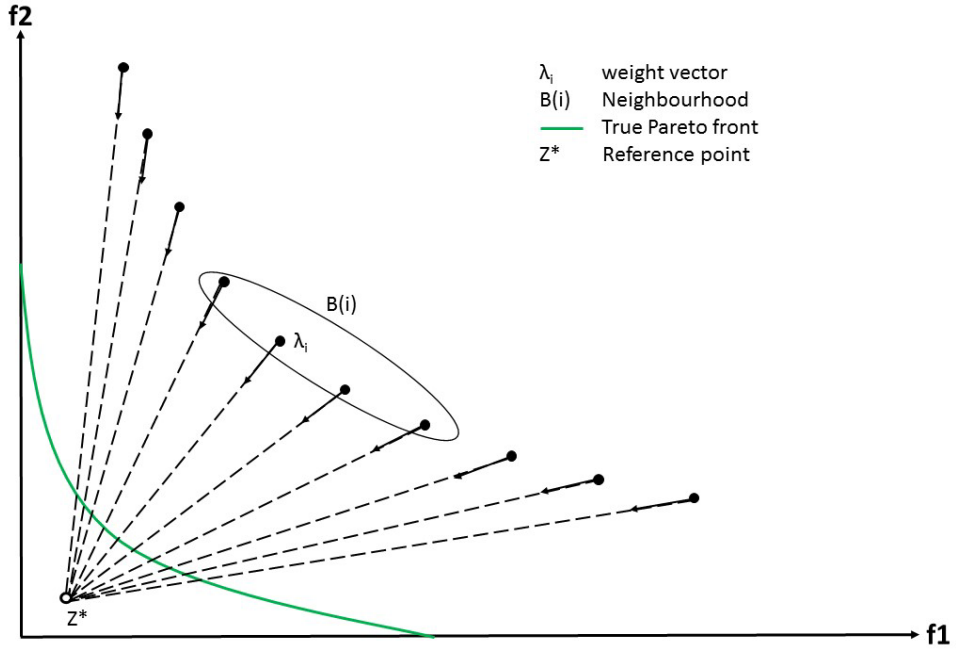

Figure 2- 4. Mechanism of MOEA/D [80]

MOEA/D, and its variants, requires a priori knowledge of the objective space or it can result in extremely poor performance and is not able to find points in negative regions. It is

hard to obtain the required knowledge of the objective space for engineering optimisation problems before solving them, making these algorithms difficult to use, and this knowledge, and likelihood of using these algorithms, would be improved through better documentation of the literature. Therefore, these algorithms may not be (currently) suitable for solving composite optimisation problems. When solving discontinuous problems or constrained problems, these algorithms struggle with large gaps where there are no feasible solutions as the weight vectors point straight through the gaps and the individuals struggle to go around these spaces, resulting in a waste of computational power. In order to utilise these decomposition algorithms for engineering optimisation problems it will be necessary to simplify the tuning process or increase the knowledge about the current problems, focusing on problems which require strong convergence but where diversity of the population is less important.

2.2.2.3 Co-evolutionary algorithms

The origins of co-evolutionary theory are in the works of Darwin [101] who clearly describes the interactions between plants and insects. The term is formalised much later by Ehrlich and Raven in 1964 [102] to describe the coexistence of plants and butterflies, as one group cannot survive without the other, meaning that their evolution is intertwined. Groups of organisms can co-evolve in a number of different ways [103] such as: symbiosis [104], coadaptation [105], host-parasite [106] and hunter-prey [107]. These form into two broad forms: cooperation [108] , where organisms coexist and "support" each other or competition [109], where an "arms race" occurs between species and only the strongest may survive in the given environment.

The idea of introducing co-evolution into GAs is first proposed by Potter and De Jong in 1994 [108]. In these approaches multiple populations coexist and evolve in parallel. This usually takes the form of using distinct reproduction mechanisms in each population, effectively using two different algorithms at the same time, with a method to exchange data between them. The sub-populations can operate on the same search space [110], or can be divided into several regions by problem decomposition or additional separation mechanisms [84]. The form of data exchange between groups depends on the type of co-evolution: competitive or cooperative. In cooperative co-evolution the information is shared by different species to form a valid solution when the problem is decomposed e.g. along the decision variable space [108]; or different sub-populations may cooperate to form the Pareto objective front with different subpopulations focusing on different regions [111]. In competitive algorithms different groups compete in the creation of new sub-populations [112], or

populations [79], with fitter sub-populations gaining a wider proportion of children in the next generation or via “arms race” where losing subpopulations try to counter the winning ones by adaptation [113]. The mechanisms are illustrated in Figure 2-5a and an example of a Pareto front from a co-evolutionary genetic algorithm is illustrated in Figure 2-5b.

In the literature multiple algorithms can be found which are inspired by co-evolution. Competitive-Cooperative Coevolutionary algorithm (COEA) [112] is a methodology inspired by symbiosis where cooperation and competition can occur. The cooperation improves the convergence while the competition retains the diversity in the population. The resulting methodology shows high performance on various dynamic problems [114] but the adaptability is limited. The utilisation of a NSGA-II like Pareto-dominance principle and decomposition along the variable space means that performance on irregular or discontinuous spaces and problems with strong variable-linkage is likely to be low. Two new co-evolutionary Genetic Algorithms were developed in 2016, Bi-Criterion Evolution (BCE) [78] and Hybrid Evolutionary Immune Algorithm (HEIA) [79] for solving multi-objective optimisation problems with both showing strong performance. In these algorithms cooperation is introduced between sub-populations. The population is divided into ‘solution’ sub-populations and ‘test’ sub-populations where different operations are performed on each of them. The individuals from the sub-population can be exchanged and there is cooperation between the sub-groups. The fitness of individuals in each sub-population is determined by comparing with the randomly selected individuals in the other sub-population. In BCE the sub-populations operate on the same search space and individuals are selected based on two fitness indicators: Pareto-based criterion and Non-Pareto-based. In this case the Pareto criterion increases the convergence using the standard Pareto dominance and the Non-Pareto fitness increases the divergence using the Hyper-Volume metric. The combination of these mechanisms leads to an overall improvement in diversity and provides particularly good performance on irregular search spaces, those with variable linkages and many-objective cases. A similar approach is utilised in Hybrid Evolutionary Immune Algorithm (HEIA) [79] where two different evolutionary methods are used in each sub-population, rather than separate quality indicators. At each generation the best individuals are moved to a shared pool and cloned before the sub-populations are recreated. This method shows strong convergence but good performance across quite a broad range of different problem types, though this is poor on imbalanced problems.

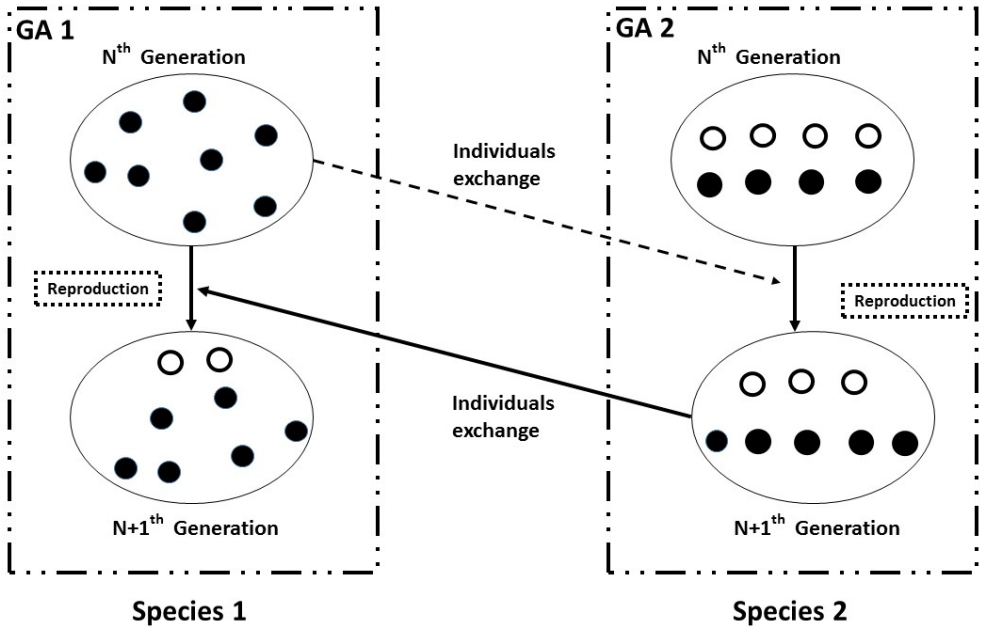

(a)

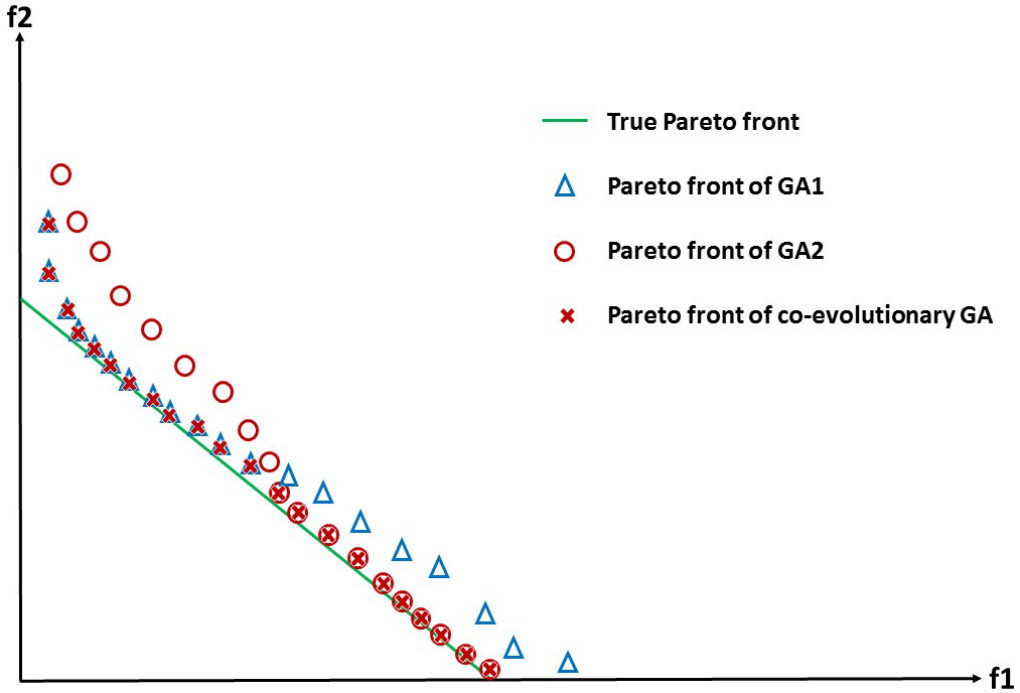

(b)

Figure 2- 5. Summary co-evolutionary genetic algorithm: (a) example co-evolutionary mechanism; (b) an example of a Pareto front from a co-evolutionary genetic algorithm

2.2.2.4 Multi-Level selection algorithms

Multi-Level Selection Genetic Algorithm (MLSGA) was first introduced by Sobey and Grudniewski in 2017 [86,87]. The algorithm mimics the Multi-Level Selection Theory introduced by Wilson and Sober [85,115] where the different theories are discussed in an

excellent review by Okasha [116]. This leads to the introduction of a collective level reproduction mechanism, in addition to the individual level used in the standard Genetic Algorithm, and a split in the fitness function between the two levels. It is unusual as it is a diversity first optimisation approach and also provides a general solver, working well across all problem types.

The algorithm starts with a randomly generated initial population which is classified into collectives, via the linear support vector machine (SVM), according to the design variables. SVMs are a class of supervised learning algorithm that builds a representation of the examples in the training data as points in space and marks each point into one or the other of two categories by dividing them by a clear gap that is as wide as possible. New points are then mapped into the same space and predicted to belong to a class based on which side of the gap they fall on. The predefined categories in the SVM become the collectives in the MLSGA and they are determined by the mean and standard deviation of the points. At the individual level, each individual is evaluated through their objective function and standard genetic operators are utilised to perform individual reproduction [117]. Simultaneously, each collective is evaluated through all of its individuals by calculating the collective objective function at the collective level. The competition is performed among the collectives and the lowest fitness collectives are eliminated. These collectives are replaced by copying the best individuals from each of the remaining collectives into a new collective. The process is stopped when the termination condition is satisfied. This mechanism is illustrated in Figure 2-6. There are two main variants, each with a different fitness definition at the individual and collective level, MLS1 and MLS2(R) [116], where MLS2R is the reverse of MLS2. MLS1 defines the fitness as the aggregate of the individuals in the population to calculate the fitness of a generation. However, the MLS2(R) calculates different objectives at each level. Therefore, MLS1 focuses its search at the middle of the Pareto front and MLS2 and MLS2R enhance the search at the two sides of the real Pareto front. MLSU combines these two variants, simplifying the multi-objective optimisation process in MLSGA and reducing the hyperparameter tuning. An example of the MLSU search is shown in Figure 2-7.

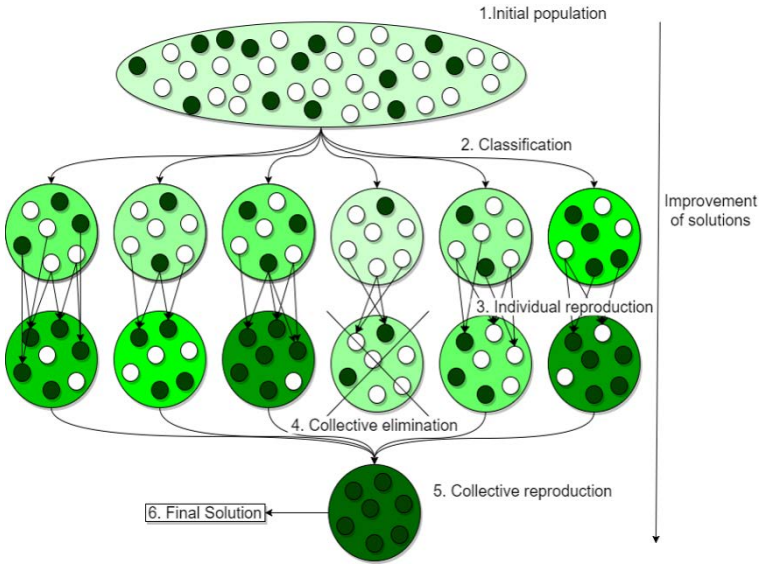

Figure 2- 6. Mechanism of MLSGA [86,87]*: individual and collective reproduction*

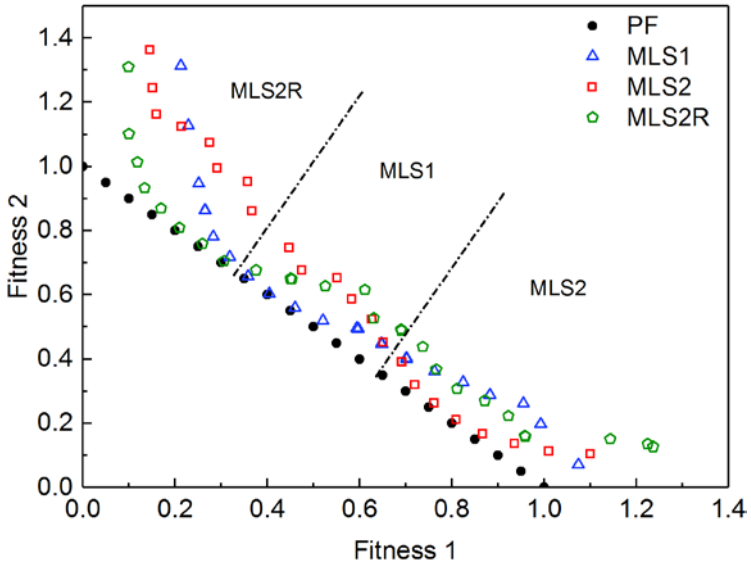

Figure 2- 7. Mechanism of MLSGA [86,87]*: an example of MLS1, MLS2 and MLS2R search preference*

MLSGA can be combined with any other Genetic Algorithm by using these algorithms at the individual reproduction level which has been demonstrated on NSGA-II, MOEA/D and Multiple Trajectory Search (MTS) [87]. The hybrid MLSGAs achieve higher performance than their original algorithms when benchmarked on the CEC'09 test functions [82] except for MOEA/D on unconstrained problems [87]. The MLSGA-MTS exhibits the best performance when solving both the constrained and unconstrained test problems among all the benchmarked algorithms, showing excellent performance as a general solver. This approach has been demonstrated practically on the optimisation of triaxial weave fabric patterns where MLSGA-NSGAII is shown to be more suitable for solving discontinuous Pareto fronts with large gap between sub-fronts [30]. The collectives are distributed in the search space, which maintains

the diversity of the entire population and improves the ability to find all of the sub-fronts. This approach is combined with the co-evolutionary approach, which improves the convergence while retaining the increase in diversity while also improving the generality of the algorithm. This leads to the best performing general solver in a recent benchmarking [88].

2.2.3 The importance of Genetic Algorithms to composite materials and structures

Optimisation techniques are widely used across many different disciplines. They are often used to provide innovative solutions or to gain insights into complex problems. Evolutionary algorithms are one of the most popular categories of optimisation techniques, especially in engineering design, as they are capable of finding solutions in large and complex search spaces. A database of applications of evolutionary algorithms, Coello Coello [118], shows 4,983 papers utilising evolutionary algorithms to solve multi-objective optimisation problems from 1988 to 2017. The proportion of different evolutionary algorithms from this database are summarised in Figure 2-8, where the papers with titles containing 'evolutionary algorithm' are not counted since it is hard to distinguish and summarise which evolutionary algorithm is used in each of those papers. The main evolutionary algorithms used are: Genetic Algorithms (GAs), Particle Swarm Optimisations (PSOs), Ant Colony (AC), Simulated Annealing (SA), Differential Evolution (DE), Immune Algorithms (IA), Artificial Bee Colony (ABC) and Firefly Algorithm (FA). The largest proportion of algorithms being used are Genetic Algorithms which occupy over 56% of applications, showing the continued popularity of this type of optimisation algorithm despite the increasing competition from other methods.

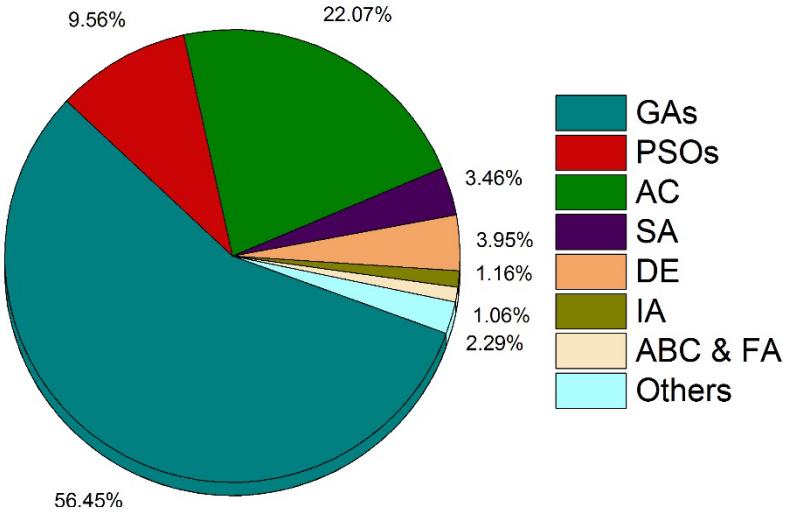

Figure 2- 8. Popular evolutionary algorithms in the past 30 years [118]

The publications from this database, related to Genetic Algorithms, fall into 23 research broad fields. These fields, and the number of publications in each field, are shown in Figure 2-

9 where the composite structures optimisation theme is ranked in the lower half, indicating that there might be room for greater uptake of these methods to help understand the behaviour of these materials. As a field optimisation algorithms are used less than in similar engineering themes such as Aeronautics & Astronautics and Material Manufacturing, though there might be some overlap between them. Whilst Composite Structures might be considered to be a small field, its complexity and importance require consideration for how optimisation techniques can be better utilised to help future research and industrial applications.

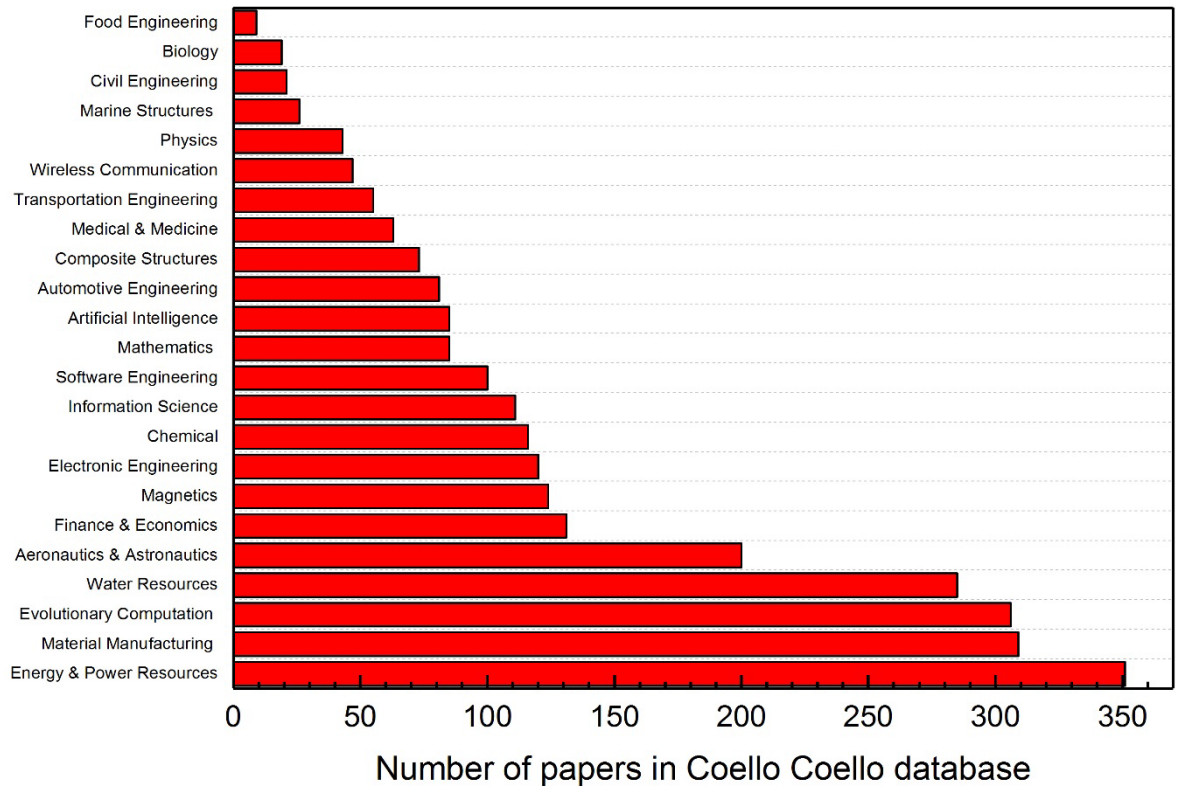

Figure 2- 9. Multi-objective optimisation papers published in different fields in the last 30 years [118]

Due to the importance of optimisation to the future of composite structures, and the significance of Genetic Algorithms within the field of optimisation, the use of Genetic Algorithms in Composite Structures/Materials is reviewed in this Chapter. In order to cover all relevant papers on this topic, allowing a more critical review of the state-of-the-art, the publications related to composite material/structure optimisation in 17 journals are reviewed: *Composites Science and Technology (CST), Composites Part A: Applied Science and Manufacturing (CPA), Composites Part B: Engineering (CPB), Composite Structures (CS), Applied Composite Materials (AppCM), International Journal of Solids and Structures (IJSS), Journal of Composite Materials (JCM), Journal of Sandwich Structures & Materials (JSSM), Thin-Walled Structures (TWS), Computer Methods in Applied Mechanics and Engineering*

(CMAME), International Journal of Mechanical Sciences (IJMS), American Institute of Aeronautics and Astronautics journal (AIAA), Steel and Composite Structures (SCS), Journal of Composites for Construction (JCC), Marine Structures (MS), Materials and Design (MD) and Structural and Multidisciplinary Optimisation (SMO) are selected over a decade from 2008-2017. These journals are deemed to be representative of best practice in composite optimisation in the rest of the literature. There are 63,780 total publications in these 17 journals from 2008 to 2017 with 1,458 papers found by searching the keywords "Genetic Algorithm for composite material and structure". These are reduced to 321 papers by removing overlapping papers or those that mention Genetic Algorithms but do not use them. The details of these 321 papers are listed in a data attachment[2]. The quantity of composite optimisation papers using Genetic Algorithms over the last decade has been summarised in Figure 2-10a. The top five journals that having the highest number of composite optimisation papers using Genetic Algorithms have been broken down by year and is illustrated in Figure 2-10b. It shows that in most of the journals the interest in this area has been increasing over the last 5 years; this is especially true in *Composite Structures*.

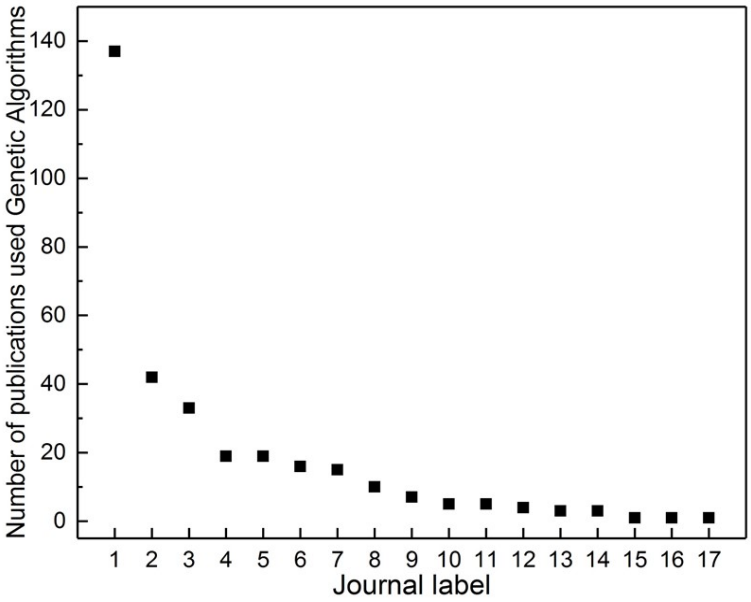

(a)

[2] https://doi.org/10.1016/j.compstruct.2019.111739

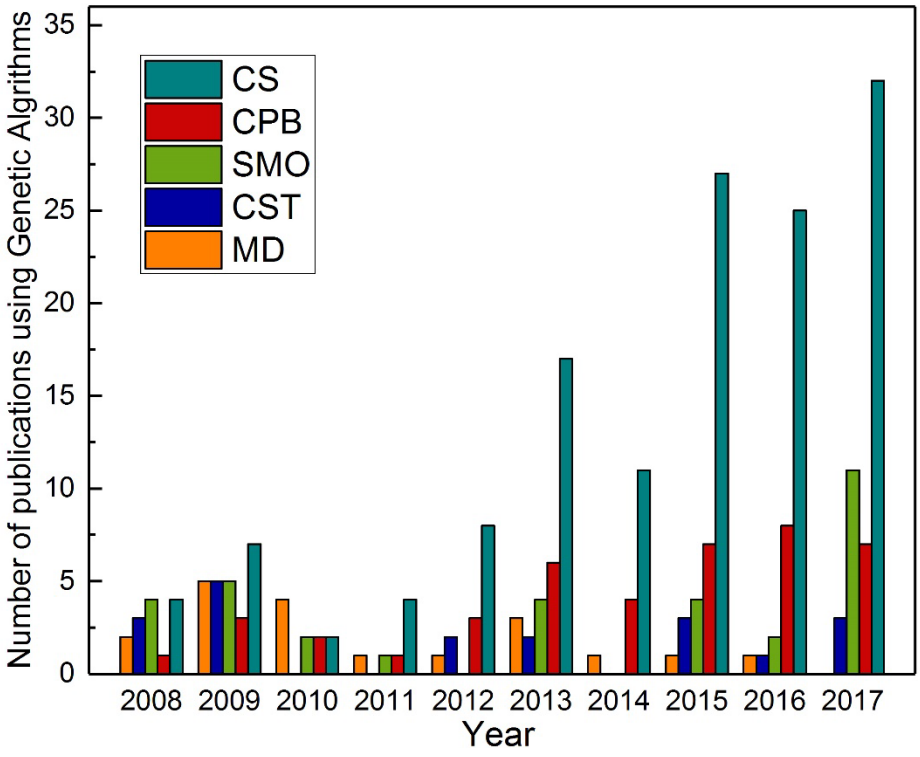

(b)

Figure 2- 10. Number of optimisation papers utilising Genetic Algorithms published: (a) in each journal; (b) in the selected journals by year

This growth in publications using Genetic Algorithms indicates that the complexity of the problems being solved is increasing, and will continue to do so. To solve these problems the selection of the Genetic Algorithms, and how they are used, is important. The 'no free lunch' theorem states that two optimisation algorithms have the same performance when averaged over all possible optimisation problems. The design space in each problem has different characteristics for example: multimodal, biased, deceptive, concave/convex, continuous/discontinuous, single, multi- and many-objective and dynamic; and general solvers have generally good performance across all of the characteristics but cannot reach the performance spike of a specialist solver when used to solve a problem dominated by that characteristic. Conversely these specialist solvers own performance quickly degrades on problems with different characteristics to its own speciality. This is supported by work in evolutionary computation where there is a difference between the performance of specialist algorithms and the general solvers across a range of constrained and unconstrained problems [82]. This choice between general and specialist solvers creates a problem when selecting the correct algorithm as it is possible that practical problems are dominated by multiple characteristics, meaning that specialist solvers will perform poorly. However, some composite optimisation problems have simpler design spaces, dominated by one characteristic, and as

these problems become more complex general solvers may not find the optimal results, or may require a larger number of function evaluations and time to solve. In addition to the type of solver in all optimisation problems there is a balance between convergence, which move the search towards the optimal solution, and diversity, which ensure the entire search space is covered. Many different types of problems require Genetic Algorithms with strong convergence mechanisms, unconstrained and dynamic problems for example, but increasingly there are cases where diversity mechanisms are shown to be important, discontinuous and constrained problems. In addition the increase in complexity of the problems seems to require solvers with stronger diversity preserving mechanisms. In some cases this diversity seems to dominate even when the problem is posed simply with limited design variables as witnessed in Wang et al. [30] and Mutlu et al. [119].

Therefore, the selection of the correct algorithm is not a simple problem and can greatly affect the performance; it requires an in-depth knowledge of evolutionary computation and composite structures/materials. This Chapter therefore reviews how Genetic Algorithms are currently being used in the literature before a technical review of some specific composite optimisation problems is performed and compared to the mechanisms of the latest evolutionary computation methods, to find compatible solutions. Recommendations are then made to help improve the performance of Genetic Algorithms on composite optimisation problems.

2.2.4 Common applications in the composite optimisation literature

2.2.4.1 Common composite optimisation applications

The main applications for optimisation within composite structures are briefly reviewed; although Nikbakt et al. [120] provide a more detailed categorisation of composite structural optimisation problems using similar categories. The literature is split into three main themes: input variables, objectives and applications. Within these there are 12 major categories which composite optimisation can be split into including design variables: laminate stacking sequence (LSS) and shape optimisation (SO); objectives: weight, cost, buckling, deflection, mechanical properties (MP) and natural frequency (NF); and applications: microwave absorption performance (MAP), woven fabric composites (WFC) problem and progressive failure (PF). The proportion of each category are summarised in Figure 2-11. The laminate stacking sequence (LSS), weight, buckling and mechanical properties (MP) optimisations occupy the highest proportions.

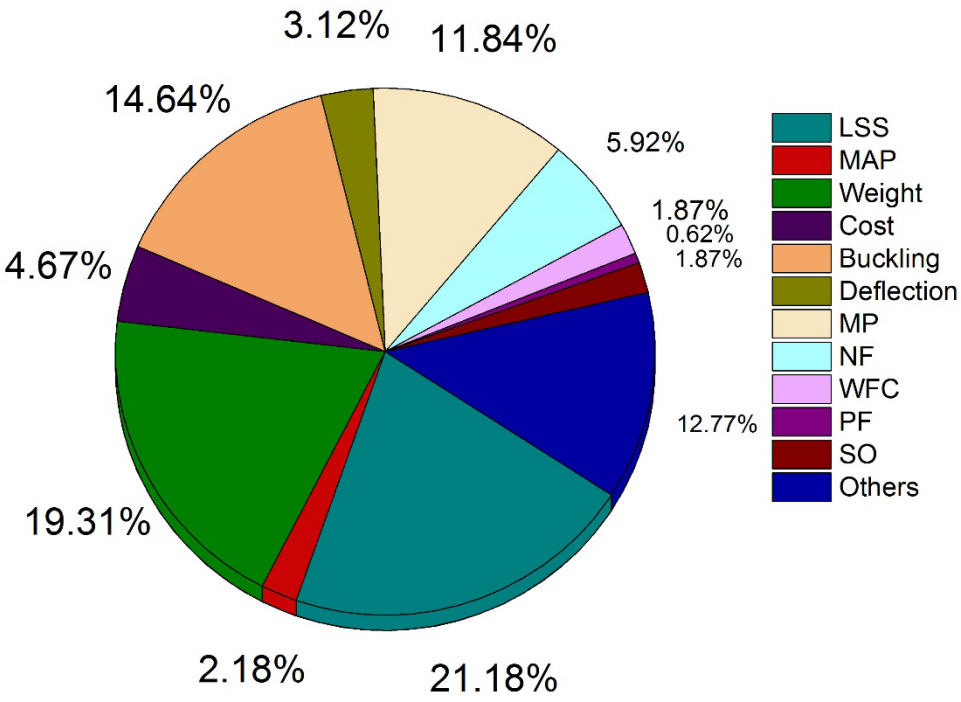

Figure 2- 11. Proportion of each optimisation topic

Within these applications there are a number of ways to evaluate the fitness of the composite structures and each method significantly influences the computational time of the optimisation. The selection of the method can restrict the total number of fitness evaluations that can be implemented during the optimisation or if rapid techniques are used can increase the importance of the computational expense of the Genetic Algorithm. The methods found in the literature are: finite element method (FEM), surrogate models which contains all types of surrogate modelling methods except artificial neural networks, such as polynomial regression and response surface methods, artificial neural networks (ANNs), analytical models and constitutive relationships, with the proportions shown in Figure 2-12. It is found that over half of the papers, ~59%, utilise FEM with the other methods having a similar representation, at 8-13%. It is considered that the main reason is that FEM models are easily obtained, robust and accurate. Furthermore, since it is considered that many authors of the 321 papers are experts on composites modelling through many types of FEM modelling methods, they prefer to use their developed FEM models as the fitness function evaluation methods in their optimisation works. Despite its accuracy the FEM process is computationally expensive when compared with the other four methods as the function evaluation methods and restricts the number of function evaluations that can be used. It is found that when using FE methods as the objective evaluation method ~90% utilised less than the average function evaluation number, 60,000 total calls, which is a low value for a complex optimisation problem and is likely to be set due to the computational time constraint. Surrogate modelling or ANNs, used as a surrogate model,

are introduced to be the fitness evaluation tool when the problem is too time consuming to utilise it. However, these methods often mean that the complexity of the problem is reduced, and the optimisation becomes more prescriptive, or accuracy might be lost, and the developed Pareto front may not relate to one developed using a more accurate method. It is therefore important to carefully consider the impact of different fitness evaluation methods; whilst FEM, or similarly more accurate methods, might provide more accuracy it reduces the number of function calls in most optimisation trials, and therefore a sub-optimal set of results might be found. Analytical or surrogate models reduce the accuracy or freedom of the model, but this might provide a set of optimal results that can be refined with a smaller number of FEM calls to adjust the final results.

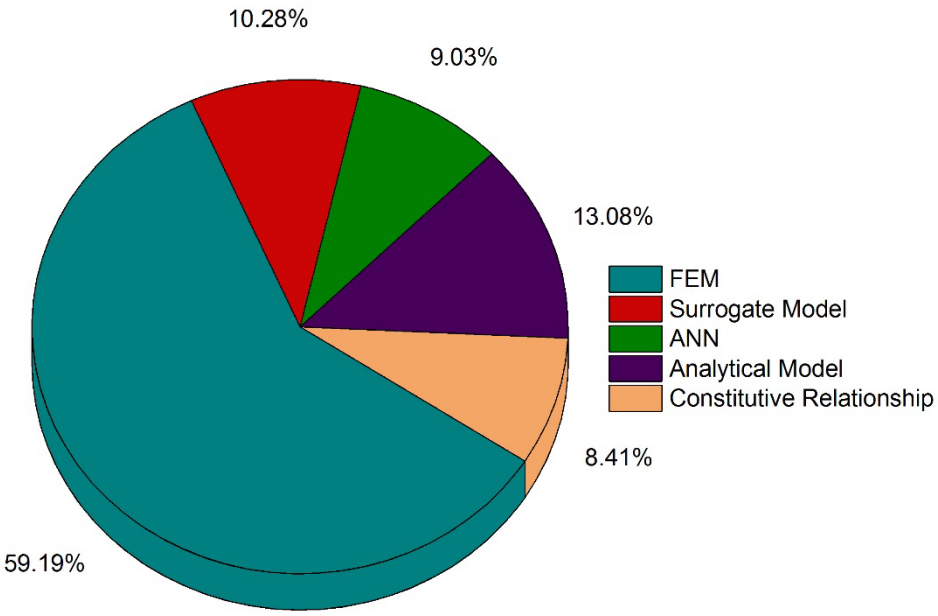

Figure 2- 12. Proportion of each fitness evaluation method

The most popular application for Genetic Algorithms is the optimal stacking sequence for composite laminates, investigated by ~21% of papers. This is because the ply angle significantly influences the performance of laminated composite structures and is affected by the loading conditions. All of the papers show improved performance of the composite laminates after achieving the optimal stacking sequence. However, it is found that the optimal stacking sequence achieved by [121–130] are similar since they limit the potential fibre orientation angles to {0°, ±15°, ±30°, ±45°, ±60°, 90°} degrees. The rest of the papers set continuous fibre orientations, so any angle from 0°-90° is possible, or discrete fibre orientations with increments of one or five degrees. However, the fibre orientation is often fixed to guarantee the manufacturing feasibility, which implies that the optimal stacking sequence achieved from continuous or discrete fibre orientations are not applicable in the real-world

composite structures [123–128]. This implies that the Genetic Algorithms are less useful for achieving optimal solutions since the best results can be achieved using an exhaustive search as these fixed patterns of the fibre orientations significantly limit the search space. This is unless the stacking sequence optimisation is in conjunction with complex loadings or structural geometries, which is not the case for much of the literature. In these scenarios bi-level optimisation of laminated composite structures will be required to reduce the complexity in these hot spot regions as other the number of variables for the entire structure will become unsearchable.

The second largest proportion of the literature is focused on weight minimisation where most papers solved single objective optimisation problems. In these studies the relationships between the weight and other features of the composite structure remain unknown. This restricts the range of applications for the optimised results, making them less interesting for real-world applications, as the structures may underperform in other areas, though there are a few multi-objective optimisation investigations. The addition of these objectives is important as illustrated by Wang and Sobey [31] who find 643 design schema that achieve an improved strength to stiffness ratio compared with an existing design of a triaxial weave fabric composite when using a multi-objective optimisation. However, this number is reduced to 15 when an additional objective of areal density is added, making the results more realistic. The results also show another 17 design schema which have slightly higher areal densities but achieve significantly improved strength to stiffness ratios that would have been lost in a single objective optimisation but inform the structural designer of more options [30].

The third most popular optimisation topic in composite literature is buckling performance. Many of the studies implement surrogate models to effectively approximate the value of objective functions due to the high computational expense in simulating buckling. The method significantly reduces the computational time caused by FE methods. However, the results from most of them are not compared to those generated with FEM, so the accuracy of these results for optimisation remains uncertain. Optimisation of mechanical properties is the fourth most popular composite optimisation problem. In these cases increasing the performance of one mechanical property can easily reduce the importance of another such as in tensile/compressive strength, tensile/compressive stiffness and shear strength/stiffness. It is therefore important to perform multi-objective optimisation to improve the applicability of the results but this topic has the lowest number of multi-objective optimisations among the four popular topics.

2.2.4.2 Bibliometric review of composite optimisation

A key issue in the current composite optimisation literature is a generally poor documentation of the Genetic Algorithm parameters, making it difficult to evaluate the validity and consistency of the optimisation results. In this section a number of parameters considered to be vital for replication of results or interpretation of performance are investigated and typical values from the literature are given to capture the current state of the art. Of the papers reviewed only ~62% of papers explicitly state the name of their employed Genetic Algorithms, shown in Figure 2-13.

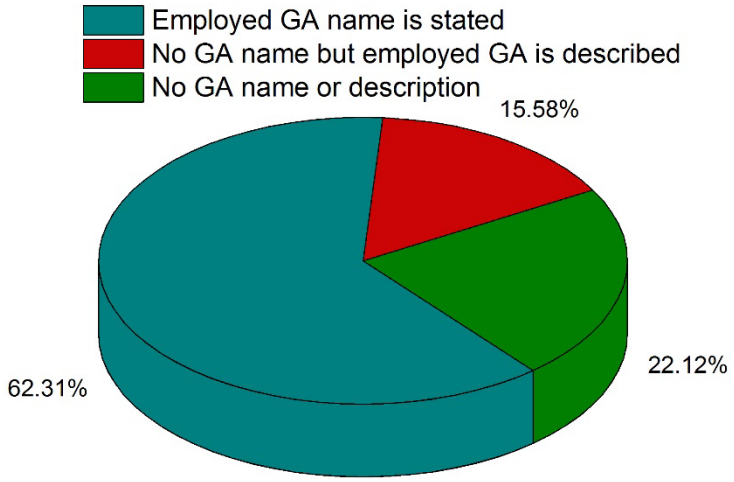

Figure 2- 13. Proportion of papers documenting the utilised Genetic Algorithm

This lack of documentation is perhaps related to a general consideration that any Genetic Algorithm can be used to solve any problem, and it is therefore suspected that many of the rest of the ~38% papers use old solvers. This is supported by the fact that ~80% of authors only published one composite optimisation paper in the last 10 years with limited authors repeatedly utilising these tools and becoming specialists, illustrated in Figure 2-14.

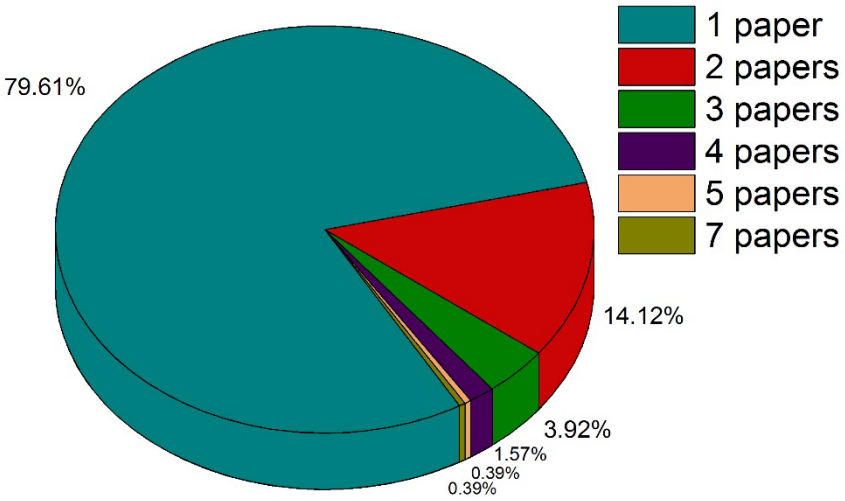

Figure 2- 14. Papers published on composite optimisation using Genetic Algorithms per author

The genetic operator types and rates have a significant influence on the performance of solvers as it is important to find a balance between the exploration and exploitation ability of the algorithms in order to achieve the global optimum [54]. Exploration means exploring the entire search landscape as comprehensively as possible, which is accomplished by mutation operators and specific diversity retaining mechanisms. While the exploitation is accomplished by the crossover operator, which pushes the search towards the current optimal solution. Most developments in the evolutionary computation field focus on increasing the convergence of the algorithm. More detailed information about the genetic operators are often not included, as shown in Figure 2-15; only ~34% of the papers state the type of selection mechanism, ~26% give the mutation operator, ~27% document the use of elitism and ~29% provide the type of crossover mechanism that they use. In terms of repeatability of these results ~58% of the 321 papers miss the crossover rate and ~61% don't state the mutation rate, though many modern algorithms are not sensitive to these specific values and the tuning performed in the original papers tends to provide close to optimal performance across most problems.

Of those papers that do incorporate this information the most popular used selection, crossover and mutation operators are roulette wheel/tournament selection, single point crossover and gene swap mutation, this indicates binary coded Genetic Algorithms developed in the 1980's and 90's. It is considered likely that the 38% of papers that did not state the Genetic Algorithm were also older solvers, defined here as those developed before 2002 as this was the year NSGA-II was developed which is the oldest Genetic Algorithm that still shows top performance on many practical problems and is considered in the evolutionary computation benchmarking. Approximately 1% of the literature does not include mutation operators, meaning that there are no mechanisms to retain the diversity of the search, and ~73% don't

mention elitism mechanisms, a key element in improving the performance of genetic algorithms since 1975. The missing genetic operator type makes it difficult to assess the validity of the results or to characterise why a given algorithm may have been successful. This means that even if the optimisation proves to be successful, with quick convergence and accurate results, the information about the type of solver optimal to this problem is lost and so it is hard to replicate the results or to generate new algorithms to solve similar, but more difficult, problems in the future.

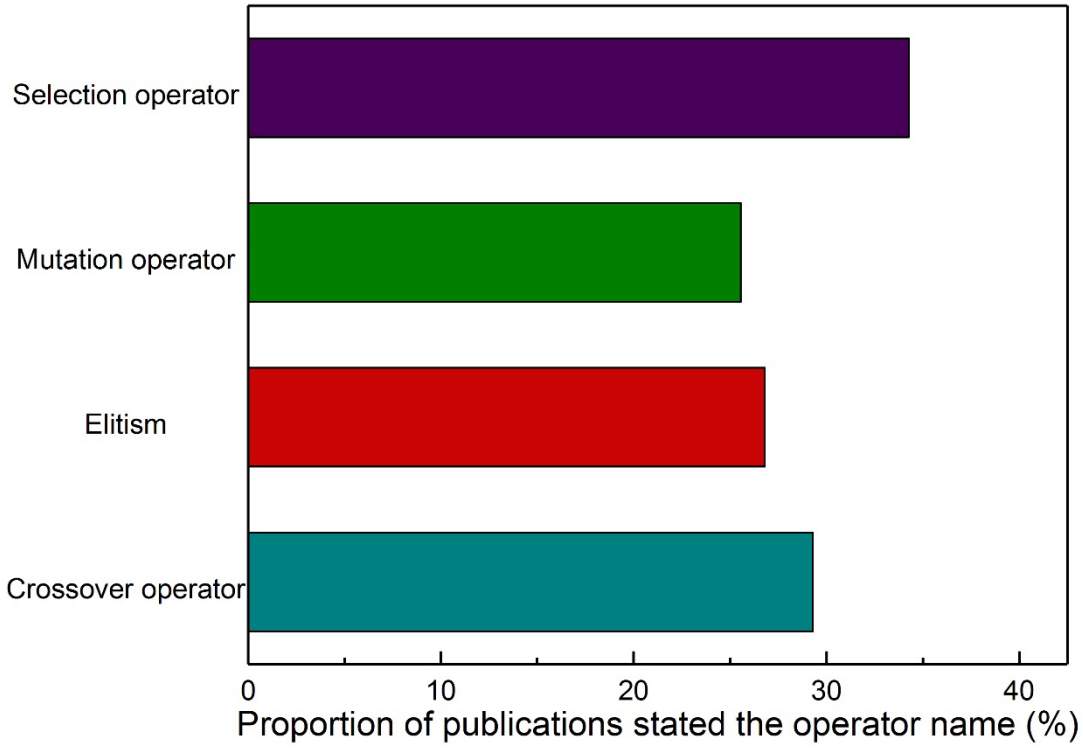

Figure 2- 15. Proportion of publications stating the name of the utilised genetic operators

In addition to the poor documentation of the mechanisms for the Genetic Algorithms the hyperparameters used within the algorithms are often not recorded. Only around 48% of papers state the population size and generation number or the total number of fitness evaluations, illustrated in Figure 2-16. It is suspected that many of the papers that do not state the information for the number of function evaluations use smaller numbers of calls to reduce the computational time but this may compromise the quality of the solutions. In addition the population size must be appropriate to the problem type and solver, which effects the diversity of the population and convergence rate. These values are vital in allowing a fair benchmarking and demonstrating improvements in methodologies, in addition the use of a small number of function evaluations may reduce confidence in the final result.

Of those papers documenting the hyperparameters the most frequently used number of population size is 50 and the most frequently used generation numbers are jointly 50 and 100 meaning that the most frequently used number of total function evaluations is 5,000 and ~93% of the 321 papers use less than 100,000 total function evaluations for solving complex composite optimisation problems. However, the computational science literature utilises 300,000 total function calls as standard to solve mathematical optimisation problems, where the optimal solutions has not been found even when using the state-of-the-art solvers. This indicates that the problems selected for testing in the composite science literature are less complicated than the benchmarking problems in the evolutionary computation literature or that the optimal designs may not have been found. Recent studies [30,119,131,132] show that the complexity of even simple composite optimisation problems is high in comparison to those found in evolutionary computation, possibly due to the problems being dominated by multiple characteristics. However, there must be some realisation that not all of the applied literature will be seeking to find the optimal results and that an improvement on the current performance may be all that is required.

In terms of population size then the standard from most of composite optimisation literature is 50 and most of the evolutionary computation is 600 with some authors recently showing better results with 1500 population sizes [30]. In many cases engineers use a much smaller population size, but this may not contain the necessary diversity of species to ensure a full search of the design space in many cases, though it may help convergence. In many cases it is likely that the optimisation converges early in the generation cycle, supported by many of the documented Pareto fronts in the literature looking unresolved or where graphs of the fitness function remain static for long periods towards the end. This means these function calls are wasted and a larger diversity is required to search more of the space, a more powerful algorithm is required or the optimal results have indeed been obtained. For biological systems it is estimated that at least 10,000 population sizes are required to retain genetic diversity, so even these numbers, 600-1500, are small by evolutionary standards [9].

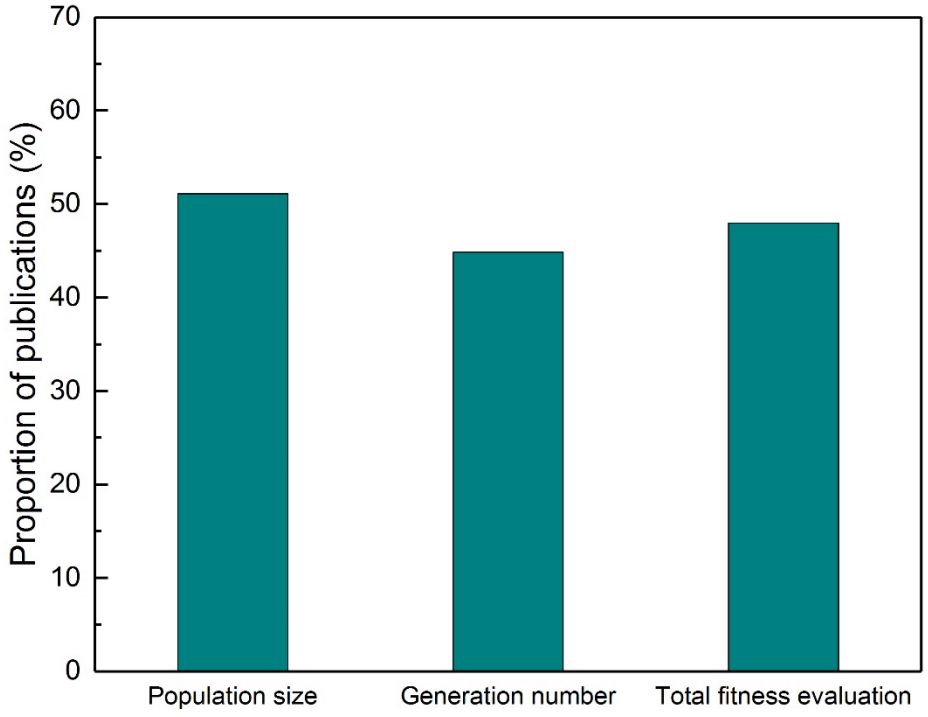

Figure 2- 16. Documentation status of hyperparameters

It addition to ensuring the function calls are utilised to match diversity and convergence it is important to have several independent run cycles to ensure that the final solutions have been achieved as Genetic Algorithms are stochastic solvers and the final solution is dependent on the initial population in a number of algorithms. However, only ~14% of papers state the number of repeated run cycles as shown in Table 2-1, where it is shown that a range of values are used from 2-100. It is suspected that many of the papers that do not provide a value for the number of repetitions give results from a single run meaning that the authors of these papers are not able to evaluate the robustness of the algorithm and it is difficult to determine the accuracy of the final results. Of those papers with a higher number of run cycles, two papers with high values are not independent cycles to determine statistical distributions of the solutions [133,134] but are used to generate the Pareto front using a weighted sum approach to solve a multi-objective problem by changing the weights 50 and 100 times to find the Pareto front, requiring many more function calls than a standard multi-objective approach. In evolutionary computation the standard value for benchmarking of Genetic Algorithms is 30 run cycles, of which 15 papers used this value or higher, to ensure enough data to determine the performance of a methodology. This is perhaps too high where the solution is the output, rather than a justification of the method, but recent papers are showing that many solvers require multiple attempts to find the entire Pareto front [30].

Table 2- 1. Documented distribution for the number of independent run cycles

No. of independent run cycles	No. of papers	References
Unrecorded	276	-
1	2	[133,134]
2	2	[135,136]
3	2	[137,138]
4	3	[139–141]
5	8	[124,142–147][148]
6-20	12	[149–156][157–160]
25	1	[27]
30	3	[130,162,163]
40	1	[164]
50	3	[165–167]
100	8	[168–175]

2.2.4.3 Categorisation of the optimisation problems

The optimisation problems are categorised into single objective, multi-objective and weighted multi-objective problems, which reduces the multiple objectives down to one objective by using a weighted sum approach. Multi-objective is generally considered to be the most interesting category since the results can be used by engineers to better understand the design space and from which engineers can pick designs that match to other considerations that may not be included in the optimisation. In addition the lessons for other researchers are increased by having the whole front, allowing more areas of interest to be published and allowing any areas of the search space that are difficult or impossible to find to be highlighted. An additional disadvantage is that the results from a weighted sum approach are highly dependent on the selection of the weights and it is hard to accurately select the correct weights between objectives to precisely achieve solutions, even for experts. However, many authors select this approach as, for the same optimisation problem, using single objective and weighted sum approaches can help to simplify the problem and more traditional Genetic Algorithms are able to solve these problems, especially if the design variable spaces are small and/or simple.

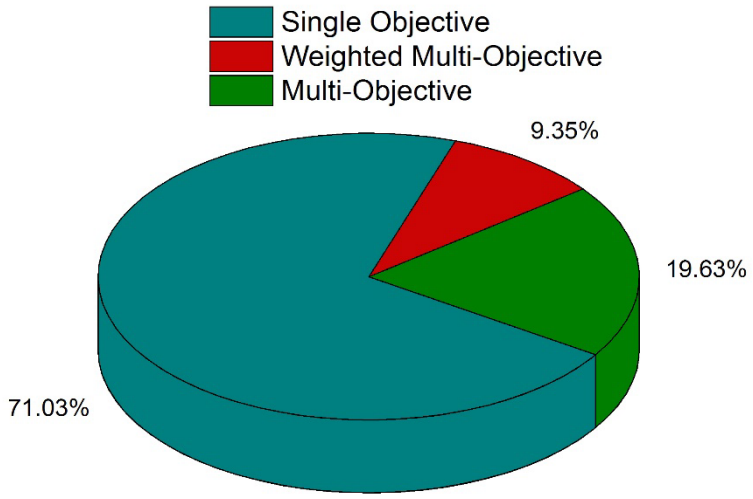

Figure 2- 17. Proportion of publications solving single objective and multi-objective problems

The composite optimisation literature relies heavily on single objective optimisation problems, illustrated in Figure 2-17. In total ~80% of papers focus on single objective and weighted multi-objective problems. This may explain the lack of more modern Genetic Algorithms in the composite optimisation literature, as these are designed with diversity retaining mechanisms rather than the convergence dominated algorithms required for single objective problems. For the single objective and weighted multi-objective problems the convergence information is not comprehensively documented, summarised in Figure 2-18, where over half of the papers do not state the converge information. It is suspected that the final solutions in much of this ~56% of the single objective optimisation may stop at a local optima. In total ~29% of papers solve problems with multiple objectives, where ~9% of the total are weighted multi-objective optimisation and ~20% of the total are multi-objective optimisation.

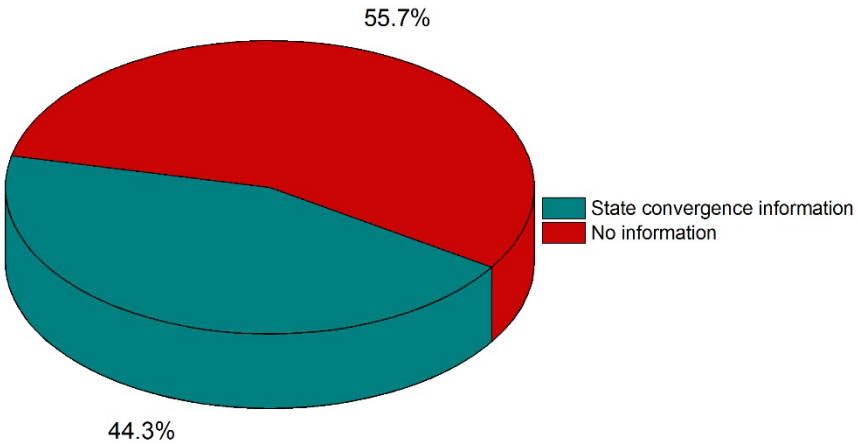

Figure 2- 18. Proportion of papers providing convergence information for single objective problems

In terms of the variable space then ~17% of papers don't have or miss documentation of the variables used or the range over the simulations are performed and ~31% of papers don't document the constraints, illustrated in Figure 2-19. The maximum and median number of variables through all the 321 papers are 217 and 5 respectively and the maximum and median number of constraints are 16 and 3. These numbers indicate the complexity of composite optimisation problems, requiring the state-of-the-art Genetic Algorithms with the correct hyperparameters. The missing design variables and constraint information makes it difficult to determine the accuracy of the optimisation results and the lack of details defining the relationship between the variable space and objective space makes it impossible to replicate.

In large-scale real-world composite structures there are potentially thousands of dimensions in the variable space. The main difficulties in solving these problems are the computational cost and the multi-modal shape of the search space, which contain many local optima. The computer science literature is developing methods to improve Genetic Algorithm performance on these problems using different methodologies, such as applying compression and decompression on the encoding chromosome to reduce the search space [176], parallel implementations of Genetic Algorithms on Central Processing Unit (CPU) and Graphic Processing Unit (GPU) [177–179] and developing a customised Genetic Algorithm for finding near-optimal solutions [180], to reduce the complexity of the problems and to improve the computational efficiency. The problems being tackled can contain billions of variables but are still flat in comparison to real-world problems, with limited multi-modality, and reduce the complexity by looking at single objective problems. In the composite optimisation literature there is still limited literature discussing and developing methodologies for solving these large-scale optimisation problems, limiting the practicality of these problems.

In the 29% of papers that solve problems with multiple objectives 15 papers solved problems with more than 2 objectives. The highest number of objectives is 21 and second highest is 6 but in both cases one fitness function is formed using a weighted average approach, the rest of the papers use 3 objectives. 8 of the 15 papers generate a Pareto front surface to illustrate the optimal solutions for the 3 objectives including one paper which generates a Pareto front surface by tuning the weights. There are 8 papers which use a weighted average approach to solve these problems. Solving many-objective optimisation problems, defined as problems with 4+ objectives, provides additional challenges as the solutions must simultaneously satisfy several design requirements. The main difficulty in solving many-objective optimisation problems is that with the additional objectives it is less likely that one

solution dominates the other solutions in the population. While the complexity of solving these problems is difficult, they provide the most interest as the additional complexity means that humans struggle to make rational decisions about the design but where computational analysis can be most helpful in visualising the trade-off between objectives. There is a strong focus in computer science literature for improving the performance of algorithms on problems with four and more objectives and several Genetic Algorithms for solving many-objective optimisation problems have been developed, such as cMLSGA [132], U-NSGA-III [97], HEIA [79] and BCE [78]. However, the test functions for these problems are still relatively few and biased towards certain types of search space. This means the performance of algorithms on these problems is particularly difficult to relate to composite structural optimisation and there must be more emphasis on developing benchmarking problems of this complexity in the composite structures field in the future.

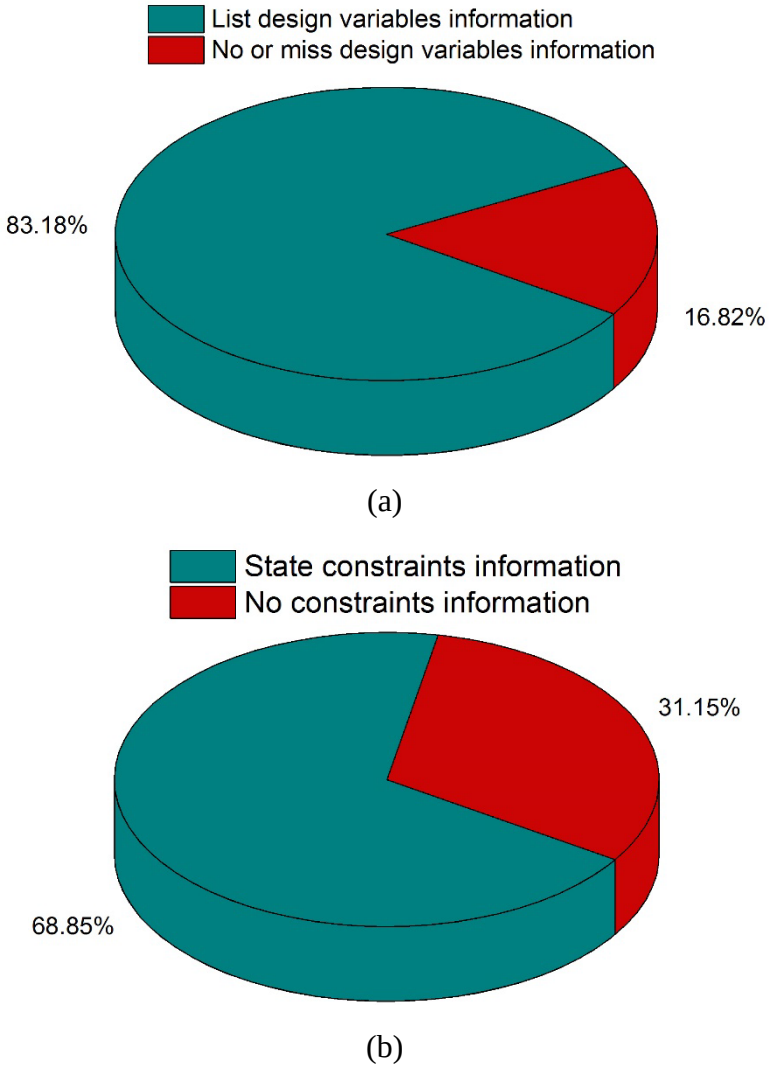

Figure 2- 19. Proportion of papers stating (a) design variables information (b) constraints information

2.2.4.4 Multi-objective optimisation in composites structures

Pareto fronts provide the set of non-dominated solutions for a multi-objective problem, with an example illustrated in Figure 2-20. This is based on Pareto optimality first proposed by Pareto [181] in 1906 which is the set of optimal results for a given problem. Each point represents an optimal design point, each with a different weighting for the objectives. This allows the objective space to be visualised and for users to quickly determine how changes to a composite design are reflected in performance. They can also provide a clear link between how the objective space relates to the variable space, for instance are points next to each other in objective space next to each other in variable space? If they are then small changes to the variables relate to small changes in the objectives and the space is easy to interpret for an engineer.

Finding the Pareto front reflects best practice in multi-objective optimisation with 61 papers illustrating the final Pareto fronts [130,133,187–196,140,197–206,145,207–216,155,217–226,182,227–236,183,237,184–186]. Of these 55 papers perform multi-objective optimisation and 8 papers utilise a weighted average approach to generate Pareto fronts, including two papers which present both methods across different problems, preferring the weighted sum approach for the 3 objective problem. The proportion of papers finding the Pareto front in solving multi-objective optimisation and weighted multi-objective optimisation problems are summarised in Figure 2-21. Weighted multi-objective optimisation generate Pareto fronts by repeatedly changing weights in repeated runs, for example the weights 1 and 0 are run followed by 0.99 and 0.01 through to 0 and 1, and all of these points are plotted as the Pareto front. Although the weighted sum approach is a straightforward implementation since single objective Genetic Algorithm can be utilised through minor modifications and weighted multi-objective Genetic Algorithms are efficient, they are not recommended as all of the Pareto-optimal solutions cannot be achieved through this method especially when the real Pareto front is non-convex and the process is slow to achieve a good density of points. For example a typical Pareto front would contain 400-1000 points from one simulation which would require the same number of repetitions from a weighted sum approach. The reason why multi-objective optimisation papers are performed that don't provide Pareto front is unknown. However, these Pareto Fronts are complex to find and require advanced Genetic Algorithms to produce good results on modern problems, for example NSGA-II or more recent but most modern Genetic Algorithms are developed to find these Pareto Fronts. These modern algorithms will not work properly with single-objective or weighted multi-objective

approaches, so it is important that more optimisation is performed using multi-objective problems so that more modern algorithms can be used in addition to the beneficial information these Pareto Fronts provide.

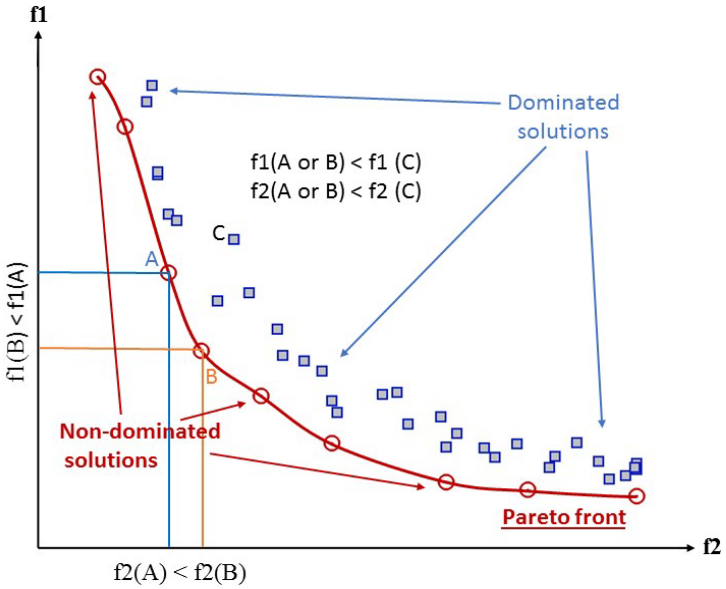

Figure 2- 20. Illustration of a Pareto front, including non-dominated and dominated solutions, on a bi-objective minimisation example

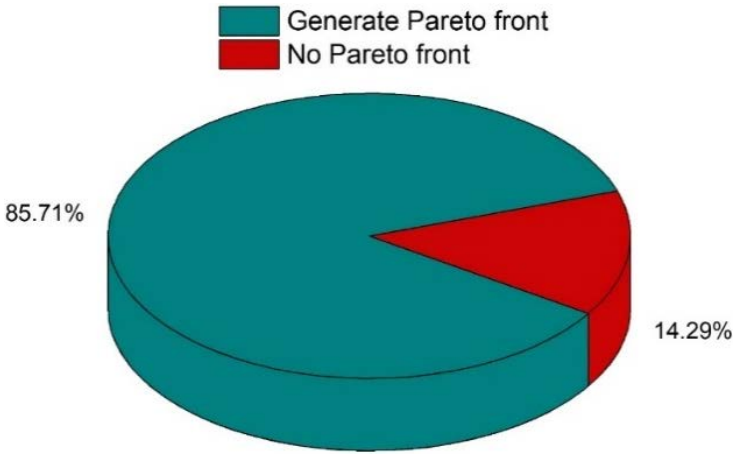

(a)

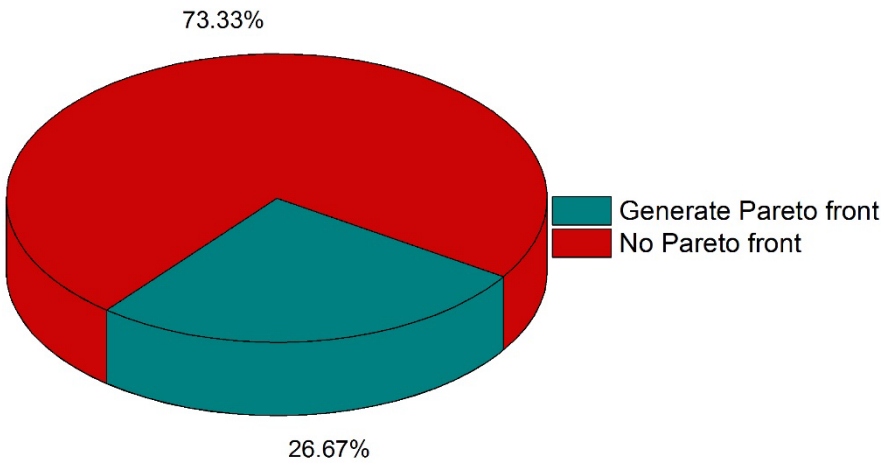

(b)

Figure 2- 21. Proportion of papers generating Pareto fronts when solving (a) multi-objective problems (b) weighted multi-objective problems

The final Pareto fronts should have three basic elements [238]: (1) the best achieved Pareto front should be as close as possible to the true Pareto front; (2) the best achieved Pareto front should be uniformly distributed and as diverse as possible in order to provide the decision-maker a true picture of trade-offs; (3) the best achieved Pareto front should capture the entire spectrum of the Pareto front. However, for engineering optimisation, as for most real world optimisation, the true Pareto front is not known. Wang et al. [30,239] propose a mimicked inverted generational distance (mIGD) approach inspired by the IGD value calculated in the evolutionary computation literature to evaluate the accuracy and diversity of Pareto fronts. They combine all of the Pareto front solutions from all of the independent run cycles, from each of the algorithms that are benchmarked. Non-domination and duplication checks are implemented on this combined Pareto front set to filter it and create a 'true Pareto front'. They then calculate the mIGD values of the obtained Pareto fronts from each algorithm to this mimicked 'true' Pareto front to assess the performance of each benchmarking algorithm and whether the obtained Pareto front has been resolved, mIGD is defined in eq. (2.1),

$$mIGD(O, M^*) = \frac{\sum_{v \in M} d(v,O)}{|M^*|}, \tag{2.1}$$

where M^* is a set of points along the mimicked Pareto front, O is a set of points on the currently obtained Pareto front, v represents each point in the set M^* and $d(v, O)$ is the minimum Euclidean distance between v and the points in O; lower mIGD values reflect a better quality and diversity of the obtained Pareto front.

Another indicator which can be utilised to evaluate the performance of the obtained Pareto fronts is Hyper Volume (HV). This metric is more representative in determining the diversity of the population that has been found and using the IGD and HV together give a strong indication of how an algorithm has performed on a problem both in terms of convergence and diversity. The Hyper Volume demonstrates the volume of the objective space between the obtained Pareto front points and a predefined reference point [240]. A fast way of calculating the HV is demonstrated in [241]. Both the HV and IGD are sensitive to the selection of reference points. This is especially the case for the IGD indicator as it requires a large number of uniformly distributed reference points to guarantee the accuracy. However, HV has problems when sorting objectives with different ranges [241]. In the benchmarking of Genetic Algorithms it is best practice to use both indicators to evaluate the solvers with IGD indicating the accuracy of the obtained Pareto fronts and HV the diversity.

2.2.4.5 Review of available Genetic Algorithm benchmarks on composite structures

The proportion of papers performing benchmarking is shown in Figure 2-22. Of these papers only ~13% of papers compare different methods, or 43 papers [134,136,160,163,165,166,168,169,171–174,137,175,187,233,242–248,143,249–258,145,259–261,146,150,154,155,157], which means that the characteristics of most problems are difficult to determine and the selection of future algorithms on similar problems is not possible. This lack of documentation makes algorithm selection and development difficult, moving the literature towards general solvers.

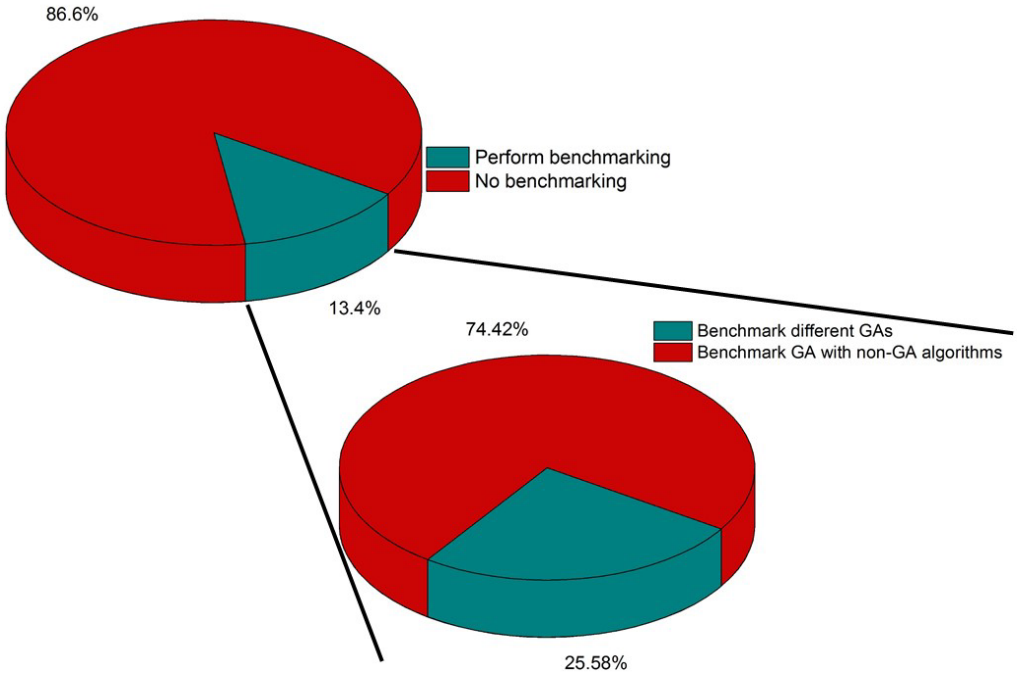

Figure 2- 22. Proportion of papers performing benchmarks

The evolutionary computation literature benchmarks algorithms across a range of problems, for static optimisation this is normally dominated by whether problems are constrained or unconstrained. Wang et al [30] demonstrates that the triaxial weave fabric problem is not dominated by these characteristics and that algorithms performing well on these problems perform extremely poorly. The highest performing solvers are general solvers with good diversity of searches, indicating that a number of characteristics are important to these problems and/or that diversity of search is important. This indicates that the benchmarking in the evolutionary computation literature cannot be used for selecting the correct algorithms in the composite optimisation problems until these problems are better understood. Therefore, it is necessary to perform benchmarking on composite problems to allow the selection of the correct Genetic Algorithms and increase their use. Of those that perform benchmarking 26% of them compare different Genetic Algorithms and 74% compare Genetic Algorithms with other non-GA solvers, such as Particle Swarm Optimisation (PSO) and Simulated Annealing (SA), shown in Figure 2-22. Of the 12 papers that benchmark different Genetic Algorithms, micro-GA is presented as the best algorithm three times but all of these benchmark the micro-GA against only the standard Genetic Algorithm. NSGA-II and hybrid NSGA-II are stated as the best algorithms in two papers respectively. Montemurro et al. [247] benchmarked GA BIANCA with the MATLAB GA and found that the GA BIANCA achieved better optimisation results but that the MATLAB GA is more efficient. It is difficult to determine best practices through these benchmarking results.

The rest of the 31 papers benchmark Genetic Algorithms with non-Genetic Algorithms. Four papers state that hybrid Genetic Algorithms outperform the Genetic Algorithms and the non-GA algorithms that the hybrid algorithms are made from [146,244,255,257]. There are five papers benchmarking non-Genetic algorithms with the standard Genetic Algorithm [143,154,165,168,250] and 10 papers benchmarking against unspecified Genetic Algorithms [169,171,172,245,251,254,258–261]. Of these papers 14 [134,136,253,259–261,154,168,171,175,233,248–250] state that the non-Genetic algorithms perform better. Eight papers [137,143,150,165,166,187,252,258] result in a draw between the Genetic Algorithms and the non-GA optimisation approaches according to the outcomes from the benchmarking metrics in each paper. Two of the Genetic Algorithms win the benchmarking among these papers [157,172]. However, 11 of the 24 papers are missing the GA hyperparameters and only four papers include a modern Genetic Algorithm, NSGA-II, making it hard to assess whether these benchmarks are fair tests. It is therefore necessary to extend these benchmarking exercises to composite optimisation problems utilising a more modern selection of Genetic Algorithms and a full documentation of the hyperparameters.

2.2.5 Application of Genetic Algorithms to composites

A range of Genetic Algorithms are used from the most basic versions, which are similar to those developed in the 1970's, to BIANCA which is developed in 2010 and utilised by the same authors [262] in the composite optimisation literature. The proportion of the literature using each algorithm is illustrated in Figure 2-23. Of those papers that document the name of the Genetic Algorithm 75% of the papers use: standard GA, MATLAB GA, NSGA-II, Micro-GA, Multi-island GA, BIANCA and hybrid GAs, where more than one mechanism works on the same population. It is shown that the NSGA-II and MATLAB GA toolbox have the highest proportion making up 48% of all the frequently used Genetic Algorithms. This means that most of the literature uses older GAs or those that are less popular in the computer science literature. NSGA-II shows the top performance on a range of practical problems, making it an excellent selection especially where the optimisation problem has not been categorised or where there is more than one dominant characteristic to the optimisation problem, though there are now more recent algorithms showing both high diversity and convergence of search leading to better performance as general solvers.

Genetic Algorithms are good at solving problems with large search spaces but traditionally require substantial computational effort to find the true Pareto front. Therefore,

other search methods are combined with Genetic Algorithms to push the solutions to the real optimal solutions with an acceptable computational cost, such as particle swarm optimisers (PSOs) and local search methods. NSGAIILS [95], BCE [78] and MTS [263] are good examples for hybridisation with local search methods. In the composite literature PSOs are the most frequently used algorithm in the hybridization with Genetic Algorithms, used in six papers of the total 29 papers, followed by a local search method, such as the Levenberg-Marquardt method that is used in three papers. However, of the hybrid algorithms ~59% use unknown Genetic Algorithms. Furthermore, only three papers perform benchmarking of hybrid Genetic Algorithms and therefore to assess the capability of these hybrid Genetic Algorithms for solving composite optimisation problems becomes difficult.

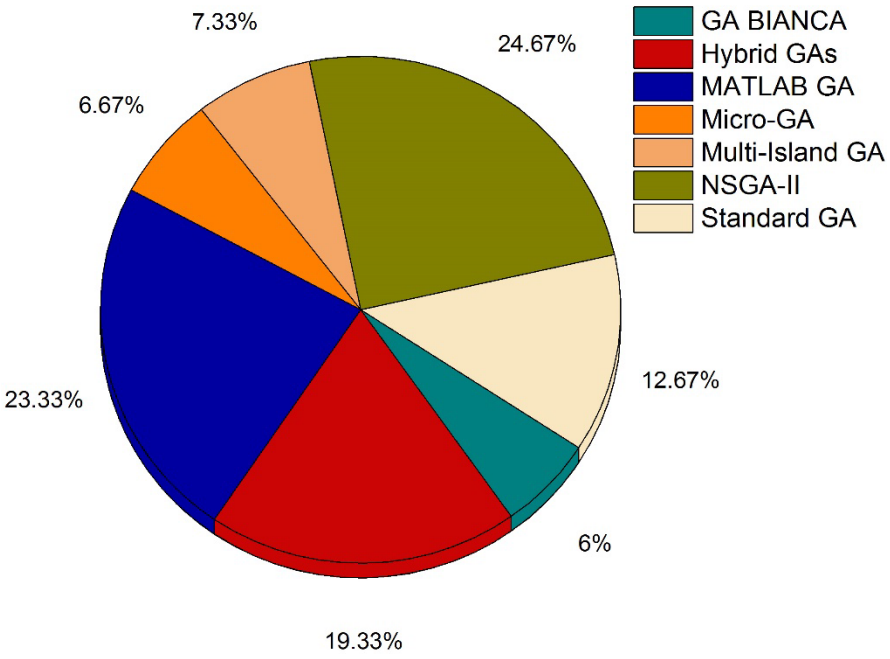

Figure 2- 23. Frequently utilised Genetic Algorithms in the composite optimisation literature

2.2.6 Comparison between composite and computational science literature

The state-of-the-art Genetic Algorithms are frequently benchmarked using mathematical optimisation problems to evaluate the performance of the new solvers in the computational science literature. Understanding these problems is a key aspect in selecting the correct algorithm for a composite problem. A variety of these test functions have been reviewed by Grudniewski and Sobey [88,117]. These problems are increasingly close to the level of complexity in engineering optimisation problems but often focus on one dominant characteristic. The problems in both literatures have similar features including:

- nonlinear,

- multi-modal,
- imbalanced, where the number of solutions on each Pareto front are different,
- discontinuous objective spaces,
- non-uniform real Pareto fronts where the density of the Pareto front points are different at different parts of the Pareto front and where the lower density part has a significantly lower possibility of being found,
- multiple constraints or complicated constraints which increase the complexity of the fitness function,
- large boundaries for the variable space
- variable linkages where the objectives are determined by a set of variables and the variables for different objectives overlap [264,265].

The test functions are categoried into four types according to the type of dynamics. In the static problems, where the objective functions are not changing with time, Grudniewski and Sobey [88] classify 42 bi-objective test functions and 31 three-objective problems into nine categories. Additionally, most test functions have secondary properties, such as multi-modal search spaces, where there are many local optima in the objective space and some local optima are close to the global optimum. Wider benchmarking exercises are performed each year on dynamic and static problems and best practice is frequently found in the *IEEE CEC* competitions, for instance CEC09 for constrained and unconstrained optimisation problems [82], CEC11 for real-world numerical optimisation problems [131], CEC13 and CEC15 for multimodal optimisation problems [266,267] and CEC17 for many-objective optimisation problems [268].

The test problems generated in the computational science literature have a bias towards problems with a single dominating characteristic, meaning that the drive in this literature is towards specialist solvers, which are less likely to be the case in composites optimisation applications. In addition the benchmarking problems in the computational science literature have the Pareto fronts provided meaning that researchers can select or produce suitable state-of-the-art Genetic Algorithms for solving the problems according to the type of the real Pareto front. However, for real-world optimisation problems the characteristics of the problem are likely to be unknown, making engineering optimisation problems even harder to be solved than the mathematical optimisation problems in computational science literature. These two factors

drive practical optimisation towards general solvers, which have a reduced performance on specific problems but are likely to give a reasonable result.

A variety of Genetic Algorithms are developed with new algorithms developed each year in the computational science literature. The Genetic Algorithm community stated that problem-specific Genetic Algorithms frequently achieve improved performance in solving specific optimisation problems [269]. However, as illustrated in Figure 2-1, the Genetic Algorithms utilised in the composite optimisation literature are taken from those developed between 1989 and 2010. Only eight of the 321 papers developed specialist Genetic Algorithms for composite optimisation problems and only three specialist solvers are benchmarked with other solvers, with two papers comparing against two algorithms and the other paper showing that the specialist algorithm didn't achieve the best performance in the benchmarking. The new or improved Genetic Algorithms should be benchmarked with existing algorithms [270]. Furthermore, a variety of algorithms are benchmarked in the competition on evolutionary computation to find the best practice of algorithms. The competition demonstrates the best practice on each type of optimisation problem and helps researchers to develop better algorithms based on these best performing algorithms. However, there is no competition or documentation of optimisation algorithms for solving specific problems in the composite optimisation literature and few papers performed benchmarking, meaning that best practice and the dominant characteristics of the problems that influence the performance of Genetic Algorithms remain unknown.

2.2.7 Summary of Genetic Algorithms in composite materials and structural optimisation

2.2.7.1 Conclusions

The application of Genetic Algorithms to solving composite optimisation problems is increasing, especially over the last five years. In this Chapter, 321 papers published between 2008 and 2017 from 17 journals which cover composite structures and materials are reviewed to understand the technical challenges related to Genetic Algorithm use and to determine the implications for the future. Also included is a detailed review of the Genetic Algorithms from the evolutionary computation literature, with a description of their mechanisms and a prediction for their suitability to different composite optimisation problems. The review shows that in general old algorithms are used and that the hyperparameters are poorly selected, necessitating the need for simple optimisation problems. The database of the papers collected for this

analysis is made available in an attached datasheet where the link is shown in Section 2.2.3. A number of problems are presented in the literature and can be summarised as follows:

1) Poor documentation: ~38% of the 321 papers reviewed don't state the name of the Genetic Algorithm used, ~71% have incomplete information about the genetic operators. Among the rest ~29% papers ~41% of them miss the genetic operator rates. Around ~52% of the 321 papers do not list the hyperparameters, including population size and generation number or total function evaluations. Only ~14% of papers document the use of several independent cycles of Genetic Algorithms, which have been shown to be dependent on the initial population. It is therefore difficult to assess the validity of the optimisation results and to be confident that the optimal solution is found. This makes benchmarking performance of different methodologies on these problems impossible and there is no consensus on which Genetic Algorithms are best aligned to different problems or what type of mechanisms should be developed; for example is convergence or diversity most important in these problems? Categorising the success, or indeed failure, of a given methodology in the optimisation leads to insight about the characteristics of the problem, for example determining whether it is discontinuous or concave, but also the type of mechanisms most suited to solving it. Defining the necessary documentation to understand the performance of an algorithm will allow the determination of which Genetic Algorithms are best suited to different types of problems, allowing more rapid progress. Since many algorithms converge on a solution early in the generation cycle, using the computational time for a higher numbers of simulations, rather than fewer, longer runs, is likely to result in better solutions and resolved Pareto fronts. A similar argument can be made about how best to use the function calls, whether for population or generations. In composite structures the tendency is towards generations but this will reduce the diversity of search. The field cannot develop its own best practice without the ability to learn from past examples.

2) Little focus on categorising the optimisation problems: related to the previous issues of documentation ~80% of authors only published one paper on optimisation of composites through Genetic Algorithms indicating that there is often a lack of experience on using Genetic Algorithms. A number of outdated Genetic Algorithms are still prevalent in the composite optimisation literature with ~56% of single objective

optimisation papers and ~58% of weighted multi-objective optimisation papers missing information about convergence. When multi-objective optimisation is performed ~14% of multi-objective optimisation papers and ~73% of weighted multi-objective optimisation papers don't generate Pareto fronts, which is the standard approach in most fields to make the most use of multi-objective optimisation techniques. Only ~13% of the papers perform benchmarking and normally compare just two or three different algorithms, without justifying the selection for why these are the state-of-the-art for this problem type and stating what measures are used to guarantee fair tests are performed. Only eight of the 321 papers develop specialist Genetic Algorithms for specific composite optimisation problems; however, only three of these eight papers performed benchmarking, with two papers comparing against two algorithms and the other paper showing that the specialist algorithm didn't achieve the best performance in the benchmarking. The lack of categorisation of the problems makes tackling the problems that have already been solved more efficiently a difficult task, helping new authors understand the current state-of-the-art in composite optimisation must be a key feature in an area where so many authors are using these tools for the first time.

3) A small range of Genetic Algorithms from the computational science literature are used: A range of Genetic Algorithms are used from the most basic versions similar to those developed in the 1970's and the latest frequently used version is GA BIANCA. However, the state-of-the-art Genetic Algorithms, such as MOEA/D for unconstrained problems, cMLSGA, BCE, HEIA as general solvers, cMLSGA for constrained and discontinuous problems and cMLSGA, U-NSGA-III, HEIA and BCE for many-objective problems are not documented in the composite optimisation literature in the past 10 years. The most frequently used Genetic Algorithm is NSGA-II, which performs well on a wide range of problems as a general solver where it is likely that there are multiple dominant characteristics for the optimisation problem. However, its performance will be compromised on specialist problems and its performance is now below a number of different algorithms in the computational evolution literature, meaning it would be ideal to test some of these algorithms on real problems. The small range of Genetic Algorithms used in composite optimisation literature restricts the probability of achieving optimal designs and stops progress in this field. But the poor documentation of the problem types means that specialist solvers for these problems can't be developed.

4) A focus on simplifying the problems: ~71% of papers solve single objective optimisation problems. In addition ~9% of papers reduce the multi-objective optimisation problems down to single objective problems by using the weighted sum approach. ~17% of papers don't provide information of design variables and ~31% don't document the constraints, indicating that they solve simple optimisation problems with limited numbers of variables and constraints. The optimisation results of these may have limited use in real-world applications and these problems are all within the bounds of complexity that Genetic Algorithms are capable of solving. Much of the literature focuses on solving problems which have previously been tackled, such as layup optimisation, with incremental steps. While exciting and complex problems such as bi-level optimisation of the structure and material together, multi-disciplinary optimisation and fibre weave optimisation are less well explored. Moving the boundaries of what is possible in optimisation will result in more useful results and make it easier to define what is not possible.

This has made determining which methods are most appropriate and effective difficult. In addition the results are impossible to replicate and best practice has not been collated over this period, meaning that the field has not evolved. Many of the best Genetic Algorithms in the computational science literature are not utilised, such as MOEA/D for unconstrained problems, cMLSGA, BCE, HEIA, MTS as general solvers, cMLSGA and MLSGA-NSGAII for constrained and discontinuous problems and cMLSGA, U-NSGA-III, HEIA and BCE for many-objective problems, meaning there is the potential for more complex problems to be solved, and the focus on simple problems means that the real benefits of Genetic Algorithms are not seen. Importantly there is no documentation linking the mechanisms of the Genetic Algorithm to the problem type, making it impossible to solve difficult and exciting problems of interest to industry. Therefore, a series of recommendations are listed in this review, categorised corresponding to the problems found in literature, to help improve composite optimisation.

2.2.7.2 Recommendations

Based on these findings a series of recommendations are made in the hope of improving research into optimisation of composite structures.

1. **Accurate documentation:** better documentation, standardisation, of the information of the Genetic Algorithm and the methods utilised in the optimisation are required to allow readers to evaluate the results, repeat their research and make improvements.

2. **Treat Genetic Algorithms as a specialisation:** understanding the features and mechanisms of the state-of-the-art Genetic Algorithms and select the most suitable solvers for the specific composite optimisation problems. There is limited technical understanding of evolutionary computation demonstrated in the literature. Understanding the search space and dominant characteristics through benchmarking of state-of-the-art Genetic Algorithms. Adequate benchmarking processes will help to select the correct Genetic Algorithms and increase their use.

3. **Perform rigorous benchmarking**: it is necessary to benchmark state-of-the-art Genetic Algorithms on composite optimisation problems as these engineering problems are dominated by different characteristics. The current computational benchmarking is simple, making it difficult to select the correct algorithm in these cases. Benchmarking helps to determine the dominant characteristics of the problem and investigate the best practices of Genetic Algorithms for the specific problem rather than using them as optimisation tools. The problem type (e.g constrained or unconstrained, single, multi-objective or many objectives and continuous or discontinuous variable or objective space) should be considered when selecting a Genetic Algorithm. Though it is possible to utilise general solvers such as NSGA-II, HEIA and cMLSGA to ensure a reasonable result and these often perform well on problems with more than one characteristic. Additionally, due to the stochastic nature of Genetic Algorithms, it is necessary to run several cycles to ensure the final solutions have been found depending on the nature of the objective space. Using metrics to determine the quality of the solution, such as HV and IGD, will improve the performance. These should be used along with the robustness of solutions and number of generations to convergence to improve the understanding generated from the literature being tackled.

4. **Solve problems with multiple (many) objectives:** Adding more objectives will make the optimisation more complicated and more realistic for use in industrial applications. Multi-objective or many-objective problems, those with 4+ objectives, Genetic Algorithms are recommended over weighted multi-objective Genetic Algorithms when

solving these problems. Better documentation and using state-of-the-art algorithms will allow these problems to be tackled, with a subsequent evolution in the composite optimisation literature.

2.3 Chapter Summary

This chapter comparatively reviews both the state-of-the-art woven fabric composite modelling methods and the Genetic Algorithms used in composite materials and structural optimisation and compared with evolutionary computation.

The task of providing optimal composite structures is increasingly difficult. New analysis approaches seek to model the material at the fibre/matrix scale and increasingly more control is sought over the material, for example optimising individual tows, and the structure, where new manufacturing techniques are proposed that will allow revolutionary new topologies. This additional complexity will stretch design engineers and as such it is important that state-of-that-art design methods are implemented to help take advantage of these exciting new opportunities, including optimisation methods. To determine best practice and the limitations on using the techniques in practice a review of Genetic Algorithms in optimisation of composite materials and structures is performed over the last 10 years. This is compared to the development of Genetic Algorithms in the evolutionary computation literature. It is found that a range of old Genetic Algorithms that developed before 2002 are still retained in the current composite optimisation literature, which are similar to those developed in the 1970's. NSGA-II is the only widely acknowledged state-of-the-art solver that frequently used in the composite optimisation literature but it has already shown insufficient power on solving a range of complex optimisation problems since these complicated problems require both high diversity and convergence of search. On the contrast, the evolutionary computational literature continues to propose novel high performance Genetic Algorithms each year for solving problems with different dominant characteristics. However, these novel solvers are not investigated and utilised in the composite optimisation literature. This information asymmetry drags the development of composite optimisation. Furthermore, the composite optimisation problems may not be fully solved even using state-of-the-art Genetic Algorithms from evolutionary computational literature since the problems in the composite optimisation literature tend to be more complicated with several dominant characteristics. However, the proposed Genetic Algorithms in evolutionary computational literature commonly solve problems with one dominant characteristic. Therefore, it is considered that the current composite optimisation problems become difficult to be fully solved without a better understanding of the Genetic

Algorithms and the dominant characteristics of the optimisation problems. By better understanding how Genetic Algorithms are used in composite structures and comparing to evolutionary computational literature, recommendations are provided for better utilising of Genetic Algorithms for solving composite optimisation problems in the future.

The comparative review of Genetic Algorithms use in composite materials/structures optimisation has provided the methodology of selecting the best practice of Genetic Algorithms. A comparative review of 2D woven fabric composite modelling methods is implemented to find the most appropriate fitness evaluation method for realizing the optimisation of 2D woven fabric composites. It has shown that several finite element method models have been developed to analyse the mechanical properties of 2D woven fabric composites. Most of them have shown high precision on predicting the mechanical properties but all of them are computationally expensive to be used in the optimisation. Even the most efficient 'binary model' requires thousands of times the computational cost of using analytical methods when having hundreds of thousands of fitness evaluations in the optimisation. In order to avoid degrading the performance of Genetic Algorithms by the limitation of increased population size and generation number due to the use of computationally expensive fitness evaluation methods, this research considers to use analytical methods. The review shows that the current literature has a lack of analytical methods on predicting the tensile strength of 2D woven fabric composites. The available uniaxial tensile strength prediction models show relatively low prediction accuracy, nearly 20%. The available biaxial tensile strength prediction models require a given uniaxial tensile strength and it can only predict the equal biaxial tensile strength. Therefore, this research has developed a novel analytical method to accurately and robustly predict the biaxial tensile strength of 2D woven fabric composites under different biaxial tensile loading ratios. In addition, there is a limited number of analytical methods predicting the shear properties. However, it is found that these methods are either not accurate on predicting the shear strength, which have a mean error of 22%, or not robust on predicting shear modulus for different material types. Therefore, this research has developed a new analytical method to accurately and robustly predict both the shear modulus and strength. According to the results of the comparative review and the balance between computational efficiency and prediction accuracy, the analytical models with the best prediction accuracy are chosen as the composite structure modelling methods for different types of 2D woven fabric composites in the optimisation studies in this work.

Chapter 3. Methodology

This research aims to develop a methodology to better design woven fabric composite materials with the aid of computationally efficient micromechanics-based analytical model. A series of research works have been done to achieve the aim. To perform optimisation of woven fabric composites, analytical models with accurate, robust and computationally efficient features are required as the fitness evaluation methods. Since two required analytical method models are unavailable from the current literature, the current research has developed them. To achieve many-objective optimisation, an initial attempt on solving bi-objective optimisation problems is necessary. All of these works are summarised and discussed. The result of the discussion develops a methodology to determine the dominant characteristics of woven fabric composite optimisation problems. This helps to select the best practices of Genetic Algorithms for solving woven fabric composite optimisation problems. The relationships between these Chapters are shown in Figure 3-1.

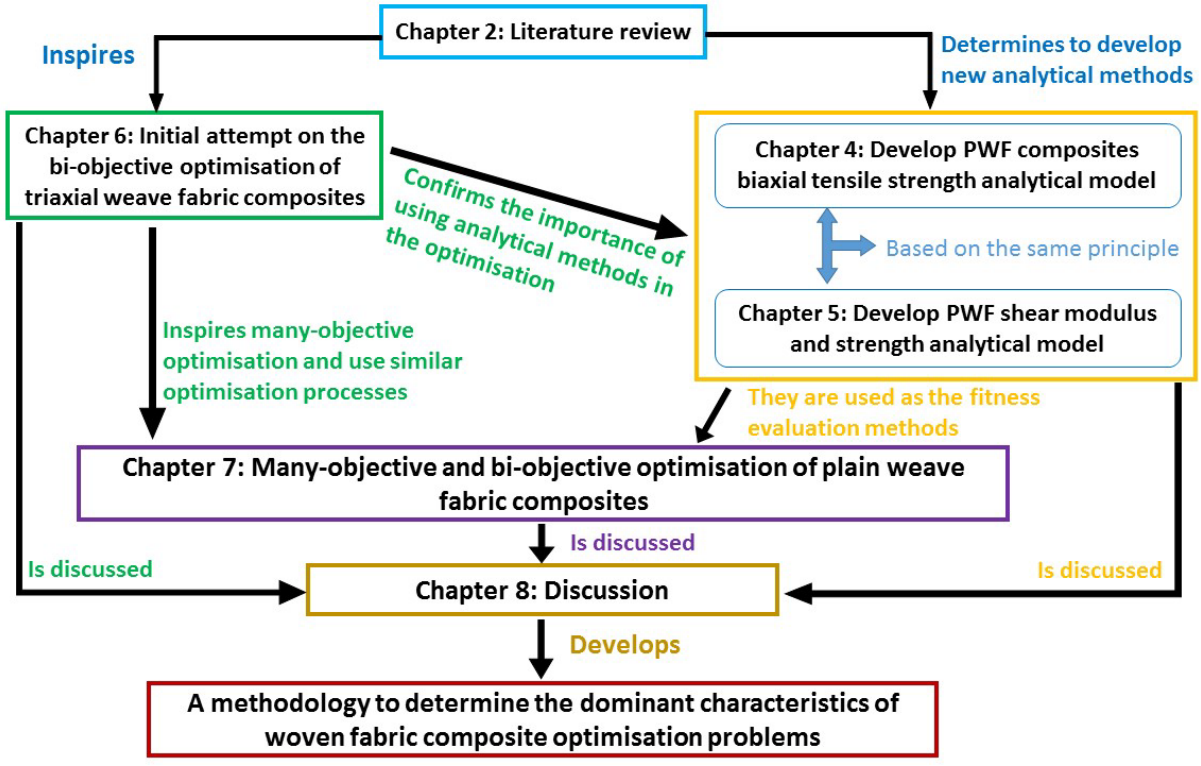

Figure 3- 1. The structure of the thesis and the relationship between the Chapters

3.1 Initial attempt on the bi-objective optimisation

The first trial of optimisation is performed on the triaxial weave fabric composites with two objectives and two cases. The details of the optimisation study are documented in the Chapter 6. The reasons of selecting triaxial weave fabric (TWF) composites are: (1) triaxial

weave fabric composites are one of new materials that utilised on novel ultralight applications; (2) the triaxial weave fabric composites provide mechanically quasi-isotropic properties, thus the initial study is able to obtain improved material performance by improving one-direction mechanical properties; (3) an available robust, accurate and computationally efficient analytical method for predicting both tensile modulus and strength of the triaxial weave fabric composites provides the indispensable condition to implement the optimisation study since it is capable to be used as the fitness evaluation method in the Genetic Algorithms; (4) there are only three geometry parameters that mainly influence the mechanical properties and areal density of the material and the limited number of variables makes the initial trial implementable; (5) investigating the optimisation of triaxial weave fabric composites inspires to propose a methodology which helps to solve the optimisation problems of plain weave fabric composites that having more variables and are more complicated.

The shape of the objective space and its relationship with the variable space is unknown for triaxial weave fabric composites under tensile loadings before the study. This means that the problem type is not defined and that the corresponding algorithms suitable to that problem type cannot be selected. In this case the CEC'09 benchmarking [82] is used to select the algorithms for comparison: NSGA-II which has generally good performance across all problem sets, MOEA/D for unconstrained problems and MTS which came second and third on unconstrained and constrained problems; in addition a more recently developed Genetic Algorithm, MLSGA-NSGAII, is also included which performs well on constrained problems. Better constrained performance is shown by DMOEA-DD and LiuLi algorithms but the available versions of the code cannot be converted to solve new problems and the documentation of the original algorithms is not enough to reproduce them.

Performing a fair benchmarking is important since the dominant characteristics of the optimisation problem and the best practices of Genetic Algorithms can be determined by analysing the benchmarking results and the Pareto fronts generated by each solver. Since the selected state-of-the-art Genetic Algorithms for the benchmarking are either general solver or solvers specialist for constrained or unconstrained problems, the bi-objective optimisation problem studied in the first case, maximising tensile strength and modulus, is formulated in both a constrained and unconstrained format for the TWF composite material in order to perform a fair test. Furthermore, in order to perform a fair test across the different Genetic Algorithms the same genetic operator types: selection, crossover and mutation, use the same operator rate, which is the same as those selected for the CEC'09 benchmarking [271]. MTS is

a population based optimisation algorithm with a different set of hyper-parameters; these are kept the same as in the CEC'09 competition, except the population size and total number of function calls which are kept the same as the other three algorithms.

T300/Hexel8552 is selected as the combination to be optimised as the most mature Triaxial Weave Fabric composite. The variables yarn undulation length, *L*, yarn width, *w*, and height, *h*, are the parameters influencing the strength and modulus in the analytical model. The ranges of these variables are selected to ensure suitability for a range of existing applications for the triaxial weave fabric composites. A constraint is in place to ensure the weave patterns can be manufactured.

In order to quantitatively evaluate the performance of the state-of-the-art Genetic Algorithms, an indicator is proposed in the current study which is the mimicked inverted generational distance (mIGD). The mimicked IGD value is based on IGD [82], which quantifies the quality and diversity of a Pareto front by representing the average value of distances from each point on the real Pareto front to its closest point on the obtained Pareto front; lower mIGD values reflect a better quality and diversity of the obtained Pareto front.

The bi-objective optimisation problem studied in the second case, maximising tensile strength while minimising the areal density and maximising the tensile modulus while minimising the areal density, are investigated by the same methodology. However, the problems are only formulated in unconstrained format since all the four solvers benchmarked in the first case show better performance on solving the problem in unconstrained format.

3.2 Analytical models developed for the many-objective optimisation

The review in Chapter 2 and the initial attempt of optimisation studied in the Chapter 6 have concluded that using analytical methods as the fitness evaluation method in the optimisation is important. In order to find out the most appropriate analytical methods to be used as the fitness evaluation methods in the woven fabric composite optimisation, the reviewed analytical methods in the Chapter 2 are compared in Table 3-1.

Table 3- 1. Comparison of the reviewed analytical methods

Precision, Robust and Efficient analytical methods	Plain weave fabric composites	Tensile properties	[39] [40]
		Shear properties	[47]
		Compressive properties	
	Triaxial weave fabric composites	Tensile properties	[51] [52]
		Shear properties	[51] [52]
		Compressive properties	
Precision and Efficient but **Not Robust** analytical methods	Plain weave fabric composites	Tensile properties	[37] [38] [33]
		Shear properties	[44] [45]
		Compressive properties	[32] [33]
	Triaxial weave fabric composites	Tensile properties	
		Shear properties	
		Compressive properties	
Efficient but **Not Robust** and **Imprecision** analytical methods	Plain weave fabric composites	Tensile properties	[34] [35]
		Shear properties	[42] [43] [46]
		Compressive properties	
	Triaxial weave fabric composites	Tensile properties	
		Shear properties	
		Compressive properties	
Precision and Robust but **inefficient** analytical methods	Plain weave fabric composites	Tensile properties	[272]
		Shear properties	
		Compressive properties	
	Triaxial weave fabric composites	Tensile properties	[48] [49]
		Shear properties	[49] [50]
		Compressive properties	[48] [49] [50]

The ‘blue’ highlights shown in the Table 3-1 are the analytical models available from current literature which are suitable to be used as the fitness evaluation methods in the current research. It is shown that the precise, robust and computationally efficient analytical methods for the predictions of tensile strength and shear properties of plain weave fabric composites are not available in the current literature. Therefore, the current research develops the two required analytical models which are highlighted in ‘green’ in Table 3-1. The details of the two analytical methods are demonstrated in Chapters 4 and 5.

The two analytical methods are both based on the minimum total complementary potential energy principle since there are several undetermined internal forces and moments after micromechanical analysis and the principle states that the solution of the unknown variables is the one that minimises the total complementary potential energy in all possible statically admissible stress fields [53]. Therefore, all the undetermined internal forces and moments can be derived using the Cramer’s rule after minimising the total complementary potential energy.

Both analytical models use the same geometrical assumptions and the same equations to build up the yarn and lamina geometries. Both analytical models assume the shape of the tow path is fixed as smooth and continuous sinusoidal curve under external loadings in order to avoid dynamic analysis getting involved which increases the complexity of the model. Both analytical models consider the fibre tows as the curved beam elements and both models use the same equations to calculate the moment of inertia along the transverse and through-thickness directions and polar inertia moment of warp and weft tows. Therefore, both analytical models use the same control parameters, which are the undulation length, width and thickness of the warp and weft tows and the fibre and resin material properties. This helps to build up the optimisation of 2D woven fabric composites since the fitness evaluation methods are based on the same control parameters.

The biaxial loadings ratio from the biaxial tensile strength prediction model, which is in the Chapter 4, is also introduced to the shear prediction model, which is in the Chapter 5, but it is changed to actual and virtual loadings ratio. The verification of the biaxial tensile strength prediction model is based on both experimental measurements and finite element method model but the verification of the shear prediction model is purely based on the experimental measurements. One of the experimental results used in the Chapter 4 is obtained by the co-author of the submitted journal paper but the rest experimental results are obtained from the literature. All the experimental measurements used for the verification of the proposed model in the Chapter 5 are obtained from the literature. In addition, it is difficult to extract the two directional tensile strengths while simultaneously applying biaxial tensile loadings due to the stress concentration at the boundary of the specimens between the loading arm and central area. This is a common problem with no available biaxial data for plain weave fabric composites despite some attempts such as Cai et al. [273] where the biaxial tensile strengths measured were inaccurate due to stress concentrations. Therefore, the finite element method model is used to verify the model proposed in Chapter 4. It is common to use experimentally measured mechanical properties of the plain weave fabric composite lamina in a composite laminate Finite Element Method model for accurately predicting the biaxial tensile strengths. Since the finite element method is a widely accepted numerical method as well as it is established by the actual specimen and experimentally measured properties, it is used as the benchmark in the verification.

The accuracy and robustness of both proposed models are determined by the mean prediction errors and standard deviations of all the verifications for different material types.

The models are chosen as the fitness evaluation methods since they achieve outperformance on both the accuracy and robustness when compare with other available analytical methods.

3.3 Perform many-objective and bi-objective optimisation

Since the first attempt of bi-objective optimisation in the Chapter 6 states the importance of studying the optimisation problems with more objectives, a many-objective optimisation is performed on the plain weave fabric (PWF) composites in the Chapter 7. The reasons of selecting plain weave fabric composites are: (1) plain weave fabric composites are typical 2D weave fabric composites; (2) plain weave fabric composites are increasingly utilised in aerospace structures in recent years, thus improved tensile and shear properties and reduced density are important for plain weave fabric composites; (3) robust, accurate and computationally efficient analytical methods have been developed in the Chapter 4 and 5 and they are capable to be used as the fitness evaluation method in the Genetic Algorithms; (4) although it is more complicated than the optimisation of triaxial weave fabric composites, the limited number of variables, six geometry parameters, make the many-objective optimisation of plain weave fabric composites still achievable; (5) investigating the many-objective optimisation of plain weave fabric composites inspires a methodology which can solve the many-objective optimisation of other types of woven fabric composites.

Similar as the optimisation problem of triaxial weave fabric composites, it is unknown about the shape of the objective space and the relationship between variable space and objective space for the optimisation of plain weave fabric composites under tension and shear before the investigation. It means the problem type is not defined and it is unknown about the best practice of Genetic Algorithms for solving this problem. In this case 10 top performing Genetic Algorithms are selected for benchmarking: MOEA/D [80], MOEA/D-PSF [84], MOEA/D-MSF [84], HEIA [274], BCE [275], IBEA [77], MTS [276], NSGA-II [75], U-NSGA-III [97], and co-evolutionary MLSGA (cMLSGA) [277]. The benchmarking Genetic Algorithms can be categorised into five categories. MOEA/D [80] and MOEA/D-PSF/MSF [84] are based on weight vector and decomposition. HEIA [274], BCE [275] and IBEA [77] all use indicator-based selection approach. MTS [276] is population based local search method. NSGA-II [75] and U-NSGA-III [97] are non-dominated sorting based niching algorithms and co-evolutionary Multi-Level Selection Genetic Algorithm (cMLSGA) [277] is multi-level selection method based co-evolutionary algorithm.

In order to perform a fair benchmarking across these Genetic Algorithms, the values of parameters in the solvers are selected from their original paper, which is the same as in Wang et al. [30]. All the Genetic Algorithms are benchmarked using the same population size and total number of function calls. MTS is a population based optimisation algorithm having a different set of hyper-parameters from other algorithms. HEIA is based on immune algorithm and uses both genetic operators and differential evolution operators. MOEA/D [80] has good performance on unconstrained problems; MOEA/D-PSF/MSF [84] is an updated version of MOEA/D with improved convergence and diversity. HEIA [274] and BCE [275] are hybrid/co-evolutionary algorithms that having high performance on solving many-objective optimisation problems. IBEA [77] is the first and also the mostly used indicator-based Genetic Algorithm, which improves the efficiency of finding the final Pareto front. MTS [276] has generally good performance across all problem sets as a general solver; NSGA-II [75] is the most popular general solver with high performance on multi-objective optimisation and U-NSGA-III [97] shows high performance on many-objective optimisation which unifies NSGA-III to be suitable for mono-, multi- and many-objective optimisation problems. co-evolutionary MLSGA (cMLSGA) [277], which uses a state-of-the-art Genetic Algorithm for half of the collectives and utilises a second state-of-the-art Genetic Algorithm for the other half, is currently known best general solver for many-objective optimisation.

EW220/5284 is chosen to be optimised as a type of glass plain weave fabric composite currently used on aerospace applications. The variables the coefficient for calculating one quarter of yarn undulation length, l_1 and l_2, the yarn width, w_1 and w_2, and the yarn thickness, h_1 and h_2, are the parameters influencing the tensile and shear strengths and moduli and the areal density of the plain weave fabric composites in the analytical models. The range of these variables are determined to ensure the applicability for a range of existing applications for plain weave fabric composites. In order to fairly compare the optimised designs with a current design, the fibre volume fraction and the yarn fibre volume fraction of the EW220/5284 plain weave fabric composites are fixed as 0.55 and 0.73 in the optimisation. In order to make sure the optimal designs can be manufactured, the sum of warp and weft tow thickness should be smaller than the thickness of the ply. The half of the undulation length of warp tow, $2L_1$, must be larger than the width of weft tow, w_2, and vice versa.

In order to quantitatively evaluate the performance of the state-of-the-art Genetic Algorithms, two indicators are introduced in the current study which are the mimicked inverted

generational distance (mIGD) and mimicked hyper volume (mHV). The mIGD is introduced in Chapter 6 and [30] and it is evaluated in eq. (6.8); lower mIGD value reflects a better quality and diversity of the obtained Pareto front. The mHV is inspired by the HV indicator proposed by [278,279]. The HV indicator calculates the summation of the objective space volume between the obtained Pareto front points and a predefined reference point. The predefined reference point in the mHV is determined using the mimicked Pareto front which is found by using the non-dominated filtering and by removing any duplications from the combined Pareto front results from all the benchmarked solvers; a higher mHV value indicates a solver with a better performance. When comparing the results from the two metrics, the mHV metric is more representative of the diversity of the population but mIGD is more representative of the accuracy and uniformity of the obtained Pareto fronts, which is especially true when there are a small number of points in the Pareto Front. Therefore, using both indicators together allows an evaluation of the accuracy and the diversity of the obtained Pareto fronts for each solver.

A league table is created to illustrate the best practices of Genetic Algorithms on solving five-objective, three-objective and bi-objective plain weave fabric composite optimisation problems. According to the league table and the obtained Pareto fronts, the dominant characteristics of each problem are evaluated.

Chapter 4. Rapid prediction of plain weave fabric composite strengths under biaxial tension using micromechanical model

4.1 Introduction

According to the comparative review of woven fabric composite modelling methods in Chapter 2, available finite element methods are computationally expensive, even using the most efficient 'binary model', when used in the optimisation since the complexity of the optimisation problem prompts hundreds of thousands of evaluations implemented to find the optimal designs. Therefore, analytical methods are better choices to be used in the optimisation. However, the available analytical methods have large prediction errors on uniaxial tensile strength predictions, which have mean errors ~20%, and there are a limited number of analytical methods for the prediction of biaxial tensile strengths. Thus, the analytical model developed by this research for the prediction of biaxial tensile strengths is the best choice as the fitness evaluation method used in the optimisation of plain weave fabric composites since it is computationally efficient, accurate, robust and applicable for a range of material types. The details of the analytical model are presented in this Chapter.

Previously, the biaxial tensile moduli of plain weave fabric composites have been investigated using the minimum complementary potential energy principle. However, the biaxial tensile strength is also a key property and there are few current analytical models to determine it. Therefore, a new method is derived in this Chapter meaning that damage under complex loading conditions can be represented using this simple approach. The model allows the prediction of the failure locations and the resulting analysis allows the influence of the different biaxial tensile loading ratios on the biaxial tensile strengths to be better understood. Plain weave fabric composites are increasingly used in aerospace structures as they provide a balance between excellent specific strength and stiffness, impact resistance and low cost [37,280,281]. These structures encounter complex loading conditions during operation but the current literature focuses uniaxial tensile properties to improve the accuracy. Therefore, it is necessary to investigate the strength of plain weave fabric composites under biaxial tension.

Plain weave fabric composites are produced from yarns placed orthogonally to each other which provide compact weaves where each tow in the warp and weft direction alternates between passing over or under the next tow, illustrated in Figure 4-1; as opposed to twill or satin weaves where a tow may pass over multiple tows in the other direction. In these materials the crimp, or undulation, of the yarns significantly influences the biaxial tensile strengths and so as the range of applications for plain weave fabric composites grows there is an increasing

interest in predicting the mechanical properties and the failure mechanisms to be able to optimise these properties.

There are several undetermined internal forces and moments that need to be solved after the micromechanical analysis of the RVE. The minimum total complementary potential energy principle states that the solution of the unknown variables is the one that minimises the total complementary potential energy in all possible statically admissible stress fields [53]. The minimum potential energy principle has a similar definition but it is for solving the undetermined internal displacements or strains [53]. According to this definition the undetermined internal forces can be determined by the known external loadings using the minimum total complementary potential energy principle rather than using the minimum potential energy principle. This approach has been used to accurately predict the tensile strengths and moduli of triaxial weave fabric composites [30,298] and the biaxial tensile moduli of plain weave fabric composites [39]. Therefore, this work proposes an analytical model for strength using the same principle. The similar curved beam assumptions of the idealised yarn geometry and the micromechanical analysis of a unit cell remain valid in the proposed model [39]. In order to validate the model, the predictions from the new analytical model are compared with experimental measurements for uniaxial loading cases. Due to the difficulties of measuring biaxial tensile strengths through experiments, the strengths of plain weave fabric composites under biaxial tensile loadings are verified with FEM in ABAQUS. The predicted failure locations and the influences of different biaxial tensile ratios on the biaxial tensile strengths are discussed. The model is verified against four types of materials with a range of different properties, including glass and carbon fibre plain weave fabric composites, to prove the general applicability of the method[3].

4.2 Geometrical representation of plain weave fabric composites

Plain weave fabrics exhibit a regular, periodical weave pattern. This simplifies the problem as they can be characterised by identical repeated unit cells, where Figure 4-2 illustrates a unit cell for a plain weave fabric composite laminate; where the coordinate axes *x*, *y* and *z* represent the longitudinal, transverse and through-thickness directions of the tows. The geometrical assumptions of the tows are inherited from the literature [39,298] for establishing the analytical model through the unit cells, which are:

[3] The model has been uploaded for Open Access: https://doi.org/10.5281/zenodo.1476559

(1) the cross-section of the tow is constituted by a flat rectangle with two semicircles at each end of width, w_1 and w_2, and thickness, h_1 and h_2, illustrated in Figure 4-1;
(2) the tows are idealised as curved beams, meaning that the neutral axis of the undulated tows is assumed to be a smooth and continuous sinusoidal curve, shown in Figure 4-2.

For the first assumption, since the width and thickness of yarns of glass and carbon plain weave fabric composites are less than 2 mm and 0.2 mm, using a flat rectangle with two semicircles at each end of width, rather than using an ellipse, to represent the cross-section of the tows doesn't reduce the accuracy of the analytical model. In addition, using the assumed cross-sectional shape is able to better represent the plain weave fabric composites with thick tows, which improves the applicable range of the analytical model. For the second assumption, since the undulation angle is small due to the thin yarns in common plain weave fabric composites, using a smooth and continuous sinusoidal curve to represent the neutral axis of the undulated tows not only maintains the model accuracy but also reduces the complexity of derivation in the following steps.

Furthermore, in order to avoid complexity, the analytical model assumes that the shape of the tow path is fixed as a smooth and continuous sinusoidal curve and does not change as the load is applied. According to the assumptions, the cross-sectional area, A, and the moment of inertia, I, of the biaxial tows are expressed the same as eqs. (1)-(2) in [39], which are summarised as eqs. (4.1) and (4.2),

$$A_i = \frac{\pi h_i^2}{4} + h_i\left(w_i - h_i\right), \tag{4.1}$$

$$I_i = \frac{1}{64}\pi h_i^4 + \frac{1}{12} h_i^3\left(w_i - h_i\right), \tag{4.2}$$

where h_i and w_i are the yarn thickness and width, illustrated in Figure 4-1, where the subscript i is equal to 1 to represent the warp tows and is 2 when representing the weft tows. According to assumption (2) and Figure 4-2, the undulated neutral axis of the yarns, z, is expressed as eq. (4.3) for warp tow, which are the same definition as in [39,299],

$$z_1 = \frac{h_2}{2}\sin\frac{\pi x}{2L_1}, \tag{4.3}$$

and eq. (4.4) for weft tow,

$$z_2 = \frac{h_1}{2}\sin\frac{\pi x}{2L_2}, \tag{4.4}$$

where L_i is one quarter undulation length of the tow, illustrated in Figure 4-2, since one period of the tow is rotationally symmetric and a half period of the tow is axially symmetric. The tangent of the off-axial angle for the undulated tows, $\tan\theta$, which is shown in Figure 4-2, is expressed as eq. (4.5),

$$\tan\theta_i = \frac{dz_i}{dx}, \tag{4.5}$$

for a differential segment, dx, on a warp or weft yarn. According to Figure 4-2, the relationship between the *dx* and *dx'* is demonstrated in eq. (4.6),

$$dx' = \frac{dx}{\cos\theta} = \sec\theta dx = \sqrt{1+\tan^2\theta}dx = \sqrt{1+\left(\frac{dz}{dx}\right)^2}dx = \sqrt{1+\left(\frac{\pi h_m}{4L_n}\cos\frac{\pi x}{2L_n}\right)^2}dx, \tag{4.6}$$

where the subscript *n* equals 1 representing warp tows and 2 representing weft tows and the subscript *m* equals 2 for z_1 and 1 for z_2. Therefore, the tow volume fraction, V_y, and the tow fibre volume fraction, V_f, are summarised as eqs (4.7) and (4.8), which are the same as eqs. (4)-(6) in [39],

$$V_y = \left(4L_1L_2H\right)^{-1}\left(2\int_0^{L_1}A_1\sqrt{1+\left(\frac{\pi h_2}{4L_1}\cos\frac{\pi x}{2L_1}\right)^2}dx + 2\int_0^{L_2}A_2\sqrt{1+\left(\frac{\pi h_1}{4L_2}\cos\frac{\pi x}{2L_2}\right)^2}dx\right), \tag{4.7}$$

$$V_f = V_{f0}/V_y, \tag{4.8}$$

where *H* is the thickness of the plain weave fabric composite ply and V_{f0} represents the fibre volume fraction of the unit cell.

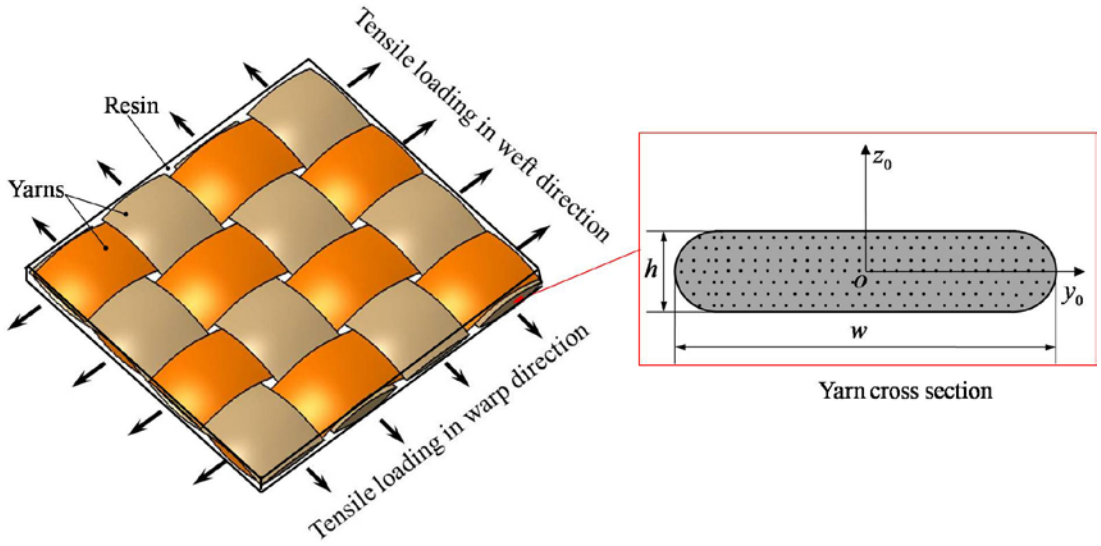

Figure 4- 2. Plain weave fabric composites under biaxial tensile loadings [39]

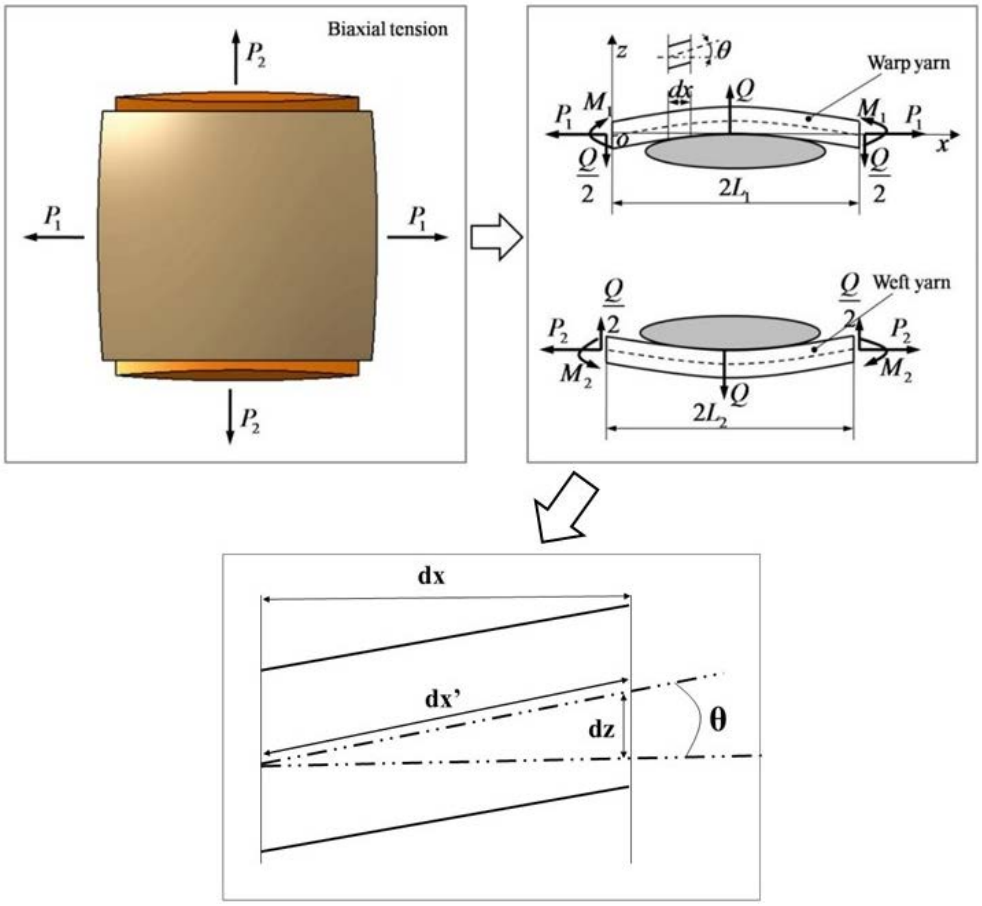

Figure 4- 3. Internal forces and bending moments on warp and weft yarns (with resin) in biaxial tensile state and a segment of the yarn [39]

4.3 Rapid strength predictions of plain weave fabric composites under biaxial tension

The ratio between the biaxial tensile loadings is defined in eq. (4.9) as,

$$\lambda = \frac{P_1}{P_2}, \tag{4.9}$$

where P_1 and P_2 are the tensile forces along the warp and weft directions respectively, shown in Figure 4-2. According to the micromechanical analysis the internal forces, $F_n(x)$, on any cross-section of the warp and weft tows are defined in eq. (4.10) as,

$$F_n(x) = P_n \cos\theta + \frac{Q}{2}\sin\theta, \tag{4.10}$$

where the subscript *n* equals 1 representing warp tows and 2 representing weft tows. Since it is an in-plane biaxial tension problem, the main interaction between the warp and weft yarns is the normal force at the interlaced section. *Q* represents the interaction force, which is caused by the yarn interactions under either biaxial or uniaxial tension. The bending moments on the warp and weft tows for each cross-section, $M_n(x)$, are expressed in eq. (4.11),

$$M_n(x) = M_n + P_n z - \frac{Q}{2}x, \tag{4.11}$$

where M_1 and M_2 are the moments on warp and weft tows induced by tensile loadings. However, the values of M_1, M_2 and Q in eqs. (4.10) and (4.11) are unknown. According to the definition of the minimum total complementary potential energy principle demonstrated in the introduction of the current Chapter [53], the minimum total complementary potential energy principle is employed to find these undetermined values. The complementary potential energies for the warp and weft tows in the unit cells are calculated in eq. (4.12),

$$\begin{aligned} U_n^* &= U_{n_{\text{Bending}}}^* + U_{n_{\text{Tensile}}}^* \\ &= 2\times\frac{1}{2EI_n}\int_0^{L_n} M_n^2(x)\,dx' + 2\times\frac{1}{2EA_n}\int_0^{L_n} F_n^2(x)\,dx'. \end{aligned} \tag{4.12}$$

Therefore, the complementary potential energies for the warp and weft tows in the unit cells are calculated in eq. (4.13),

$$U_n^* = \frac{1}{EI_n}\int_0^{L_n} M_n^2(x)\sqrt{1+\left(\frac{\pi h_m}{4L_n}\cos\frac{\pi x}{2L_n}\right)^2}\,dx + \frac{1}{EA_n}\int_0^{L_n} F_n^2(x)\sqrt{1+\left(\frac{\pi h_m}{4L_n}\cos\frac{\pi x}{2L_n}\right)^2}\,dx, \tag{4.13}$$

by substituting eq. (4.6) into eq. (4.12), where the subscript *m* equals 2 for U_1^* and 1 for U_2^*. E is the elastic modulus of a yarn in the longitudinal direction, which is calculated using the rule of mixtures. The complementary potential energies of the warp and weft tows can be obtained by substituting eqs. (4.10) and (4.11) into eq. (4.13). The resulting equations are summarised in eq. (4.14) for the warp direction,

$$U_1^* = C_1 M_1^2 + \left(C_2 + C_7\right) P_1^2 + \left(C_3 + C_8\right) Q^2 + C_4 M_1 P_1 + \left(C_5 + C_9\right) P_1 Q + C_6 M_1 Q, \qquad (4.14)$$

and eq. (4.15) for the weft,

$$U_2^* = C_{10} M_2^2 + \left(C_{11} + C_{16}\right) P_2^2 + \left(C_{12} + C_{17}\right) Q^2 + C_{13} M_2 P_2 + \left(C_{14} + C_{18}\right) P_2 Q + C_{15} M_2 Q, \quad (4.15)$$

where C_i $\left(i = 1,2,3\ldots\ldots 18\right)$ are the transformation variables [39] which are listed in Appendix I-A. Therefore, the total complementary potential energy of the unit cells, Π^*, is the summation of eqs. (4.14) and (4.15). To minimise the total complementary potential energy for the unit cell the partial derivatives are taken with respect to M_1, M_2 and *Q*, which are expressed in eq. (4.16) [39],

$$\begin{cases} \dfrac{\partial \Pi^*}{\partial M_1} = 0, \\ \dfrac{\partial \Pi^*}{\partial M_2} = 0, \\ \dfrac{\partial \Pi^*}{\partial Q} = 0, \end{cases} \qquad (4.16)$$

and the relationships are represented using P_1 and P_2 in eq. (4.17) [39],

$$\begin{cases} 2C_1 M_1 + C_6 Q = -C_4 P_1, \\ 2C_{10} M_2 + C_{15} Q = -\dfrac{C_{13}}{\lambda} P_1, \\ C_6 M_1 + C_{15} M_2 + 2\left(C_3 + C_8 + C_{12} + C_{17}\right) Q = -\left[\left(C_5 + C_9\right) + \dfrac{1}{\lambda}\left(C_{14} + C_{18}\right)\right] P_1, \end{cases} \qquad (4.17)$$

where P_2 is replaced by $\frac{P_1}{\lambda}$, which allows biaxial loadings to be incorporated. Cramer's rule can be utilised to solve eq. (4.17) to give a simple formulation, eq. (4.18), for the bending moment in the warp direction,

$$M_1 = D_1 P_1, \tag{4.18}$$

eq. (4.19) for the bending moment in the weft direction,

$$M_2 = D_2 P_1, \tag{4.19}$$

and eq. (4.20) for the internal force,

$$Q = D_3 P_1, \tag{4.20}$$

where D_i $(i = 1,2,3)$ are the determinants [39] which are listed in Appendix I-B.

The maximum normal stresses on the warp tow is the summation of axial stress and bending stress [300], which is formulated as eq. (4.21),

$$\sigma_{1\max} = \sigma_{1\text{axial}} + \sigma_{1\text{bending}} = \frac{P_1}{A_1} - \frac{M_1(x) z_0}{I_1}, \tag{4.21}$$

where z_0 represents the maximum normal stress location, I_1 is the moment of inertia obtained from eq. (4.2) and $M_1(x)$ is obtained from eq. (4.11). According to the micromechanical analysis the maximum normal stresses at the crest and trough of the warp tow path, $\sigma_{1\max}$, are formulated in eq. (4.22) for the trough $z_0 = -h_1/2$,

$$\sigma_{1\max 1} = \frac{P_1}{A_1} + \frac{h_1}{2I_1}\left(\frac{P_1 h_2}{2}\sin\frac{\pi L_1}{2L_1} - \frac{Q}{2}L_1 + M_1\right), \quad (z_0 = -h_1/2), \tag{4.22}$$

where x equals L_1 when $z_0 = -h_1/2$, which is illustrated in Figure 4-2. The maximum normal stress at the trough of the warp tow path is derived by substituting eqs. (4.18) and (4.20) into eq. (4.22), as eq. (4.23),

$$\sigma_{1\max 1} = P_1\left(\frac{1}{A_1} + \frac{h_1 h_2}{4I_1} - \frac{D_3 L_1 h_1}{4I_1} + \frac{D_1 h_1}{2I_1}\right), \quad (z_0 = -h_1/2), \tag{4.23}$$

and using the same process the maximum normal stress at the crest of the warp tow path, $z_0 = h_1 / 2$, is expressed in eq. (4.24),

$$\sigma_{1\max 2} = P_1\left(\frac{1}{A_1} - \frac{h_1 h_2}{4I_1} + \frac{D_3 L_1 h_1}{4I_1} - \frac{D_1 h_1}{2I_1}\right), \quad (z_0 = h_1 / 2). \tag{4.24}$$

The maximum normal stresses at the crest and trough of the weft tow path, σ_{2max}, in the unit cells are expressed as eq. (4.25) for the trough $z_0 = -h_2 / 2$,

$$\sigma_{2\max 1} = \frac{P_2}{A_2} + \frac{h_2}{2I_2}\left(\frac{P_2 h_1}{2} - \frac{Q}{2}L_2 + M_2\right), \quad (z_0 = -h_2 / 2), \tag{4.25}$$

and eq. (4.26) for the crest $z_0 = h_2 / 2$,

$$\sigma_{2\max 2} = \frac{P_2}{A_2} + \frac{h_2}{2I_2}\left(-\frac{P_2 h_1}{2} + \frac{Q}{2}L_2 - M_2\right), \quad (z_0 = h_2 / 2), \tag{4.26}$$

through a similar derivation process as that used to generate (4.22) from eqs. (4.21). By substituting eqs. (4.9) and (4.19)-(4.20) into eqs. (4.25)-(4.26), a similar derivation process as used to determine eqs. (4.22) and (4.23) can be used to find the maximum normal stresses at the crest and trough of the weft tow path, σ_{2max}, in the unit cells, expressed as eq. (4.27) for the trough $z_0 = -h_2 / 2$,

$$\sigma_{2\max 1} = P_1\left(\frac{1}{\lambda A_2} + \frac{h_1 h_2}{4\lambda I_2} - \frac{D_3 L_2 h_2}{4I_2} + \frac{D_2 h_2}{2I_2}\right), \quad (z_0 = -h_2 / 2), \tag{4.27}$$

and eq. (4.28) for the crest $z_0 = h_2 / 2$,

$$\sigma_{2\max 2} = P_1\left(\frac{1}{\lambda A_2} - \frac{h_1 h_2}{4\lambda I_2} + \frac{D_3 L_2 h_2}{4I_2} - \frac{D_2 h_2}{2I_2}\right), \quad (z_0 = h_2 / 2), \tag{4.28}$$

where the first term $\frac{P_1}{\lambda A_2}$ is the transformation of $\frac{P_2}{A_2}$, the second term $\frac{P_1 h_1 h_2}{4\lambda I_2}$ is the transformation of $\frac{P_2 h_1 h_2}{4I_2}$ and the last two terms are transformed from $\frac{QL_2 h_2}{4I_2}$ and $\frac{M_2 h_2}{2I_2}$.

Since the failure of the plain weave fabric composites is dominated by the failure of the fibre

bundle in the direction of the fibre when under tensile loading, the maximum stress failure criterion is used in the model. The critical external biaxial tensile forces, P_f, at each crest and trough location are obtained by the tensile failures of warp and weft tows. The failure force for the trough of the warp tow, subscript 1, is given in eq. (4.29),

$$P_{f1} = X_{t0}\left(\frac{1}{A_1} + \frac{h_1 h_2}{4I_1} - \frac{D_3 L_1 h_1}{4I_1} + \frac{D_1 h_1}{2I_1}\right)^{-1}, \tag{4.29}$$

and the failure force for the crest of the warp tow, subscript 2, is given in eq. (4.30),

$$P_{f2} = X_{t0}\left(\frac{1}{A_1} - \frac{h_1 h_2}{4I_1} + \frac{D_3 L_1 h_1}{4I_1} - \frac{D_1 h_1}{2I_1}\right)^{-1}. \tag{4.30}$$

The failure force for the trough of the weft tow, subscript 3, is given in eq. (4.31),

$$P_{f3} = X_{t0}\left(\frac{1}{\lambda A_2} + \frac{h_1 h_2}{4\lambda I_2} - \frac{D_3 L_2 h_2}{4I_2} + \frac{D_2 h_2}{2I_2}\right)^{-1}, \tag{4.31}$$

and the failure force for the crest of the weft tow, subscript 4, is given in eq. (4.32),

$$P_{f4} = X_{t0}\left(\frac{1}{\lambda A_2} - \frac{h_1 h_2}{4\lambda I_2} + \frac{D_3 L_2 h_2}{4I_2} - \frac{D_2 h_2}{2I_2}\right)^{-1}, \tag{4.32}$$

by switching the maximum normal stresses with the tensile force P_1 in eqs. (4.23), (4.24), (4.27) and (4.28) and replacing the maximum normal stresses in these equations by the tensile strength of the tows where X_{t0} is the tensile strength of the tows in the longitudinal direction. Since the ultimate tensile strain of the fibre, ε_{ft}^{u}, is lower than that of the matrix, ε_{mt}^{u}, the fibre bundle will fail when its longitudinal strain reaches the ultimate tensile strain in the fibre [301]. The longitudinal tensile strength of the yarn, X_{t0}, can be approximated by eq. (4.33) [301],

$$X_{t0} \cong X_t V_f + \sigma_m^* V_m, \tag{4.33}$$

where X_t is the fibre tensile strength in the longitudinal direction, V_m is volume fraction of the matrix in the yarn and σ_m^* is the average longitudinal matrix stress when ultimate fibre strain

is reached. Assuming liner elastic behaviour for the constituents, the tensile strength of the tows is derived from eq. (4.33) as the eq. (4.34) [301],

$$X_{t0} \cong X_t V_f + E_m \varepsilon_{ft}^u V_m = X_t V_f + X_t E_f^{-1} E_m \left(1 - V_f\right), \tag{4.34}$$

where E_f is the Young's modulus of the fibre and E_m is the Young's modulus of the matrix. The critical external tensile force along the warp direction, P_f, for the plain weave fabric composite ply can be defined as the lowest failure force from eqs. (4.29)-(4.32). Therefore, the biaxial tensile strength of the plain weave fabric composites in the warp loading direction is obtained through the critical force divided by the cross-sectional area and shown in eq. (4.35),

$$X_{1\mathrm{t}} = \frac{P_f}{2L_2 H} = \frac{\min\left(P_{f1}, P_{f2}, P_{f3}, P_{f4}\right)}{2L_2 H}. \tag{4.35}$$

The critical external force along weft direction can be found by P_f dividing by λ. Thus the biaxial tensile strength in the weft direction is shown in eq. (4.36),

$$X_{2\mathrm{t}} = \frac{P_f}{2\lambda L_1 H}. \tag{4.36}$$

The analytical model can predict the uniaxial tensile strength of the plain weave fabric composites by setting $\lambda = \infty$ (i.e. $P_2 = 0$) in the warp direction and $\lambda = 0$ (i.e. $P_1 = 0$) in the weft direction.

4.4 Biaxial verification and uniaxial validation of the analytical model

In order to validate the analytical model an E-glass/epoxy, EW220/5284, plain weave fabric cruciform composite specimen is designed with 55% fibre volume fraction; the geometry and dimensions of the biaxial tensile specimen are shown in Figure 4-3. The ply thickness of the composite specimens is 0.167 mm with 13 stacked layers. One quarter of the undulation length, *L*, is 0.714 mm for the warp and 0.556 mm for the weft. The width, *w*, and the thickness, *h*, of the tows are 1.0 mm and 0.080 mm for the warp direction and 1.2 mm and 0.067 mm for weft direction. The fibre and the epoxy resin properties are listed in Table 4-1. The specimen is designed to replicate geometries tested previously in the literature [39,273]. The length and width of the cruciform specimens are 130 mm with a 2.16 mm thickness for the four loading arms. In order to reduce the influences of the stress concentrations, four elliptical chamfers are designed with a 33.94 mm length in the major axis and 28.28 mm length in the minor axis. A

diamond-shaped central thinner area is made with three layers of plain weave fabric composite with 0.5 mm thickness plies. In the specimens, the warp and weft tows are along the X and Y directions in Figure 4-3, respectively. It is difficult to extract the two directional tensile strengths while simultaneously applying biaxial tensile loadings due to the stress concentration at the boundary of the specimens between the loading arm and central area. This is a common problem with no available biaxial data for plain weave fabric composites despite some attempts such as Cai et al. [273] where the biaxial tensile strengths measured were inaccurate due to stress concentrations. It is common to use experimentally measured mechanical properties of the plain weave fabric composite lamina in a composite laminate FEM model for accurately predicting the biaxial tensile strengths. Since the finite element method is a widely accepted numerical method as well as being established by the actual specimen and experimentally measured properties, it is used as the benchmark in the verification. Therefore, in order to verify the accuracy and robustness of the model for both uniaxial and biaxial tensile strength predictions, four sets of uniaxial tensile experimental results and the FEM model predictions in ABAQUS with six sets of biaxial loading ratios: 1:1, 2:1 (1:2) and 3:1 (1:3) are used to add confidence to the results.

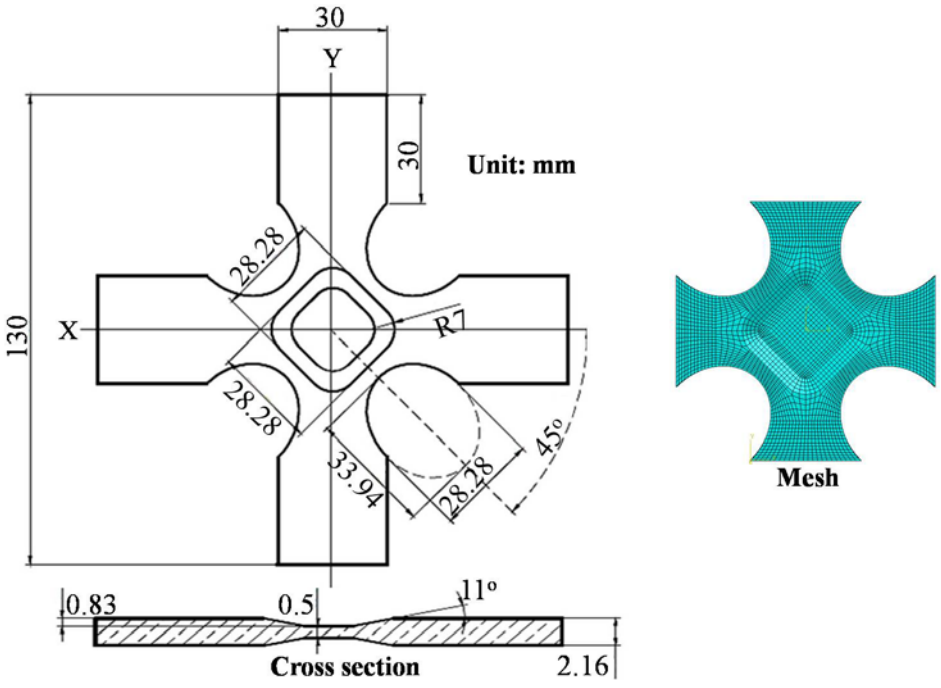

Figure 4- 4. Geometry and finite element model of the biaxial tensile specimen [39]

Table 4- 2. Fabric dimensions and mechanical properties of the test specimens [39]

Parameters	Values	Parameters	Values
h_1 (mm)	0.080	w_2 (mm)	1.2
h_2 (mm)	0.067	H (mm)	0.167
L_1 (mm)	0.714	E_f (GPa)	73.0
L_2 (mm)	0.556	E_m (GPa)	3.4
w_1 (mm)	1.0	X_t (MPa)	2000

4.4.1 Uniaxial tensile tests

The uniaxial tensile test specimens are manufactured with EW220/5284 plain weave fabric composite using the resin transfer moulding technique within closed steel mould and cutting method. The composite preforms are laid-up in the mould and heated at a speed of 5 ℃/min to 160 ℃ where the temperature is held for 1 hour. The resin is transferred to the closed steel mould with pressure at the inlet and vacuum at the outlet. The temperature is then increased to 180 ℃ with the same heating rate and the temperature held for a further 2 hours. The resin transfer continues throughout this period. This process is to reduce defects like voids within the laminates. The plain weave fabric laminates are consolidated under a room-temperature curing process. Finally, the laminates are cut according to ASTM D3039M-2000(R06) to obtain the uniaxial tensile specimens.

The warp and weft direction tensile tests are repeated six times using a MTS880-100Kn servo-hydraulic machine, meaning there are 12 specimens in total. The static tensile tests are executed at a 3 mm/min loading rate, and the load to strain curves are recorded, where the strain is measured by strain gauges taped on the specimens. The straightening of the crimped in-plane tows causes bilinear behaviour in the stress-strain plot in both the uniaxial and biaxial tensile experiments [39,302]. However, the bilinear behaviour of glass plain weave fabric composites is different from the elastoplastic behaviour exhibited by metal matrix composites [303] and nanocomposites [304], as the behaviour is caused by an initial hardening phase as the crimped tows straighten rather than a plastic deformation. Therefore, the ultimate tensile strength in the warp and weft directions is measured according to ASTM D3039M-2000(R06). The average tensile strengths are 492.52 MPa in warp direction and 379.57 MPa in weft direction with a standard deviation of 21.61 for the warp direction and 21.49 for the weft direction loadings.

The details of the measured tensile strengths in warp and weft directions are listed in the Table 4-2.

Table 4- 3. Experimental uniaxial tensile strengths of EW220/5284 PWF composites

Specimen No.	Warp (i.e. $\lambda = \infty$)	Weft (i.e. $\lambda = 0$)
	Strengths (MPa)	Strengths (MPa)
1	479.79	384.44
2	480.47	345.23
3	536.10	366.70
4	486.11	387.64
5	488.69	384.67
6	483.98	408.73
Average	492.52	379.57
Standard deviation	21.61	21.49

4.4.2 Biaxial tensile simulation in ABAQUS

The biaxial tensile specimens shown in Figure 4-3 are modelled in ABAQUS, resulting in a model shown in the same figure. The plain weave fabric composite specimen is simplified as an anisotropic laminate with 13 plies defined as a solid composite layup in the FEM model. The experimentally measured mechanical properties of the EW220/5284 plain weave fabric composite lamina from uniaxial tensile tests are used in the FEM model and summarised in Table 4-3.

Table 4- 4. Mechanical properties of the EW220/5284 plain weave fabric composite lamina

Property	Value
Longitudinal elastic modulus E_1/GPa	14.2
Transverse elastic modulus E_2/GPa	19.3
Poisson's ratio ν_{12}	0.15
In-plane shear modulus G_{12} /GPa	4.3
Longitudinal tensile strength X_{1t}/MPa	380
Transverse tensile strength X_{2t}/MPa	493
In-plane shear strength X_{12}/MPa	111

A static analysis is implemented using a linear solver. In order to accurately replicate the boundary conditions of the experiments, the loads are added to the four ends at the

different loading ratios and four sets of displacement/rotation boundary conditions are implemented at the ends to constrain the displacements along the loading directions. The yarn undulation lengths in the warp and weft directions are different, 1.428 mm for the warp tows and 1.112 mm for the weft tows. The external forces on a unit cell, P_1 and P_2, need to be transformed to external loadings in order to be equivalent to the external loadings added on the FEM model. Therefore, the biaxial loadings set in the FEM model are not the same as biaxial loadings set in the analytical model. Since a unit cell of plain weave fabric composite, illustrated in Figure 4-1, is a cuboid, it has the same thickness in warp and weft directions but it has different length of side due to the different undulation length of warp and weft tows. When the proposed model is verified with the FEM model, the biaxial tensile loading ratios should be set using the ratio of $P_1/2L_2$ over $P_2/2L_1$ for the analytical model, which is $\lambda\frac{L_1}{L_2}$.

Therefore, in order to calibrate the model, the loading ratios set in the FEM model, 3:1, 2:1, 1:1, 1:2 and 1:3, are respectively set as 3.852:1, 2.568:1, 1.284:1, 1.284:2 and 1.284:3 for the external biaxial forces in the analytical model. In order to increase the accuracy of the FEM model a structured mesh is created using 8-node brick solid elements with reduced integration, C3D8R, and a mesh convergence study is implemented. Seven meshes are compared under 100 MPa biaxial tensile loadings. The stresses in the weft and warp directions and shear stress are plotted to illustrate the convergence, which are shown in the Figure 4-4 and Table 4-4.

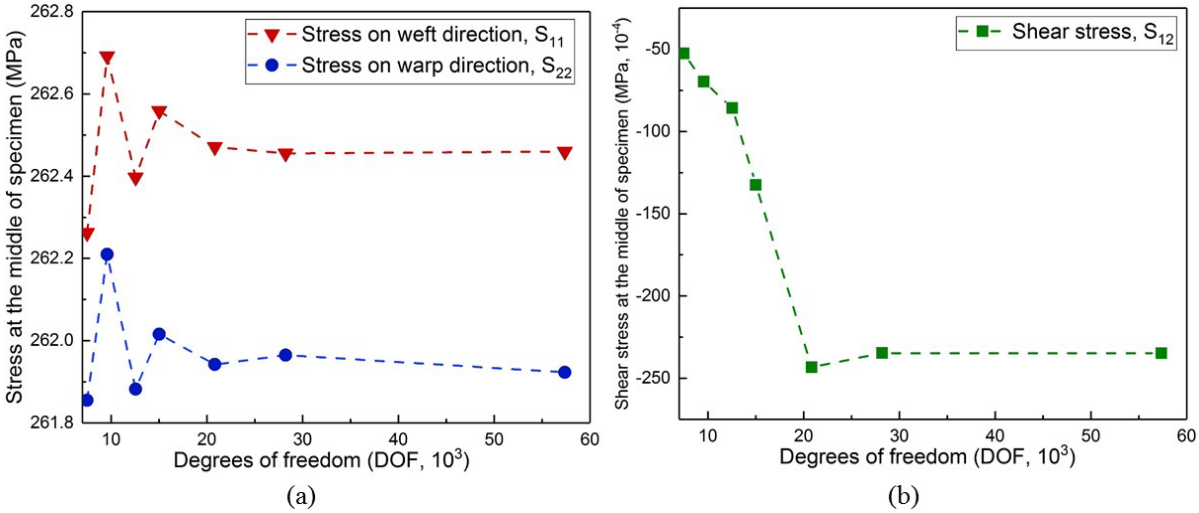

Figure 4- 5. Mesh convergence study: (a) stresses in warp and weft directions; (b) shear stress

Table 4- 5. Statistics of mesh in mesh convergence study

Mesh	No. of nodes	No. of elements	DoF	CPU time (s)
1 (Coarse)	2496	1526	7488	7.19
2	3195	1928	9585	8.05
3	4188	2610	12564	11.97
4	5007	3136	15021	13.67
5	6945	4392	20835	18.90
6	9405	5984	28215	21.60
7 (Fine)	19120	13806	57360	58.18

It is shown that the three stresses converge when the degree of freedom reaches 28215 and therefore, it is selected as the final mesh with an illustration in Figure 4-3. Since the in-plane biaxial tensile loadings are the dominant loadings applied to the finite element model and it assumes there are no defects in the model, the biaxial tensile strength is predicted using Tsai-Hill failure criterion [305],

$$\frac{\sigma_1^2}{X^2}-\frac{\sigma_1\sigma_2}{X^2}+\frac{\sigma_2^2}{Y^2}+\frac{\tau_{12}^2}{S^2}=1, \tag{4.37}$$

where the σ_1 and σ_2 are tensile stresses in longitudinal and transverse directions for the plain weave fabric composite lamina and τ_{12} is the in-plane shear stress. *X* and *Y* are the longitudinal and transverse tensile strengths of the plain weave fabric composite lamina and *S* is the in-plane shear strength of the lamina. The in-plane failure is iteratively evaluated, layer by layer on the element with highest stress at the central thinning area, until the value of Tsai-Hill failure criterion is equal to one. Using this method the biaxial tensile strengths under each biaxial tensile loading ratio are obtained.

4.5 Behaviour of plain weave fabric under biaxial loading

4.5.1 Verification of analytical method on a range of materials

In order to investigate the range of applications for the current proposed model another three plain weave fabric composite materials are selected [306,307]. Due to the lack of biaxial tensile tests in the literature, only uniaxial tensile strengths are compared. The fibre specifications, material properties and verification results are shown in Table 4-5, where the prediction results from the proposed model are compared to the experimental data from the literature. It is shown that the prediction errors for E-Glass/Epoxy, AS4 Carbon/3501-6 Epoxy and TC33 Carbon/Aradur3486 Epoxy plain weave fabric composites are respectively 6.74%,

12.20% and 11.78%. There are another two analytical model found in the literature for the predictions of uniaxial tensile strengths of 2D woven fabric composites. The analytical model developed by Scida et al. [34] provides a mean error of uniaxial tensile strength predictions of 15.55% for twill and satin weave fabric composites. The model developed by Naik et al. [33] provides a mean error of uniaxial tensile strength predictions of 15.92% for plain weave fabric composites. According to the verification results demonstrated above, the proposed analytical model is judged to be valid and most accurate for predicting the uniaxial tensile strengths of plain weave fabric composites produced from a range of different materials under uniaxial tension.

Table 4- 6. Experimental and predicted uniaxial tensile strengths with three types of material

Material		E-Glass[1]	AS4-Carbon[2]	TC33 Carbon[3]
Yarn Specifications	L_1 (mm)	0.376	0.5	0.998
	L_2 (mm)	0.376	0.5	0.998
	w_1 (mm)	0.732	1	1.651
	w_2 (mm)	0.732	1	1.651
	h_1 (mm)	0.1	0.04	0.1
	h_2 (mm)	0.1	0.04	0.1
Ply Thickness	H (mm)	0.201	0.081	0.208
Fibre Volume Fraction	V_{f0}	0.35	0.6	0.5
Elastic Modulus of Fibre	E_f (GPa)	72.4	221	230
Elastic Modulus of Matrix	E_m (GPa)	3.45	4.4	3.0
Fibre Tensile Strength in Longitudinal Direction	X_t (MPa)	2413	3585	3450
Uniaxial Tensile Strengths Verification (Warp = Weft)	Experiments (MPa)	353.27	737.5	588.43
	Predictions (MPa)	329.45	827.46	657.76
	Errors (%)	6.74	12.20	11.78

1. E-Glass/Epoxy [306]
2. AS4-Carbon/3501-6 Epoxy [306]
3. TC33 Carbon/Aradur3486 Epoxy [307]

4.5.2 Effect of loading ratio

Predicted results from the proposed analytical model are compared with the biaxial predictions from the FEM model and the uniaxial measurements from experiments, summarised in Table 4-6. The tensile strengths of the plain weave fabric composites under biaxial loading ratios 1:1, 2:1 (1:2), 3:1 (1:3) and ∞:1 (1:∞) are evaluated through eqs. (4.35) and (4.36). Over these ratios it is demonstrated that the maximum error between the warp biaxial tensile strength prediction and the FEM prediction is 11.18%. The warp uniaxial tensile strength prediction shows a similar level of accuracy as the three uniaxial strength verification cases in the previous section, which has an error of 11.64%. For the weft direction the maximum error is 14.67% between the predictions from the FEM model and the analytical model. The error between the analytical model prediction under weft uniaxial tension and the average of experimental measurements is 16.74%. The mean errors are 10.51% for warp direction predictions and 12.65% for weft direction predictions. Figure 4-5 shows the comparison between the experimental and predicted results for the different loading ratios, illustrating the predicted results accurately match with the experimental measurements and FEM predictions. The difference between the analytical predictions and the experimental and FEM predicted results is caused by the assumption that the yarns retain a non-deformable smooth and continuous sinusoidal yarn path, even after loading, and that the cross-section is represented as a flat rectangle with a semicircle at each end. Although a simple basis transform rule can be used for the calculation of the biaxial tensile strength, it requires the macroscopic material parameters, such as the fabric and lamina anisotropic moduli and strengths. The proposed model is able to predict the uniaxial and biaxial tensile strengths without experimental investigations at the fabric and laminate level and only requires the yarn mechanical properties and specifications.

Table 4- 7. Experimental and predicted warp and weft biaxial tensile strengths for EW220/5284 plain weave fabric composite

		$\lambda = 1$	$\lambda = 2$	$\lambda = 3$	$\lambda = \infty$
Warp strengths X_{1t} (MPa)	FE predictions &Experiments	409.77^{FEM}	556.13^{FEM}	499.16^{FEM}	492.52^{Exp}
	Theoretical Predictions	374.75	493.93	552.51	549.88
	Errors	8.55%	11.18%	10.68%	11.64%
	Critical locations*	warp yarn, $z_0 = h_1/2$	warp yarn, $z_0 = h_1/2$	warp yarn, $z_0 = h_1/2$	warp yarn, $z_0 = -h_1/2$
		$\lambda = 1$	$\lambda = 1/2$	$\lambda = 1/3$	$\lambda = 1/\infty$
Weft strengths X_{2t} (MPa)	FE predictions &Experiments	264.57^{FEM}	461.35^{FEM}	406.21^{FEM}	379.57^{Exp}
	Theoretical Predictions	291.82	393.67	370.07	312.60
	Errors	10.30%	14.67%	8.90%	16.74%
	Critical locations*	warp yarn $z_0 = h_2/2$	warp yarn $z_0 = h_2/2$	weft yarn $z_0 = -h_2/2$	weft yarn $z_0 = -h_2/2$

*See Figures 4-1 and 4-2 for details of cross-section at the path peaks and valleys of yarns
^{FEM} the value is obtained from Finite Element Method
^{Exp} the value is obtained from experiments

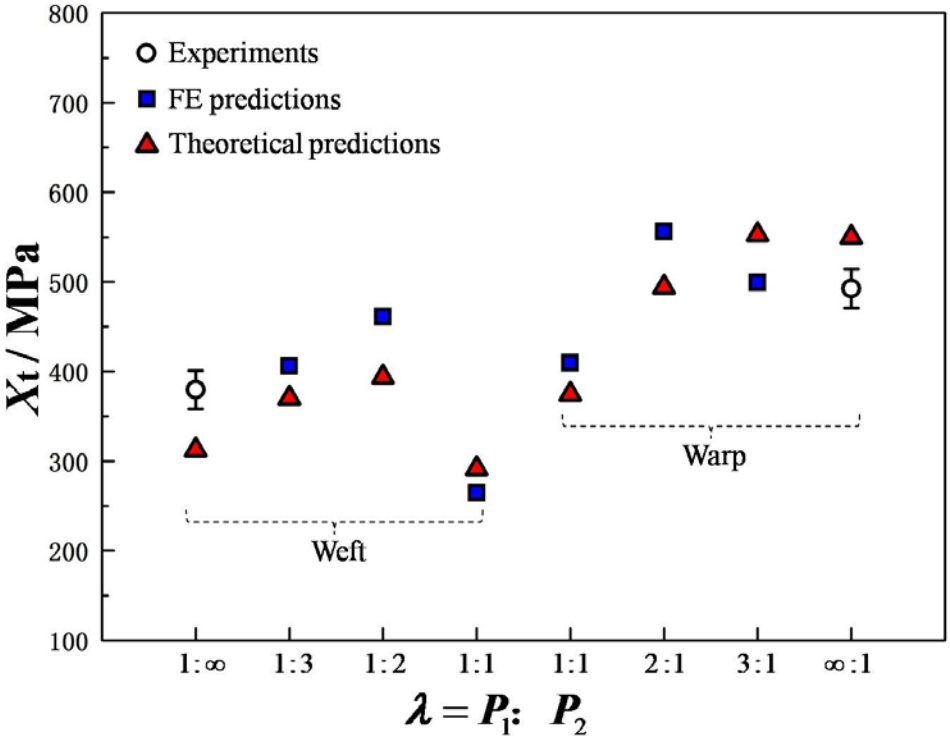

Figure 4- 6. Comparison between the experimental data, FE predictions and analytical predictions for EW220/5284 plain weave fabric composite

4.6 Discussion

The critical locations for the weave fabric are demonstrated for each biaxial loading ratio, shown in Table 4-6. The damage occurs at the peaks of the warp yarn when $\lambda = 1$, 2 and 3 but at the troughs of the warp yarn when $\lambda = \infty$. For the weft yarns, the damage occurs at the peaks of the warp yarns when $\lambda = 1$ and $\lambda = 1/2$. The damage occurs at the troughs of the weft yarns when $\lambda = 1/3$ and $1/\infty$. It is found that the failure starts at the warp yarn under biaxial tension until the weft direction loading is three times higher than the warp direction loading. This is caused by the fabric specifications, where the warp yarns are thicker with longer undulation lengths resulting in higher bending stresses due to a higher internal force, *Q*, and external force, *P*, which induces the moments, $\frac{Qx}{2}$ and Pz, in eq. (4.11). The strengths in both the warp and weft direction initially increase and then decrease from $\lambda = 1$ to ∞ in the warp direction and from $\lambda = 1$ to $1/\infty$ in the weft direction; this is shown in Table 4-6 and Figure 4-5 and applies to both the FEM and analytical models. This phenomenon is caused by the variation in the total stresses caused by the internal bending moments and change of the failure location. When the loading changes from equal biaxial tension to warp uniaxial tension, λ from 1:1 to ∞:1, or from equal biaxial tension to weft uniaxial tension, λ from 1:1 to 1:∞, the failure location

changes from the crest of the tows to the trough of the tows in both directions. The change in stress is caused by the internal force induced bending moment which is increased to balance the increased loading in the warp or weft direction. Since the stress caused by the internal force induced bending moment, $\frac{Qx}{2}$, is opposite to the stresses caused by the tension induced bending moment, *M*, and the tensile forces induced bending moment, *Pz*, the total stresses caused by the internal bending moments are reduced; increasing the strength of the material. When the warp direction loading is three times larger than the weft direction loading or the weft direction loading is two times larger than the warp direction loading, the total stress is dominated by the stresses caused by the tensile forces. The increased tensile forces result in a higher total stress, and therefore the strength is reduced. These relationships are reflected in the eqs. (4.23)-(4.24) and (4.27)-(4.28). Furthermore, the total stresses under uniaxial tension are lower than under equal biaxial tension since the contribution of the stresses caused by the tension induced bending moment, *M*, and the internal force induced bending moment, $\frac{Qx}{2}$, are both significantly lower under uniaxial tension. Therefore, the strength under uniaxial tension is higher than that under equal biaxial tension. This phenomenon is also demonstrated by Escárpita [297] where the strength under equal biaxial tensions is calculated by reducing the uniaxial strength.

The fabric specification has a substantial impact on the strength of the plain weave fabric composites, but this is also dependant on the type of load it will see in service. This means there is the potential to optimise the weave fabric to improve its properties but this can be further improved if its operation loads are known, for example a composite under uniaxial loading may differ in weave pattern from that expecting a more complex loading scenario. The model provided here gives a simple and rapid analysis to determine this specification.

Twill and satin weave fabrics are also common in composite applications, since they can be used to produce structures with curved geometries due to their lower crimp. The current model is developed to accurately predict the biaxial tensile strengths of plain weave fabric composites. However, initial feasibility studies show that the model can be extended to predict the biaxial tensile strengths of twill and satin weave fabric composites. To develop these models, the same steps can be followed, where the first step is to obtain the micromechanical behaviour of the satin and twill weave fabric composite unit cells. Then the total complementary potential energy can be calculated and minimised, so that all of the undetermined internal forces and moments can be obtained. Finally, the biaxial tensile strength can be derived.

A limitation of the current research is the difficulty in obtaining the biaxial tensile strength through experiments, due to the inevitable stress concentrations at the transition regions between the loading arms and the central thinning area of the specimens, and therefore the proposed model is verified with the FEM model. While the FEM provides confidence in the accuracy of the method, the ability to determine experimental data will increase the confidence in the approach.

4.7 Chapter summary

A novel analytical model is proposed in this chapter for rapid prediction of the biaxial tensile strengths of plain weave fabric composites. The model is derived based on the minimum total complementary potential energy principle with micromechanical analysis of orthogonally interlaced yarns. The proposed model is verified against the FEM under different biaxial loading cases and validated by experimental measurements under uniaxial tensile loading. Different biaxial tensile loading ratios and various types of materials, ranging in material properties from carbon to glass fibres, are used to show the general applicability of the method. By analysing the predicted results, it is demonstrated that the biaxial tensile strengths can be determined from the fibre specifications and biaxial loading ratios. The result is a model giving a mean error of 11.22% and a maximum error of 16.74% over the six biaxial tension cases, five uniaxial tension cases and four types of materials, which indicates the accuracy of the proposed model. Furthermore, the standard deviation of prediction errors among the total 11 cases is 2.66, which demonstrates the robustness of the model for a range of applications.

Chapter 5. Computationally efficient prediction of plain weave fabric composite shear moduli and strengths using a micromechanical model

5.1 The requirement for new analytical models predicting shear properties

As mentioned in the comparative review of woven fabric composite modelling methods in Chapter 2, the current available analytical methods for the predictions of shear modulus are not robust and the predictions of shear strength are not precise. Therefore, another analytical model is developed in this research for the prediction of the shear moduli and strengths, which is computationally efficient as the fitness evaluation method used in the optimisation of plain weave fabric composites. It is also accurate, robust and applicable for a range of material types, which is similar to the analytical model proposed in the previous Chapter. The details of the analytical model have been demonstrated in this Chapter.

According to the literature review in Chapter 2, there is a comprehensive determination of the tensile properties for plain weave fabric composites [33,37,39,299,308,309]. However, there are fewer examples of the shear property predictions, either through virtual or physical experiments. This is because the shear properties are more difficult to derive experimentally, or to simulate, than the tensile behaviours because of the complicated stress conditions. There are already a limited number of analytical models that show good accuracy for the shear modulus predictions of plain weave fabric composites, approximately 15%, but the prediction is not consistent across the entire range of composite material types. However, the strength predictions are less common and are performed with a lower accuracy, 23%. Therefore, this Chapter proposes a new analytical method building on the minimum total complementary potential energy principle to model the shear modulus and strength of plain weave fabric composites. It aims to mimic the bias extension experiment which is used for measuring the shear modulus and strength of the plain weave fabric composites. A set of equations are derived based on the applied tensile loadings which can be used to calculate the minimum total complementary potential energy, as opposed to previous literature which applies pure shear forces. The new approach allows both the shear modulus and strength to be predicted using the minimum total complementary potential energy. The result is a method with an improved robustness of shear modulus prediction and accuracy of the shear strength prediction. The model is rapid and provides an accurate tool for computational expensive simulation methods and as a tool for virtual experiments. The predictions from the analytical model are validated against experimental measurements with four types of materials and seven fabric specifications

to prove the general applicability and robustness of the method. The proposed analytical model has been uploaded to an open access platform[4].

5.2 Formulation of the micromechanical model

To replicate the bias extension experiment a pair of tensile loads is applied to the warp and weft tows at $\pm 45°$. A virtual biaxial loading with an actual P_2 tensile load and a virtual P_1 tensile load is applied in order to obtain the strain along the loading direction and its orthogonal direction to calculate the shear strain, illustrated in Figure 5-1. The ratio between the two tensile loadings, λ, is defined as eq. (5.1),

$$\lambda = \frac{P_1}{P_2}. \tag{5.1}$$

The strains along both directions and several undetermined internal forces and moments obtained after the micromechanical analysis of the unit cell are calculated using the minimum total complementary potential energy principle, since the definition states that the solution of the unknown variables is the one that minimises the total complementary potential energy in all possible statically admissible stress fields [53]. This methodology has already been used successfully to predict the tensile and shear, strengths and moduli of triaxial weave fabric composites [280,298] as well as the uniaxial and biaxial tensile moduli and strengths and shear modulus of plain weave fabric composites [39,44,299].

The shear strain of an experimental specimen is calculated as the difference value of strains along the loading direction and its orthogonal direction according to the ASTM D3518M-1994(R01) standard [314], illustrated in Figure 5-1. Therefore, the shear strain of the plain weave fabric composite, $\varepsilon_{\text{Shear}}$, is calculated through eq. (5.2),

$$\varepsilon_{\text{Shear}} = \varepsilon_{P_2} - \varepsilon_{P_1}, \tag{5.2}$$

by setting the ratio, λ in eq. (5.1), to zero; ε_{P_1} and ε_{P_2} are the tensile strains along the P_1 and P_2 directions, respectively. The shear stress of the specimen, τ, is calculated as half of the tensile loading stress, which is defined in eq. (5.3),

[4] The model has been uploaded for Open Access: https://doi.org/10.5281/zenodo.2630555

$$\tau = \frac{\sigma_{P_2}}{2} = \frac{P_2}{2L_1\left(h_1 + h_2\right)}, \tag{5.3}$$

where σ_{P_2} is the tensile loading stress along the P_2 direction; L_1 is one quarter of the undulation length of the weft tow and h_1 and h_2 are the thicknesses of the weft and warp tows, respectively. Therefore, the shear modulus can be obtained from the shear stress divided by the shear strain. For the shear strength of plain weave fabric composites, the interlaminar shear stress on the interlacing surface between weft and warp tows is critical as this is where the shear debonding failure is frequently found. Therefore, the maximum interlaminar shear stress at the interlacing interface is evaluated to obtain the shear strength.

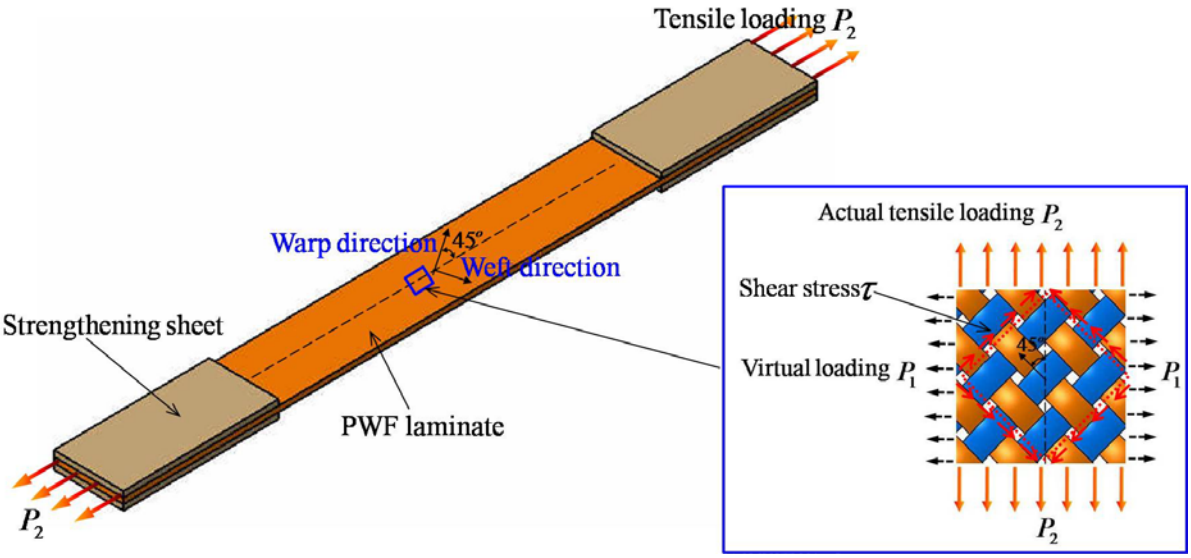

Figure 5- 1. Schematic experimental specimen and plain weave fabric composites under virtual ±45° off-axis biaxial tensile loadings

5.3 Rapid shear modulus prediction of plain weave fabric composites

Plain weave fabric composites have regular and periodical features and therefore, a repeated unit cell is utilised in the current model to reduce complexity and computational cost; this is identified in Figure 5-2. Two geometrical assumptions are inherited from Chapter 4 and the literature [39,44,299] to establish the geometrical expression of the plain weave fabric composites as follows:

(1) The cross-section of the tow is constituted by a flat rectangle with two semicircles at each end of width, w_1 and w_2, and thickness, h_1 and h_2, illustrated in Figure 5-2.

(2) The tows are idealised as curved beams, meaning that the neutral axis of the undulated tows is assumed to be a smooth and continuous sinusoidal curve, shown in Figure 5-3.

Furthermore, the analytical model assumes the shape of the tow path is fixed as smooth and continuous sinusoidal curve under biaxial tensile loadings in order to avoid dynamic analysis getting involved which increases the complexity of the model. Therefore, according to assumption (1) and Figure 5-2, the cross-sectional area, A_i, and moment of inertia along the transverse direction of the warp and weft tows, I_{yi}, are the same as the eqs. (4.1) and (4.2) in Chapter 4. The moment of inertia along the through-thickness directions of the tows, I_{zi}, and the polar inertia moment, I_{pi}, are respectively formulated as eqs. (5.4)-(5.5), which are the same as in [39,44,299],

$$I_{zi} = \frac{1}{64}\pi h_i^4 + \frac{1}{12} h_i \left(w_i - h_i\right)^3, \tag{5.4}$$

$$I_{pi} = I_{yi} + I_{zi}, \tag{5.5}$$

where h_i and w_i are the yarn thickness and width, where the subscript i is equal to 1 to represent the weft tows and is 2 when representing the warp tows. According to the assumption (2) and Figure 5-3, the undulated neutral axis of the yarns, z, is expressed the same as eq. (4.3) for weft tow and eq. (4.4) for warp tow in Chapter 4. The tow volume fraction, V_y, and the fibre volume fraction in a single yarn, V_f^y, are summarised as eqs. (4.7) and (4.8) of Chapter 4.

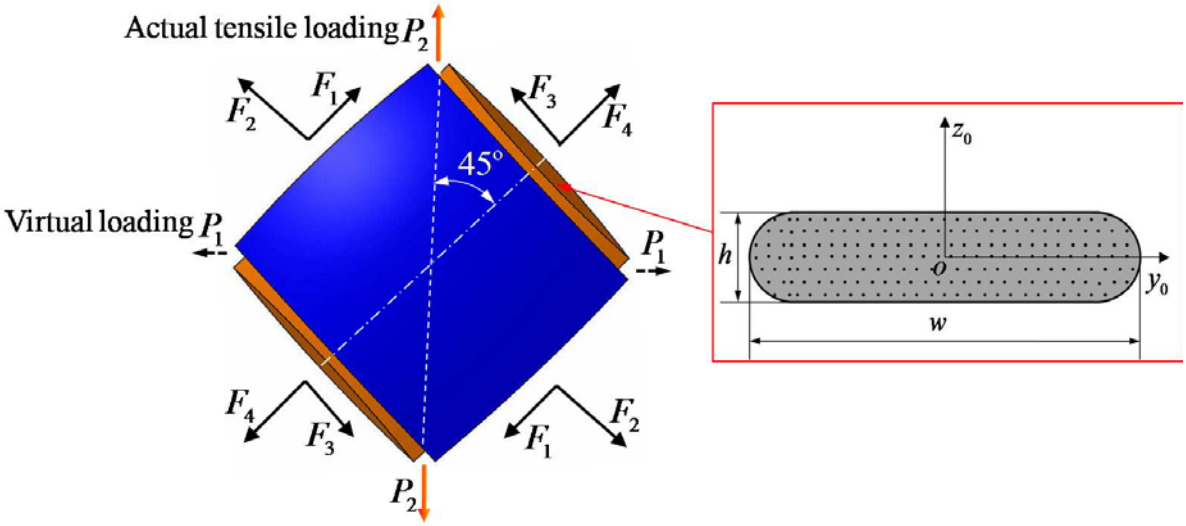

Figure 5- 2. External forces on warp and weft yarns under virtual ±45° off-axis biaxial tension with the schematic yarn cross-section

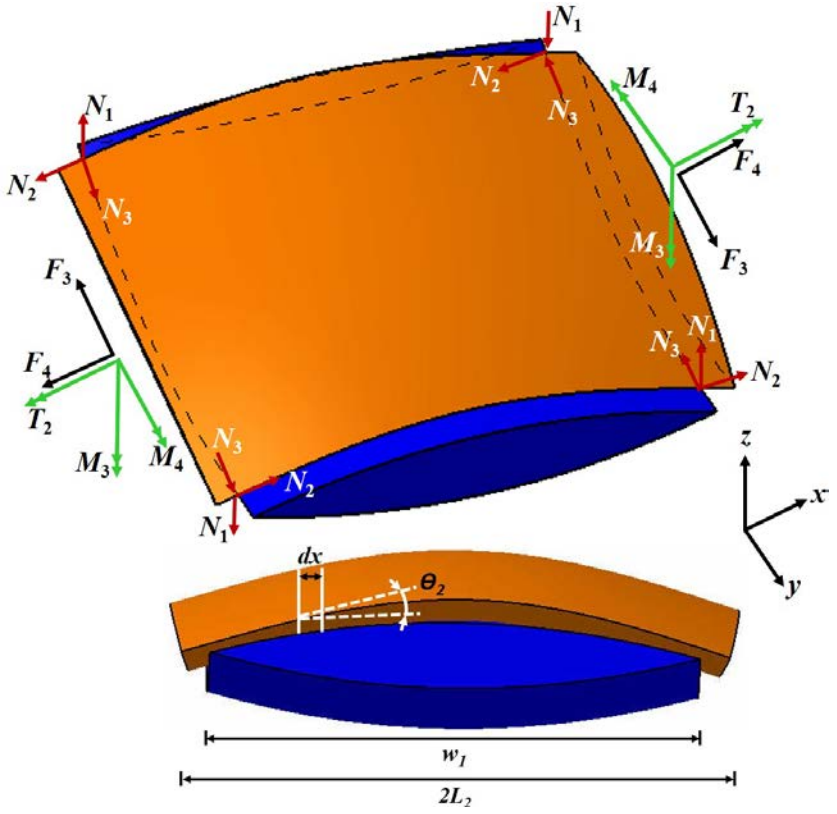

(A)

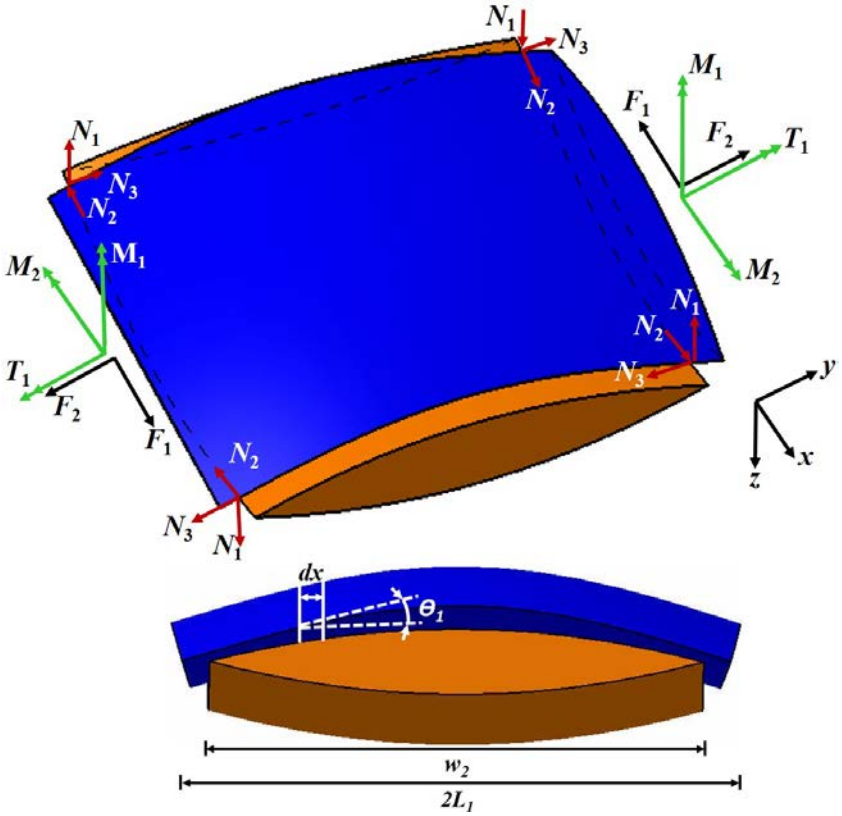

(B)

Figure 5- 3. Internal forces and bending moments on (A) warp and (B) weft yarns under virtual ±45° off-axis biaxial tension

The force decomposition of P_1 and P_2 can be represented as eqs. (5.6) and (5.7), according to the illustration in Figure 5-2,

$$P_1 = \frac{\sqrt{2}}{2}\left(F_4 - F_3 + F_2 - F_1\right), \tag{5.6}$$

$$P_2 = \frac{\sqrt{2}}{2}\left(F_1 + F_2 + F_3 + F_4\right), \tag{5.7}$$

where F_1 and F_3 are decomposed shear forces applied to the weft and warp yarns respectively and F_2 and F_4 are the decomposed tensile forces on the weft and warp yarns. Since the unit cell satisfies the moment balance, three moment balancing equations are summarised in eq. (5.8),

$$\begin{cases} M_1 + F_1 L_1 = N_2 w_2 + N_3 w_1, \\ M_3 + F_3 L_2 = N_2 w_2 + N_3 w_1, \\ F_1 L_1 = F_3 L_2, \end{cases} \tag{5.8}$$

where M_1 and M_3 are the bending moments induced by the shear forces, N_2 and N_3 are the in-plane forces induced by the rotation of the yarns; these moments and internal forces are illustrated in Figure 5-3. Eq. (5.8) can therefore be simplified to eq. (5.9),

$$\begin{cases} M_1 = M_3 = M_v, \\ \dfrac{F_1}{F_3} = \dfrac{L_2}{L_1} = \gamma, \end{cases} \tag{5.9}$$

where M_1 and M_3 are replaced by M_v and the relationship between F_1 and F_3 is established by γ to reduce the number of undetermined variables in the model. Eqs. (5.6), (5.7) and (5.9) can be combined by assuming P_1, P_2 and F_2 are known variables and therefore the decomposed forces are represented as eq. (5.10),

$$\begin{cases} F_1 = \gamma \dfrac{P_2 - P_1}{\sqrt{2}\left(1+\gamma\right)}, \\ F_3 = \dfrac{P_2 - P_1}{\sqrt{2}\left(1+\gamma\right)}, \\ F_4 = \dfrac{P_1 + P_2}{\sqrt{2}} - F_2. \end{cases} \tag{5.10}$$

The micromechanical analysis is illustrated in Figure 5-3, where T_1 and T_2 are internal torques and M_2 and M_4 are tensile force induced bending moments on the weft and warp tows. N_1 is an internal force along the through-thickness direction at the interaction area between the weft and warp yarns. According to the micromechanical analysis illustrated in Figure 5-3 and eqs. (5.9) and (5.10) and eq. (4.6) of Chapter 4, the total internal forces along x axes, *F(x)*, y axes bending moments, $M_y(x)$, z axes bending moments, $M_z(x)$, and torque moments, $T_x(x)$ at each cross-section for weft tow are defined as eqs. (5.11)-(5.14),

$$F_1(x) = F_2 \cos\theta_1 = \frac{F_2}{\sqrt{1+\left(\frac{\pi h_2}{4L_1}\cos\frac{\pi x}{2L_1}\right)^2}} \qquad \left(0 \le x < L_1\right), \tag{5.11}$$

$$M_{y1}(x) = M_2 + \frac{F_2 h_2}{2}\sin\frac{\pi x}{2L_1} \qquad \left(0 \le x < L_1\right), \tag{5.12}$$

$$M_{z1}(x) = \begin{cases} M_v + \gamma\dfrac{P_2 - P_1}{\sqrt{2}\left(1+\gamma\right)}x & \left(0 \le x < L_1 - \dfrac{w_2}{2}\right), \\ M_v + \gamma\dfrac{P_2 - P_1}{\sqrt{2}\left(1+\gamma\right)}x - 2N_2\left[x - \left(L_1 - \dfrac{w_2}{2}\right)\right] - N_3 w_1 & \left(L_1 - \dfrac{w_2}{2} \le x < L_1\right), \end{cases} \tag{5.13}$$

$$T_{x1}(x) = \begin{cases} T_1 + \gamma\dfrac{\left(P_2 - P_1\right)h_2}{2\sqrt{2}\left(1+\gamma\right)}\sin\dfrac{\pi x}{2L_1} & \left(0 \le x < L_1 - \dfrac{w_2}{2}\right), \\ T_1 + \gamma\dfrac{\left(P_2 - P_1\right)h_2}{2\sqrt{2}\left(1+\gamma\right)}\sin\dfrac{\pi x}{2L_1} - N_1 w_1 - N_2 h_2\left[\sin\dfrac{\pi x}{2L_1} - \sin\dfrac{\pi\left(L_1 - \dfrac{w_2}{2}\right)}{2L_1}\right] & \left(L_1 - \dfrac{w_2}{2} \le x < L_1\right), \end{cases} \tag{5.14}$$

where L_i is one quarter undulation length of the tow since one period of the tow is rotationally symmetric and a half period of the tow is axially symmetric. Using the same methodology, the total internal forces, bending and torque moments at each cross-section for warp tow are derived as eqs. (5.15)-(5.18),

$$F_2(x)=F_4\cos\theta_2=\frac{\frac{P_1+P_2}{\sqrt{2}}-F_2}{\sqrt{1+\left(\frac{\pi h_1}{4L_2}\cos\frac{\pi x}{2L_2}\right)^2}}\qquad \left(0\le x<L_2\right), \tag{5.15}$$

$$M_{y2}(x)=M_4+\left(\frac{P_1+P_2}{\sqrt{2}}-F_2\right)\frac{h_1}{2}\sin\frac{\pi x}{2L_2}\qquad \left(0\le x<L_2\right), \tag{5.16}$$

$$M_{z2}(x)=\begin{cases}M_v+\dfrac{P_2-P_1}{\sqrt{2}\left(1+\gamma\right)}x & \left(0\le x<L_2-\dfrac{w_1}{2}\right),\\ M_v+\dfrac{P_2-P_1}{\sqrt{2}\left(1+\gamma\right)}x-N_2w_2-2N_3\left[x-\left(L_2-\dfrac{w_1}{2}\right)\right] & \left(L_2-\dfrac{w_1}{2}\le x<L_2\right),\end{cases} \tag{5.17}$$

$$T_{x2}(x)=\begin{cases}T_2+\dfrac{\left(P_2-P_1\right)h_1}{2\sqrt{2}\left(1+\gamma\right)}\sin\dfrac{\pi x}{2L_2} & \left(0\le x<L_2-\dfrac{w_1}{2}\right),\\ T_2+\dfrac{\left(P_2-P_1\right)h_1}{2\sqrt{2}\left(1+\gamma\right)}\sin\dfrac{\pi x}{2L_2}-N_1w_2-N_3h_1\left[\sin\dfrac{\pi x}{2L_2}-\sin\dfrac{\pi\left(L_2-\dfrac{w_1}{2}\right)}{2L_2}\right] & \left(L_2-\dfrac{w_1}{2}\le x<L_2\right).\end{cases} \tag{5.18}$$

The minimum complementary potential energy principle is used to obtain the nine undetermined variables in the eqs. (5.19)-(5.26): T_1, T_2, M_2, M_4, M_v, N_1, N_2, N_3 and F_2. Keeping a similar format to [39,44,299], which is similar as in eqs. (4.12)-(4.13) of Chapter 4, the newly derived complementary potential energy of the weft yarns, U_1^*, in the unit cell is derived as eq. (5.19),

$$\begin{aligned}U_1^*=&\frac{1}{EA_1}\int_0^{L_1}\left(F_1(x)\right)^2\sqrt{1+\left(\frac{\pi h_2}{4L_1}\cos\frac{\pi x}{2L_1}\right)^2}\,dx\\ &+\frac{1}{EI_{y1}}\int_0^{L_1}\left(M_{y1}(x)\right)^2\sqrt{1+\left(\frac{\pi h_2}{4L_1}\cos\frac{\pi x}{2L_1}\right)^2}\,dx\\ &+\frac{1}{EI_{z1}}\int_0^{L_1}\left(M_{z1}(x)\right)^2\sqrt{1+\left(\frac{\pi h_2}{4L_1}\cos\frac{\pi x}{2L_1}\right)^2}\,dx\\ &+\frac{1}{GI_{p1}}\int_0^{L_1}\left(T_{x1}(x)\right)^2\sqrt{1+\left(\frac{\pi h_2}{4L_1}\cos\frac{\pi x}{2L_1}\right)^2}\,dx,\end{aligned} \tag{5.19}$$

and the complementary potential energy of the warp yarns, U_2^*, is derived as eq. (5.20),

$$
\begin{aligned}
U_2^* = & \frac{1}{EA_2}\int_0^{L_2}\left(F_2(x)\right)^2\sqrt{1+\left(\frac{\pi h_1}{4L_2}\cos\frac{\pi x}{2L_2}\right)^2}\,dx \\
& + \frac{1}{EI_{y2}}\int_0^{L_2}\left(M_{y2}(x)\right)^2\sqrt{1+\left(\frac{\pi h_1}{4L_2}\cos\frac{\pi x}{2L_2}\right)^2}\,dx \\
& + \frac{1}{EI_{z2}}\int_0^{L_2}\left(M_{z2}(x)\right)^2\sqrt{1+\left(\frac{\pi h_1}{4L_2}\cos\frac{\pi x}{2L_2}\right)^2}\,dx \\
& + \frac{1}{GI_{p2}}\int_0^{L_2}\left(T_{x2}(x)\right)^2\sqrt{1+\left(\frac{\pi h_1}{4L_2}\cos\frac{\pi x}{2L_2}\right)^2}\,dx,
\end{aligned}
\tag{5.20}
$$

where E is the elastic modulus and G is the in-plane shear modulus of the tows, and they are obtained by using the rule of mixtures, which has been shown to provide accurate results for unidirectional fibres in resin, with fibre elastic and shear moduli, E_f and G_f, and resin elastic and shear moduli, E_m and G_m, and the fibre volume fraction in a single yarn, V_f^y (derived from eq. (4.8) in Chapter 4), which has been shown to provide accurate results. By substituting eqs. (5.11)-(5.18) into eqs. (5.19) and (5.20), the complementary potential energy of weft tows is summarised as eq. (5.21),

$$
\begin{aligned}
U_1^* = & Q_1P_1^2 + Q_2P_2^2 + Q_3F_2^2 + Q_4M_2^2 + Q_5M_v^2 + Q_6N_1^2 + Q_7N_2^2 + Q_8N_3^2 + Q_9T_1^2 + Q_{10}P_1P_2 + Q_{11}P_1M_v \\
& + Q_{12}P_1N_1 + Q_{13}P_1N_2 + Q_{14}P_1N_3 + Q_{15}P_1T_1 + Q_{16}P_2M_v + Q_{17}P_2N_1 + Q_{18}P_2N_2 + Q_{19}P_2N_3 \\
& + Q_{20}P_2T_1 + Q_{21}F_2M_2 + Q_{22}M_vN_2 + Q_{23}M_vN_3 + Q_{24}N_1N_2 + Q_{25}N_1T_1 + Q_{26}N_2N_3 + Q_{27}N_2T_1,
\end{aligned}
\tag{5.21}
$$

and the complementary potential energy of warp tows is summarised as eq. (5.22),

$$
\begin{aligned}
U_2^* = & Q_{28}P_1^2 + Q_{29}P_2^2 + Q_{30}F_2^2 + Q_{31}M_4^2 + Q_{32}M_v^2 + Q_{33}N_1^2 + Q_{34}N_2^2 + Q_{35}N_3^2 + Q_{36}T_2^2 + Q_{37}P_1P_2 \\
& + Q_{38}P_1F_2 + Q_{39}P_1M_4 + Q_{40}P_1M_v + Q_{41}P_1N_1 + Q_{42}P_1N_2 + Q_{43}P_1N_3 + Q_{44}P_1T_2 + Q_{45}P_2F_2 \\
& + Q_{46}P_2M_4 + Q_{47}P_2M_v + Q_{48}P_2N_1 + Q_{49}P_2N_2 + Q_{50}P_2N_3 + Q_{51}P_2T_2 + Q_{52}F_2M_4 + Q_{53}M_vN_2 \\
& + Q_{54}M_vN_3 + Q_{55}N_1N_3 + Q_{56}N_1T_2 + Q_{57}N_2N_3 + Q_{58}N_3T_2,
\end{aligned}
\tag{5.22}
$$

where $Q_n\left(n=1,2,3,.....,58\right)$ are the transformation variables that listed in Appendix II-A. The transformation variables $K_n\left(n=1,2,3,.....,72\right)$ are contained in the $Q_n\left(n=1,2,3,.....,58\right)$, which are summarised in Appendix II-B. By aggregating the eqs. (5.21) and (5.22), the total complementary potential energy of the unit cell, $\prod^*$, is obtained, which is expressed in eq. (5.23).

$$
\begin{aligned}
\Pi^* = U_1^* + U_2^* = {} & \left(Q_1 + Q_{28}\right)P_1^2 + \left(Q_2 + Q_{29}\right)P_2^2 + \left(Q_3 + Q_{30}\right)F_2^2 + Q_4 M_2^2 + Q_{31} M_4^2 \\
& + \left(Q_5 + Q_{32}\right)M_v^2 + \left(Q_6 + Q_{33}\right)N_1^2 + \left(Q_7 + Q_{34}\right)N_2^2 + \left(Q_8 + Q_{35}\right)N_3^2 + Q_9 T_1^2 + Q_{36} T_2^2 \\
& + \left(Q_{10} + Q_{37}\right)P_1 P_2 + Q_{38} P_1 F_2 + Q_{39} P_1 M_4 + \left(Q_{11} + Q_{40}\right)P_1 M_v + \left(Q_{12} + Q_{41}\right)P_1 N_1 \\
& + \left(Q_{13} + Q_{42}\right)P_1 N_2 + \left(Q_{14} + Q_{43}\right)P_1 N_3 + Q_{15} P_1 T_1 + Q_{44} P_1 T_2 + Q_{45} P_2 F_2 + Q_{46} P_2 M_4 \\
& + \left(Q_{16} + Q_{47}\right)P_2 M_v + \left(Q_{17} + Q_{48}\right)P_2 N_1 + \left(Q_{18} + Q_{49}\right)P_2 N_2 + \left(Q_{19} + Q_{50}\right)P_2 N_3 \\
& + Q_{20} P_2 T_1 + Q_{51} P_2 T_2 + Q_{21} F_2 M_2 + Q_{52} F_2 M_4 + \left(Q_{22} + Q_{53}\right)M_v N_2 + \left(Q_{23} + Q_{54}\right)M_v N_3 \\
& + Q_{24} N_1 N_2 + Q_{55} N_1 N_3 + Q_{25} N_1 T_1 + Q_{56} N_1 T_2 + \left(Q_{26} + Q_{57}\right)N_2 N_3 + + Q_{27} N_2 T_1 + Q_{58} N_3 T_2 .
\end{aligned}
\tag{5.23}
$$

By minimising the total complementary potential energy for all the nine unknown variables and using eq. (5.1), the nine undetermined variables are transformed as eq. (5.24),

$$
\begin{bmatrix} F_2 \\ M_2 \\ M_4 \\ T_1 \\ T_2 \\ M_v \\ N_1 \\ N_2 \\ N_3 \end{bmatrix}
= -P_2
\begin{bmatrix}
2\left(Q_3 + Q_{30}\right) & Q_{21} & Q_{52} & 0 & 0 & 0 & 0 & 0 & 0 \\
Q_{21} & 2Q_4 & 0 & 0 & 0 & 0 & 0 & 0 & 0 \\
Q_{52} & 0 & 2Q_{31} & 0 & 0 & 0 & 0 & 0 & 0 \\
0 & 0 & 0 & 2Q_9 & 0 & 0 & Q_{25} & Q_{27} & 0 \\
0 & 0 & 0 & 0 & 2Q_{36} & 0 & Q_{56} & 0 & Q_{58} \\
0 & 0 & 0 & 0 & 0 & 2\left(Q_5 + Q_{32}\right) & 0 & \left(Q_{22} + Q_{53}\right) & \left(Q_{23} + Q_{54}\right) \\
0 & 0 & 0 & Q_{25} & Q_{56} & 0 & 2\left(Q_6 + Q_{33}\right) & Q_{24} & Q_{55} \\
0 & 0 & 0 & Q_{27} & 0 & \left(Q_{22} + Q_{53}\right) & Q_{24} & 2\left(Q_7 + Q_{34}\right) & \left(Q_{26} + Q_{57}\right) \\
0 & 0 & 0 & 0 & Q_{58} & \left(Q_{23} + Q_{54}\right) & Q_{55} & \left(Q_{26} + Q_{57}\right) & 2\left(Q_8 + Q_{35}\right)
\end{bmatrix}^{-1}
\begin{bmatrix}
\lambda Q_{38} + Q_{45} \\
0 \\
\lambda Q_{39} + Q_{46} \\
\lambda Q_{15} + Q_{20} \\
\lambda Q_{44} + Q_{51} \\
\lambda\left(Q_{11} + Q_{40}\right) + \left(Q_{16} + Q_{47}\right) \\
\lambda\left(Q_{12} + Q_{41}\right) + \left(Q_{17} + Q_{48}\right) \\
\lambda\left(Q_{13} + Q_{42}\right) + \left(Q_{18} + Q_{49}\right) \\
\lambda\left(Q_{14} + Q_{43}\right) + \left(Q_{19} + Q_{50}\right)
\end{bmatrix},
\tag{5.24}
$$

and each undetermined variable is defined in eqs. (5.25)-(5.33) using Cramer's rule,

$$F_2 = D_1 P_2, \tag{5.25}$$

$$M_2 = D_2 P_2, \tag{5.26}$$

$$M_4 = D_3 P_2, \tag{5.27}$$

$$T_1 = D_4 P_2, \tag{5.28}$$

$$T_2 = D_5 P_2, \tag{5.29}$$

$$M_v = D_6 P_2, \tag{5.30}$$

$$N_1 = D_7 P_2, \tag{5.31}$$

$$N_2 = D_8 P_2, \tag{5.32}$$

$$N_3 = D_9 P_2, \tag{5.33}$$

where the transformation variables $D_n\left(n=1,2,3,.....,9\right)$ are demonstrated in Appendix II-C. Since P_1 is a virtual tensile loading utilised for obtaining the strains along the P_1 direction, λ in eq. (5.1) is set to zero to make $P_1 = 0$. The strains along the P_1 and P_2 tensile loading directions are defined through dividing the displacement along P_1 direction, $\delta_{P_1(\lambda=0)}$, and P_2 direction, $\delta_{P_2(\lambda=0)}$, by their original length, $2L_1$ and $2L_2$, respectively. They are calculated by taking the partial differentials of the total complementary potential energy with respect to the actual and virtual tensile forces in eqs. (5.34) and (5.35),

$$\varepsilon_{P_1} = \frac{\delta_{P_1(\lambda=0)}}{2L_1} = \frac{\partial \Pi^*}{\partial P_1}(2L_1)^{-1} = \Big[\left(Q_{10}+Q_{37}\right)+Q_{38}D_{1(\lambda=0)}+Q_{39}D_{3(\lambda=0)}+\left(Q_{11}+Q_{40}\right)D_{6(\lambda=0)}$$
$$+\left(Q_{12}+Q_{41}\right)D_{7(\lambda=0)}+\left(Q_{13}+Q_{42}\right)D_{8(\lambda=0)}+\left(Q_{14}+Q_{43}\right)D_{9(\lambda=0)}+Q_{15}D_{4(\lambda=0)}+Q_{44}D_{5(\lambda=0)}\Big]\frac{P_2}{2L_1}, \tag{5.34}$$

$$\varepsilon_{P_2} = \frac{\delta_{P_2(\lambda=0)}}{2L_2} = \frac{\partial \Pi^*}{\partial P_2}(2L_2)^{-1} = \Big[2\left(Q_2+Q_{29}\right)+Q_{45}D_{1(\lambda=0)}+Q_{46}D_{3(\lambda=0)}+\left(Q_{16}+Q_{47}\right)D_{6(\lambda=0)}$$
$$+\left(Q_{17}+Q_{48}\right)D_{7(\lambda=0)}+\left(Q_{18}+Q_{49}\right)D_{8(\lambda=0)}+\left(Q_{19}+Q_{50}\right)D_{9(\lambda=0)}+Q_{20}D_{4(\lambda=0)}+Q_{51}D_{5(\lambda=0)}\Big]\frac{P_2}{2L_2}. \tag{5.35}$$

The shear strain of the plain weave fabric composite is defined in eq. (5.2) and the shear stress of the plain weave fabrics is defined in eq. (5.3). Therefore, the shear modulus of the plain weave fabrics is expressed as eq. (5.36),

$$G_{f12} = \frac{\tau}{\varepsilon_{\text{Shear}}}. \tag{5.36}$$

According to the rule of mixtures and yarn volume fraction, the shear modulus of the plain weave fabric composite is expressed as eq. (5.37),

$$G_{12} = \frac{G_{f12}G_m}{G_m V_y + G_{f12}\left(1-V_y\right)}. \tag{5.37}$$

5.4 Rapid shear strength predictions of plain weave fabric composites

The shear strength is obtained by finding the maximum interlaminar shear stress on the interlacing surface, which is approximated as a rectangular section. According to the elastic mechanics theory of rectangular section torque [315], the maximum shear stress is located at the mid-point of the long edge of the section. Therefore, the maximum shear stress, τ_{max}, is expressed as eq. (5.38) for weft tow width larger than warp tow width,

$$\tau_{\max} = \frac{T_{\text{in}}}{\alpha w_1 w_2^2} \qquad \left(w_1 \geq w_2\right), \tag{5.38}$$

and eq. (5.39) for warp tow width larger than weft tow width,

$$\tau_{\max} = \frac{T_{\text{in}}}{\alpha w_2 w_1^2} \qquad \left(w_1 < w_2\right), \tag{5.39}$$

where T_{in} is the internal torque moment between the weft and warp tows' interlacing surface. The torque moment is induced by the internal forces N_2 and N_3, which is defined in eq. (5.40),

$$T_{in} = 2N_2 w_2 + 2N_3 w_1 = 2P_2\left(D_{8(\lambda=0)} w_2 + D_{9(\lambda=0)} w_1\right), \tag{5.40}$$

by substituting eqs. (5.32) and (5.33). The α in eqs. (5.38) and (5.39) is a coefficient table related to the torque moment, which is controlled by the rectangular edge ratio [315]. The coefficient table is shown in Table 5-1,

Table 5- 1. The coefficient related to the torque moment of rectangular cross-section [315]

w_l / w_s	1.0	1.2	1.5	1.75	2.0	2.5	3.0	4.0	6.0	8.0	10.0	∞
α	0.208	0.219	0.231	0.239	0.246	0.258	0.267	0.282	0.299	0.307	0.313	0.333

where w_l represents the yarn having larger width between the weft and warp tows and w_s represents the yarn having smaller width between the weft and warp tows. The table is transferred to two nonlinear regression equations as eqs. (5.41) and (5.42),

$$\alpha = 0.3401 - 0.2923\left(w_1 / w_2\right)^{-1} + 0.2570\left(w_1 / w_2\right)^{-2} - 0.0968\left(w_1 / w_2\right)^{-3} \qquad \left(w_1 \geq w_2\right), \tag{5.41}$$

$$\alpha = 0.3401 - 0.2923\left(w_2 / w_1\right)^{-1} + 0.2570\left(w_2 / w_1\right)^{-2} - 0.0968\left(w_2 / w_1\right)^{-3} \qquad \left(w_1 < w_2\right). \tag{5.42}$$

By substituting eqs. (5.40)-(5.42) into (5.38) and (5.39), the critical equivalent external force on the plain weave preforms, P_2, is expressed as eqs. (5.43) and (5.44),

$$P_2 = \frac{\alpha \tau_{\max} w_1 w_2^2}{2\left(D_{8(\lambda=0)} w_2 + D_{9(\lambda=0)} w_1\right)} \qquad \left(w_1 \geq w_2\right), \tag{5.43}$$

$$P_2 = \frac{\alpha \tau_{\max} w_2 w_1^2}{2\left(D_{8(\lambda=0)} w_2 + D_{9(\lambda=0)} w_1\right)} \qquad \left(w_1 < w_2\right). \tag{5.44}$$

The ratio of stresses on textiles and resin is related to the elastic moduli of textiles, the resin and the yarn volume fraction. Therefore, the critical equivalent external force on the plain weave fabric composite, P_c, is expressed as eq. (5.45) [301], which is derived by the same processes as in eqs. (4.33)-(4.34) of Chapter 4,

$$P_c = P_2 + P_{\text{resin}} = P_2\left[1 + \frac{E_m\left(1 - V_y\right)}{E_{t2} V_y}\right]. \tag{5.45}$$

where E_{t2} is the elastic modulus of tow obtained from the analytical model proposed by Bai et al. [39] and P_{resin} is the external force distributed on the resin. Similar as eq. (5.2), the in-plane shear strength of the plain weave fabric composites, S, is obtained through the critical force divided by cross-sectional area as eqs. (5.46) and (5.47),

$$S = \frac{\sigma_{P_{\max}}}{2} = \frac{P_c}{2L_2 H} = \frac{\alpha \tau_{\max} w_1 w_2^2}{4L_2 H\left(D_{8(\lambda=0)} w_2 + D_{9(\lambda=0)} w_1\right)}\left[1 + \frac{E_m\left(1 - V_y\right)}{E_{t2} V_y}\right] \qquad \left(w_1 \geq w_2\right), \tag{5.46}$$

$$S = \frac{\sigma_{P_{\max}}}{2} = \frac{P_c}{2L_2 H} = \frac{\alpha \tau_{\max} w_2 w_1^2}{4L_2 H\left(D_{8(\lambda=0)} w_2 + D_{9(\lambda=0)} w_1\right)}\left[1 + \frac{E_m\left(1 - V_y\right)}{E_{t2} V_y}\right] \qquad \left(w_1 < w_2\right), \tag{5.47}$$

where H is the thickness of the plain weave fabric composite ply.

5.5 Validation of the analytical model

The results of the proposed analytical model are validated against E-glass/epoxy plain weave fabric composite specimens, EW220/5284, from the literature [44]. These specimens are manufactured with 55% fibre volume fraction (V_{f0}) using the resin transfer moulding technique. The details of the manufacturing process and cutting method are demonstrated in the literature [44].

The shear modulus and shear strength are both measured from bias extension experiments. The specimens are cut as illustrated in Figure 5-1 so that the angle between the tensile loading and the warp and weft tows are $\pm 45°$. The shear modulus and shear strength tests are respectively repeated five times using a MTS880-100Kn servo-hydraulic machine and the experimental results are shown in Table 5-2 [44]. The average shear modulus is 6.45 GPa and the average shear strength is 111.09 MPa with a standard deviation of 0.14 for the shear modulus and 0.39 for the shear strengths.

Table 5- 2. The experimental data of shear moduli and shear strengths of PWF composites [44]

Specimen No.	Shear Moduli (GPa)	Shear Strength (MPa)
1	6.58	111.63
2	6.19	110.97
3	6.58	111.42
4	6.46	110.91
5	6.43	110.53
Mean	6.45	111.09
Standard Deviation	0.14	0.39

Additional materials for validation are not available due to the lack of literature investigating the shear strength of the plain weave fabric composites and for those that are available the required material properties and yarn specifications are not fully documented. Therefore, only the shear strengths measured in these experiments are used to verify the proposed analytical model. Due to the lack of information about the yarn interlaminar shear strength of the EW220/5284 tows, the interlaminar shear strength of the E-glass/Epoxy tows are obtained from the available literature [316–321]. Those with the most similar properties are selected, determined by the material type, the fibre volume fraction, yarn fibre volume fraction or fibre weight fraction and manufacturing method. The yarn specifications are listed in Table 5-3, from which the fibre weight fraction can be calculated as 69% and the yarn fibre volume fraction as 67%. Nine values are found from the literature and the details of these specimens used in each study are summarised in Table 5-3 and are substituted into the analytical model. The interlaminar shear strengths from the most similar specimens are 32.49, 40 and 42 MPa [317,320] which provide prediction errors of 17.62%, 1.43% and 6.50%, giving mean error of 8.51%. This gives a higher level of accuracy compared to the previous literature, which has a 23% error when predicting the strength [46]. When all of the nine specimens are analysed the lowest prediction error is 0.67% when using the 39.7 MPa interlaminar shear strength and the highest error is 18.92% for the 46.9 MPa interlaminar strength.

The shear modulus prediction obtained from the proposed analytical model is compared with the shear modulus measured in the experiments in [44] to validate the method. The EW220/5284 is a specific type of composite material for aviation structures. The fibre specifications, material properties and verification results are listed in Table 5-3. The Young's and shear moduli of the fibre are derived by the paper from the fibre volume fraction and tensile and shear moduli of the yarn. It is shown that the prediction error for E-Glass/Epoxy plain weave fabric composites is 10.85%. To test the robustness and universality of the new model for the shear modulus predictions, another three types of plain weave fabric composite materials with six sets of yarn specifications, ply thickness and fibre volume fractions [45,322] are selected from the literature. The tow width, tow thickness and fibre and matrix material properties used in the new analytical model are the same as in the previous literature. However, the new analytical model requires a value for one quarter of the warp and weft tow undulation length and these values are calculated using half of the sum of the warp or weft tow widths and the gap between the adjacent warp or weft tows from the literature. The properties for each of these different materials are specified in Table 5-4. The previous literature both use the $\pm 45°$ bias extension experiments to obtain the shear moduli of the plain weave fabric composites. By comparing with their experimental results, it is shown that the prediction errors for Graphite/Epoxy, T-300 Carbon/Epoxy and four sets of E-Glass/Epoxy plain weave fabric composites are respectively 10.26%, 16.40%, 18.37%, 15.41%, 21.63% and 17.45%.

Table 5- 3. Experimental and predicted shear modulus and shear strength for EW220/5284 plain weave fabric composites

Material		EW220/5284 [44]					
Yarn Specifications		Values		Material Properties		Values	
L_1 (mm)		0.53		H (mm)		0.17	
L_2 (mm)		0.66		V_{f0}		0.55	
w_1 (mm)		1.17		E_f (GPa)		91.63	
w_2 (mm)		1.02		E_m (GPa)		3.20	
h_1 (mm)		0.07		G_f (GPa)		11.53	
h_2 (mm)		0.08		G_m (GPa)		1.10	
Shear Modulus		Experiments (GPa) [44]			6.45		
		Predictions (GPa)			5.75		
		Errors (%)			10.85		
Shear Strength	Experiments (MPa) [44]	111.09					
	Yarn Interlaminar Shear Strength τ_{max} (MPa)	33.4 & 37.4 [321][1]	32.49 [320][2]	37.8 & 46.9 [319][3]	33.06 [318][4]	39.7 [316][5]	40 to 42 [317][6]
	Predictions (MPa)	94.09 & 105.35	91.52	106.48 & 132.11	93.13	111.83	112.68 to 118.31
	Errors (%)	15.30 & 5.17	17.62	4.15 & 18.92	16.17	0.67	1.43 to 6.50

1. Both E-glass (Fothergill & Harvey Ltd.)/Ciba-Geigy XD 927 epoxy plain weave fabric; 53% & 57% fibre volume fraction; Both ply lay-up; Both impact test.
2. E-glass (Saint-Goban Vetrotex Company)/SC-15 epoxy (Applied Polymetric Inc.) plain weave fabric; 55% fibre volume fraction; Resin transfer moulding; Short beam shear test.
3. LY5052 E-glass/HY5052 epoxy & LY556 E-glass/HT972 epoxy unidirectional laminates; Both 62% fibre weight fraction; Both wet lay-up; Both short beam shear test.
4. E-glass (Feihuangtongda Co. Ltd., China)/DER354 epoxy (Dow Chemical Co., USA) plain weave fabric; 73% fibre weight fraction; Pre-preg hot-press process; Short beam shear test.
5. E-glass/epoxy plain weave fabric; 70% yarn fibre volume fraction; Obtained from the provided table of properties.
6. E-glass/epoxy unidirectional laminates; 64% fibre weight fraction; Resin transfer moulding; Short beam shear test; E_f is 85 GPa, E_m is 3.20 GPa and G_m is 1.16 GPa.

Table 5- 4. Experimental and predicted shear modulus with three types of materials and six sets of fibre specifications

Material		Graphite [1]	T300-Carbon[2]	E-Glass[3]	E-Glass[4]	E-Glass[5]	E-Glass[6]
Yarn Specifications	L_1 (mm)	1.25	0.96	0.45	0.54	0.43	0.47
	L_2 (mm)	1.25	1.10	0.45	0.53	0.43	0.47
	w_1 (mm)	1.80	1.80	0.45	0.68	0.86	0.60
	w_2 (mm)	1.80	1.45	0.45	0.62	0.84	0.60
	h_1 (mm)	0.35	0.10	0.048	0.09	0.11	0.09
	h_2 (mm)	0.35	0.10	0.048	0.09	0.11	0.09
Ply Thickness	H (mm)	1.002	0.20	0.096	0.18	0.3	0.18
Fibre Volume Fraction	V_{f0}	0.41	0.27	0.373	0.43	0.46	0.38
Elastic Modulus of Fibre	E_f (GPa)	387.875	230	72	72	72	72
Elastic Modulus of Matrix	E_m (GPa)	3.50	3.50	3.50	3.50	3.50	3.50
Shear Modulus of Fibre	G_f (GPa)	4.16	24	27.70	27.70	27.70	27.70
Shear Modulus of Matrix	G_m (GPa)	1.30	1.30	1.30	1.30	1.30	1.30
Shear Modulus (GPa)	Experiments	2.34	5.00	2.94	3.57	5.50	3.84
	Predictions	2.58	5.82	2.40	3.02	4.31	3.17
	Errors (%)	10.26	16.40	18.37	15.41	21.63	17.45

1. Graphite/Epoxy [322]
2. T300-Carbon/Epoxy [45]
3. E-Glass/Epoxy GLE2 [45]
4. E-Glass/Epoxy GLE3 [45]
5. E-Glass/Epoxy GLE5 [45]
6. E-Glass/Epoxy GLE8 [45]

The proposed model has an average accuracy of 15.24% with four types of materials and seven verification cases. This gives a similar accuracy to the prediction of shear moduli as the models proposed by Cheng et al. [44], 15.56%, with two types of verified materials and three cases, and Naik and Ganesh [45], 14.47%, with two types of materials and five cases. However, the current proposed model is more robust for different material types than both of these models, where the standard deviation of the prediction errors are 8.86 in Cheng et al., 12.76 for Naik and Ganesh's and 4.10 for the new method.

Additionally, the proposed model is able to predict both shear moduli and strengths but the model proposed by Cheng et al. [44] is only for shear modulus prediction and the prediction

of the strength is better than the Naik and Ganesh 23% as it has a worst case of 18.92% and a mean error of 8.51% using data from the most similar specimens. It is considered that the proposed analytical model is accurate and robust for the prediction of the shear modulus and strength of plain weave fabric composites.

Despite the improvements shown by the method there are some limitations. It is found that the model is not applicable for cases where the yarn dimensions of *2L/h* and *w/h* approximate 40 or larger, where these specifications are not representative of currently manufactured plain weave fabric composites. At this point the yarn no longer behaves like a beam, and is closer to a shell structure, due to the large span/height and width/height ratios. As the yarns are thin when the span/height and width/height ratios are large the dominant characteristic for determining the strength is the failure of the yarns under shear stress, instead of the maximum interlaminar shear stress on the interlacing surface between the interlaced yarns.

5.6 Chapter summary

This chapter proposes a novel analytical model for rapid prediction of the shear modulus and strength of plain weave fabric composites. The model is derived based on the minimum total complementary potential energy principle with virtual ±45° off-axis tensions on the orthogonally interlaced yarns. The proposed model is validated by experimental measurements from the literature for both shear modulus and shear strength. Additionally, the shear modulus from four types of materials with seven fabric specifications are verified against to demonstrate the general applicability of the method. The prediction errors for the shear modulus from the new model are compared with another five analytical models, showing an improved accuracy and higher robustness for different material types. A mean error of 15.24% and a maximum error of 21.63% in shear modulus and a mean error of 8.51% in shear strength from the experimental verification indicates the practical and effective use of the proposed model. The prediction error standard deviation of 4.10 for the seven cases reflects the improved robustness of the proposed model for a range types of materials.

Chapter 6. Optimal design of triaxial weave fabric composites under tension

6.1 Introduction

Novel ultralight applications are creating a demand for new materials. These new materials need to have good mechanical properties despite the low mass requirement. Triaxial weave fabrics (TWF), illustrated in Figure 6-1, are an example of materials finding growing usage in these structures. They are composites with longitudinal fibres in three directions, 0° and ± 60°, which provide mechanically quasi-isotropic properties, are lightweight due to the high degree of porosity and reduce the impact from air loads, which are achieved by the hexagonal openings on the material. It is also possible to design these structures with a small number of layers, as low as 1. The tensile strength to stiffness ratio and areal density of the material are the most important material properties in many applications of triaxial weave fabric composites, especially for deployable antenna on spacecraft and ultra-thin wing skins of unmanned aerial vehicles (UAVs) as these properties provide flexible structures that are damage resistant. The crimp, or undulation, of the yarns significantly influences the mechanical properties and areal density and requires an optimal weave pattern to maximise the strength to stiffness ratio while minimising the areal density of the material. However, it is not fully known how close the currently available fabric design schemes are to optimal, since these materials are relatively new.

It is essential to utilise a suitable algorithm for solving an optimisation problem. The 'no free lunch' theorem states that an algorithm that improves its performance on a category of problems inevitably degrades its performance on other types; optimisation algorithms are designed to be specialist to a problem type or have lower performance across all problems. Therefore, a variety of Genetic Algorithms have been developed to solve multi-objective problems categorised by their performance on different types of problems. As an example to demonstrate the importance of selecting the correct algorithm, Mutlu et al. [323] benchmark the performance of a number of popular algorithms on a composite grillage optimisation problem. The problem has limited input variables but even this simple problem demonstrates the need for state-of-the-art algorithms to evolve the entire Pareto front, and that these should be specialist algorithms reflecting the problem type. Reviewing the multi-objective optimisation papers, where a Pareto front is developed, the most popular Genetic Algorithm was NSGA-II but a number of older algorithms are still prevalent in this literature. However,

in much of the literature the names of the Genetic Algorithms used are not stated, making it difficult to assess the validity of the results.

In addition to the algorithm selection, the hyper-parameters, such as population size, number of generations and mutation and crossover type, affect the performance. From the reviewed literature the median number of the population sizes is approximating 600 individuals; this is consistent with the computer science literature where the popular algorithms selected for comparison in the CEC'09 benchmarking use this value or smaller [82]. The reviewed literature generally uses 100 generations or less, totalling 60,000 function calls, including the reviewed woven roving optimisation literature [10–13], with some papers using as few as 350 function evaluations [324]. There is a tendency for the number of function calls to be poorly documented in the composite material/structural optimisation literature and it is suspected that many use smaller numbers to reduce computational time but which may compromise the quality of the final solution. Additionally, the number of repeated independent run cycles is not stated in many papers, with a focus on fewer long runs, indicating that the optimisation results were obtained from one run making it difficult to determine the consistency of the results.

The literature review in Chapter 2 shows promising properties for Triaxial Weave Fabric composites but there is no consensus on which weave patterns provide optimal mechanical characteristics, for example high strength to stiffness ratios. The literature indicates that genetic algorithms are a popular method for optimising composite materials and structures but non-specialist Genetic Algorithms are utilised, many of which are out of date, on single objective or weighted multi-objective problems. It is proposed that current composite structural problems are becoming too complex for these non-specialist algorithms, leading to unresolved Pareto fronts. However, the selection of the correct Genetic Algorithm is difficult as the evolutionary computation literature is not categorised in a manner that reflects composite structures, defining the dominant categories as only constrained or unconstrained formulations for static multi-objective optimisation. Therefore the current study benchmarks state-of-the-art Genetic Algorithms on a multi-objective problem to find optimal designs, Pareto fronts, for TWF composites. The Genetic algorithms considered for the benchmarking are a specialist constrained, MLSGA-NSGAII, a specialist unconstrained, MOEA/D, the most popular, NSGA-II, and one population based local search method, MTS, which demonstrates generally good performance over both formulation types.

6.2 Triaxial weave fabric model for tensile strength and modulus

The tensile modulus and strength of the TWF composites are predicted using the minimum total complementary potential energy principle developed by Bai et al. [52]. Figure 6-1 shows the geometry parameters of a unit cell of a TWF composite with the idealized undulation shape of the yarn shown in comparison to a micrograph of the actual undulation. The shape of the cross-section of yarns were assumed as rectangle in [52]. The undulating neutral axis of the triaxial yarns is expressed using a sinusoidal function. The tensile loading is along the 0 degree yarn direction, where the internal forces and bending moments are shown in Figure 6-2.

The total complementary potential energy of the triaxial weave fabric composite is obtained after the micro-mechanical analysis. The undetermined internal forces and moments are obtained by minimising the total complementary potential energy. The strain of the triaxial weave fabric composite is obtained from the partial differential equation of total complementary potential energy over the external force. The tensile modulus is derived based on the obtained strain and the external force. Since the equation between the undetermined internal forces and external force are obtained, the critical external forces along 0 and 60 degrees yarns are able to be determined. The tensile strength of triaxial weave fabric composite is derived using the maximum stress failure criterion.

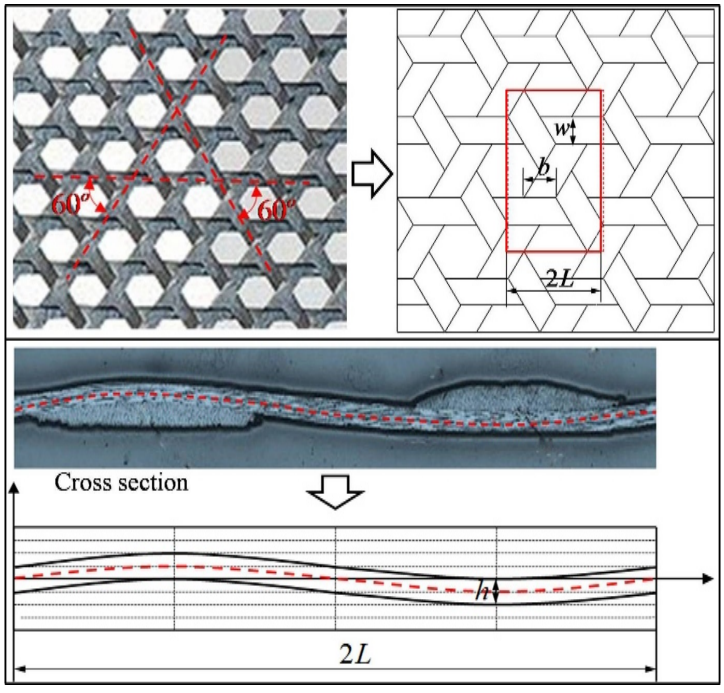

Figure 6- 1. Unit cell and micrograph of TWF composites [52]

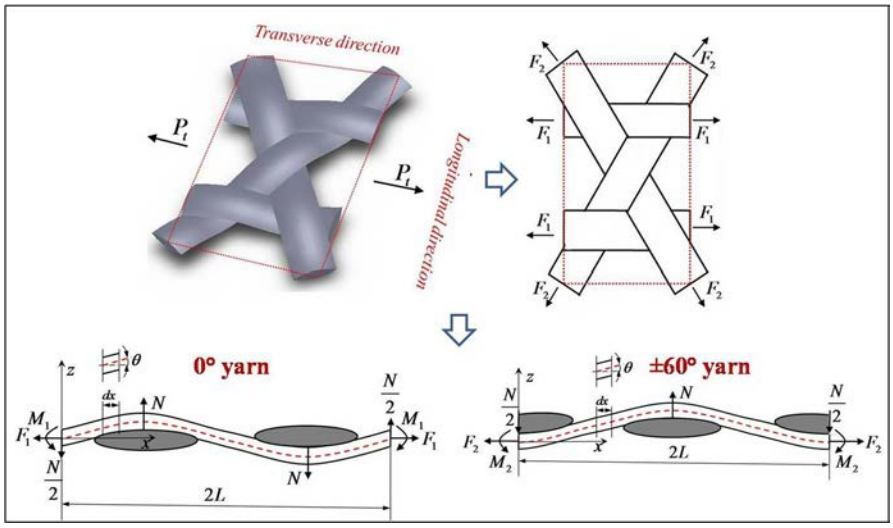

Figure 6- 2. Internal forces and bending moments on a unit cell [52]

It is referred to Bai et al. [52] for a detailed introduction to the analytical model. In brief the tensile modulus, E_T, is expressed in eq. (6.1) as,

$$E_T = \frac{P_T}{2\sqrt{3}\delta_T h} = \frac{1}{2\sqrt{3}h}[4(B_1 + B_4)C_1^2 + 8(B_5 + B_{11})(0.5 - C_1)^2 + 4(B_2 + 2B_6)C_2^2 + 8B_7C_3^2 + 4B_3C_1C_2 + 8B_8C_2(0.5 - C_1) + 8B_9C_3(0.5 - C_1) + 8B_{10}C_2C_3]^{-1}, \tag{6.1}$$

and strength per unit length, X_t, in eq. (6.2) as,

$$X_t = \frac{\min(P_{tf1}, P_{tf2})}{4\sqrt{3}hL}, \tag{6.2}$$

where the P_{tf1} and P_{tf2} are the internal tensile loading along the 0 degree and $\pm$ 60 degree yarns, L is a half of undulation length of tows and h is the thickness of the tows. B_i $(i = 1,2,\cdots,11)$ and C_i $(i = 1,2,3)$ are the transformation variables defined in Bai et al. [52].

The areal density of the triaxial weave fabric composites is evaluated according to the geometry parameters and idealised undulation shape. The fibre volume faction is 0.65, which is the same as the experimental sample in the Kueh and Pellegrino technical report [325]. The areal density of the T300/Hexcel 8552 fibre tow, ρ_c, is expressed in eq. (6.3),

$$\rho_c = \rho_f \times V_f^y + \rho_m \times \left(1 - V_f^y\right), \tag{6.3}$$

where the ρ_f is the density of the fibre 1760 kg/m^3, V_f^y is the fibre volume fraction of a yarn and ρ_m is the density of the matrix 1301 kg/m^3.

The surface density of the TWF composites can then be expressed in eq. (6.4) as,

$$\rho = 2\rho_c wh * 4\left[\int_0^{\frac{L}{2}} \sqrt{1+\left(\frac{\pi h}{2L}\cos\frac{\pi x}{L}\right)^2}\,dx + \int_0^{L} \sqrt{1+\left(\frac{\pi h}{2L}\sin\frac{\pi x}{L}\right)^2}\,dx\right] * \frac{1000000}{4\sqrt{3}L^2}, \quad (6.4)$$

where w is the width of the fibre tows. The surface density from eq. (6.4) is utilised with strength and stiffness to evaluate the fitness of a given weave.

In order to validate the analytical model the predictions are compared to mechanical properties taken from experiments performed by Kueh and Pellegrino [325] for T300/Hexel8552, Aoki and Yoshida [326] and Aoki et al. [327] for T300/NM35 and Zhao et al. [328] for a carbon fibre/epoxy resin; the yarn specifications are shown in Table 6-1. The comparison between the experimental results of the three types of TWF composites are compared to the analytical method in Table 6-2. The maximum error for the prediction of the tensile modulus and strength compared to the experiments are respectively 13.77% and 3.40%. The model provides an adequate prediction for the tensile modulus and strength analysis of TWF composites.

Table 6- 1. Manufacturer's data for fabric schema and yarn mechanical properties

	w / mm	h / mm	L / mm	E_f / GPa	G_f / GPa	E_m / GPa	G_m / GPa	E_y / GPa	G_y / GPa	X_{t0} / MPa
T300/Hexel8552 [325]	0.803	0.078	1.56	233	8.96	4.67	1.704	153.09	4.408	2296
T300/NM35 [326,327]	0.89	0.07	1.55	N/A	N/A	N/A	N/A	176	6.86	2673
Carbon fibre/ epoxy resin[328]	0.85	0.07	1.59	500	24	3.5	1.3	338.57	5.61	3400

Table 6- 2. Verification of tensile modulus and strength predictions from analytical model

		T300/Hexel8552[325]	T300/NM35[326, 327]	Carbon fibre/epoxy resin[328]
Modulus E_T (GPa)	Experiments	13.53	22.01	32.24
	Predictions	14.93	18.97	35.23
	Error	10.29%	13.77%	9.27%
Strength X_t (MPa)	Experiments	165.71	218.43	239.43
	Predictions	161.86	210.36	247.29
	Error	2.32%	3.40%	3.28%

In order to validate the areal density calculation the predictions are compared to the areal density taken from measurements performed by Kueh and Pellegrino [325]. The T300/Hexel8552 is used in the validation which has an undulation length of 1.56mm, a width of 0.803mm and a thickness of 0.078mm. The comparison between the measurements of TWF composites and the analytical method are shown in Table 6-3.

Table 6- 3. Verification of the areal density predictions from analytical model

		Density [g/m^2]
Measurements[325]	Specimen 1	104.62
	Specimen 2	112.35
	Specimen 3	112.31
	Specimen 4	114.20
	Specimen 5	115.08
	Mean	111.71
Prediction		111.36
Error		0.31%

6.3 Multi-objective design methodology

The shape of the objective space and its relationship with the variable space is currently unknown for TWF composites under tensile loading. This means that the problem type is not defined and that the corresponding algorithms suitable to that problem type cannot be selected. In this case the CEC'09 benchmarking [82] is used to select the algorithms for comparison: NSGA-II which has generally good performance across all problem sets, MOEA/D for unconstrained problems and MTS which came second and third on unconstrained and constrained problems; in addition a more recently developed Genetic Algorithm, MLSGA-NSGAII, is also included which performs well on constrained problems. Better constrained performance is shown by DMOEA-DD and LiuLi algorithms but the available versions of the

code cannot be converted to solve new problems and the documentation of the original algorithms is not enough to reproduce them.

A general schematic diagram of the optimisation process is illustrated in Figure 6-3. The four Genetic Algorithms are substituted into the selection and reproduction stage, where MTS has no crossover and mutation mechanisms. All individuals from the population are evaluated through the analytical model. In order to perform a fair test across the different Genetic Algorithms the same genetic operator types: selection, crossover and mutation, use the same operator rate, which is the same as those selected for the CEC'09 benchmarking [271]. MTS is a population based optimisation algorithm with a different set of hyper-parameters; these are kept the same as in the CEC'09 competition, except the population size and total number of function calls which are kept the same as the other three algorithms.

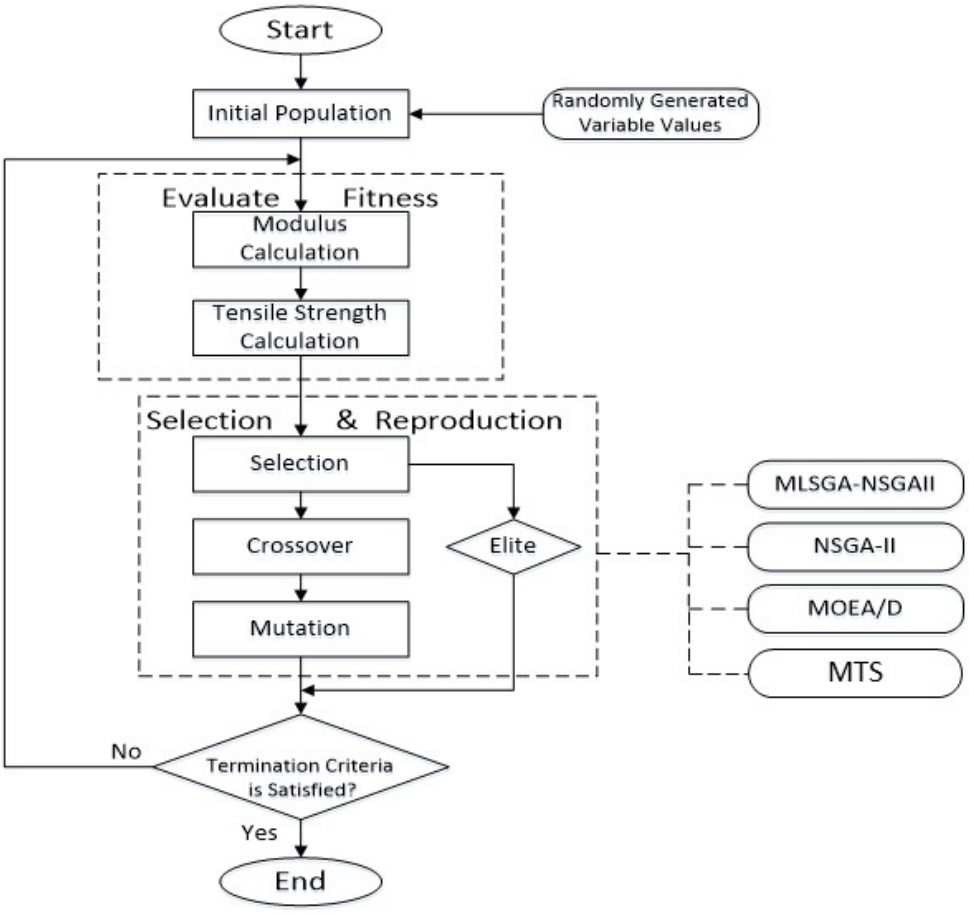

Figure 6- 3. General optimisation procedure

6.3.1 Formulation of multi-objective optimisation problem

The multi-objective optimisation problem, maximising tensile strength and modulus, is formulated in both a constrained and unconstrained format for the TWF composite material in eqs. (6.5) and (6.6),

$$\begin{cases} Minimise\ \{1/Tensile\ Strength(L,w,h), 1/Modulus(L,w,h)\}, \\ Subject\ to\ constraint: L \geq \sqrt{3} * w, \\ The\ range\ of\ variables: 0mm < L \leq 50mm, \\ 0mm < w \leq 10mm, \\ 0mm < h \leq 2mm. \end{cases} \tag{6.5}$$

$$\begin{cases} Minimise\ \{1/Tensile\ Strength(n,w,h), 1/Modulus(n,w,h)\}, \\ L = n * \left(50 - \sqrt{3} * w\right) + \sqrt{3} * w, \\ The\ range\ of\ variables: n \in [0,1], \\ 0mm < w \leq 10mm, \\ 0mm < h \leq 2mm. \end{cases} \tag{6.6}$$

These are to provide a material with a maximum strength and modulus under tensile load.

Since the elimination of the constraint simplifies the optimisation problem and reduces the computational cost, the multi-objective optimisation problems, maximising tensile strength and stiffness while minimising the areal density, are formulated as unconstrained for the TWF composite material in eq. (6.7),

$$\begin{cases} Minimise\ \{1/Tensile\ Strength(n,w,h), Surface\ Density(n,w,h)\}, \\ or \\ Minimise\ \{1/Tensile\ Stiffness(n,w,h), Surface\ Density(n,w,h)\}, \\ L = n * \left(50 - \sqrt{3} * w\right) + \sqrt{3} * w, \\ The\ range\ of\ variables: n \in [0,1], \\ 0mm < w \leq 10mm, \\ 0mm < h \leq 2mm. \end{cases} \tag{6.7}$$

T300/Hexel8552 is selected as the combination to be optimised as the most mature TWF composite. The variables yarn undulation length, L, yarn width, w, and height, h, are the parameters influencing the strength and modulus in the analytical model which are shown in Figure 6-1. The ranges of these variables are selected to ensure suitability for a range of existing applications for TWF composites. A constraint is in place to ensure the weave patterns can be manufactured. Current manufacturing precision can be controlled to 10^{-2} millimetres; this can be extended to three decimal places but is more expensive. The interval between variables has been selected at 10^{-10} millimetres, substantially beyond the capability of current manufacturing,

because the optimisation procedure seeks to fully document the objective space and uses an extended search space to benchmark the different optimisation algorithms.

6.3.2 NSGA-II

NSGA-II is the most commonly used Genetic Algorithm due to its success as a general solver with good performance across a range of problem types. It is commonly applied in the optimisation of composite materials and structures. The algorithm was first published by Deb et al. [75] in 2002 and is based on non-domination of solutions. Individuals in initial generated population are reproduced by real variable simulated binary crossover (SBX) and polynomial mutation. All solutions are real value coded. It is not like binary coded solutions where all the real value variables are transformed into binary strings to mimic the reproduction of chromosome in sexual reproductions. In real value coded algorithms, all the variables are kept as their real values limited in the boundary of each variable. In SBX, two real value coded solutions crossover to generate two children with the help of polynomial probability distribution and the children have the same average value as their parents. In polynomial mutation operator, a polynomial probability distribution is used to perturb a solution in a parent's vicinity. The mutation is not normally happened to each individuals in the population, which is only triggered when the randomly generated number is lower than the mutation rate.

If a solution is not simultaneously dominated on all objectives by any other solutions in the population, the solution is defined as non-dominated. Solutions not dominated by each other are classified into the same non-domination rank. The previous non-domination ranks are temporarily discounted when sorting out a new rank. It is recommended to Deb et al. [75] and Section 2.2.2.1 of Chapter 2 for a detailed introduction to NSGA-II and niching algorithms. The NSGA-II parameters used within this optimisation are listed in Table 6-4 where the selection, crossover and mutation types are default settings.

Table 6- 4. NSGA-II parameter definition

Initialisation	Initialisation type	Random
	Encoding type	Real value coded
Reproduction	Selection type	NSGAII – crowding distance
	Crossover type	Real variable SBX
	Crossover rate	0.7
	Mutation type	Polynomial mutation
	Mutation rate	0.08
Termination	Stopping criteria	Total number of iterations are reached

6.3.3 MOEA/D

MOEA/D is the top performer on unconstrained problems and was first published in Zhang and Li [80] in 2007. This algorithm is based on weight vector and decomposition, splitting the problem into a number of sub-problems and optimising each sub-problem separately. This algorithm is complex for the user as substantially different Pareto optimal solutions can be obtained by changing the weight vector. Since each generation uses only 5 to 10 percent of the total population size in MOEA/D, the generation number is much higher when compared to NSGA-II and MLSGA-NSGAII with the same population size and total function calls. For detailed information about MOEA/D and decomposition algorithms, it is referred to Zhang and Li [80] and Section 2.2.2.2 of Chapter 2. The MOEA/D parameters are summarised in Table 6-5. The selection, crossover and mutation types are MOEA/D default settings with default settings for crossover rate but the mutation rate is kept the same as NSGA-II and MLSGA-NSGAII. The multiple-parent crossover operator selects three parents each time to reproduce one offspring. For a particular variable, one of the three parents will be randomly chosen to be the basis and one of the rest two parents will be selected to crossover. The crossover is based on adding the randomly generated number between the rest two selected parents' values on the basis parent's value.

Table 6- 5. MOEA/D parameter definition

Initialisation	Initialisation type	Random
	Encoding type	Real value coded
Reproduction	Selection type	MOEA/D
	Crossover type	Multiple parents
	Crossover rate	1
	Mutation type	Polynomial mutation
	Mutation rate	0.08
Termination	Stopping criteria	Total number of iterations are reached

6.3.4 MLSGA-NSGAII

MLSGA was first introduced by Grudniewski and Sobey [329] in 2017 and introduces a collective level reproduction mechanism, in addition to the individual level used in standard genetic algorithms, and a split fitness function. The collectives are determined by a support vector machine (SVM), which is a popular type of machine learning algorithms for classification and regression analysis. In the MLSGA, there is a training process at the beginning for the SVM. A training set of individuals are marked as belong to different collectives according to their mean value and standard deviation. The SVM training algorithm builds a model that assigns new individuals to one category or the others, making it a non-probability classifier. MLSGA-NSGAII is a hybrid Genetic Algorithm that utilises the crowding distance of NSGA-II as the individual reproduction step in MLSGA. It is shown to have improved performance over NSGA-II on constrained and unconstrained problems, showing particularly strong performance on constrained problems. It is suggested to read Grudniewski and Sobey [329] and Section 2.2.2.4 of Chapter 2 for information about MLSGA in details. Table 6-6 summarises the specific parameters of MLSGA-NSGAII in the current paper. The selection, crossover and mutation types and rates are MLSGA-NSGAII default settings.

Table 6- 6. MLSGA-NSGAII parameter definition

Initialisation	Initialisation type	Random
	Encoding type	Real value coded
Classification	Classification method	Support Vector Machine
	Number of collectives	8
Individual Level	Individual fitness evaluation	MLSU
	Individuals selection type	NSGAII – crowding distance
	Individuals crossover type	Real variable SBX
	Crossover rate	0.7
	Individuals mutation type	Polynomial mutation
	Mutation rate	0.08
	Elite rate	0.1
Collective Level	Collective fitness evaluation	MLSU
	Number of collectives elimination	1
	Number of new collectives	1
	Total number of skipped collectives elimination	25% of generation number
Termination	Stopping criteria	Total number of iterations are reached

6.3.5 MTS

MTS was first introduced by Tseng and Chen [276] in 2007 and shows good performance on both unconstrained and constrained multi-objective optimisation problems. This algorithm is a population based local search method. The initial solutions are randomly generated where the local search starts around each solution. It is referred to Tseng and Chen [276] for detailed information about MTS. The MTS parameters are listed in Table 6-7 which are set to the default values from the literature. The same number of function calls with the same size of initial population as the other algorithms are used.

Table 6- 7. MTS parameter definition

Initialisation	Initialisation type	Random
	Number of initial solutions	Population size
Reproduction	Local search grade bonus 1	9
	Local search grade bonus 2	2
	Number of local search test	5
	Number of local search	45
	Number of foreground	0.125 Population size
Termination	Stopping criteria	Total fitness evaluation number reached

6.4 Optimisation of TWF composites tensile strength and modulus

6.4.1 Benchmarking of Genetic Algorithms

A study of population size is used to benchmark the different algorithms on the TWF problem. Many examples in the composite structures literature use generation sizes of 100 or less; which is selected for this investigation. In order to determine the optimal population size for each algorithm, population sizes of 200, 600, 1000, 1500, 2000 and 3000 were compared for the four selected algorithms using both unconstrained and constrained formulations. All four solvers achieve better results on the unconstrained formulation and so only these are documented. The runs generating the best Pareto front from the 30 simulations are illustrated in Figure 6-4 for the highest and lowest population sizes for each of the four algorithms.

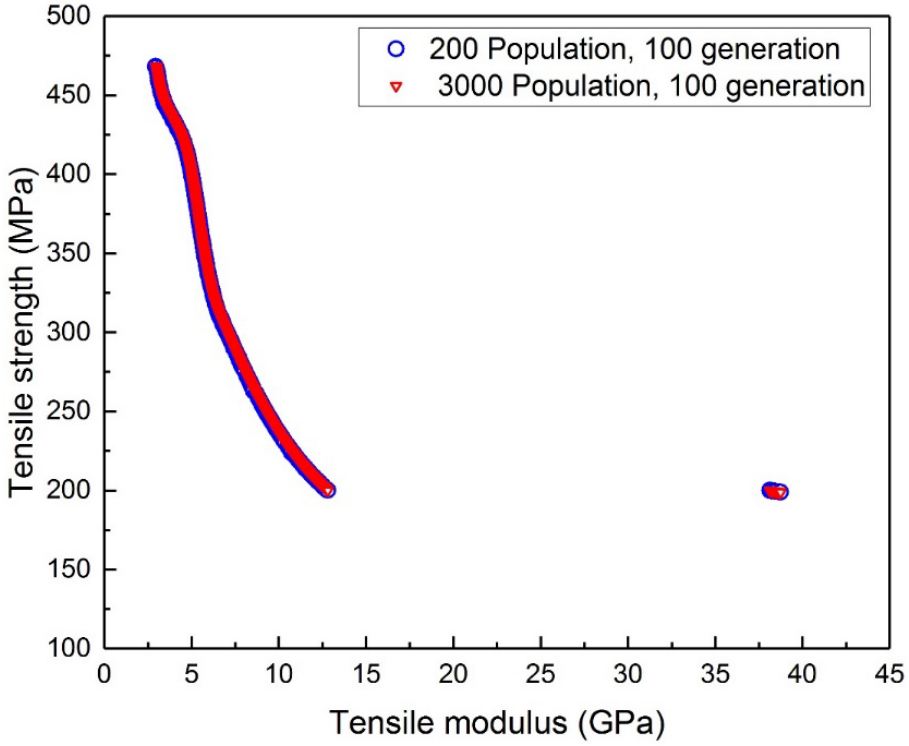
200 Population, 100 generation
3000 Population, 100 generation
Tensile strength (MPa)
Tensile modulus (GPa)
500
450
400
350
300
250
200
150
100
0
5
10
15
20
25
30
35
40
45

(a)

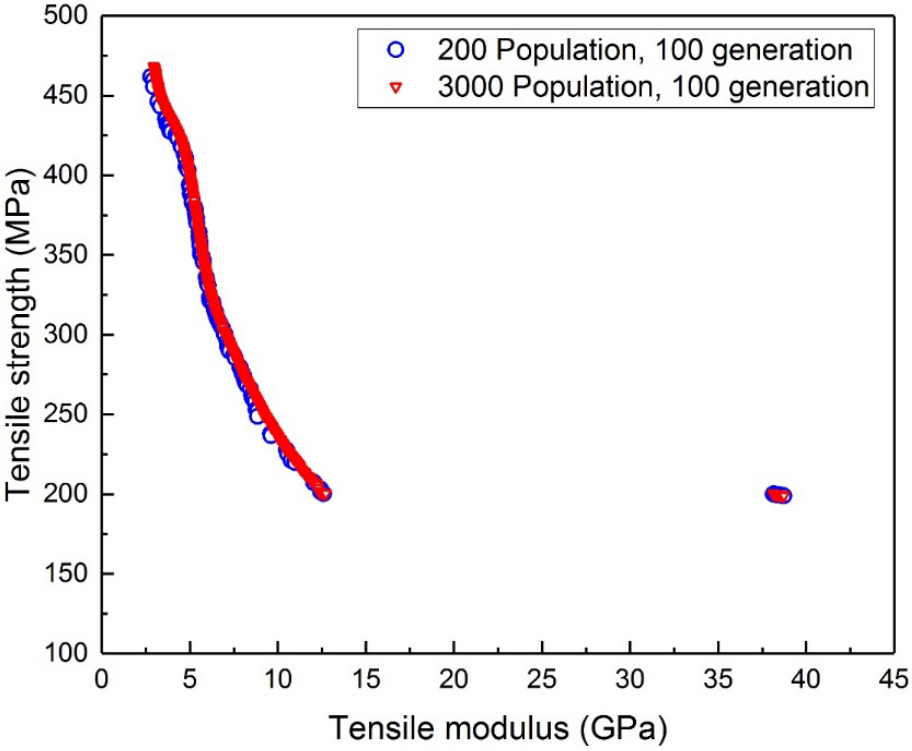
200 Population, 100 generation
3000 Population, 100 generation
Tensile strength (MPa)
Tensile modulus (GPa)
500
450
400
350
300
250
200
150
100
0
5
10
15
20
25
30
35
40
45

(b)

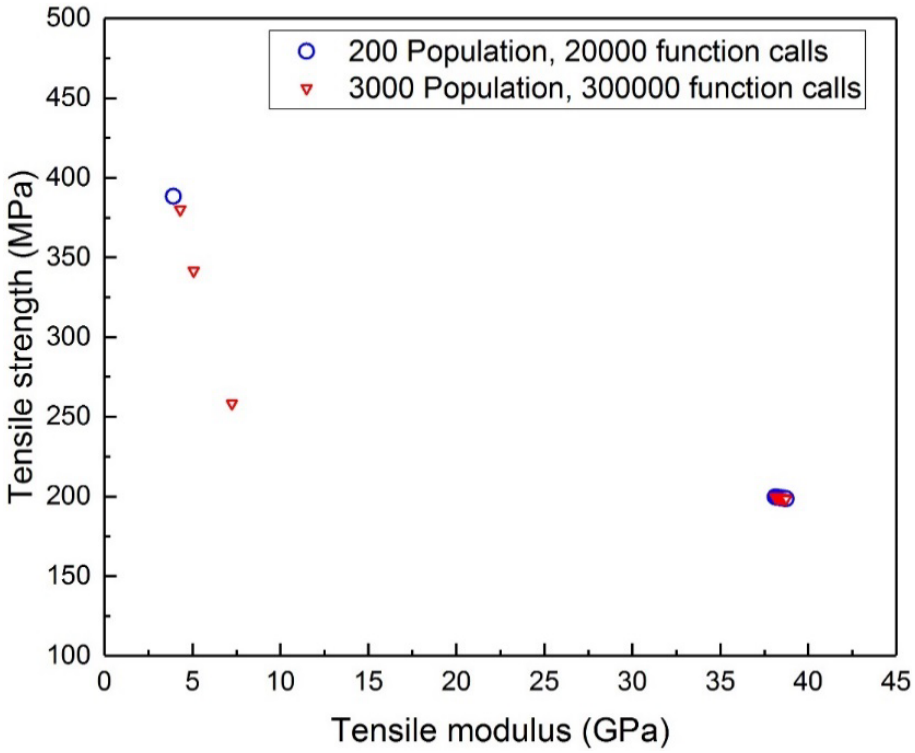

(c)

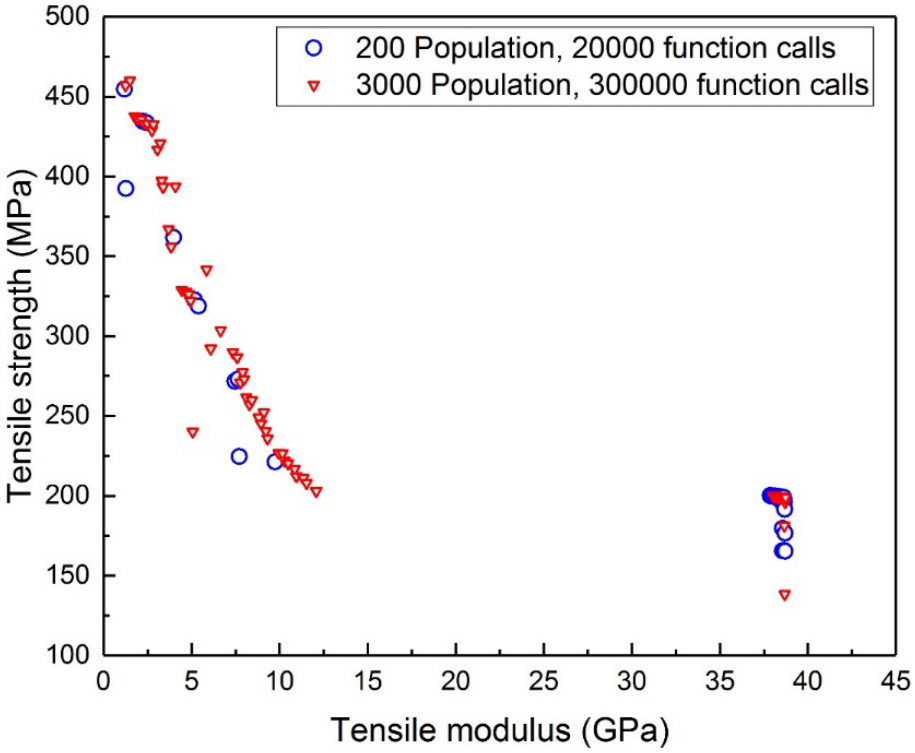

(d)

Figure 6- 4. Comparison of Pareto fronts for different populations sizes: (a) NSGA-II (b) MLSGA-NSGAII (c) MOEA/D (d) MTS

MLSGA-NSGAII and NSGA-II both find the disconnected Pareto front with a good spread of results, covering a similar range, but with little difference in terms of the population

size. MTS is expected to obtain good results on both problem formulations but it performs poorly, finding few points on the left side of the Pareto front. MOEA/D performs the worst among the four algorithms with only a small number of points near the Pareto front, despite being a specialist algorithm for unconstrained problems. The population size has a large influence on the quality of the best optimisation results from MTS, unlike the other algorithms. Since MTS and MOEA/D show such poor performance, they are not discussed further.

6.4.2 Usability of the Pareto front

The results in Figure 6-4 show the best obtained results which show a disconnected Pareto front with two main fronts, which are not equally easy to capture. The front on the right side, with higher tensile moduli, is easier to capture but exhibits lower strengths under tension. The left side has higher strength and lower modulus weave patterns but none of the algorithms can always obtain these results. Therefore the robustness of the algorithms is investigated here determining how regularly they capture the entire Pareto front.

The influence of population size on the frequency of finding the entire disconnected Pareto front is studied, with 600 individuals selected as a representative value from the reviewed literature and is compared against a larger value of 1500. The frequencies for finding the two separated Pareto fronts from 30 runs and the maximum points found on the left side of the Pareto front for each algorithm are summarised in Table 6-8, where the Pareto fronts are extracted every 50 generations from each run until 200 generations.

Table 6- 8. Success finding the entire Pareto front over 30 cycles

		Max. points found on left side PF (total PF storage of 1000)		Frequency	
Population Size	Generation	NSGA-II	MLSGA-NSGAII	NSGA-II	MLSGA-NSGAII
1500	50	808	508	17	26
1500	100	828	568	17	26
1500	150	873	637	17	27
1500	200	964	643	17	28
600	50	806	393	6	11
600	100	908	418	6	14
600	150	960	418	6	15
600	200	969	547	6	16

Both algorithms achieve 1000 points across the entire Pareto front for every run. In all cases MLSGA-NSGAII finds the disconnected Pareto front more frequently than NSGA-II. MLSGA-NSGAII shows a greater probability of finding the entire front after a greater number of generations whereas the frequency of finding the disconnected Pareto front through NSGA-II does not change after 50 generations. It is found that the ability of the algorithm to find the whole Pareto front is higher with larger population sizes, even for the same number of total function evaluations. This shows that the size of the population, which is proposed here to be larger than the values normally used, is important in achieving the best results for both NSGA-II and MLSGA-NSGAII.

In the cases where NSGA-II finds the left hand front it obtains more points than MLSGA-NSGAII. The number of points on the left side Pareto front increases with higher generations in both NSGA-II and MLSGA-NSGAII. To determine the quality of the Pareto front on the runs that successfully find the left side front, a convergence study is performed on NSGA-II and MLSGA-NSGAII at a population size of 1500. Since the real Pareto front is unknown for these cases a mimicked inverted generational distance (mIGD) is derived by generating the best Pareto front from all of the available data. As mentioned in Section 2.2.4.4 of Chapter 2, the mimicked IGD value is based on IGD [82], which quantifies the quality and diversity of a Pareto front by representing the average value of distances from each point on the real Pareto front to its closest point on the obtained Pareto front. In this case a mimicked Pareto front is achieved by filtering all of the dominated and duplicated Pareto front solutions from both MLSGA-NSGAII and NSGA-II. mIGD is defined in eq. (6.8),

$$mIGD(O, M^*) = \frac{\sum_{v \in M^*} d(v,O)}{|M^*|}, \tag{6.8}$$

where M^* is a set of points along the mimicked Pareto front, O is a set of points on the currently obtained Pareto front, v represents each point in the set M^* and $d(v, O)$ is the minimum Euclidean distance between v and the points in O; lower mIGD values reflect a better quality and diversity of the obtained Pareto front. The mIGD values are calculated only for the cases which achieve the entire Pareto front, and are illustrated in Figure 6-5. The results show that MLSGA-NSGAII converges five times faster than NSGA-II, which converges at 250 generations. All of the mean mIGD values from MLSGA-NSGAII are lower than that of NSGA-II, indicating a better accuracy and diversity of the front. The best cases from MLSGA-NSGAII are better than the best from NSGA-II and the worst cases also achieve lower mIGD values than the worst NSGA-II cases until 200 generations. MLSGA-NSGAII shows a

considerable improvement in the probability of finding the left side front, with a slightly smaller density of points, but with better quality, diversity and faster convergence.

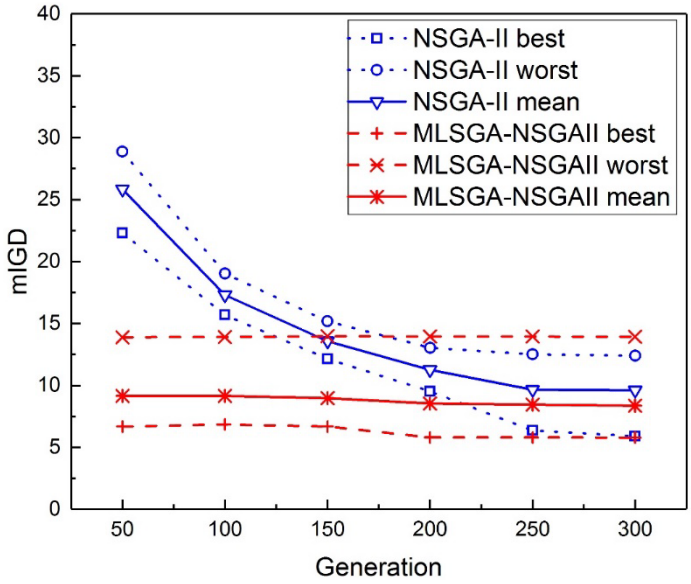

Figure 6- 5. Comparison of the mIGD values for NSGA-II and MLSGA-NSGAII

6.4.3 Design schema for triaxial weave fabric composites

The results for the MLSGA-NSGAII algorithm with 1500 population size and 200 generations are chosen to demonstrate the implications for TWF composite design, as they have the best performance. Due to the repeatability of the results across the algorithms and number of simulations, each point on the Pareto front is assumed close to the optimal design for the TWF composites. Three points on the disconnected Pareto front were randomly selected by hand to demonstrate the three different types of designs; their location in the objective space and the resulting topologies are shown in Figure 6-6. Further examples of how changes in objective and variable space vary are summarised in Appendix III which shows that the relationship between the objectives and variables is nonlinear on the left hand front, making design decisions more difficult but offering a wide range of potential designs, but linear on the right.

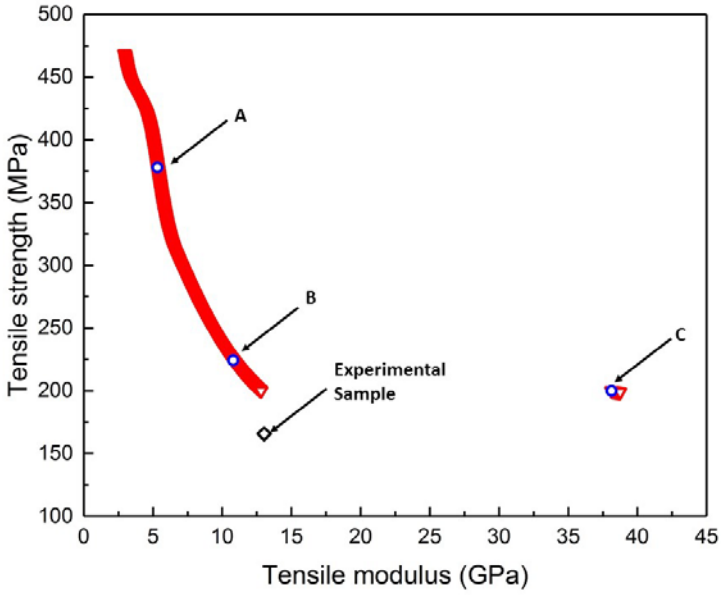
Tensile strength (MPa)
Tensile modulus (GPa)
A
B
C
Experimental
Sample

(a)

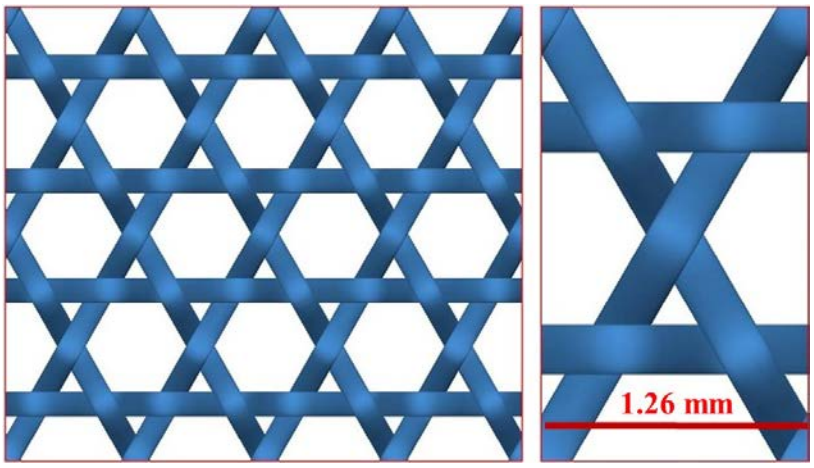
1.26 mm

(b)

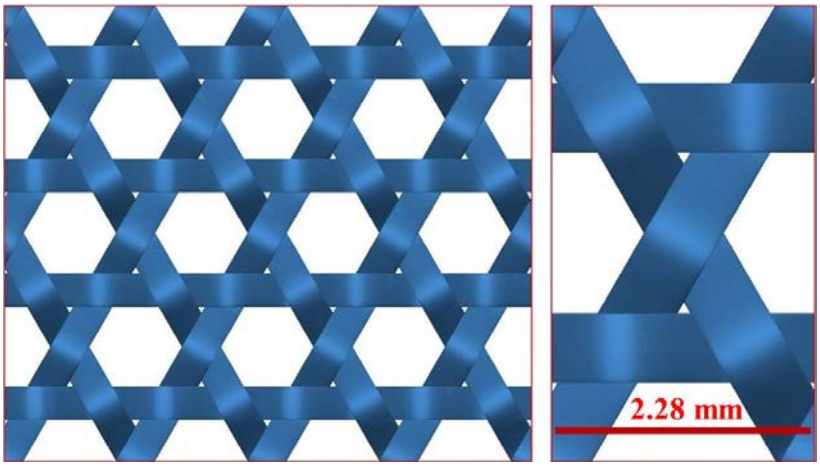
2.28 mm

(c)

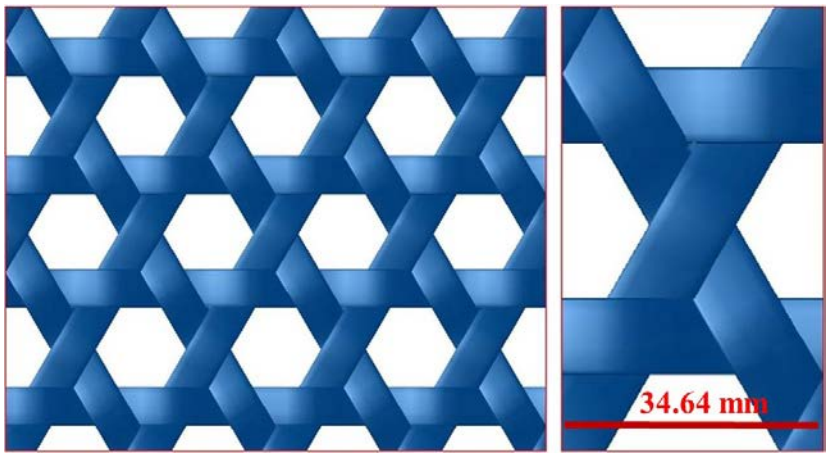

(d)

Figure 6- 6. Optimal designs of TWF composites: (a) sample points in Pareto front (b) Point A: L=0.63, w=0.35, h=0.44; (c) Point B: L=1.14, w=0.65, h=0.96; (d) Point C:L=17.32, w=9.98, h=0.94

For the randomly selected points in Figure 6-6a, the left of Figures 6-6b, 6-6c and 6-6d, illustrate the weave pattern and the right shows the unit cell. The three sub-figures are at different magnifications, with a range of unit cell widths from 1.26mm in 6-6b to 34.64mm in 6-6d. In Figure 6-6a, all of the left side Pareto front solutions are potentially applicable for ultralight structures under tension, with high strength to stiffness ratios which are suitable for producing flexible structures. Points A and B are representative of the general size of the points in the left side front. Compared with a current T300/Hexel8552 weave pattern [325], L=1.559, w=0.803, h=0.78, points A and B both have smaller unit cells; where the area of a T300/Hexel8552 unit cell is 612 times point A and 1.9 point B. The bottom point of the left hand front, L=1.23, w=0.71, h=1.12, with the lowest strength to modulus ratio of the optimised designs is improved by 28.80% compared to the experimental construction with the same modulus. The left hand front solutions above this provide higher strength to stiffness ratios where the top point shows an improvement of 1191%. Between these two designs there are 643 points in the best Pareto front, providing a range of designs exhibiting different secondary properties. The tensile strength and modulus are related to all three variables, but are dominated by more compact weave patterns than the current T300/Hexel8552. The right side of the Pareto front provides results with significantly wider yarns and long undulation lengths, an example of which is point C illustrated in Figure 6-6d. The right hand materials are similar to Xu et al. [330] who performed a bi-axial buckling analysis of TWF composite structures with similar geometric parameters, indicating the potential for these weave patterns to resist compression despite poor tensile performance. The sample optimal designs, points A and B in Figure 6-6 illustrate triangular gaps in the unit cell. The extreme top point shows similar-sized triangular

gaps as point B, but point A illustrates significantly larger triangular voids. Examples from the literature, [325–328], and the bottom point of the left hand front are similar to point C, with no triangular gaps between the yarns. The size of triangular voids is controlled by the relationship between the undulation length and yarn width. These hexagonal and triangular holes help to reduce the load by increasing the penetrability of impacting air [330].

6.5 Optimisation of TWF composites specific strength and stiffness with areal density

Since the areal density of triaxial weave fabric composites are not considered in the previous optimisation, two bi-objective optimisations are performed on strength-density and stiffness-density problems respectively to investigate the relationship between strength, stiffness and areal density. In order to avoid the influences caused by the stochastic characteristics of the solvers 30 independent runs are performed for each study. To determine the quality of the Pareto front, a numerical comparison is performed between NSGA-II and MLSGA-NSGAII at a population size of 1500. The mimicked inverted generational distance (mIGD) from previous study [30] is utilised in this numerical comparison, which is defined in eq. (6.8).

In the stiffness-density optimisation, the relationship between the stiffness and surface density is linear in the Pareto front. Both solvers achieved the same density of points on the Pareto front, covering the same range of designs. However, all of the designs on the Pareto front have large fibre tow undulation lengths, meaning that the woven fibre tows are as straight as possible to increase the stiffness but that all of the optimal designs are distributed on one side of the variable space. Since they have a linear relationship and are less interesting for real applications, the stiffness-density problem is not discussed further.

For the strength-density optimisation, the mIGD values at each generation are illustrated in Figure 6-7 for the best and worst cases as well as the average from the 30 simulations. The figure shows that MLSGA-NSGAII converges faster than NSGA-II, except in the worst case where MLSGA-NSGAII takes 200 generations to converge. MLSGA-NSGAII achieves the best result in the case of 1500 population size and 200 generation and obtains better results than those from the NSGA-II after running the first 50 generations. This indicates that the advantage of MLSGA-NSGAII over NSGA-II is reduced in these cases compared to the previous study [30]. Additionally, it is illustrated that both algorithms obtain large differences in convergence between the best and worst results among the 30 independent simulations.

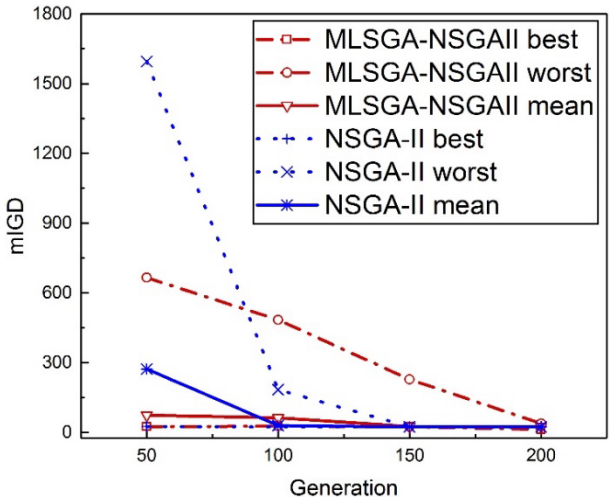

Figure 6- 7. Convergence of NSGA-II and MLSGA-NSGAII on the strength-density optimisation

According to the mIGD results the runs generating the best Pareto front from the 30 simulations for strength-density problem are illustrated in Figure 6-8 for each of the two algorithms. When optimising for strength and density, MLSGA-NSGAII and NSGA-II both find a disconnected Pareto front with a good spread of results, covering a similar range; the discontinuities are highlighted in Figure 6-8. NSGA-II achieves a lower density of Pareto front points on the bottom left part of the front relative to MLSGA-NSGAII. It is found that MLSGA-NSGAII and NSGA-II both capture the entire disconnected Pareto front in all the 30 independent runs with 500 points across the entire Pareto front each run, making this Pareto front easier to capture than the results from the previous study [30]. This is because the discontinuities are smaller than the Pareto front achieved in the previous study and the diversity mechanism of NSGA-II, crowding distance, maintains a higher diversity in its population and across the gaps. The advantages of the collective evolutionary mechanism in MLSGA-NSGAII are smaller in this case, as diversity of the population is less important.

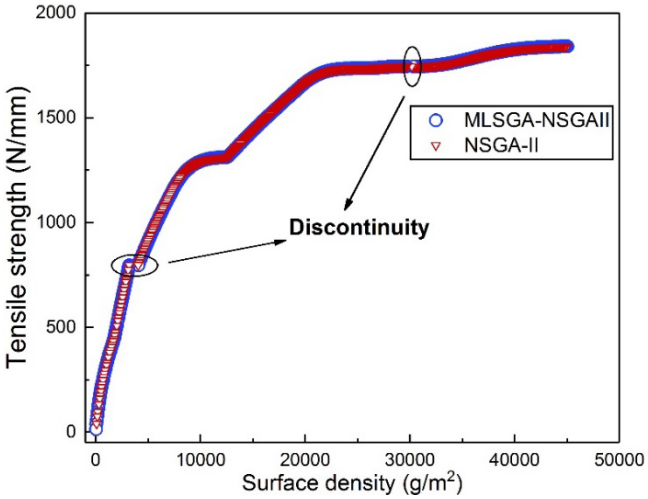

Figure 6- 8. Strength-density Pareto fronts for strength vs density

The designs at the extreme points of the Pareto front are L = 0.67 mm, w = 0.39 mm and h = 0.02 mm for the extreme bottom left point and L = 0.39 mm, w = 0.22 mm and h = 2 mm for the extreme top right point. The point at the extreme top right is more dense with a 100 times greater thickness and is about two times more compact. The extreme top right design has a high strength per unit length value, 1839.92 N/mm, but the two extreme point designs achieve similar strength per unit cross-sectional area values, 459.98 MPa at extreme top right design and 457.37 MPa at extreme bottom left design, which are high among all the optimal designs. The two points on either side of the right hand side discontinuity have the same strength per unit length, 1744.56 N/mm, and the same thickness, 2 mm, but one is much denser than the other, 29599.3 g/m^2 and 30326.9 g/m^2, again the denser design is more compact. However, these designs are not applicable in the current applications of triaxial weave fabric composites since the weights are significantly larger than the normal requirements of these materials, which are typically lower than 200 g/m^2. These designs are included in this study to artificially enlarge the search space for evaluating the Genetic Algorithm performance. The lower left discontinuity has similar designs as in the previous study [30], the point at the left of the disconnection has a large undulation length and yarn width, similar to the weave pattern shown in Figure 6-6d. However the point at the right side of the discontinuity has a significantly more compact weave pattern with slightly smaller thickness, which looks similarly to the weave pattern illustrated in Figure 6-6c. This shows that compact weave patterns increase the strength per unit cross-sectional area and thick yarns tend to decrease this value.

The results for the MLSGA-NSGAII algorithm are chosen to demonstrate the implications for the TWF composite designs, as they have the best performance. The optimal designs from the previous study [30] are compared with the Pareto front of the current study which include the areal density. It is shown that the Pareto front of the previous study covers the same range of points as the bottom left front in the current study up until the first discontinuity, which is shown in Figure 6-9a. This demonstrates that the optimal designs from the previous study are also useful for real applications. In order to compare the optimal designs with the experimental samples, the unit of tensile strength is transferred from N/mm to MPa by dividing by the thickness of the TWF composites, 2h, since each interlacing point has two yarns stacked together; the new Pareto front is shown in Figure 6-9b. The designs on the lower left front in Figure 6-9b illustrate high stiffness despite having the lowest strengths. The right side front contains designs having similar strengths with lower stiffness compared to the designs from the upper left front. They achieve slightly higher strength to stiffness ratios than

the optimal designs in the previous study but are significantly denser. The designs in the top left hand front are therefore judged to have properties most useful for ultra-lightweight applications. TWF composites usually consist of 3-5 layers in applications [325]. If a material is made from five layers of the experimental sample this gives an areal density of around 550 g/m^2. The top left hand front contains 17 designs having areal density lower than 550 g/m^2 which has a larger tensile strength, from 370 MPa to 467.5 MPa, and lower stiffness, from 6.6 GPa to 12 GPa, than the experimental specimen [325].

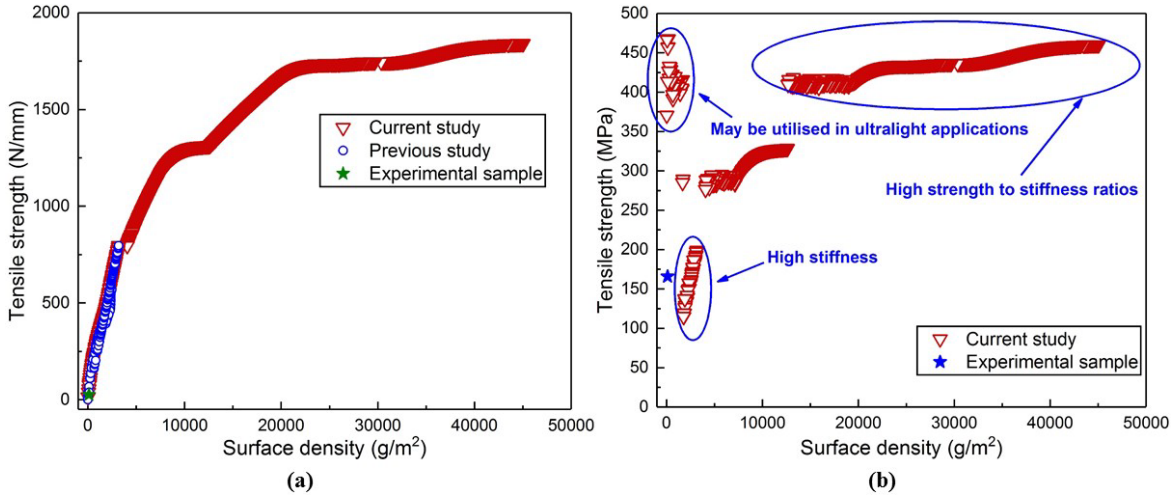

Figure 6- 9. Implication of TWF composite designs: (a) Comparison between the current study and the previous study [30]*; (b) Pareto front of tensile strength from current study after unit transfer*

Of these samples three designs have areal density lower than the experimental sample and a higher strength to stiffness ratio. The extreme strength to stiffness ratio of the current study is 1230%, which is larger than the experimental sample but the density is 40216% denser than the experimental sample, where the previous study achieved a highest improvement of strength to stiffness ratio by 1191%. However, the previous specific design with highest strength to stiffness ratio has larger density, 303.86 g/m^2, and thicker than the experimental sample, 111.75 g/m^2. A point with an areal density closer to the experimental sample but thinner [325], 110.86 g/m^2, is shown to have a tensile strength of 413.43 MPa, showing an increase of 149.49% in strength compared to the experimental sample. Furthermore, the stiffness is decreased by 15.94% from 13.53 GPa in the experiment to 10.30 GPa for the optimal design, meaning that the strength to stiffness ratio increases by 228.05% compared with the experimental sample. The previous study illustrated one design with similar areal density as the specific design in the current study and the experimental sample, 129.98 g/m^2, showing an increased strength to stiffness ratio of 896.29% with a tensile strength of 441.66 MPa and stiffness of 3.62 GPa. The specific design in the previous study achieves a significant

improvement of strength to stiffness ratio with an acceptable increase of areal density. It is demonstrated that the optimal designs from the two studies extend the selection of TWF composite designs for engineers and that if a material with a similar areal density to those currently available was required, that there is are still a number of design available that can increase the strength to stiffness ratio.

6.6 Discussion and limitations

There is 'no free lunch', improving an algorithms performance on a category of problems inevitably degrades its performance on other problem types. This results in specialist algorithms for a given problem that may perform badly on problems not of this type, and general solvers, with a lower performance on these specific problems but generally good performance across all the problems. The composite structures literature generally does not consider the problem type when selecting Genetic Algorithms for optimisation, meaning that general or outdated solvers are used in many cases. The complexity of the composite structural optimisation problems is getting larger and it has been shown in Mutlu et al. [323] to lead to unresolved Pareto fronts, even on simple problems. To investigate optimal designs of triaxial weave fabric composites four leading Genetic Algorithms are compared with the tensile strength and tensile modulus maximisation problem posed using both a constrained and an unconstrained formulation. MOEA/D, which in previous benchmarking provides top performance on unconstrained problems, shows the worst results on both formulations, which for the unconstrained results is unexpected. MTS also performs poorly on both formulation types, despite its excellent performance in benchmarking on both constrained and unconstrained problems. This demonstrates that these engineering problems are dominated by different characteristics than whether they are formulated as constrained or unconstrained; making current computational benchmarking unfit for selecting the correct algorithm in these cases. The results indicate that more composite structural optimisation problems need to be investigated, to determine the dominant features. It is likely that the literature increasingly will need to look at specialist solvers, rarely referenced in the current composite structural literature, but that these benchmarking exercises will more easily allow the selection of the correct algorithm and increase the use of these algorithms.

For the TWF composite tensile strength and modulus optimisation MLSGA-NSGAII and NSGA-II are the best performers, with MLSGA-NSGAII showing the greatest accuracy. NSGA-II cannot regularly find the optimal Pareto front on the left side but when successful it achieves the highest density of points. The NSGA-II mechanism is based on non-domination

ranking through the whole population to find the Pareto front. Once part of the disconnected Pareto front is found, all of the solutions are pushed to this front and the possibility of missing the other parts of the front is increased. The crowding distance is used to maintain the diversity of solutions in NSGA-II and this indicates that the crowding distance is too weak to maintain diversity when the disconnected Pareto front has a large gap between two fronts. Based on these findings it is proposed that for NSGA-II the initial population determines the likelihood of success on disconnected objective spaces like this problem. MLSGA-NSGAII utilises its own collective evolutionary mechanism, incorporating separate crowding distances to keep the diversity of solutions. In MLSGA-NSGAII the population is divided into eight collectives meaning that different collectives find different parts of the entire front, though this leads to a reduction in the number of points found. The eight collectives are distributed throughout the search space giving it robust performance in finding the disconnected Pareto front. In this case it is proposed that the disconnected nature of the Pareto front favours MLSGA-NSGAII in both constrained and unconstrained formulations. This indicates that the disconnected nature of the front is the dominant characteristic of the search space but which isn't generally considered a dominant characteristic in the literature.

In addition to the algorithm selection, many composite structures papers obtain results from a single run. However, due to the stochastic nature of the solvers, it is demonstrated that it is necessary to run several cycles to ensure the entire Pareto front has been found depending on the nature of the objective space. Many algorithms converge on a solution early in the generation cycle. Using the computational time for a higher numbers of simulations, rather than fewer, longer runs, is likely to result in better solutions and resolved Pareto fronts. In the TWF composite tensile strength and modulus optimisation study increasing the population size also results in a higher possibility for finding the whole Pareto front, even with the same number of function calls. This goes against the prevalence of the micro-GAs, small population sizes with a large number of generations, often found in engineering optimisation literature to reduce the computational time.

The focus of the TWF composite tensile strength and modulus optimisation in the first case is tensile properties, but due to the number and diversity of points, designers should be able to find a suitable weave pattern matching their required secondary characteristics, such as low areal density or shear stiffness. To benchmark the different algorithms and to provide an ideal Pareto front, the size of the search space is artificially enlarged with gaps of 10^{-10} millimetres. However, to solve the problem practically the variable interval could be reduced

to 10^{-2} millimetres. This will result in achieving the optimal results through fewer total function calls but the results here provide a more complete Pareto front for interest. A many-objective optimisation will provide more interest for designers than the bi-objective optimisation but is a significantly more complex problem to solve. Insight from the current optimisation will allow a method to be developed to include compression, shear and density properties into the design of triaxial weave fabric composites but will provide a refinement to the current selection due to the importance of the properties selected.

In order to investigate the proportion of optimal designs from the TWF composite tensile strength and modulus optimisation satisfies the ultralight requirement, the low areal density is added into the optimisation as an objective. The best two algorithms from the TWF composite tensile strength and modulus optimisation are used in the specific tensile strength and modulus optimisation. The study demonstrates similar results to the previous study, where the MLSGA-NSGAII achieves the best results and converges faster on average. However, both Genetic Algorithms find the entire Pareto front on every run when solving the strength-density optimisation problem, since the disconnected Pareto front has significantly smaller gaps compared with the previous study. Furthermore, both algorithms achieve better robust performance with increased numbers of fitness evaluations, where the differences between the best and worst results are significantly reduced. The addition of the areal density makes the problem easier to solve, and more useful. However, the previous results still demonstrate some solutions that a designer might be interested in, that are not available in this set of results. The advantages of MLSGA-NSGAII in maintaining a more diverse population through collective evolutionary mechanisms and crowding distance are smaller when solving the strength-density optimisation problem. However, it is worth solving this as a many-objective optimisation problem and to perform further benchmarking to evaluate the dominant characteristics of the problem helping to determine the selection of solvers for further exploration of these problems in the future.

The designs in the bottom left part of the front in Figure 6-8 demonstrate similar strength per unit cross-sectional area compared to those on the right side part of the front but are much lighter. This is because the right side front designs have more compact weave patterns and are much thicker than the bottom left part front designs, making the cross-sectional area much larger. The previous TWF composite tensile strength and modulus optimisation study concluded that compact weave patterns provide high strength but it is found in the specific tensile strength and modulus optimisation study that compact weave patterns and high

thicknesses significantly increase the surface density, which conflicts with the purpose of producing ultralight weight structures. Therefore, it is essential to select suitable weave patterns of TWF composites. The previous study found 643 designs that achieve higher strength to stiffness ratios than the experimental sample. However, after accounting for the areal density of the TWF composites, only three designs achieve higher strength to stiffness ratios with lower density than the experimental sample in the current study. However, there are also 17 optimal designs in the previous study which have similar densities as the experimental sample whilst having higher strength to stiffness ratios. This is because the specific tensile strength and modulus optimisation study achieved the Pareto front providing optimal designs for a wide range of density, which inevitably reduce the density of Pareto front points at the most interesting areas. Therefore, it is worth searching for optimal designs at the most interesting area by restricting the TWF composite density range. The focus of the current study is tensile properties and density, but due to the diversity of points, designers should be able to find a suitable weave pattern matching their required additional characteristics, such as buckling performance.

6.7 Chapter summary

Triaxial weave fabrics (TWF) are increasingly used in novel ultralight applications and there is a requirement to improve material properties. The material properties are dependent on the weave pattern, so optimising the designs can lead to improved TWFs. In this chapter Genetic Algorithms are firstly used to find optimal weave patterns of TWF composites for maximisation of tensile modulus and strength. Since the dominant characteristics of the problem are not understood, four leading Genetic Algorithms specific to different problem types are compared to find the Pareto front for the TWF designs. Computational science literature defines constrained and unconstrained as the dominant features of an optimisation problem; with a recent benchmarking showing that MTS provides top performance on both problem types and MOEA/D on unconstrained problems. Poor performance from both of these algorithms demonstrates that this problem is dominated by different characteristics and that the selection of the correct algorithm is critical to find the optimal solutions. This indicates that it will be impossible to select the correct Genetic Algorithm for composite optimisation problems from the current literature. Therefore, there is a requirement for characterisation and benchmarking of composite optimisation problems to allow selection of algorithms capable of finding solutions to the more complex problems. The benchmarking demonstrates that for this problem MLSGA-NSGAII provides the best performance, providing a weave pattern which is

seemingly dominated by the disconnected nature of the Pareto front. This process results in a left hand front which is suitable for producing flexible structures with 643 optimal designs. Of the proposed weave patterns one matching the modulus of a current experimental sample [325] gives an increase in the strength to stiffness ratio of 28.80%. However, the lowest modulus solution achieves a greater tensile strength to stiffness ratio improvement of 1191% compared to the experimental sample.

In order to investigate the influences of weave patterns on the areal density of the TWF composites, the areal density is introduced in the second study as an objective. In this study the best two Genetic Algorithms, selected as being the best performing based on the previous study, are used to find optimal weave patterns of TWF composites in tension. The benchmarking demonstrates that for this problem MLSGA-NSGAII achieves the best results and converges faster, similar to the results in the previous study. Of the proposed strength-density Pareto front results there are three designs which have a lower density, higher strength and stiffness than the experiment. One design, 110.86 g/m^2, which is slightly lighter than the areal density of a current experimental sample [325], 111.75 g/m^2, gives an increase in the strength of 149.49% and an increase in the strength to stiffness ratio of 228.05%. One design with slightly higher areal density than the experimental sample, 129.98 g/m^2, shows an increased strength to stiffness ratio of 896.29% with a tensile strength of 441.66 MPa and stiffness of 3.62 GPa. Additionally, since TWF composites are usually layup for 3-5 layers in the applications, there are 17 of designs having a surface density lower than the five layers of experimental sample, 550 g/m^2, with tensile strength larger than 370 MPa and strength to stiffness ratios higher than the experimental sample [325], which may be capable of being designed for flexible ultralight structures.

Chapter 7. Determination of best Genetic Algorithms and dominant characteristics for many-objective optimal design of plain weave fabric composites through benchmarking

7.1 Many-objective optimisation in the design of plain weave fabric composites

Plain weave fabric (PWF) composites are a low-cost material often found in civil, offshore, marine and automobile structures. They are generally limited to these applications because they exhibit lower mechanical properties than unidirectional composite laminates which becomes a problem in lightweight applications. In order to utilise them in aerospace structures, such as for wing stiffeners, truss members and rotor blades, they must have improved specific tensile and shear properties. However, the combination of modern manufacturing and optimisation techniques makes the use of bespoke high-performance plain weave fabric composites a possibility in a wider range of applications. The yarn specifications, including the undulation length, the width and the thickness of the yarns, significantly influence the mechanical properties and the density of the material. To maximise the tensile and shear properties while reducing the weight of the material requires an optimal weave pattern. However, this is a complex problem and it is currently unknown which optimal design will simultaneously satisfy these requirements.

Bai et al. [39,299] and Wang and Sobey [47] develop models that show robust and accurate predictions of the mechanical properties of plain weave fabric composites under tension and shear. However, there is no knowledge about which weave patterns provide optimal mechanical properties and lowest density under tensile and shear loadings. The five-objective composite optimisation problem is complicated to be solved and it is difficult to select the correct Genetic Algorithm from the evolutionary computation literature since the dominant characteristics are different between composite optimisation problems and the evolutionary computation literature [9,30,323]. Therefore, the current study benchmarks 10 state-of-the-art Genetic Algorithms, including a number of variants of the top performing methodologies, to find the optimal designs for plain weave fabric composites and the dominant characteristics of these optimisation problems.

7.2 Plain weave fabric model for the areal density, strengths and moduli under tension and shear

The tensile modulus of the plain weave fabric composites is predicted by analytical model developed by Bai et al. [39]. The tensile strength of the plain weave fabric composites is predicted by the analytical model demonstrated in Chapter 4. The shear modulus and strength

of the plain weave fabric composites are predicted by an analytical model developed by Wang and Sobey [47], which is demonstrated in Chapter 5. All three analytical models provide accurate and robust predictions for a set of different materials and yarn specifications, where the mean errors of the three models proposed by Bai et al. and Wang and Sobey are respectively 5.50% for biaxial tensile modulus, 11.22% for biaxial tensile strength, 15.24% for shear modulus and 8.51% for shear strength and the standard deviation of prediction errors are respectively 2.27, 2.66, 4.10 and 6.76. All of them use the same geometric parameters, which are shown in Figure 7-1. Bai et al. [39] and Chapter 4 and 5 provide a detailed derivation and verification of these analytical models.

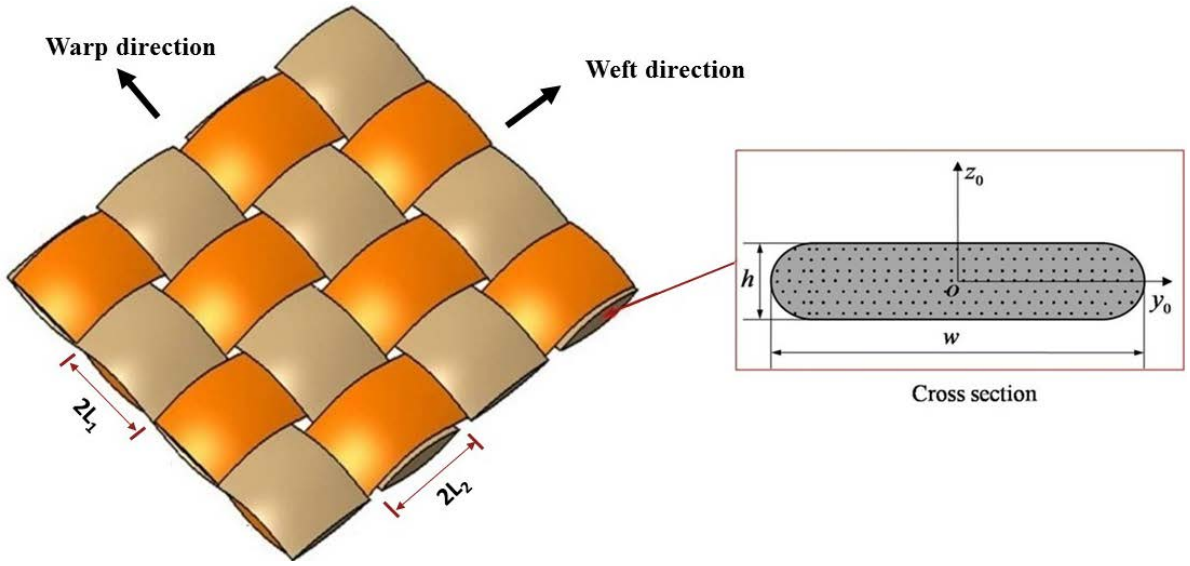

Figure 7- 1. Geometric parameters of plain weave fabric composite lamina [39,299]

In order to evaluate the areal density of the plain weave fabric composites, the same geometry parameter and idealised undulation shape as in Bai et al. [39,299] and Chapter 4 and 5 are used. The cross-sectional area, A_i, for the yarns is formulated the same as eq. (4.1) of Chapter 4, which is summarised as eq. (7.1),

$$A_i = \frac{\pi h_i^2}{4} + h_i\left(w_i - h_i\right), \tag{7.1}$$

where the subscript *i* is 1 when represents warp tows and equals 2 for weft tows. w_i and h_i are width and thickness of the tows. The yarn volume fraction, V_y, of the unit cell can be calculated from the eq. (4.7) of Chapter 4, which is reprinted as eq. (7.2),

$$V_y = \left(4L_1L_2H\right)^{-1}\left(2\int_0^{L_1} A_1\sqrt{1+\left(\frac{\pi h_2}{4L_1}\cos\frac{\pi x}{2L_1}\right)^2}\,dx + 2\int_0^{L_2} A_2\sqrt{1+\left(\frac{\pi h_1}{4L_2}\cos\frac{\pi x}{2L_2}\right)^2}\,dx\right), \tag{7.2}$$

where L_i is one quarter of the tow undulation length since one period of a tow is rotational symmetric and a half period of the tow is axial symmetric. *H* is the thickness of a composite ply. The tow fibre volume fraction, V_f^y, is expressed as eq. (4.8) of Chapter 4, which is reprinted as eq. (7.3),

$$V_f^y = V_{f0}/V_y, \tag{7.3}$$

where V_{f0} is fibre volume fraction, which is 55% in the current study. Therefore, the density of a tow, ρ_{tow}, is expressed similar as eq. (6.3) of the Chapter 6, summarised as eq. (7.4),

$$\rho_{\text{tow}} = \rho_{\text{fibre}}V_f^y + \rho_{\text{resin}}\left(1-V_f^y\right), \tag{7.4}$$

where the density of the EW220 glass fibre, ρ_{fibre}, is 2.5 g/cm^3 and the density of the 5284 epoxy resin, ρ_{resin}, is 1.2 g/cm^3. The areal density of a EW220/5284 plain weave fabric composite ply is expressed as in eq. (7.5),

$$\begin{aligned} AD = \Bigg\{ & \rho_{\text{tow}}\left(2\int_0^{L_1} A_1\sqrt{1+\left(\frac{\pi h_2}{4L_1}\cos\frac{\pi x}{2L_1}\right)^2}\,dx + 2\int_0^{L_2} A_2\sqrt{1+\left(\frac{\pi h_1}{4L_2}\cos\frac{\pi x}{2L_2}\right)^2}\,dx\right) \\ & + \rho_{\text{resin}}\left[\left(4L_1L_2H\right) - \left(2\int_0^{L_1} A_1\sqrt{1+\left(\frac{\pi h_2}{4L_1}\cos\frac{\pi x}{2L_1}\right)^2}\,dx + 2\int_0^{L_2} A_2\sqrt{1+\left(\frac{\pi h_1}{4L_2}\cos\frac{\pi x}{2L_2}\right)^2}\,dx\right)\right]\Bigg\}\frac{1000000}{4L_1L_2}. \end{aligned} \tag{7.5}$$

In order to validate the constitutive equations for calculating the areal density of plain weave fabric composites, the prediction is compared against a weight measurement. The fabric parameters are: one quarter of the tow undulation length, L_1, is 0.714 mm and L_2 is 0.556 mm; the tow width, w_1, is 1.0 mm and w_2 is 1.2 mm; the thickness of tow, h_1, is 0.08 mm and

h_2 is 0.067 mm and the thickness of the EW220/5284 plain weave fabric composite plies, *H*, are 0.167 mm.

The mean value of the measured areal density of the EW220/5284 plain weave fabric composite ply is 330.18 g/m^2 from experiments. The predicted areal density is 319.81 g/m^2 and the prediction error is 3.14% from the comparison. The constitutive equations provide adequate accuracy for the areal density prediction of plain weave fabric composites.

7.3 Many-objective design methodology

In this case the 10 top performing Genetic Algorithms from the evolutionary computation literature are selected for benchmarking: MOEA/D [80], MOEA/D-PSF [84], MOEA/D-MSF [84], HEIA [274], BCE [275], IBEA [77], MTS [276], NSGA-II [75], U-NSGA-III [97], and co-evolutionary MLSGA (cMLSGA) [277]. All individuals in the population are evaluated by the three analytical models for the tensile and shear properties and one constitutive equation model for the areal density.

7.3.1 Formulation of many-objective optimisation problem

A set of 5 optimisation problems are select to maximise the strengths and moduli under tensile and shear loads and minimum areal density for a Plain Weave Fabric. Since many-objective optimisation problems are complex, transforming the constraints to the limits of the range of variables helps to resolve the problem. The benefits have been shown in Chapter 6, where all of the benchmarked Genetic Algorithms achieve better Pareto fronts when solving the unconstrained formulation of bi-objective optimisation of the triaxial weave fabric tensile strength and stiffness. Therefore, the optimisation problems in the current study are formulated using an unconstrained formulation for the plain weave fabric composite material in eqs. (7.6) - (7.10). Eq. (7.6) is a five-objective optimisation problem maximising the moduli and strengths under tension and shear while minimising the areal density,

$$\begin{cases} \text{Minimise}\begin{Bmatrix} 1/\mathit{TensileStrength}(l_1,l_2,w_1,w_2,h_1,h_2), 1/\mathit{Modulus}(l_1,l_2,w_1,w_2,h_1,h_2), \\ 1/\mathit{ShearStrength}(l_1,l_2,w_1,w_2,h_1,h_2), 1/\mathit{Modulus}(l_1,l_2,w_1,w_2,h_1,h_2), \\ \mathit{ArealDensity}(l_1,l_2,w_1,w_2,h_1,h_2) \end{Bmatrix}, \\ L_1 = l_1 \times (2 - 0.5 \times w_2) + 0.5 \times w_2, \\ L_2 = l_2 \times (2 - 0.5 \times w_1) + 0.5 \times w_1, \\ 2 \times L_1 / h_1 \geq 7 \quad \text{and} \quad 2 \times L_2 / h_2 \geq 7, \\ 2 \times L_1 / h_1 \leq 40 \quad \text{and} \quad w_1 / h_1 \leq 40, \\ 2 \times L_2 / h_2 \leq 40 \quad \text{and} \quad w_2 / h_2 \leq 40, \\ h_1 + h_2 < H, \\ \text{The range of variable:} l_1 \in [0.0001,1], l_2 \in [0.0001,1], \\ \qquad\qquad 0.2\text{mm} \leq w_1 \leq 2\text{mm}, 0.2\text{mm} \leq w_2 \leq 2\text{mm}, \\ \qquad\qquad 0.04\text{mm} \leq h_1 \leq 0.2\text{mm}, 0.04\text{mm} \leq h_2 \leq 0.2\text{mm}. \end{cases} \tag{7.6}$$

eq. (7.7) is a three-objective problem optimising the specific tensile and shear moduli,

$$\text{Minimise}\begin{Bmatrix} 1/\mathit{TensileModulus}(l_1,l_2,w_1,w_2,h_1,h_2), \\ 1/\mathit{ShearModulus}(l_1,l_2,w_1,w_2,h_1,h_2), \\ \mathit{ArealDensity}(l_1,l_2,w_1,w_2,h_1,h_2), \end{Bmatrix} \tag{7.7}$$

eq. (7.8) is a three-objective problem optimising the specific tensile and shear strengths,

$$\text{Minimise}\begin{Bmatrix} 1/\mathit{TensileStrength}(l_1,l_2,w_1,w_2,h_1,h_2), \\ 1/\mathit{ShearStrength}(l_1,l_2,w_1,w_2,h_1,h_2), \\ \mathit{ArealDensity}(l_1,l_2,w_1,w_2,h_1,h_2), \end{Bmatrix} \tag{7.8}$$

eq. (7.9) is a bi-objective problem optimising the tensile strength to stiffness ratio,

$$\text{Minimise}\begin{Bmatrix} 1/\mathit{SpecificTensileStrength}(l_1,l_2,w_1,w_2,h_1,h_2), \\ 1/\mathit{SpecificTensileModulus}(l_1,l_2,w_1,w_2,h_1,h_2), \end{Bmatrix} \tag{7.9}$$

and eq (7.10) is a bi-objective problem optimising the shear strength to stiffness ratio,

$$\text{Minimise}\begin{Bmatrix} 1/\mathit{SpecificShearStrength}(l_1,l_2,w_1,w_2,h_1,h_2), \\ 1/\mathit{SpecificShearModulus}(l_1,l_2,w_1,w_2,h_1,h_2). \end{Bmatrix} \tag{7.10}$$

The optimisation problems all use the same range of variables and variable constraints, which are shown in eq. (7.6).

EW220/5284 is selected as a type of glass plain weave fabric composite currently used on aerospace applications and where the required material properties are available in the open literature. The range of these variables shown in eq. (7.6) are determined to ensure the applicability for a range of existing applications for plain weave fabric composites. In order to fairly compare the optimised designs with a current design, the fibre volume fraction and the yarn fibre volume fraction of the EW220/5284 plain weave fabric composites are fixed as 0.55 and 0.73 in the optimisation and the thickness of the composite ply, *H*, is calculated using a

combination of eqs. (7.1) and (7.2). According to the material properties of the current EW220/5284 plain weave fabric composite design, the tensile modulus of the EW220 fibre is 73 GPa and the shear modulus is 11.53 GPa; the tensile modulus of the 5284 resin is 3.4 GPa and the shear modulus is 1.1 GPa; the tensile strength of the fibre is 2000 MPa and the interlaminar shear strength of the yarn is 40 MPa. These material properties are fixed values in the optimisation to allow a comparison with the currently available materials. In order to make sure the optimal designs can be manufactured, the sum of warp and weft tow thickness must be smaller than the thickness of the ply and half of the undulation length of the warp tow, $2L_1$, must be larger than the width of the weft tow, w_2, and vice versa. In order to ensure the accuracy of the models the half of the undulation length over thickness ratio is set to be larger than or equal to seven according to all the verification cases of the analytical models, as the analytical models proposed in Chapter 4 and 5 are based on curved beams and this formulation breaks down at larger values. Additionally, Chapter 5 demonstrates that the proposed model for predicting shear properties is not accurate when the half of the undulation length over thickness ratio and width over thickness ratio are simultaneously larger than 40; therefore, the variables are also constrained under these limits.

7.3.2 Genetic algorithms selection

The benchmarking Genetic Algorithms can be categorised into five categories. MOEA/D [80] and MOEA/D-PSF/MSF [84] are based on weight vector and decomposition. HEIA [274], BCE [275] and IBEA [77] all use indicator-based selection approach. MTS [276] is population based local search method. NSGA-II [75] and U-NSGA-III [97] are non-dominated sorting based niching algorithms and co-evolutionary Multi-Level Selection Genetic Algorithm (cMLSGA) [277] is multi-level selection method based co-evolutionary algorithm. The details of these algorithms are documented in their original paper and Chapter 2 has summarised the main mechanisms of these algorithms.

In order to perform a fair benchmarking across these Genetic Algorithms, the values of parameters in the solvers are selected from their original paper, which is the same as in Chapter 6. All the Genetic Algorithms are benchmarked using the same population size and total number of function calls. MTS is a population based optimisation algorithm having a different set of hyper-parameters from other algorithms. HEIA is based on immune algorithm and uses both genetic operators and differential evolution operators. High-affinity antibodies are cloned in HEIA, where the high-affinity is defined as non-dominated solutions located at less crowded

area. MOEA/D [80] has good performance on unconstrained problems; MOEA/D-PSF/MSF [84] is an updated version of MOEA/D with improved convergence and diversity. HEIA [274] and BCE [275] are hybrid/co-evolutionary algorithms that having high performance on solving many-objective optimisation problems. IBEA [77] is the first and also the mostly used indicator-based Genetic Algorithm, which improves the efficiency of finding the final Pareto front. MTS [276] has generally good performance across all problem sets as a general solver; NSGA-II [75] is the most popular general solver with high performance on multi-objective optimisation and U-NSGA-III [97] shows high performance on many-objective optimisation which unifies NSGA-III to be suitable for mono-, multi- and many-objective optimisation problems. co-evolutionary MLSGA (cMLSGA) [277], which uses a state-of-the-art Genetic Algorithm for half of the collectives and utilises a second state-of-the-art Genetic Algorithm for the other half, is currently known best general solver for many-objective optimisation.

The parameters of the genetic operators for NSGA-II, U-NSGA-III, MOEA/D, MOEA/D-PSF/MSF and MTS are available in Chapter 6. The genetic operator parameters of HEIA, BCE, IBEA and cMLSGA are listed in Tables 7-1 to 7-4. The parameters of cMLSGA are the same as those selected in [277] since Grudniewski and Sobey have tuned these parameters to give the best general performance. All algorithms are real value coded, random initialised and terminated when reach the total number of iterations. In order to quantitatively evaluate the performance of the state-of-the-art Genetic Algorithms, two indicators are introduced in the current study which are the mimicked inverted generational distance (mIGD) and mimicked hyper volume (mHV). The mIGD is introduced in Chapters 2 and 6 [30] and evaluated in eq. (6.8); lower mIGD value reflects a better quality and diversity of the obtained Pareto front. The mHV is inspired by the HV indicator proposed by [278,279]. The HV indicator calculates the summation of the objective space volume between the obtained Pareto front points and a predefined reference point. The predefined reference point in the mHV is determined using the mimicked Pareto front which is found by using the non-dominated filtering and by removing any duplications from the combined Pareto front results from all of the benchmarked solvers; a higher mHV value indicates a solver with a better performance. When comparing the results from the two metrics, the mHV metric is more representative of the diversity of the population but mIGD is more representative of the accuracy and uniformity of the obtained Pareto fronts, which is especially true when there are a small number of points in the Pareto Front. Therefore, using both indicators together allows an evaluation of the accuracy and the diversity of the obtained Pareto fronts for each solver. 300,000 total function

calls are used for all the benchmarked algorithms, which results in a population size of 1500 and 200 generations for most of the algorithms, in the current study and each solver is run over 30 independent cycles to obtain the entire statistical distributions of the Pareto front solutions.

Table 7- 1. HEIA parameter definition

Cloning	Clone the high-affinity antibody to perform hyper-mutation		
Evolutionary strategy	Selection	Pareto domination & crowding distance	
	Evolution 1	Simulated binary crossover (SBX) rate	1.0
		Polynomial mutation rate	0.08
	Evolution 2	Differential evolution crossover rate	0.9
		Polynomial mutation rate	0.08

Table 7- 2. BCE parameter definition

Reproduction	Selection type	Non-Pareto criterion & Pareto criterion
	Crossover type	Simulated binary crossover (SBX)
	Crossover rate	1.0
	Mutation type	Polynomial mutation
	Mutation rate	0.08

Table 7- 3. IBEA parameter definition

Reproduction	Selection type	Indicator-based selection
	Crossover type	Simulated binary crossover (SBX)
	Crossover rate	1.0
	Mutation type	Polynomial mutation
	Mutation rate	0.08

Table 7- 4. cMLSGA parameter definition

Classification	Classification method	Support vector machine (SVM)
	No. of collectives	8
Individual Level	Individual fitness evaluation	MLS-U with 4 collectives of HEIA and 4 collectives of IBEA
Collective Level	No. of eliminated and new generated collectives	1
	Total No. of skipped collectives elimination	10

7.4 Optimisation of plain weave fabric composites

7.4.1 Selection of the genetic algorithms

In order to evaluate the convergence of each of the benchmarked algorithms, the Pareto front results are extracted from each run at every 50 generations, or every 75,000 function calls, until 200 generations are reached, or 300,000 function calls. To reduce the number of results the best of the three MOEA/D variants, MOEA/D-PSF, is chosen for the illustration, U-NSGA-III is used for many-objective and three-objective optimisation and NSGA-II for the bi-objective optimisation. The convergence of the mIGD and mHV values for the seven solvers for one five-objective, two three-objective and two bi-objective optimisation problems are illustrated in Figures 7-2 to 7-6, where these figures show the mean values of mIGD and mHV extracted at each 50-generation until 200 generations. In addition, there is a league table of the 10 solvers in Appendix IV-A, where the mIGD and mHV values of each solver are extracted at every 50 generations or every 75,000 function calls.

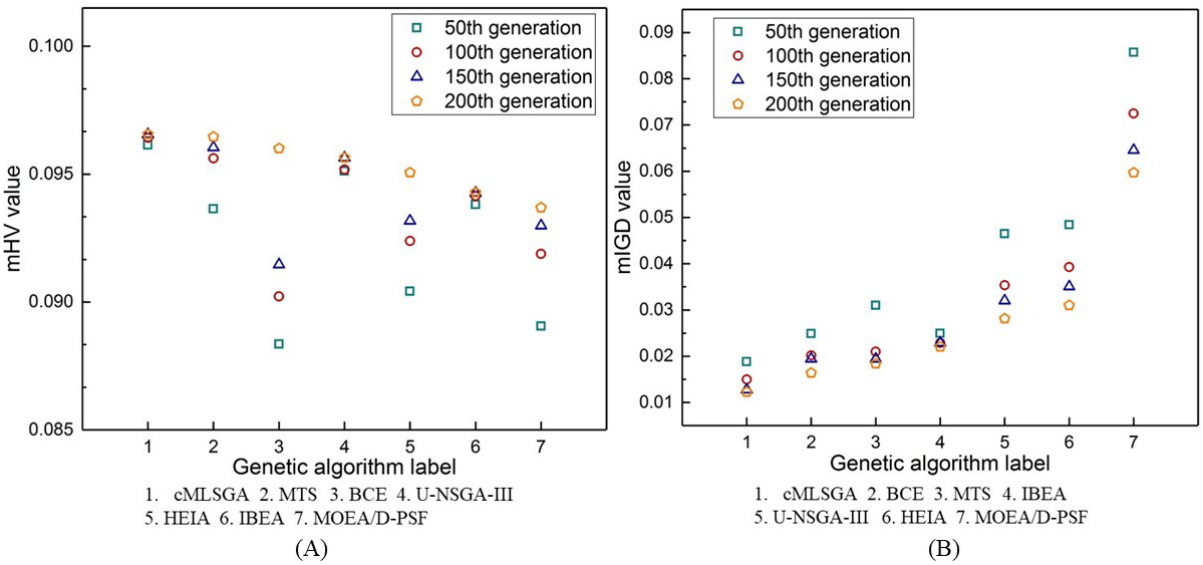

Figure 7- 2. The rank of the seven solvers for the five-objective optimisation problem based on the two indicators: (A) mHV mean value; (B) mIGD mean value.

cMLSGA achieves the best performance according to the ranking of the different algorithms with an mHV of 0.0966 at 200 generations and mIGD of 0.0123 at 200 generations in comparison to MTS which performs second best for mHV with a value of 0.0964 and BCE which performs second best for mIGD with a value of 0.0164. cMLSGA starts as the strongest solver after 50 generations and retains this position for both metrics. For the five-objective optimisation problem, only cMLSGA and IBEA obtain both converged mHV and mIGD values according to the results shown in Figure 7-2. All the rest solvers require more generations to achieve their converged mHV and mIGD values, which consume more computational resource. IBEA is the fastest solver to converge at 100 generations for both metrics, mHV and mIGD. However, the rank of IBEA is fifth by rearrangement according to the calculated average mHV and mIGD rank of the seven solvers. Therefore, cMLSGA is the only solver obtaining the best results while maintaining low computational cost. In addition, there is a surprising result that U-NSGA-III shows the top performance by some margin on many-objective problems [97], but has ordinary performance when solving this five-objective optimisation problem.

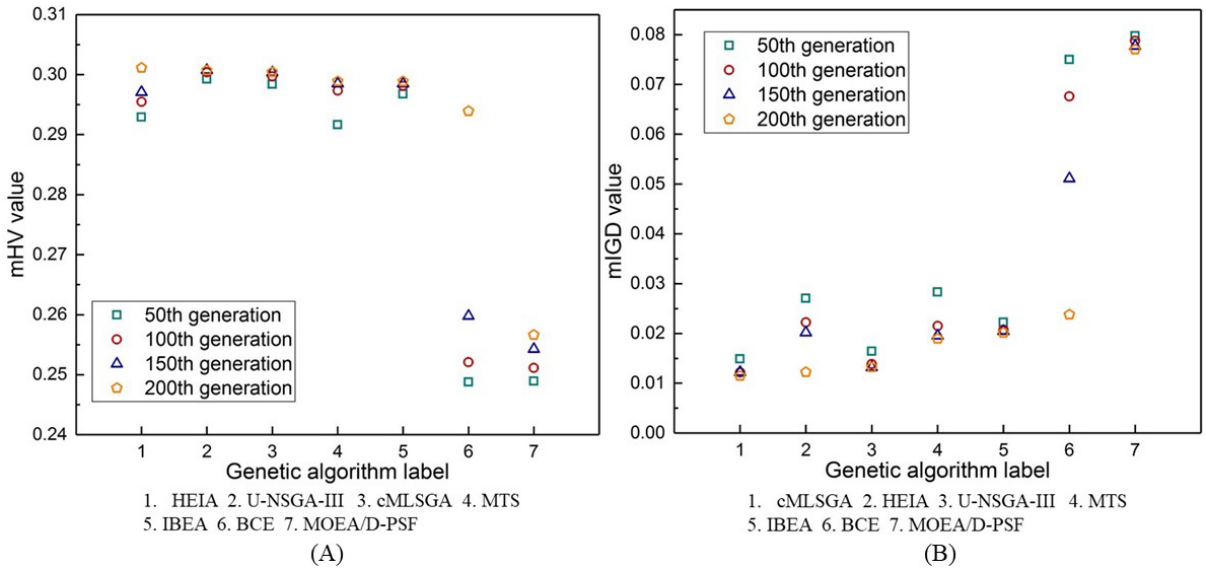

Figure 7- 3. The rank of the seven solvers for the tensile and shear moduli and areal density three-objective optimisation problem: (A) mHV mean value; (B) mIGD mean value.

For the three-objective moduli optimisation problem, HEIA performs best when measured using the mHV metric, with the results shown in Figure 7-3a, which has a value of 0.3011 at 200 generations compared to U-NSGA-III with a value of 0.3007. cMLSGA has the lowest mIGD metric, shown in Figure 7-3b, with a value of 0.0115 at 200 generations with HEIA in second place with a value of 0.0122. For these metrics cMLSGA, HEIA and U-NSGA-III share the top three places, confirming results from [132] that the more modern and diversity based algorithms are the strongest at solving these problem types, based due to the complexity of the search space when using a larger number of variables. U-NSGA-III has been developed for many-objective problems, but performs more strongly on this lower objective problem, contradicting the results seen in the evolutionary computation literature. It is considered that the different dominant characteristics between the plain weave fabric composite optimisation problems and the benchmark problems in the evolutionary computation literature make the selection of the best practices of Genetic Algorithms for solving composite optimisation problems difficult, which is similar as found in [30].

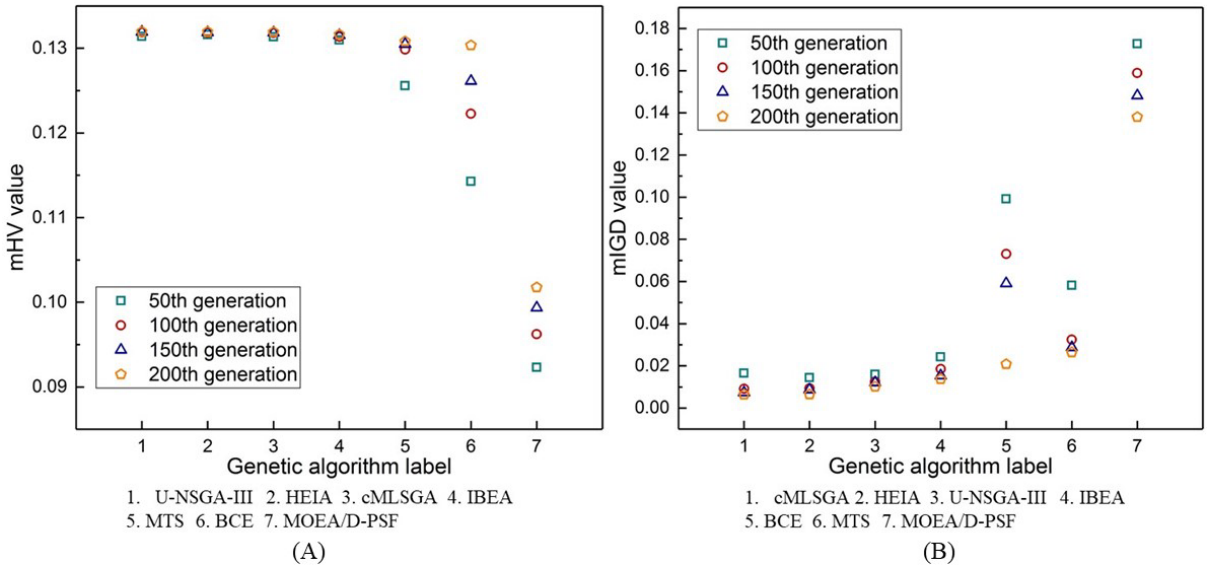

Figure 7- 4. The rank of the seven solvers for the tensile and shear strengths and areal density three-objective optimisation problem: (A) mHV mean value; (B) mIGD mean value.

For the three-objective strengths optimisation problems in eq. (7.8), all cMLSGA, HEIA and U-NSGA-III have achieved converged solutions and tied for the first place in the comprehensive rank. According to the results shown in Figure 7-3 and 7-4, it confirms cMLSGA, HEIA and U-NSGA-III are the best solvers for the two three-objective optimisation problems.

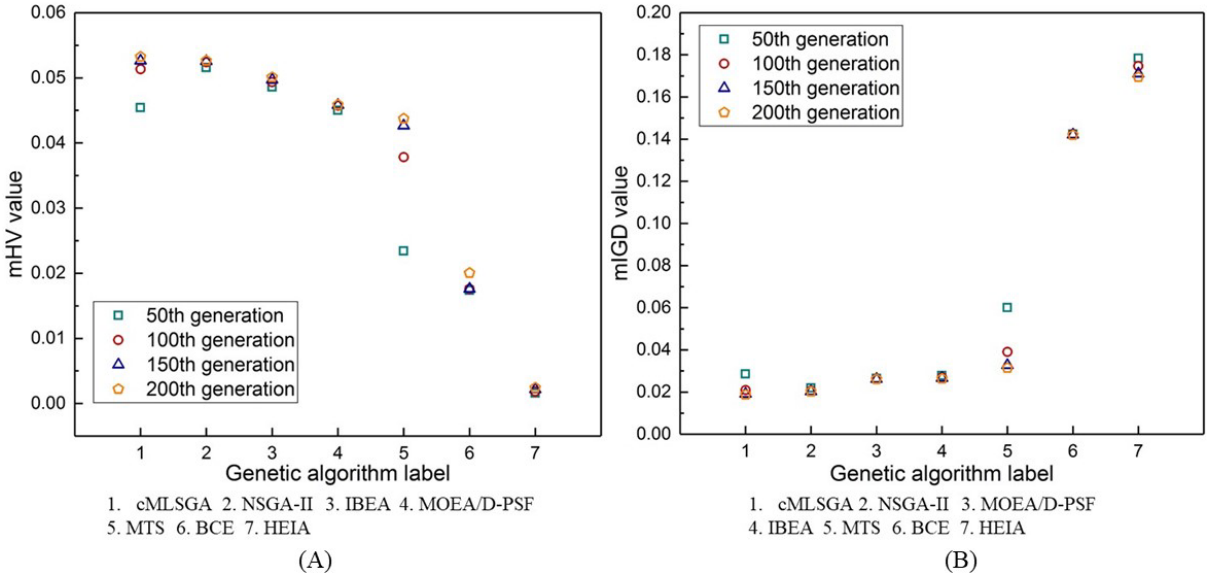

Figure 7- 5. The rank of the seven solvers for the specific tensile strength and modulus bi-objective optimisation problem: (A) mHV mean value; (B) mIGD mean value.

cMLSGA achieves the first place and NSGA-II achieves the second on optimising the tensile strength to stiffness ratio according to Figure 7-5. The mHV values of cMLSGA and

NSGA-II are respectively 0.0532 and 0.0526 and the mIGD values of them are 0.0187 and 0.0202. It is considered that the feature of the disconnected Pareto front shown in Figure 7-9 makes the cMLSGA perform better since the collective mechanism in cMLSGA guarantees the diversity of the obtained Pareto front and the co-evolutionary mechanism improves the accuracy of the solutions. However, this advantage is not obvious when the disconnected Pareto front has small gap, which is reflected by comparing the performance of cMLSGA on solving bi-objective problem in eq. (7.9), where the results of mHV and mIGD are shown in Figure 7-5, with its performance on solving the problem in eq. (7.10), where the results are illustrated in Figure 7-6.

It is considered that NSGA-II is the best solver for the two bi-objective optimisation problems since NSGA-II is the best solver on optimising the shear strength to stiffness ratio and second-best solver on optimising the tensile strength to stiffness ratio according to Figures 7-5 and 7-6. Furthermore, it converges fast for both problems, where the mean values of both mHV and mIGD converge from 50 generations in Figure 7-5 and converge from 100 generations in Figure 7-6.

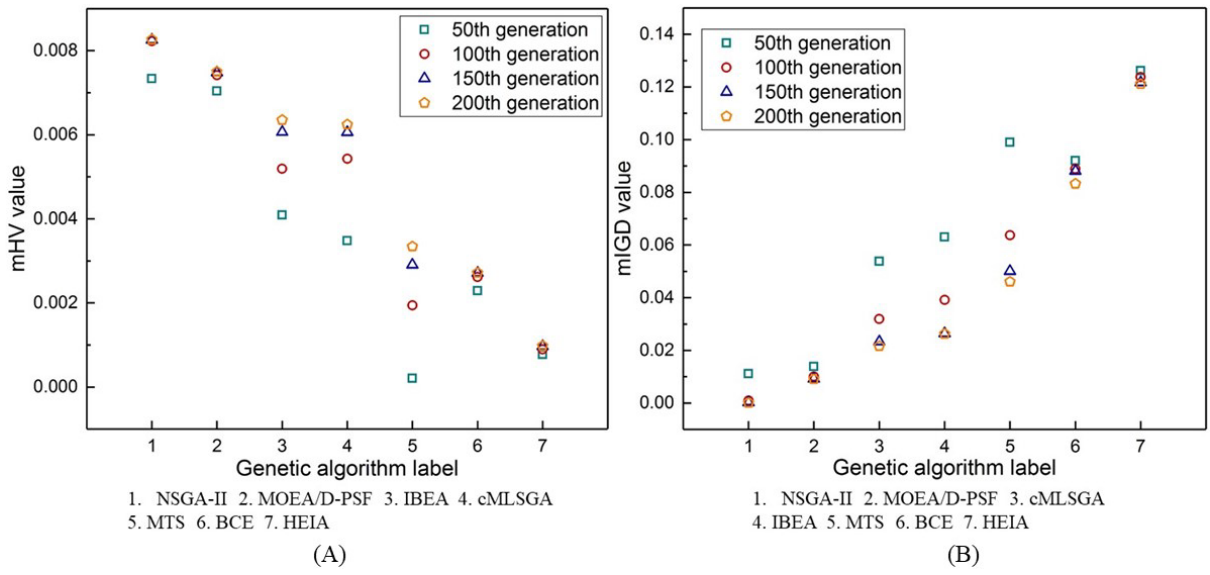

Figure 7- 6. The rank of the seven solvers for the specific shear strength and modulus bi-objective optimisation problem: (A) mHV mean value; (B) mIGD mean value.

7.4.2 Pareto fronts among five-objective, three-objective and bi-objective optimisation

In order to intuitively compare the Pareto front results among the five-objective, three-objective and bi-objective optimisation, the runs generating the best Pareto front results of the five-objective optimisation problem from cMLSGA are projected to two and three dimensions,

which are shown in Figures 7-7 to 7-10. In these figures a number of the Pareto front results overlap due to the projection from the 5-dimension to two or three dimensions. However, since all the Pareto front results found in the five-objective optimisation are non-dominated solutions, even a number of Pareto front results overlapped on the 3-dimension (or 2-dimension) plots, they have different properties on the remaining two dimensions (or the remaining three dimensions). In addition, Figures 7-7 and 7-8 illustrate all five dimensions of the optimal solutions using a colour-map to represent the fourth objective and the size of the marker to represent the fifth dimension. The runs generating the best Pareto front results of the three-objective optimisation problems from cMLSGA and of the bi-objective optimisation problems from NSGA-II are also illustrated in Figures 7-7 to 7-10.

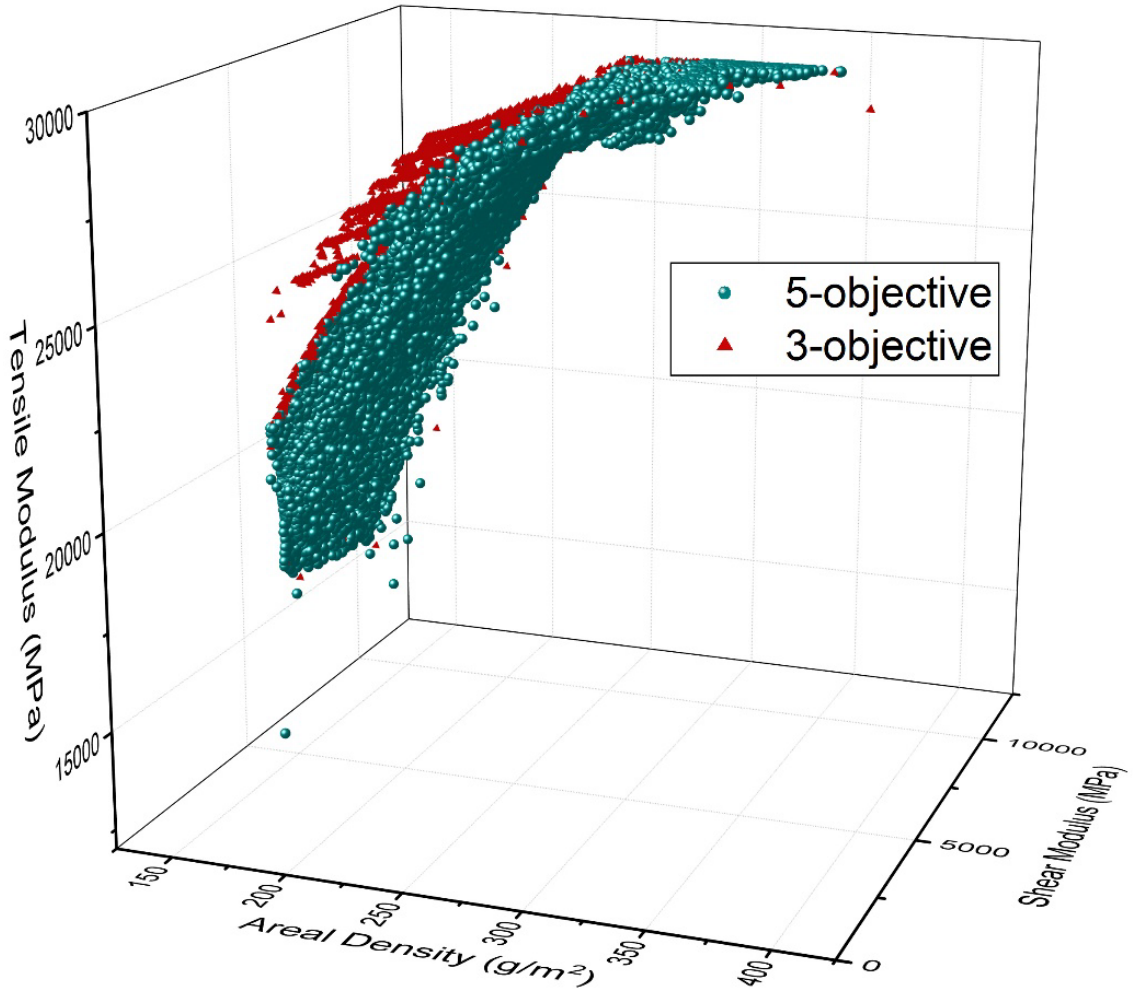

(A)

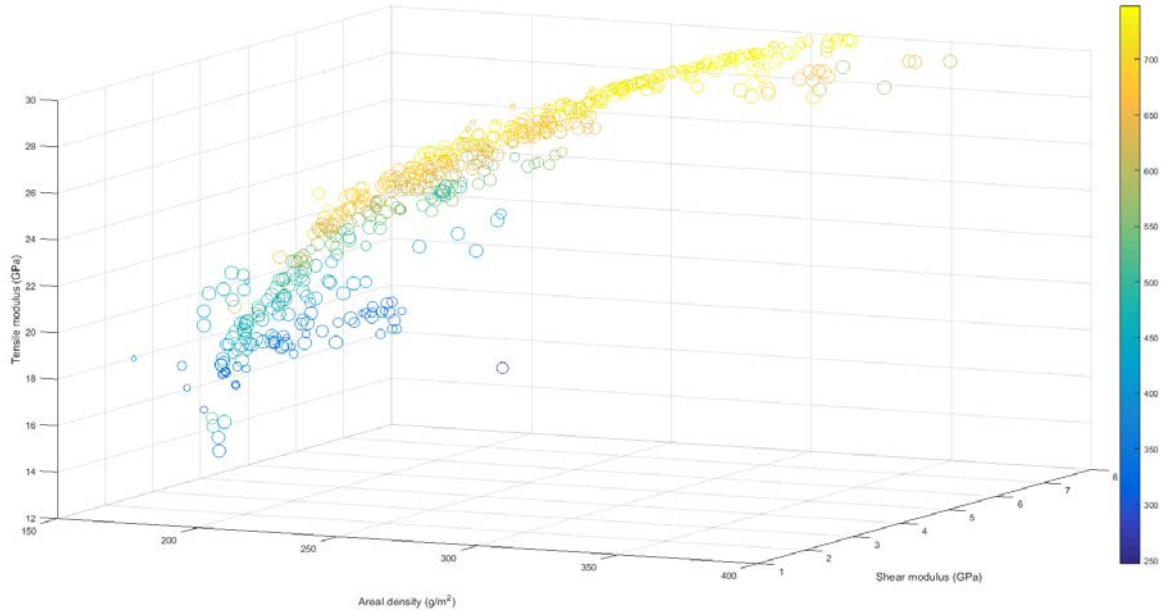

(B)

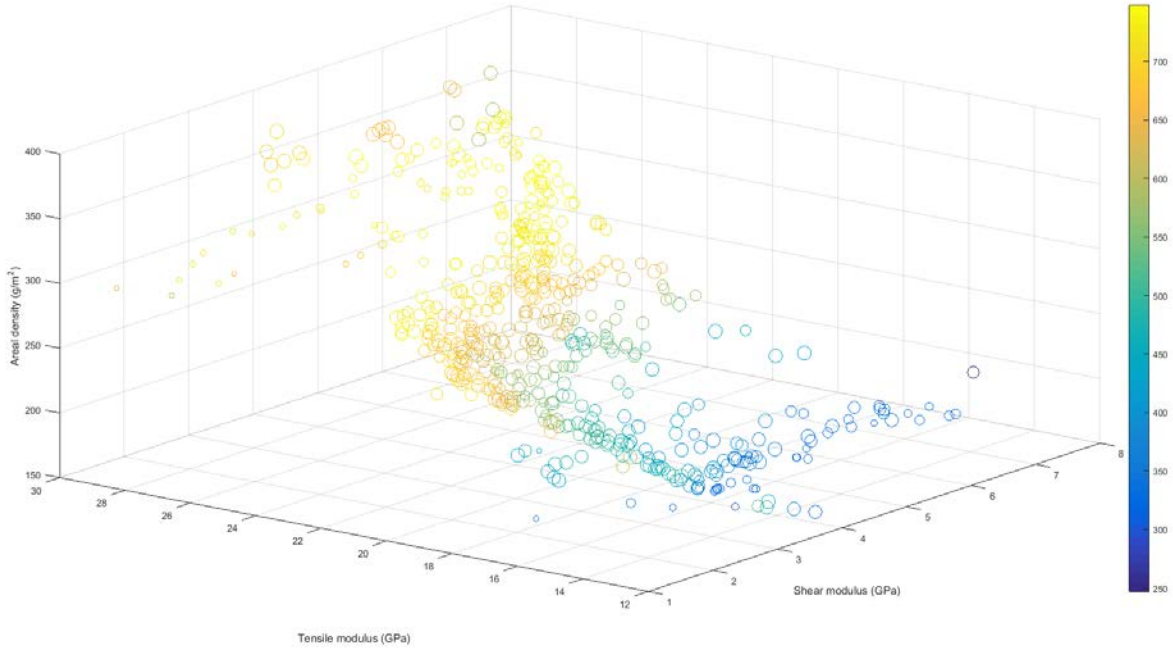

(C)

Figure 7- 7. Comparison of Pareto fronts from five-objective and three-objective optimisation of tensile modulus, shear modulus and areal density.

It is shown that the Pareto front results from the three-objective moduli optimisation in Figure 7-7A have the same shape as the projected Pareto front results from the five-objective optimisation. However, it is obvious that most of the Pareto front results from the five-objective optimisation are dominated by the Pareto front results from the three-objective optimisation. Therefore, it is considered that the properties of tensile and shear moduli and areal density must

be compromised to achieve better tensile and shear strengths in the five-objective optimisation. In addition, part of the Pareto front results from the five-objective optimisation, which are close to the Pareto front results from the three-objective optimisation, dominate the five-objective optimisation Pareto front results in Figure 7-7A. However, since all of them are non-dominated solutions, the Pareto front results shown in Figure 7-7A that dominated by other points have better tensile and/or shear strengths. Figures 7-7B and C illustrate the other two dimensions of the three-dimensional plot by a colour-map to represent the tensile strength and the size of the marker to represent the shear strength. The colour bar in the figures reflects the tensile strength. The larger the size of the marker the higher the shear strength. It is obvious the tensile modulus and tensile strength have the same trend and the areal density increases when both of them are increased.

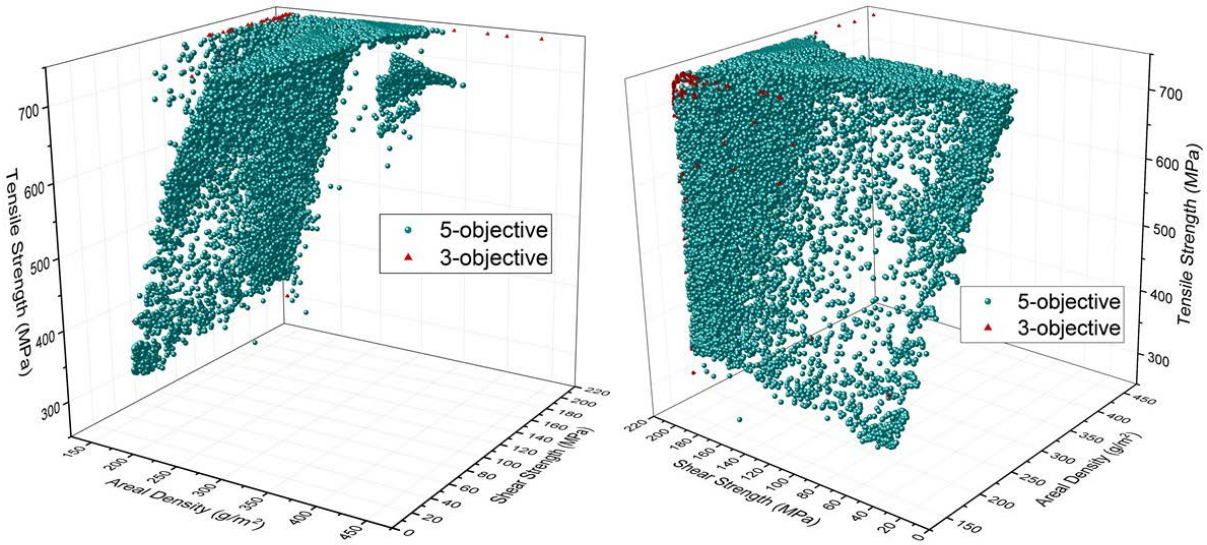

(A) Front view (B) Back view

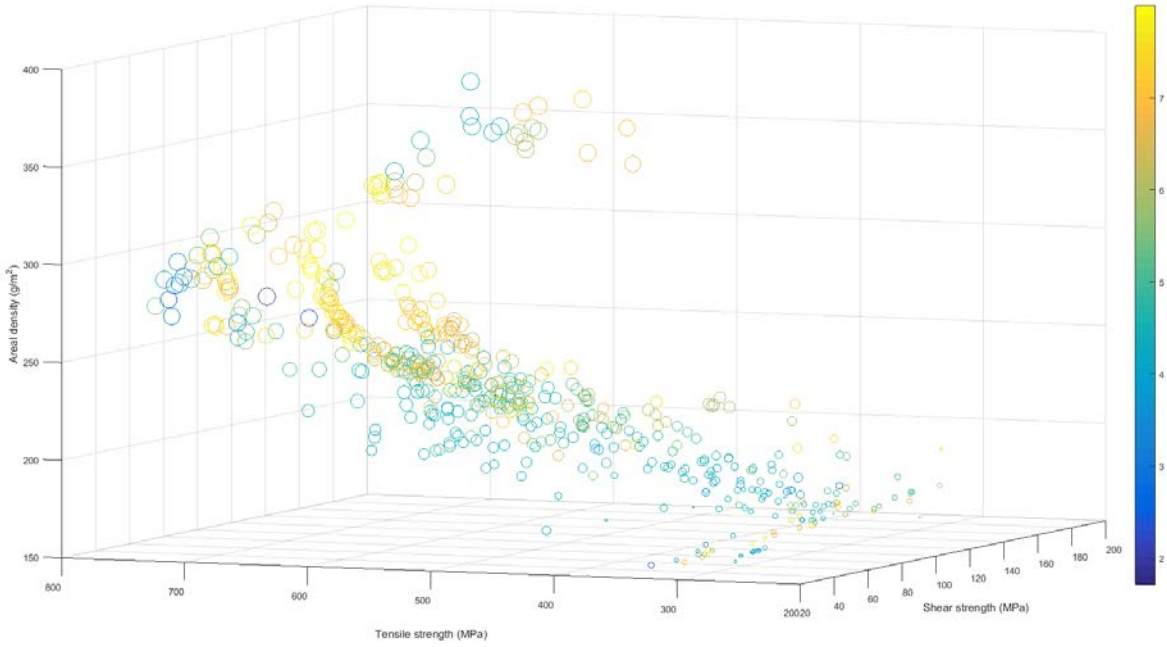

(C)

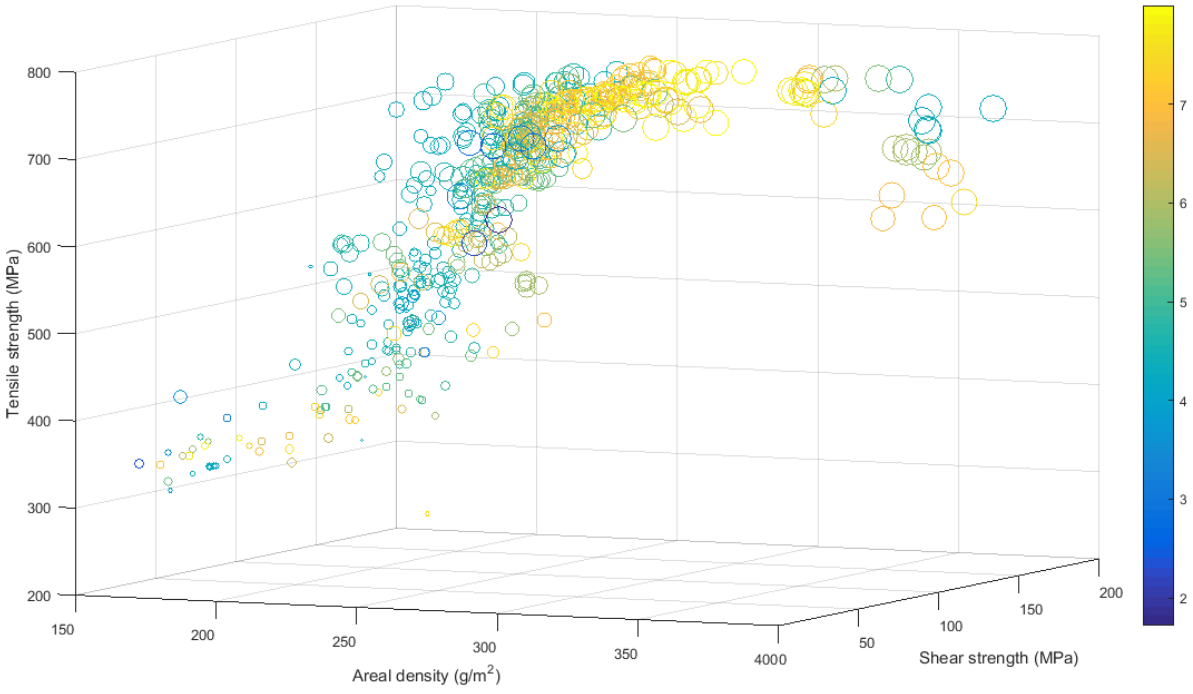

(D)

Figure 7- 8. Comparison of Pareto fronts from five-objective and three-objective optimisation of tensile strength, shear strength and areal density.

Compared with the Pareto front in Figure 7-7A, the three-objective optimisation Pareto front results shown in Figures 7-8A and B are mostly concentrated on a small area of the objective space. In Figures 7-8C and D, the colour-map represents the shear modulus and the

size of the marker represents the tensile modulus. It is found that most optimal designs that have a high shear modulus are concentrated at the region where the areal densities are between 200 g/m^2 and 250 g/m^2, but it is difficult to determine any specific rule. Furthermore, it is considered that the relationship between the shear strength and areal density are loose since the same tendency of changes are not shown in the three-objective and five-objective optimisation Pareto fronts. However, when designing a plain weave fabric composite structure, the weight of each ply is expected between 200 g/m^2 and 250 g/m^2 if high shear modulus is expected. Designers are able to estimate the weight of the structure in advance and tune the designs. In order to understand these phenomena, the relationship between the variable space and objective space are analysed. It is found that the simultaneous change of width and undulation length of yarns have positive correlation to the tensile modulus and strength but negative correlation to the shear modulus and strength. The shear modulus and strength are increased and then decreased when only the undulation length of warp or weft yarn increased. The increased undulation length of one-direction yarns causes the increased yarn spaces in the other direction. The increased yarn spaces reduce the tensile and shear strengths and moduli in that direction but reduce the total areal density. The simultaneous change of thickness and width of yarns have positive correlation to the areal density, but the thickness has negative correlation to the tensile modulus and shear modulus and strength. The increased warp/weft yarn thickness first increases and then decreases the tensile strength in warp/weft direction. In comprehensive, the relationship between the objectives and variables is nonlinear and complicated, where either the single of or the combination of the six variables influence the five objectives, confirming the complicity of the five-objective optimisation problem. Furthermore, several examples are summarised in the Appendix IV-B, which demonstrates how the variable space variation influences the changes in objective space. It is considered that the areal density and shear properties have nonlinear correlation to several design variables, such as yarn thickness, undulation length, yarn space and width, and they are also sensitive to the combination influences of these variables. These cause the obtained Pareto front results illustrate poor correlation between the shear strength and areal density.

A similar phenomenon as in Figure 7-7A is found again in Figures 7-8A, 7-9 and 7-10 that most of the results from five-objective optimisation are dominated by the results from the three-objective and bi-objective optimisation. This confirms that the optimal solutions from the simulations with fewer objectives have better results for these objectives, such as specific tensile strength and modulus optimisation in Figure 7-9, but compromise on the performance

of other objectives, such as shear. Therefore, many-objective optimisation is necessary to ensure that all the mechanical properties remain high, as changes to improve one material property degrade those of another.

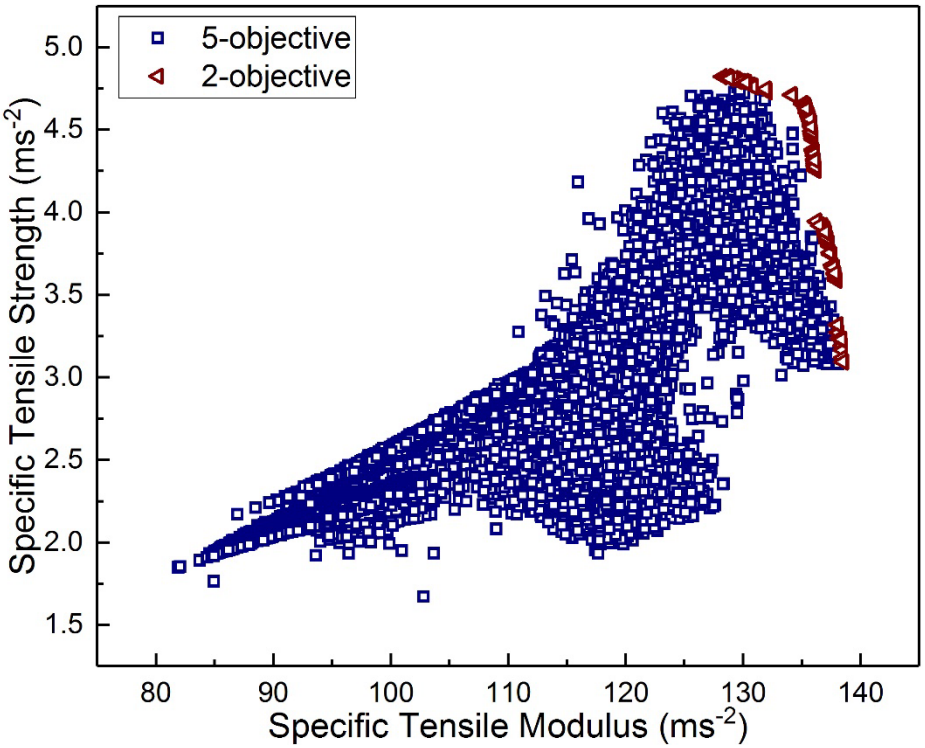

Figure 7- 9. Comparison of Pareto fronts from five-objective and bi-objective optimisation of specific tensile strength and modulus.

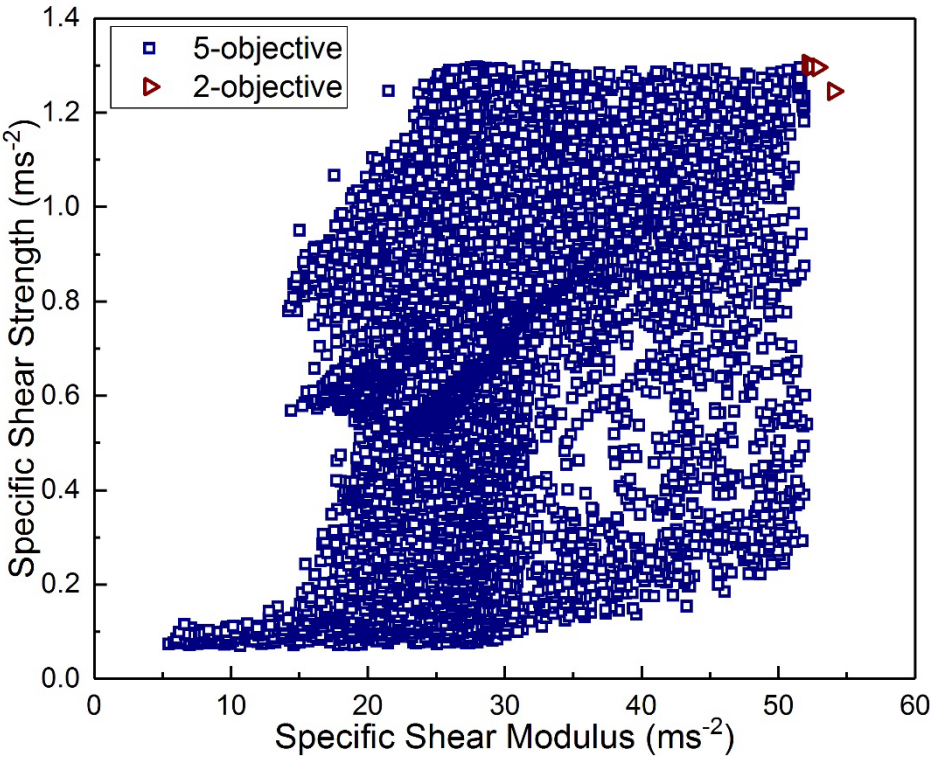

Figure 7- 10. Comparison of Pareto fronts from five-objective and bi-objective optimisation of specific shear strength and modulus.

The bi-objective optimisation Pareto fronts found in both Figures 7-9 and 7-10 are disconnected Pareto fronts but the Pareto front in Figure 7-10 has smaller gap between the two fronts and most results are concentrated on one of the two fronts. In addition, five-objective optimisation Pareto front results show the correlation between the specific tensile strength and modulus in Figure 7-9 but the correlation between specific shear strength and modulus are not obvious as the projected Pareto front results are distributed in the plot. The reason is also considered similar as that causing the uncorrelated areal density and shear strength shown in Figure 7-8.

The Pareto front results from the best run of cMLSGA from the five-objective optimisation problem with 1500 population size and 200 generations are selected to demonstrate the implications for PWF composite designs since they achieve the best performance. Each Pareto front solution is assumed close to the optimal design of the Plain Weave Fabric composites since the standard deviation of mHV and mIGD values are 0.000712 and 0.000103 among the 30 independent runs of cMLSGA and the best run has the mHV and mIGD values of 0.0968 and 0.0104, which are the best values among all the 10 solvers. Five extreme points: maximum tensile strength and modulus, maximum shear strength and modulus

and minimum areal density, on the five-dimensional Pareto front are selected to illustrate the five different types of designs. The resulting topologies are illustrated in Figure 7-11.

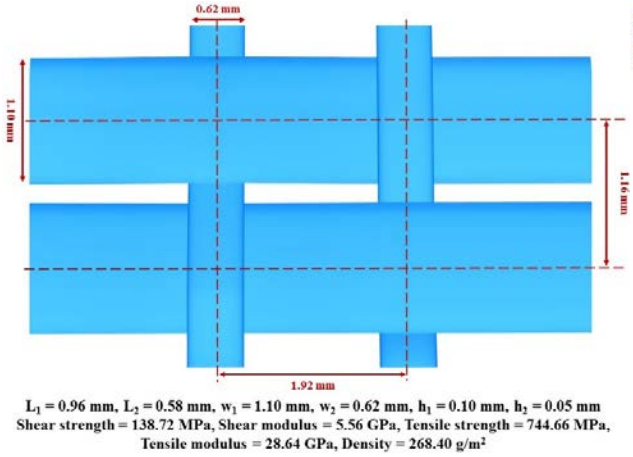

L_1 = 0.96 mm, L_2 = 0.58 mm, w_1 = 1.10 mm, w_2 = 0.62 mm, h_1 = 0.10 mm, h_2 = 0.05 mm
Shear strength = 138.72 MPa, Shear modulus = 5.56 GPa, Tensile strength = 744.66 MPa,
Tensile modulus = 28.64 GPa, Density = 268.40 g/m²

(A)

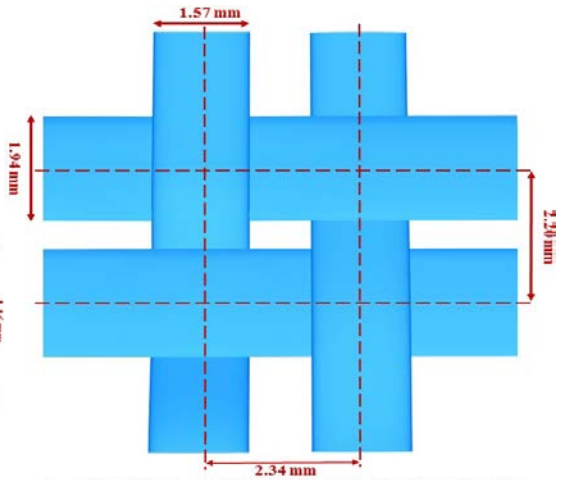

L_1 = 1.17 mm, L_2 = 1.10 mm, w_1 = 1.94 mm, w_2 = 1.57 mm,
h_1 = 0.12 mm, h_2 = 0.10 mm
Shear strength = 181.87 MPa, Shear modulus = 4.20 GPa,
Tensile strength = 629.00 MPa, Tensile modulus = 29.87 GPa,
Density = 349.28 g/m²

(B)

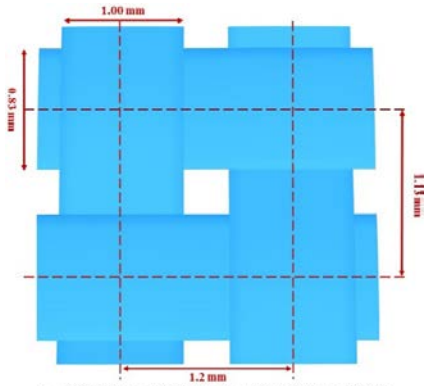

L_1 = 0.60 mm, L_2 = 0.565 mm, w_1 = 0.83 mm, w_2 = 1.00 mm,
h_1 = 0.04 mm, h_2 = 0.04 mm
Shear strength = 197.40 MPa, Shear modulus = 4.09 GPa,
Tensile strength = 452.99 MPa, Tensile modulus = 14.43 GPa,
Density = 167.25 g/m²

(C)

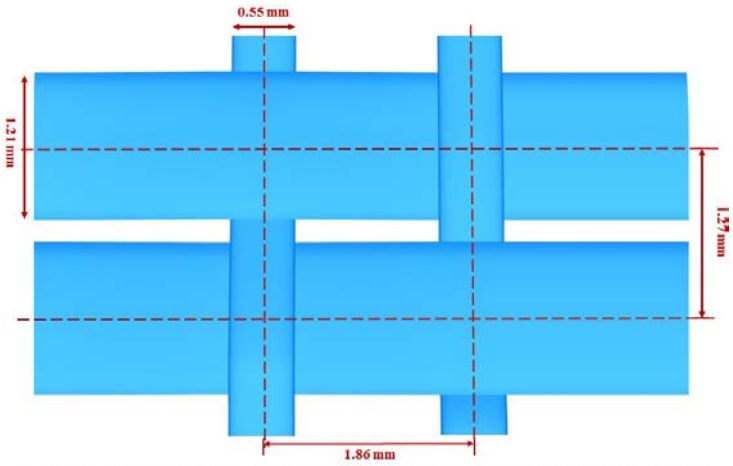

L_1 = 0.93 mm, L_2 = 0.635 mm, w_1 = 1.21 mm, w_2 = 0.55 mm, h_1 = 0.11 mm, h_2 = 0.05 mm
Shear strength = 67.64 MPa, Shear modulus = 7.88 GPa, Tensile strength = 728.29 MPa,
Tensile modulus = 28.54 GPa, Density = 310.61 g/m²

(D)

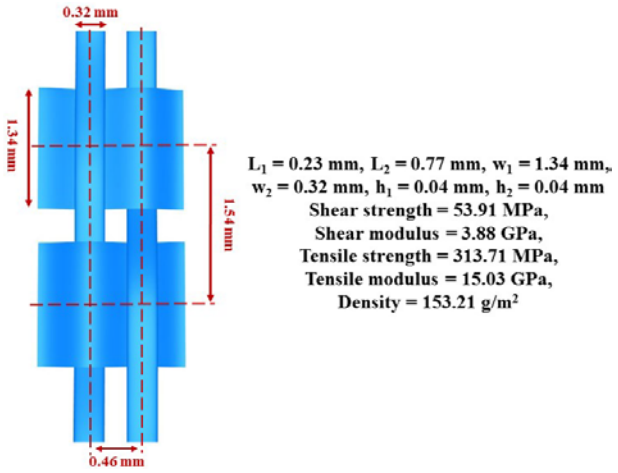

(E)

Figure 7- 11. Optimal designs of PWF composites: the design having (A) maximum tensile strength; (B) maximum tensile modulus; (C) maximum shear strength; (D) maximum shear modulus; (E) minimum areal density.

The maximum tensile strength and modulus, shear strength and modulus and minimum areal density of the five extreme optimal designs are 744.66 MPa, 29.87 GPa, 197.40 MPa, 7.88 GPa and 153.21 g/m^2, respectively. It is found that thick yarn provides high tensile strength and modulus but significantly increases the areal density of the material. In addition, the weave patterns illustrated in Figures 7-11A, B and D have large undulation length and width on warp yarns and all the three weave patterns provide high tensile strength and tensile modulus along the warp direction. When comparing Figure 7-11B with C, it is found that the proportion of warp and weft yarns geometric parameters are similar but the weave fabric in 7-11C is more compact than that in 7-11B, which provides higher shear strength. When comparing Figures 7-11C and E against Figures 7-11A, B and D, it is found that smaller undulation length, width and thickness of warp and weft tows provide lower areal density but significantly reduce the mechanical properties of the materials. Bai et al. [39,299] and Wang and Sobey [47] have summarised the fabric specifications of 10 experimental specimens with nine of them obtained from nine other papers. It is found that eight of the 10 specimens have the same fabric specifications in their both warp and weft directions and the other two specimens also have similar fabric specifications in the two directions. Seven of them have small undulation length and width of both tows, which are smaller than those in Figure 7-11C, but thick tows, which have similar thickness as those in Figure 7-11B. The yarn specifications make these experimental specimens have low tensile properties and high areal density, which are not applicable on light-weight structures.

A current EW220/5284 weave pattern [39,47,299] is introduced in Section 7.2 for the comparison, which has L_1 = 0.714 mm, L_2 = 0.556 mm, w_1 = 1.0 mm, w_2 = 1.2 mm, h_1 = 0.08 mm and h_2 = 0.067 mm, providing 492.52 MPa tensile strength, 19.30 GPa tensile modulus, 111.09 MPa shear strength, 6.45 GPa shear modulus and 330.18 g/m^2 areal density. The weave pattern shown in Figure 7-11A has 13.80% shear modulus reduction but provides 24.87% shear strength improvement, 51.19% improved tensile strength, 48.39% improved tensile modulus and 18.71% areal density reduction. The weave pattern shown in Figure 7-11C has slightly smaller geometric parameters but similar topology as the current EW220/5284 weave pattern. Compared to the current weave pattern, the optimal design in Figure 7-11C has 8.02% reduction in tensile strength, 25.23% reduction in tensile modulus and 36.59% reduction in shear modulus, but it achieves 77.69% increased shear strength and 49.35% reduced density. When compared to the five extreme optimal designs against the current weave pattern, the tensile strength is improved 51.19%, the tensile modulus is improved 54.77%, the shear strength is improved 77.69%, the shear modulus is improved 22.17% and the areal density is reduced 53.60%, respectively.

7.5 Discussion

It is important to perform benchmarking since it helps to select the most appropriate solvers of the problems. Performing benchmarking is a common method to evaluate the new developed algorithm or find out the best practices of solver for the problem in evolutionary computational literature. Hyper volume and inverted generational distance indicators are frequently simultaneously used in evolutionary computational literature to quantitatively evaluation the performance of the benchmarked solvers since HV metric is more representative of the diversity of the obtained Pareto front but IGD is more representative of the accuracy. Inspired by the mIGD proposed in Chapter 6, this Chapter proposes mHV metric from HV and use both indicators to evaluate the performance of each solver when solve composite structural optimisation problems. The combination of the mHV and mIGD quantitatively evaluates the performance of solvers when solve engineering optimisation problems and obtain best practice for solving this and similar problems. According to the mHV and mIGD results and the convergence speed of each solver shown in Section 7.4.1, cMLSGA performs the best when solve the five-objective optimisation of plain weave fabric composites, cMLSGA, HEIA and U-NSGA-III are the best solvers for the two three-objective optimisation problems and NSGA-II performs the best on the two bi-objective optimisation problems.

In addition, it is important to investigate the dominant characteristics of the optimisation problems. It helps the selection of the appropriate solvers for the similar problems and to better understand both the mechanisms of the solvers and increase the use of those solvers that represent best practice in the composites domain. For the current study, cMLSGA, HEIA, U-NSGA-III and NSGA-II are the best performers, with the cMLSGA showing the greatest accuracy in four of the five cases and the best diversity in two cases. For the five-objective and three-objective problems, the combination of the co-evolution of HEIA and IBEA on the individual level and the collective level mechanisms of the cMLSGA simultaneously enhances the ability of approximating the optimal solutions and the balance between the convergence and diversity. U-NSGA-III uses the same non-dominated rank mechanism as in the NSGA-II to efficiently approximate the optimal solutions and uses a set of reference directions rather than using the crowding distance operator as in NSGA-II to maintain the diversity for many-objective optimisation problems. These features allow U-NSGA-III to find the entire Pareto front and rapidly converge to the final solutions. However, this algorithm is an update to NSGA-II for many-objective problems, those with 4 or more objectives, and in this case the algorithm does not perform particularly strongly on these problems, contrary to the evolutionary computation literature. This demonstrates the continued importance of benchmarking these algorithms on more realistic problems with a relevant optimisation landscape.

It is found that Figures 7-7 to 7-10 show disconnection and dense points at multiple parts of projected Pareto front from the five-objective optimisation. The dense points are caused by the projection where these Pareto front results have similar or the same values in the properties corresponding to the plot axis but different values in the unshown properties. These dense Pareto front results are easily to be found but time consuming since they have similar or same values in multiple objectives of the five objectives, but the variables need to be carefully tuned by the solvers to obtain a new Pareto front result in this area, which is the place many solvers may get stuck. This is considered as the reason that eight of the ten solvers don’t obtain a converged Pareto front in 200 generations when solve the five-objective problem. The disconnected feature of Pareto fronts are also found in both three-objective and bi-objective optimisation problems illustrated in red triangle points of Figures 7-7 to 7-10. These gaps in the Pareto fronts are also shown in the mimicked Pareto front, which means none of the 10 solvers have found any Pareto front results in these gaps. Based on these findings it is proposed that the dense point area and disconnected features of the search space and the problem

complexity are the dominant characteristics of the five-objective and three-objective problems. However, these dominant characteristics aren't usually considered in the literature. It is found that the balance between the exploitation, the ability of approximating the optimal solutions, and the exploration, the ability of maintaining the diversity of population, becomes significant for solving many-objective optimisation problems.

For the two bi-objective problems, both have disconnected nature of the front, which are illustrated in red points of Figures 7-9 and 7-10, but the Pareto front of the specific tensile strength and modulus problem has larger and more gaps than that of the specific shear strength and modulus problem. When the quantity and size of the gaps are small, the crowding distance operator is still capable of maintaining the diversity and the non-dominated rank mechanism enhances the ability of finding the optimal solutions by the NSGA-II. However, cMLSGA becomes the best when multiple and large gaps appear in the search space. It is found that the disconnected nature of the front is the dominant characteristic of the bi-objective problems, which is the same as in [30].

7.6 Conclusions

The combination of cheap manufacturing and highly optimisable fabrics makes the wider application of plain weave fabric composites a possibility in industries that do not traditionally use them. In this Chapter, 10 state-of-the-art Genetic Algorithms are employed to find low density designs of Plain Weave Fabric composites under tension and shear. These algorithms are benchmarked to determine the best solvers and the dominant characteristics of the problems. The benchmarking demonstrates that for the three-objective and five-objective optimisation problems that cMLSGA, HEIA and U-NSGA-III are the top performers, where these use of the algorithms is currently rare in the composite optimisation literature. The benchmarking of the bi-objective optimisation problems shows that NSGA-II achieves the best performance, which supports its use as the most popular of the modern algorithms in the literature. The disconnected nature of the Pareto front is the main characteristic which influences the selection of these algorithms since the 'diversity first' general solver, cMLSGA, simultaneously achieves lower mIGD and higher mHV values than other solvers when the optimisation problem has disconnected feature in the Pareto front. The results show that several composites with extreme properties can be found using the bi-objective approach with the five different extreme optimal designs improving the tensile strength by 51.19%, the tensile modulus by 54.77%, the shear strength by 77.69%, the shear by 22.17% and the areal density by 53.60%. However, one design which improves four of the five properties can be found when using a many-objective approach

with 5 objectives, when compared to a current experimental sample, with one optimal design demonstrating a 13.80% shear modulus reduction, a 24.87% shear strength improvement, 51.19% improved tensile strength, 48.39% improved tensile modulus and 18.71% areal density reduction.

Chapter 8. Discussion

8.1 Benefits of current work

This work comparatively reviews the state-of-the-art woven fabric composite modelling methods. The review helps to understand the advantages and disadvantages of each modelling method. The result of the review helps other researchers to select appropriate modelling methods for their requirements. This work also comparatively reviews the use of Genetic Algorithms in composite materials and structural optimisation from the representative 17 composite journals over the past decade and compares them with the state-of-the-art in evolutionary computation. The review helps to understand the current problems in the composites optimisation literature and to determine the challenges for the coming years. The descriptions of Genetic Algorithms' history and the mechanism of main Genetic Algorithms help researchers in composites field better understand the Genetic Algorithms. The comparison with evolutionary computation helps researchers in the composites field to extend the range of the selection of Genetic Algorithms and increase the usage of the state-of-the-art Genetic Algorithms. Furthermore, it encourages researchers from both a general engineering background and computational science field to develop specific Genetic Algorithms for solving engineering optimisation problems, benchmark the state-of-the-art Evolutionary Algorithms to find the best practice of solver for the specific problem and determine the dominant characteristics of the problems for better selection of the correct solvers. The recommendations help researchers in the composites field to improve their composite optimisation works.

Plain weave fabric composites are increasingly used in many applications, especially aerospace structures. The biaxial properties of plain weave fabric composites are important as they are more representative of the performance of these materials under complex loading conditions. However, experimental determination of these properties is difficult. There are no methods to reliably determine and optimise these properties other than through finite element methods. However, using finite element methods is computationally expensive especially when they are used in the industrial design and optimisation which require hundreds of thousands of repetition. In this work, a novel micromechanical model based on the minimum total complementary potential energy principle is proposed to provide a simple way to rapidly predict the strength of plain weave fabric composites under different biaxial tensile loading ratios. The model is verified with four types of material, ranging in mechanical properties from carbon to glass fibres, giving a mean error of 11.22% and a maximum error of 16.74%, which demonstrate the effectiveness of the model. The standard deviation of prediction errors among

11 cases is 2.66, which demonstrates the robustness of the model for a range of applications. Furthermore, the failure locations for the woven fabric composite can also be predicted. The result is a method that helps manufacturers to rapidly evaluate both the biaxial and uniaxial strengths of plain weave fabric composites without experiments or finite element analysis. In addition, this model provides a reliable and rapid virtual experimental method to replace the actual experiments, which can save a huge amount of time and cost in the design process, especially for basic material tests which require many repetitions or experiments that are difficult or expensive to perform.

Except the predictions of biaxial tensile strengths of plain weave fabric composites, the investigation of the shear modulus and strength predictions are also important. However, there are a few investigations focusing on the shear properties of plain weave fabric composites, while the emphasis of the current investigations is on the tensile and compressive properties [33,37,39,299,308,309]. The main methods for the determination of these properties are various finite element methods and experimental methods but when comparing the two methods with analytical methods the finite element methods are computationally expensive and the experimental methods require skilled users. In this work, a novel micromechanical model based on the minimum total complementary potential energy principle is proposed to allow computationally efficient prediction of both shear modulus and strength of plain weave fabric composites. The new model is easy to be utilised and provides a rapid way to perform virtual experiments, which is efficient and low cost for the design of plain weave fabric composite structures, providing instant feedback in the design process. It gives a mean error of 15.24% in shear modulus predictions and 8.51% in shear strength predictions against experimental measurements with a diverse range of different materials. Furthermore, the new model has prediction error standard deviation of 4.10 for seven cases which reflects the prediction robustness for a range of materials. Compared against another two available analytical model for shear modulus prediction and one available analytical method for shear strength prediction, the new model is the most reliable model for a range of applications. The result is a method that helps manufacturers to rapidly evaluate both the shear modulus and strength of a plain weave fabric composite without actual experiments or finite element analysis which are expensive and difficult to perform. The efficiency of the new model helps the model to be an appropriate choice as the fitness evaluation method used in the optimisation of plain weave fabric composite shear properties.

Triaxial weave fabrics are increasingly used in ultralight composite structures but it is unknown how close to optimal the currently available fibre weave patterns are. In this work four state-of-the-art Genetic Algorithms are employed to find their optimal weave patterns under tension. 643 points are found in the best Pareto front providing a range of designs exhibiting higher strength to stiffness ratios when compared to a current example, where the lowest modulus solution achieves a tensile strength to stiffness ratio improvement of 1191%. By adding areal density as another objective, there are 17 designs that are potentially capable of being designed for ultralight structures. A potential increase of 228.05% in the strength to stiffness ratio with increase of 149.49% in the strength is made with the same surface density as a current example. These allow selection of designs with high specific strength to stiffness ratios, ensuring practical designs that can be used for ultra-lightweight applications. The results are found by better understanding the dominant characteristics of the optimisation problem, which is shown to be important to find the optimal weave patterns. It is shown that the selection of the Genetic Algorithm is crucial where non-specialist solvers are incapable of finding these designs and only MLSGA-NSGAII regularly finds the entire Pareto front. The benchmarking demonstrates that the disconnected nature of the front is the dominant characteristic of the search space but isn't generally considered a dominant characteristic in the literature. Finally, the paper highlights the necessity for composite structural optimisation research to determine and benchmark the dominant characteristics of composite optimisation problems, which will result in improved results from optimisation exercises.

From the triaxial weave fabric composite optimisation study, it is found that the number of optimal designs is reduced significantly from 643 designs in the first case study to 17 designs when adding a third objective into the second case study. It is considered that having a many-objective optimisation is compulsory. This helps to find more optimal designs that simultaneously satisfy all the objectives. Therefore, a many-objective optimisation is performed in the second woven fabric composite optimisation study. In this work, 10 state-of-the-art Genetic Algorithms are employed and benchmarked to find the optimal designs of plain weave fabric composites under tension and shear. The optimisation of the plain weave fabric composites helps engineers to select one or several proper designs for their applications that simultaneously match five of their requirements. In addition, the many-objective optimisation study has investigated the dominant characteristics of a five-objective, two three-objective and two bi-objective optimisation problems. The results help to select appropriate solvers for other many-objective optimisation problems and increase the use of the state-of-the-art Genetic

Algorithms. Compared with a current experimental sample, one optimal design has 13.80% shear modulus reduction but provides 24.87% shear strength improvement, 51.19% improved tensile strength, 48.39% improved tensile modulus and 18.71% areal density reduction. When comparing the five extreme optimal designs against the current weave pattern, the tensile strength is improved by 51.19%, the tensile modulus is improved by 54.77%, the shear strength is improved by 77.69%, the shear modulus is improved by 22.17% and the areal density is reduced by 53.60%, respectively.

8.2 Limitations

There are six main limitations for the two proposed micromechanical models. First, both of them are not applicable for the mechanical properties prediction of woven fabric composites under high or low temperature conditions since the temperature influences are not considered. Second, it is unknown whether the two models are accurate for mechanical properties prediction of thick woven fabric composite laminates since the interactions between layers are not considered in the two models and both models are only verified with thin experimental specimens which have three to five layers. Third, both of the models are not applicable for the mechanical properties predictions of hybrid woven fabric composites, which have the yarns that constituted by more than one type of fibre or laminates that consist of plies with different composite materials. Fourth, both models assume that the warp and weft fibre tows have the same cross-section. However, if the cross-section shape among warp tows or weft tows are significantly different, the two models have difficulties to accurately predict the mechanical properties. Therefore, it is difficult to use them for the predictions of natural plain weave fabric composite mechanical properties, such as flax fabrics. Fifth, both of them are not able to predict the mechanical properties of woven fabric composites with defects. The models are not suitable to be used to investigate the influence of defects in woven fabric composites. Sixth, both models only investigate plain weave style. Currently, the two models are not applicable to predict the mechanical properties of twill and satin weave styles, but both models have the potential to be adapted for the plain, twill and satin weave styles simultaneously after improvements.

Except these five main limitations, the model for biaxial tensile strength prediction has an additional limitation. The limitation is the difficulty in obtaining the biaxial tensile strength through experiments, due to the inevitable stress concentrations at the transition regions between the loading arms and the central area of the specimens, and therefore the proposed

model is verified with the FEM model. While FEM provides confidence in the accuracy of the method, experimental data will increase confidence in the approach.

The model for shear strength prediction also has another two limitations. It was only verified against one experimental case, which may be not enough to fully prove the robustness of the model for shear strength predictions. However, additional materials for validation are not available since there is a lack of literature investigating the shear strength of the plain weave fabric composites. Additionally, many studies found partially miss the required material properties or yarn specifications for the proposed model. Therefore, these papers are not usable for the model verification. In addition, it is found that the model is not applicable for cases where the yarn dimensions of *2L/h* and *w/h* are approximately 40 or larger. As the yarns are thin when the span/height and width/height ratios are large the dominant characteristic for determining the strength is the failure of the yarns under shear stress, instead of the maximum interlaminar shear stress on the interlacing surface between the interlaced yarns.

In the triaxial weave fabric composite optimisation, to benchmark the different algorithms and to provide an ideal Pareto front the size of the search space is artificially enlarged where the intervals of design variables are much smaller than the current manufacturing precision, which is 10^{-2} millimetres. Further optimisation might be used to explore the robustness of the designs, capable of being manufactured with a reasonable tolerance.

In the plain weave fabric composite optimisation, since there is no proper tool or methodology to visualise the Pareto front of five objectives, the Pareto fronts are illustrated by reduced-dimension Pareto front plots. This makes overlapped and distributed points illustrated on the Pareto fronts. In addition, only investigating the optimal designs of a single weave style, which is plain weave fabric style, is another limitation of the plain weave fabric composite optimisation work.

8.3 Future work

The methodology used in the proposed analytical models will be extended to predict the biaxial tensile properties and shear properties of twill and satin weave fabric composites. In addition, it is planned to extend the methodology of the proposed two micromechanical models to develop a new micromechanical model to rapidly predict the compressive properties of plain, twill and satin weave fabric composites. Currently, the compressive properties of the weave fabric composites are mainly predicted through finite element methods. There is an available analytical method but it doesn't consider the geometry nonlinearity under compressive loadings.

However, the fabrics have large deformation in the through-thickness direction and may also have local buckling when under the compression. Therefore, the same minimum complementary potential energy principle with geometry nonlinearity analysis will be utilised to derive a new micromechanical model for the rapid prediction of the compressive strength and modulus of plain, twill and satin weave fabric composites.

Once the compressive strength and modulus are available from the new model, it is planned to benchmark the state-of-the-art Genetic Algorithms for optimal designs of plain weave fabric composites to achieve high compressive properties. In addition, the tensile and shear properties are available from the models proposed in this work. The Poisson's ratio can be derived from the proposed biaxial tensile micromechanical model since the displacements in both warp and weft directions are available in the model. Therefore, once the compressive properties are achieved from the new model, all material properties of the plain weave fabric composites are available. This makes the bi-level optimisation of weave fabric composite structures become possible. It is planned to perform bi-level optimisation on weave fabric composite structures to improve the structural properties using micromechanical model at the material level and finite element methods at the structure level.

In addition, it is planned to apply many-objective optimisation on the triaxial weave fabric optimisation case. The tensile modulus and strength, shear modulus and strength and areal density will be optimised simultaneously. The state-of-the-art many-objective Genetic Algorithms will be benchmarked to characterise the dominant characteristics of the problem for better selection of the appropriate solvers for the problem.

Chapter 9. Conclusion

Since woven fabric composites are increasingly used in many applications, especially aerospace structures, the requirement of seeking better designs is increasing. However, the investigation of woven fabric composites optimisation is still at a starting point. It is difficult to find out the optimal designs of woven fabric composites without the help of optimisation since the fibre specifications and woven architecture significantly influence their behaviour and these optimisation problems contain complicated design search space. Therefore, this work comparatively reviews the Genetic Algorithms use in composite optimisation literature from the representative 17 composite journals over the past decade and they are compared with evolutionary computation. Over the past decades hundreds of journal and conference papers have been published about the optimisation of composite materials/structures. Over half of them utilise various Genetic Algorithms to achieve the optimal designs for their single or multiple objectives. However, a number of problems are found and summarised from the literature. The literature review has listed the corresponding recommendations. According to the results of the comparative review, state-of-the-art Genetic Algorithms are utilised in the optimisation of woven fabric composites in this work. In order to select the most suitable 'fitness evaluation method' for the optimisation of woven fabric composites, this work performs a comparative review of woven fabric composite modelling methods. The review recommends to use the analytical models as the fitness evaluation method used in woven fabric composites optimisation due to their computational efficiency but the required analytical methods are not available in the current literature. Therefore, this work proposes two analytical models to rapidly predict woven fabric composites mechanical properties.

The two proposed analytical models are both based on the minimum total complementary potential energy principle with micromechanical unit cells. The first model provides a simple way to rapidly predict the strength of plain weave fabric composites under uniaxial and biaxial tension. The model is able to predict the tensile strength and failure locations of plain weave fabric composites under different biaxial loading ratios. It is also capable of predicting the uniaxial tensile strengths and failure locations for both warp and weft directions. In addition, different biaxial tensile loading ratios and various types of materials, ranging in material properties from carbon to glass fibres, are used to show the general applicability of the method. The result shows a mean error of 11.22% and a maximum error of 16.74% over the six biaxial tension cases, five uniaxial tension cases and four types of materials, which indicates the accuracy and general applicability of the proposed model. Furthermore, the standard deviation

of prediction errors among the total 11 cases is 2.66, which demonstrates the robustness of the model for a range of applications.

The second model provides a convenient way for the rapid prediction of both shear modulus and shear strength of plain weave fabric composites. Different from the first model, a virtual $\pm 45°$ off-axis biaxial tension is applied on the orthogonally interlaced yarns to derive the shear properties. The proposed model is validated by experimental measurements for both shear modulus and shear strength. Additionally, four types of materials with seven fabric specifications are verified to demonstrate the general applicability of the method. Furthermore, the prediction errors of shear modulus from current proposed model are compared with another five analytical models, showing a significantly improved accuracy compared with the models proposed by Nguyen et al. [42], Sun and Pan [43] and Ganesh and Naik [46]. A mean error of 15.24% and a maximum error of 21.63% in shear modulus verifications and a mean error of 8.51% in shear strength verifications indicate the practical and effective use of the proposed model. Furthermore, the prediction error standard deviation of 4.10 for the seven cases reflects the robustness of the proposed model for a range types of materials.

The first optimisation study is performed on the triaxial weave fabric composites, which are increasingly used in novel ultralight applications and there is a requirement to improve material properties. Since the dominant characteristics of the problem are not understood, four leading Genetic Algorithms specific to different problem types are compared to find the Pareto front for the triaxial weave fabric designs. Poor performance from both of the top general solver, MTS, and the leading unconstrained solver, MOEA/D, demonstrates that this problem is dominated by different characteristics and the selection of the correct algorithm is critical to find the optimal solutions. This indicates that it will be impossible to select the correct Genetic Algorithm for composite optimisation problems from the current literature. Therefore, there is a requirement for characterisation and benchmarking of composite optimisation problems to allow selection of algorithms that are capable of finding solutions to the more complex problems. The benchmarking demonstrates that MLSGA-NSGAII provides the best performance for both tensile strength and modulus optimisation problem and strength-density optimisation problem, providing a weave pattern which is seemingly dominated by the disconnected nature of the Pareto front. In the tensile strength and modulus optimisation, there are 643 optimal designs suitable for producing flexible structures and 17 designs among them are capable for producing ultralight flexible structures from the strength-density optimisation. Of the proposed weave patterns in the tensile strength and modulus optimisation one matching

the modulus of a current experimental sample [325] gives an increase in the strength to stiffness ratio of 28.80%. However, the lowest modulus solution achieves a greater tensile strength to stiffness ratio improvement of 1191% compared to the experimental sample. One design in the strength-density optimisation, 110.86 g/m^2, which is slightly lighter than the areal density of a current experimental sample [325], 111.75 g/m^2, gives an increase in the strength of 149.49% and an increase in the strength to stiffness ratio of 228.05%. Furthermore, one design with slightly higher areal density, 129.98 g/m^2, than the experimental sample [325] shows an increased strength to stiffness ratio of 896.29% with a tensile strength of 441.66 MPa and stiffness of 3.62 GPa.

The second optimisation is performed on the plain weave fabric composites. The combination of modern manufacturing and optimisation techniques makes the wide use of bespoke high performance plain weave fabric (PWF) composites become possible for aerospace structures. The material properties are dependent on the weave pattern, thus the improved plain weave fabrics can be obtained from optimisation. In Chapter 7, 10 state-of-the-art Genetic Algorithms are employed to find optimal designs of plain weave fabric composites under tension and shear and these algorithms are benchmarked to determine the best solvers and dominant characteristics of the problems. The benchmarking results demonstrate that for the three-objective and five-objective optimisation problems cMLSGA, HEIA and U-NSGA-III achieve outperformance, where the use of these algorithms is currently rare in the composite optimisation literature. The benchmarking of the bi-objective optimisation problems shows that NSGA-II achieves the best performance, which supports its use as the most popular of the modern algorithms in the literature. The disconnected nature of the Pareto front is the main characteristic which influences the selection of these algorithms since the 'diversity first' general solver, cMLSGA, simultaneously achieves lower mIGD and higher mHV values than other solvers when the optimisation problem has disconnected feature in the Pareto front. Compare with a current experimental sample, one optimal design has 13.80% shear modulus reduction but provides 24.87% shear strength improvement, 51.19% improved tensile strength, 48.39% improved tensile modulus and 18.71% areal density reduction. When comparing the five extreme optimal designs from the five-objective optimisation against the current weave pattern, the tensile strength is improved by 51.19%, the tensile modulus is improved by 54.77%, the shear strength is improved by 77.69%, the shear modulus is improved by 22.17% and the areal density is reduced by 53.60%, respectively.

These optimisation works clearly indicate the benefits of utilising Genetic Algorithms and have shown the optimal designs of woven fabric composites, which helps to better design and understand woven fabric composite structures. However, there is a requirement for characterisation and benchmarking of composite optimisation problems to allow selection of algorithms capable of finding solutions to more complex problems. In addition, the optimisation works demonstrates the benefits of using analytical models as the 'fitness evaluation method' since it can utilise higher hyper-parameters in the optimisation to allow the leading Genetic Algorithms to achieve resolved Pareto fronts. Furthermore, analytical methods as a type of virtual experimental method are able to replace the actual experiments in the structure design process, especially for basic material tests which require many repetitions or experiments that are difficult or expensive to perform. The analytical models also provide an accurate tool for computationally expensive simulation methods. Therefore, it is worth to continuously investigate and develop novel analytical models for the rapid prediction of mechanical properties of woven fabric composites.

Bibliography

[1] Textile Composites Market by Fiber Type (Carbon, Glass, Aramid and Others), by Textile Type (Woven, Non-Woven), by Application (Electrical & Electronics, Wind, Sporting Goods, Marine, Construction and Others) & by Region - Global Forecast to 2020. Mark Res Rep 2015. http://www.marketsandmarkets.com/Market-Reports/textile-composites-market-94199765.html (accessed November 15, 2018).

[2] Aly NM. A review on utilization of textile composites in transportation towards sustainability. IOP Conf Ser Mater Sci Eng 2017;254. doi:10.1088/1757-899X/254/4/042002.

[3] Dexter HB. Innovative textile reinforced composite materials for aircraft structures. 28th Int. SAMPE Tech. Conf., 1996, p. 404–16.

[4] Whiteside JB, DeIasi RJ, Schulte RL. Measurement of preferential moisture ingress in composite wing/spar joints. Compos Sci Technol 1985;24:123–45. doi:10.1016/0266-3538(85)90055-7.

[5] Liu Z, Lu J, Zhu P. Lightweight design of automotive composite bumper system using modified particle swarm optimizer. Compos Struct 2016;140:630–43. doi:10.1016/j.compstruct.2015.12.031.

[6] Hamilton S, Schinske N. Multiaxial stitched preform reinforcement. Sixth Annu. ASM/ESD Adv. Compos. Conf., 1990, p. 433–4.

[7] Brandt J, Drechsler K. The potential of advanced textile structural composites for automotive and aerospace applications. Fourth Japan Int. SAMPE Symp., 1995, p. 679–86.

[8] Long AC, editor. Design and manufacture of textile composites. Elsevier; 2005.

[9] Wang Z, Sobey A. A comparative review between Genetic Algorithm use in composite optimisation and the state-of-the-art in evolutionary computation. Compos Struct 2020;233:111739. doi:10.1016/j.compstruct.2019.111739.

[10] Fu X, Ricci S, Bisagni C. Multi-scale analysis and optimisation of three-dimensional woven composite structures combining response surface method and genetic algorithms. CEAS Aeronaut J 2017;8:129–41. doi:10.1007/s13272-016-0227-y.

[11] Fu X, Ricci S, Bisagni C. Minimum-weight design for three dimensional woven composite stiffened panels using neural networks and genetic algorithms. Compos Struct 2015;134:708–15. doi:10.1016/j.compstruct.2015.08.077.

[12] Abu Bakar IA, Kramer O, Bordas S, Rabczuk T. Optimization of elastic properties and weaving patterns of woven composites. Compos Struct 2013;100:575–91. doi:10.1016/j.compstruct.2012.12.043.

[13] Axinte A, Taranu N, Bejan L, Hudisteanu I. Optimisation of Fabric Reinforced Polymer Composites Using a Variant of Genetic Algorithm. Appl Compos Mater 2017:1479–91. doi:10.1007/s10443-017-9594-8.

[14] Tan P, Tong L, Steven G. P. Modelling for predicting the mechanical properties of textile composites—A review. Compos Part A Appl Sci Manuf 1997;28:903–22. doi:10.1016/S1359-835X(97)00069-9.

[15] Tabiei A, Jiang Y. Woven fabric composite material model with material nonlinearity for nonlinear finite element simulation. Int J Solids Struct 1999;36:2757–71. doi:10.1016/S0020-7683(98)00127-9.

[16] Sankar B V., Marrey R V. A unit-cell model of textile composite beams for predicting stiffness properties. Compos Sci Technol 1993;49:61–9.

[17] Hahn H, Pandey R. A Micromechanics Model for Thermoplastic Properties of Plain Weave Fabric Composites. J Eng Mater Technol 1994;116:517–23.

[18] Kwon YW, Roach K. Unit-cell model of 2/2-twill woven fabric composites for multi-scale analysis. C - Comput Model Eng Sci 2004;5:63–72.

[19] Naik NK, Ganesh VK. Prediction of on-axes elastic properties of plain weave fabric composites. Compos Sci Technol 1992;45:135–52. doi:10.1016/0266-3538(92)90036-3.

[20] Naik NK, Ganesh VK. Prediction of thermal expansion coefficients of plain weave fabric composites. Compos Struct 1993;26:139–54. doi:10.1016/0263-8223(93)90062-U.

[21] Adumitroaie A, Barbero EJ. Stiffness and strength prediction for plain weave textile reinforced composites. Mech Adv Mater Struct 2012;19:169–83. doi:10.1080/15376494.2011.572245.

[22] Karkkainen RL, Sankar B V. A direct micromechanics method for analysis of failure initiation of plain weave textile composites. Compos Sci Technol 2006;66:137–50. doi:10.1016/j.compscitech.2005.05.018.

[23] Cox BN, Carter WC, Fleck N a. A binary model of textile composites-I. Formulation. Acta Metall Mater 1994;42:3463–79. doi:10.1016/0956-7151(94)90479-0.

[24] Flores S, Evans AG, Zok FW, Genet M, Cox B, Marshall D, et al. Treating matrix nonlinearity in the binary model formulation for 3D ceramic composite structures. Compos Part A Appl Sci Manuf 2010;41:222–9. doi:10.1016/j.compositesa.2009.10.020.

[25] Yang Q, Cox BN. Spatially Averaged Local Strains in Textile Composites Via the Binary Model Formulation. J Eng Mater Technol 2003;125:418. doi:10.1115/1.1605117.

[26] Yang QD, Cox B. Predicting failure in textile composites using the Binary Model with gauge-averaging. Eng Fract Mech 2010;77:3174–89. doi:10.1016/j.engfracmech.2010.08.004.

[27] Lomov S V., Gusakov a. V., Huysmans G, Prodromou a., Verpoest I. Textile geometry preprocessor for meso-mechanical models of woven composites. Compos Sci Technol 2000;60:2083–95. doi:10.1016/S0266-3538(00)00121-4.

[28] Verpoest I, Lomov S V. Virtual textile composites software WiseTex: Integration with micro-mechanical, permeability and structural analysis. Compos Sci Technol 2005;65:2563–74. doi:10.1016/j.compscitech.2005.05.031.

[29] Lin H, Zeng X, Sherburn M, Long AC, Clifford MJ. Automated geometric modelling of textile structures. Text Res J 2012;82:1689–702. doi:10.1177/0040517511418562.

[30] Wang Z, Bai J, Sobey AJ, Xiong J, Shenoi RA. Optimal design of triaxial weave fabric composites under tension. Compos Struct 2018;201:616–24. doi:https://doi.org/10.1016/j.compstruct.2018.06.090.

[31] Wang Z, Sobey AJ. Optimal design of triaxial weave fabric composites for specific strength and stiffness under tension. 18th Eur. Conf. Compos. Mater., Athens, Greece: 2018.

[32] Cheng X, Xiong JJ. A novel analytical model for predicting the compression modulus of 2D PWF composites. Compos Struct 2009;88:296–303. doi:10.1016/j.compstruct.2008.04.005.

[33] Naik NK, Tiwari SI, Kumar RS. An analytical model for compressive strength of plain weave fabric composites. Compos Sci Technol 2003;63:609–25. doi:10.1016/S0266-3538(02)00198-7.

[34] Scida D, Aboura Z, Benzeggagh ML, Bocherens E. A micromechanics model for 3D elasticity and failure of woven-fibre composite materials. Compos Sci Technol 1999;59:505–17. doi:10.1016/S0266-3538(98)00096-7.

[35] Ishikawa T, Chou TW. Stiffness and strength behaviour of woven fabric composites. J Mater Sci 1982;17:3211–20. doi:10.1007/s11270-016-3098-2.

[36] Zhang YC, Harding J. A numerical micromechanics analysis of the mechanical properties of a plain weave composite. Comput Struct 1990;36:839–44. doi:10.1016/0045-7949(90)90154-T.

[37] Xiong JJ, Shenoi RA, Cheng X. A modified micromechanical curved beam analytical model to predict the tension modulus of 2D plain weave fabric composites. Compos Part B Eng 2009;40:776–83. doi:10.1016/j.compositesb.2009.06.004.

[38] Escárpita DAA. Experimental Investigation of Textile Composites Strength Subject to Biaxial Tensile Loads. Instituto Tecnologico y de Estudios Superiores de Monterrey, 2011.

[39] Bai JB, Xiong JJ, Shenoi RA, Wang Q. A micromechanical model for predicting biaxial tensile moduli of plain weave fabric composites. J Strain Anal Eng Des 2017;52:333–43. doi:10.1177/0309324717707858.

[40] Bai J, Wang Z, Sobey AJ, Xiong J, Shenoi RA. Micromechanical model for rapid prediction of plain weave fabric composite strengths under biaxial tension (Under Review). Compos Part B Eng 2019.

[41] Wang Z, Bai J, Sobey AJ, Xiong J, Shenoi RA. Analytical model for rapid prediction of plain weave fabric composite moduli and strengths under biaxial tension 2018. doi:http://doi.org/10.5281/zenodo.1479774.

[42] Nguyen M, Herszberg I, Paton R. The shear properties of woven carbon fabric. Compos Struct 1999;47:767–79. doi:10.1533/9781845690403.151.

[43] Sun H, Pan N. Shear deformation analysis for woven fabrics. Compos Struct 2005;67:317–22. doi:10.1016/j.compstruct.2004.01.013.

[44] Cheng X, Xiong J, Bai J. Analytical solution for predicting In-plane elastic shear properties of 2D orthogonal PWF composites. Chinese J Aeronaut 2012;25:575–83. doi:10.1016/S1000-9361(11)60421-4.

[45] Naik NK, Ganesh VK. An analytical method for plain weave fabric composites. Composites 1995;26:281–9. doi:10.1016/0010-4361(95)93671-6.

[46] Ganesh K, Naik NK. Failure behaviour of plain weave fabric laminates under in-plane shear loading : effect of fabric geometry. Compos Struct 1995;30:179–92.

[47] Wang Z, Sobey AJ. A micromechanical model for computationally efficient prediction of plain weave fabric composite shear moduli and strengths (Prepare to submit). Compos Struct 2020.

[48] Kueh ABH, Soykasap O, Pellegrino S. Thermo-mechanical behaviour of single-ply triaxial weave carbon fibre reinforced plastic. Eur. Conf. Spacecr. Struct. Mater. Test., Netherlands, Noordwijk: 2005.

[49] Kueh ABH. Size-influenced mechanical isotropy of singly-plied triaxially woven fabric composites. Compos Part A Appl Sci Manuf 2014;57:76–87. doi:10.1016/j.compositesa.2013.11.005.

[50] Kueh ABH. Buckling of sandwich columns reinforced by triaxial weave fabric composite skin-sheets. Int J Mech Sci 2013;66:45–54. doi:10.1016/j.ijmecsci.2012.10.007.

[51] Bai J, Xiong J, Liu M, Man Z. Analytical Solutions for Predicting Tensile and Shear Moduli of Triaxial Weave Fabric Composites. Acta Mech Solida Sin 2016;29:59–77. doi:10.1016/S0894-9166(16)60007-1.

[52] Bai JB, Xiong JJ, Shenoi RA, Zhu YT. Analytical solutions for predicting tensile and in-plane shear strengths of triaxial weave fabric composites. Int J Solids Struct 2017;120:1339–51. doi:10.1016/j.ijsolstr.2017.05.002.

[53] Jones RM. Mechanics of composite materials. second edi. Taylor & Francis; 1999.

[54] Coley DA. An introduction to genetic algorithms for scientists and engineers. Singapore: World Scientific; 1999.

[55] Konak A, Coit DW, Smith AE. Multi-objective optimization using genetic algorithms: A tutorial. Reliab Eng Syst Saf 2006;91:992–1007. doi:10.1016/j.ress.2005.11.018.

[56] Turing A. Computing machinery and intelligence. MIND 1950;LIX:433–60.

[57] Holland JH. Adaptive plans optimal for payoff-only environments. 1969.

[58] De Jong KA. Analysis of the behaviour of a class of genetic adaptive systems 1975.

[59] Schaffer JD. Multiple objective optimization with vector evaluated genetic algorithms. First Int. Conf. Genet. Algorithms their Appl., 1985, p. 93–100.

[60] Goldberg DE. Genetic algorithms in search, optimisation and machine learning. Reading, MA Addison-Wesley 1989.

[61] Hajela P, Lin C. Genetic search strategies in multicriterion optimal design. Struct Optim 1992;4:99–107. doi:10.1007/BF01759923.

[62] Fonseca CM, Fleming PJ. Multiobjective genetic algorithms. IEE Colloq. Genet. algorithms Control Syst. Eng., 1993, p. 6–1.

[63] Chipperfield A, Fleming P, Pohlheim H, Fonseca CM. Genetic Algorithm Toolbox for use with MATLAB 1994. doi:10.1243/0954405021519915.

[64] Srinivas M, Patnaik LM. Adaptive Probabilities of Crossover and Mutation in Genetic Algorithms. IEEE Trans Syst Man Cybern 1994;24:656–67.

[65] Grefenstette JJ. Optimization of Control Parameters for Genetic Algorithms. IEEE Trans Syst Man Cybern 1986;16:122–8. doi:10.1109/TSMC.1986.289288.

[66] Hinterding R, Michalewicz Z, Peachey TC. Self-adaptive genetic algorithm for numeric functions. Int. Conf. Parallel Probl. Solving from Nat., Springer Berlin Heidelberg; 1996, p. 420–9.

[67] Srinivas N, Deb K. Muiltiobjective Optimization Using Nondominated Sorting in Genetic Algorithms. Evol Comput 1994;2:221–48. doi:10.1162/evco.1994.2.3.221.

[68] Deb K, Agrawal RB. Simulated Binary Crossover for Continuous Search Space. Complex Syst 1994;9:1–5.

[69] Whitley D, Rana S, Heckendorn RB. The island model genetic algorithm: On separability, population size and convergence. J Comput Inf Technol 1999;7:33–47. doi:10.1.1.36.7225.

[70] Zitzler E, Thiele L. Multiobjective evolutionary algorithms: a comparative case study and the strength Pareto approach. IEEE Trans Evol Comput 1999;3:257–71. doi:10.1109/4235.797969.

[71] Zitzler E, Laumanns M, Thiele L. SPEA2: Improving the Strength Pareto Evolutionary Algorithm 2001:95–100. doi:10.1.1.28.7571.

[72] Watanabe S, Hiroyasu T, Miki M. NCGA : Neighborhood Cultivation Genetic Algorithm for Multi-Objective Optimization Problems. GECCO Late Break Pap 2002:458–65.

[73] Coello CAC, Pulido GT. A Micro-Genetic Algorithm for Multiobjective Optimization. First Int Conf Evol Multi-Criterion Optim 2001:126–40. doi:10.1007/3-540-44719-9.

[74] Tiwari S, Fadel G, Koch P, Deb K. Performance Assessment of the Hybrid Archive-based Micro Genetic Algorithm (AMGA) on the CEC09 Test Problems. IEEE Congr. Evol. Comput., 2009, p. 1935–42.

[75] Deb K, Pratap A, Agarwal S, Meyarivan T. A fast and elitist multiobjective genetic algorithm: NSGA-II. IEEE Trans Evol Comput 2002;6:182–97. doi:10.1109/4235.996017.

[76] Chen H, Ooka R, Kato S. Study on optimum design method for pleasant outdoor thermal environment using genetic algorithm (GA) and coupled simulation of convection radiation and conduction: Optimum arrangement of trees for design of pleasant outdoor thermal environment. J Environ Eng 2004;69:65–71. doi:10.3130/aije.69.65_1.

[77] Zitzler E, Kunzli S. Indicator-Based Selection in Multiobjective Search. 8th Int Conf Parallel Probl Solving from Nat (PPSN VIII) 2004;3242:832–42. doi:10.1007/b100601.

[78] Li M, Yang S, Liu X. Pareto or Non-Pareto : Bi-Criterion Evolution in Multiobjective Optimization. IEEE Trans Evol Comput 2016;20:645–65. doi:10.1109/TEVC.2015.2504730.

[79] Lin Q, Chen J, Zhan Z-H, Chen W, Coello CAC, Yin Y, et al. A Hybrid Evolutionary Immune Algorithm for Multiobjective Optimization Problems. IEEE Trans Evol Comput 2016;20:711–29. doi:10.1109/TEVC.2015.2512930.

[80] Zhang Q, Li H. MOEA/D: A Multiobjective Evolutionary Algorithm Based on Decomposition. IEEE Trans Evol Comput 2007;11:712–31. doi:10.1109/TEVC.2007.892759.

[81] Paquete L, Stutzle T. A two-phase local search for the biobjective traveling salesman problem. Int. Conf. Evol. Multi-Criterion Optim., Springer Berlin Heidelberg; 2003, p. 479–93. doi:10.1007/3-540-36970-8.

[82] Zhang Q, Suganthan PN. Final Report on CEC ' 09 MOEA Competition. Congr. Evol. Comput. (CEC 2009), 2009.

[83] Liu H, Gu F, Zhang Q. Decomposition of a Multiobjective Optimization Problem into a Number of Simple Multiobjective Subproblems. IEEE Trans Evol Comput 2014;18:450–5. doi:10.1109/TEVC.2013.2281533.

[84] Jiang S, Yang S, Wang Y, Liu X. Scalarizing Functions in Decomposition-Based Multiobjective Evolutionary Algorithms. IEEE Trans Evol Comput 2018;22:296–313. doi:10.1109/TEVC.2017.2707980.

[85] Sober E, Wilson D. Unto others: The evolution and psychology of unselfish behaviour. Harvard University Press; 1999.

[86] Grudniewski PA, Sobey AJ. Multi-level selection genetic algorithm applied to CEC ' 09 test instances. IEEE Congr. Evol. Comput., 2017, p. 1613–20.

[87] Sobey AJ, Grudniewski PA. Re-inspiring the genetic algorithm with multi-level selection theory : multi-level selection genetic algorithm. Bioinspir Biomim 2018;13. doi:10.1088/1748-3190/aad2e8.

[88] Grudniewski PA, Sobey AJ. cMLSGA : Co-evolutionary Multi-Level Selection Genetic Algorithm (Under Review). Swarm Evol Comput n.d.

[89] Cavicchio D. Adaptive search using simulated evolution 1970.

[90] De Jong KA. Analysis of the behavior of a class of genetic adaptive systems 1975.

[91] Goldberg DE, Richardson J. Genetic algorithms with sharing for multimodal function optimization. Genet. algorithms their Appl. Proc. Second Int. Conf. Genet. Algorithms, 1987, p. 41–9.

[92] Beasley D, Bull DR, Martin RR. A sequential niche technique for multimodal function optimization. Evol Comput 1993;1:101–25. doi:10.1016/j.neucom.2006.02.016.

[93] Petrowski A. A clearing procedure as a niching method for genetic algorithms. Proc IEEE Int Conf Evol Comput ICEC-96 1996:798–803. doi:10.1109/ICEC.1996.542703.

[94] Deb K. Multi-objective NSGA-II code in C Revision 1.1.6. Softw Dev by KanGAL 2011. https://www.egr.msu.edu/~kdeb/codes.shtml.

[95] Sindhya K, Sinha A, Deb K, Miettinen K. Local search based evolutionary multi-objective optimization algorithm for constrained and unconstrained problems. 2009 IEEE Congr. Evol. Comput., 2009, p. 2919–26. doi:10.1109/CEC.2009.4983310.

[96] Deb K, Jain H. Handling Many-Objective Problems Using an Improved NSGA-II Procedure. 2012 IEEE Congr. Evol. Comput., 2012, p. 1–8.

[97] Seada H, Deb K. U-NSGA-III: A unified evolutionary optimization procedure for single, multiple, and many objectives. InInternational Conf. Evol. Multi-Criterion Optim., Springer, Cham; 2015, p. 34–49. doi:10.1007/978-3-319-15892-1_3.

[98] Branke J, Schmeck H, Deb K, Reddy M. Parallelizing Multi-Objective Evolutionary Algorithms : Cone Separation. CEC2004 Evol. Comput., 2004, p. 1952–7. doi:10.1109/CEC.2004.1331135.

[99] Liu M, Zou X, Chen Y, Wu Z. Performance assessment of DMOEA-DD with CEC 2009 MOEA competition test instances. 2009 IEEE Congr. Evol. Comput., 2009, p. 2913–8. doi:10.1109/CEC.2009.4983309.

[100] Liu HL, Li X. The multiobjective evolutionary algorithm based on determined weight and sub-regional search. 2009 IEEE Congr. Evol. Comput. CEC 2009, 2009, p. 1928–34. doi:10.1109/CEC.2009.4983176.

[101] Darwin C. On the origins of species by means of natural selection, Murray, London: 1859.

[102] Ehrlich PR, Raven PH. Butterflies and plants: a study in coevolution. Evolution (N Y) 1964;18:586–608. doi:10.1111/j.1558-5646.1964.tb01674.x.

[103] Nuismer S. Introduction to coevolutionary theory. Macmillan Learning; 2017.

[104] Currie C, Wong B, Stuart A, Schultz T, Rehner S, Mueller U, et al. Ancient Tripartite Coevolution in the Attine Ant-Microbe Symbiosis. Science (80-) 2003;299:386–8.

[105] Potter MA, Jong K. Cooperative coevolution: an architecture for evolving coadapted subcomponents. Evol Comput 2000;8:1–29. doi:10.1162/106365600568086.

[106] Anderson R, May R. Coevolution of hosts and parasites. Parasitology 1982;85:411–26.

[107] Downes S, Shine R. Sedentary snakes and gullible geckos: Predator-prey coevolution in nocturnal rock-dwelling reptiles. Anim Behav 1998;55:1373–85. doi:10.1006/anbe.1997.0704.

[108] Potter MA, De Jong KA. A cooperative coevolutionary approach to function optimization. Int. Conf. Parallel Probl. Solving from Nat., Springer Berlin Heidelberg; 1994, p. 249–57.

[109] Hill J. The three C's - competition, coexistence and coevolution - and their impact on the breeding of forage crop mixtures. Theor Appl Genet 1990;79:168–76. doi:10.1007/BF00225947.

[110] De Jong KA. Evolutionary computation: a unified approach. MIT; 2006.

[111] Coello CAC, Sierra MR. A coevolutionary multi-objective evolutionary algorithm. 2003 Congr. Evol. Comput. CEC 2003, vol. 1, 2003, p. 482–9. doi:10.1109/CEC.2003.1299614.

[112] Goh C, Tan KC. A competitive-cooperative coevolutionary paradigm for dynamic multiobjective optimization. IEEE Trans Evol Comput 2009;13:103–27. doi:10.1109/TEVC.2008.920671.

[113] Rosin C, Belew R. New methods for competitive coevolution. Evol Comput 1997;5:1–29. doi:10.1162/evco.1997.5.1.1.

[114] Jiang S, Yang S. Evolutionary dynamic multiobjective optimization: benchmarks and algorithm comparisons. IEEE Trans Cybern 2017;47:198–211. doi:10.1109/TCYB.2015.2510698.

[115] Wilson D, Sober E. Reviving the superorganism. J Theor Biol 1989;136:337–56.

[116] Okasha S. Evolution and the levels of selection. Oxford University Press; 2006.

[117] Grudniewski PA, Sobey AJ. Genetic Algorithm performances on constrained dynamic problem types (Under Review). IEEE Trans Evol Comput n.d.

[118] Coello CAC. Journal Papers on Evolutionary Multiobjective Optimisation. J Pap Evol Multiobjective Optim 2017. http://delta.cs.cinvestav.mx/~ccoello/EMOO/EMOOjournals.html (accessed August 20, 2018).

[119] Mutlu U, Grudniewski PA, Sobey AJ, Blake JIR. Selecting an optimisation methodology in the context of structural design for leisure boats. Des. Constr. Super Mega Yachts, Genoa, Italy: 2017.

[120] Nikbakt S, Kamarian S, Shakeri M. A review on optimization of composite structures Part I: Laminated composites. Compos Struct 2018;195:158–85. doi:10.1016/j.compstruct.2018.03.063.

[121] Deveci HA, Artem HS. Optimum design of fatigue-resistant composite laminates using hybrid algorithm. Compos Struct 2017;168:178–88. doi:10.1016/j.compstruct.2017.01.064.

[122] Naik GN, Gopalakrishnan S, Ganguli R. Design optimization of composites using genetic algorithms and failure mechanism based failure criterion. Compos Struct 2008;83:354–67. doi:10.1016/j.compstruct.2007.05.005.

[123] Paluch B, Grédiac M, Faye A. Combining a finite element programme and a genetic algorithm to optimize composite structures with variable thickness. Compos Struct 2008;83:284–94. doi:10.1016/j.compstruct.2007.04.023.

[124] Marques FD, Natarajan S, Ferreira AJM. Evolutionary-based aeroelastic tailoring of stiffened laminate composite panels in supersonic flow regime. Compos Struct 2017;167:30–7. doi:10.1016/j.compstruct.2017.01.062.

[125] Roos C, Bakis CE. Multi-physics design and optimization of flexible matrix composite driveshafts. Compos Struct 2011;93:2231–40. doi:10.1016/j.compstruct.2011.03.011.

[126] An H, Chen S, Huang H. Simultaneous optimization of stacking sequences and sizing with two-level approximations and a genetic algorithm. Compos Struct 2015;123:180–9. doi:10.1016/j.compstruct.2014.12.041.

[127] An H, Chen S, Huang H. Optimal design of composite sandwich structures by considering multiple structure cases. Compos Struct 2016;152:676–86. doi:10.1016/j.compstruct.2016.05.066.

[128] Kim DH, Choi DH, Kim HS. Design optimization of a carbon fiber reinforced composite automotive lower arm. Compos Part B Eng 2014;58:400–7.

doi:10.1016/j.compositesb.2013.10.067.

[129] Irisarri FX, Bassir DH, Carrere N, Maire JF. Multiobjective stacking sequence optimization for laminated composite structures. Compos Sci Technol 2009;69:983–90. doi:10.1016/j.compscitech.2009.01.011.

[130] Irisarri FX, Laurin F, Leroy FH, Maire JF. Computational strategy for multiobjective optimization of composite stiffened panels. Compos Struct 2011;93:1158–67. doi:10.1016/j.compstruct.2010.10.005.

[131] Suganthan APN. Testing Evolutionary Algorithms on Real-World Numerical Optimization Problems. 2011.

[132] Sobey AJ, Blanchard J, Grudniewski PA, Savasta T. There's no free lunch: A study of Genetic Algorithm use in maritime applications. Int. Conf. Comput. Appl. Inf. Technol. Marit. Ind. (COMPIT 19), Tullamore, Ireland: 2019.

[133] Almeida FS, Awruch AM. Design optimization of composite laminated structures using genetic algorithms and finite element analysis. Compos Struct 2009;88:443–54. doi:10.1016/j.compstruct.2008.05.004.

[134] Jing Z, Sun Q, Silberschmidt VV. Sequential permutation table method for optimization of stacking sequence in composite laminates. Compos Struct 2016;141:240–52. doi:10.1016/j.compstruct.2016.01.052.

[135] Maes VK, Pavlov L, Simonian SM. An efficient semi-automated optimisation approach for (grid-stiffened) composite structures: Application to Ariane 6 Interstage. Compos Struct 2016;209:1042–9. doi:10.1016/j.compstruct.2016.02.082.

[136] Ju S, Shenoi RA, Jiang D, Sobey AJ. Multi-parameter optimization of lightweight composite triangular truss structure based on response surface methodology. Compos Struct 2013;97:107–16. doi:10.1016/j.compstruct.2012.10.025.

[137] Kamarian S, Shakeri M. Thermal buckling analysis and stacking sequence optimization of rectangular and skew shape memory alloy hybrid composite plates. Compos Part B Eng 2017;116:137–52. doi:10.1016/j.compositesb.2017.01.059.

[138] Pelegri AA, Kedlaya DN. Design of composites using a generic unit cell model coupled with a hybrid genetic algorithm. Compos Part A Appl Sci Manuf 2008;39:1433–43. doi:10.1016/j.compositesa.2008.05.006.

[139] Antoine GO, Batra RC. Optimization of transparent laminates for specific energy dissipation under low velocity impact using genetic algorithm. Compos Struct 2015;124:29–34. doi:10.1016/j.compstruct.2014.12.066.

[140] Knipprath C, McCombe GP, Trask RS, Bond IP. Predicting self-healing strength recovery using a multi-objective genetic algorithm. Compos Sci Technol 2012;72:752–9. doi:10.1016/j.compscitech.2012.02.002.

[141] Axinte A, Taranu N, Bejan L, Hudisteanu I. Optimisation of fabric reinforced polymer composites using a variant of Genetic Algorithm. Appl Compos Mater 2017;24:1479–91. doi:10.1007/s10443-017-9594-8.

[142] Barnes RH, Morozov EV. Structural optimisation of composite wind turbine blade structures with variations of internal geometry configuration. Compos Struct 2016;152:158–67. doi:10.1016/j.compstruct.2016.05.013.

[143] Taetragool U, Shah PH, Halls VA, Zheng JQ, Batra RC. Stacking sequence optimization for maximizing the first failure initiation load followed by progressive failure analysis until the ultimate load. Compos Struct 2017;180:1007–21. doi:10.1016/j.compstruct.2017.08.023.

[144] Ho-Huu V, Do-Thi TD, Dang-Trung H, Vo-Duy T, Nguyen-Thoi T. Optimization of laminated composite plates for maximizing buckling load using improved differential evolution and smoothed finite element method. Compos Struct 2016;146:132–47. doi:10.1016/j.compstruct.2016.03.016.

[145] Badalló P, Trias D, Marín L, Mayugo JA. A comparative study of genetic algorithms for the multi-objective optimization of composite stringers under compression loads. Compos Part B 2013;47:130–6. doi:10.1016/j.compositesb.2012.10.037.

[146] Lieu QX, Lee J. Modeling and optimization of functionally graded plates under thermo-mechanical load using isogeometric analysis and adaptive hybrid evolutionary firefly algorithm. Compos Struct 2017;179:89–106. doi:10.1016/j.compstruct.2017.07.016.

[147] Hwang SF, Wu JC, He RS. Identification of effective elastic constants of composite plates based on a hybrid genetic algorithm. Compos Struct 2009;90:217–24. doi:10.1016/j.compstruct.2009.03.021.

[148] Stodieck O, Cooper JE, Weaver PM, Kealy P. Optimization of tow-steered composite wing laminates for aeroelastic tailoring. AIAA J 2015;53:2203–15. doi:10.2514/1.J053599.

[149] Petrone G, Meruane V. Mechanical properties updating of a non-uniform natural fibre composite panel by means of a parallel genetic algorithm. Compos Part A Appl Sci Manuf 2017;94:226–33. doi:10.1016/j.compositesa.2016.12.017.

[150] Ihesiulor OK, Shankar K, Zhang Z, Ray T. Delamination detection with error and noise polluted natural frequencies using computational intelligence concepts. Compos Part B Eng 2014;56:906–25. doi:10.1016/j.compositesb.2013.09.032.

[151] Cai H, Aref AJ. On the design and optimization of hybrid carbon fiber reinforced polymer-steel cable system for cable-stayed bridges. Compos Part B Eng 2015;68:146–52. doi:10.1016/j.compositesb.2014.08.031.

[152] Macquart T, Bordogna MT, Lancelot P, De Breuker R. Derivation and application of blending constraints in lamination parameter space for composite optimisation. Compos Struct 2016;135:224–35. doi:10.1016/j.compstruct.2015.09.016.

[153] Fan HT, Wang H, Chen XH. An optimization method for composite structures with ply-drops. Compos Struct 2016;136:650–61. doi:10.1016/j.compstruct.2015.11.003.

[154] Ashjari M, Khoshravan MR. Mass optimization of functionally graded plate for mechanical loading in the presence of deflection and stress constraints. Compos Struct 2014;110:118–32. doi:10.1016/j.compstruct.2013.11.025.

[155] Kalantari M, Dong C, Davies IJ. Multi-objective robust optimisation of unidirectional carbon/glass fibre reinforced hybrid composites under flexural loading. Compos Struct 2016;138:264–75. doi:10.1016/j.compstruct.2015.11.034.

[156] Keller D. Optimization of ply angles in laminated composite structures by a hybrid, asynchronous, parallel evolutionary algorithm. Compos Struct 2010;92:2781–90.

doi:10.1016/j.compstruct.2010.04.003.

[157] Karakaya Ş, Soykasap Ö. Natural frequency and buckling optimization of laminated hybrid composite plates using genetic algorithm and simulated annealing. Struct Multidiscip Optim 2011;43:61–72. doi:10.1007/s00158-010-0538-2.

[158] Herath MT, Natarajan S, Prusty BG, John NS. Isogeometric analysis and genetic algorithm for shape-adaptive composite marine propellers. Comput Methods Appl Mech Eng 2015;284:835–60. doi:10.1016/j.cma.2014.10.028.

[159] Baran I, Tutum CC, Hattel JH. Optimization of the thermosetting pultrusion process by using hybrid and mixed integer genetic algorithms. Appl Compos Mater 2013;20:449–63. doi:10.1007/s10443-012-9278-3.

[160] Kim SH, Kim CG. Optimal design of composite stiffened panel with cohesive elements using micro-genetic algorithm. J Compos Mater 2008;42:2259–73. doi:10.1177/0021998308094967.

[161] Perera R, Ruiz A. Design equations for reinforced concrete members strengthened in shear with external FRP reinforcement formulated in an evolutionary multi-objective framework. Compos Part B Eng 2012;43:488–96. doi:10.1016/j.compositesb.2011.10.013.

[162] Satheesh R, Narayana NG, Ganguli R. Conservative design optimization of laminated composite structures using Genetic Algorithms and multiple failure criteria. J Compos Mater 2010;44:369–87. doi:10.1177/0021998309347579.

[163] Montemurro M, Vincenti A, Vannucci P. The automatic dynamic penalisation method (ADP) for handling constraints with genetic algorithms. Comput Methods Appl Mech Eng 2013;256:70–87. doi:10.1016/j.cma.2012.12.009.

[164] Perera R, Tarazona D, Ruiz A, Martín A. Application of artificial intelligence techniques to predict the performance of RC beams shear strengthened with NSM FRP rods. Formulation of design equations. Compos Part B Eng 2014;66:162–73. doi:10.1016/j.compositesb.2014.05.001.

[165] de Almeida FS. Stacking sequence optimization for maximum buckling load of composite plates using harmony search algorithm. Compos Struct 2016;143:287–99. doi:10.1016/j.compstruct.2016.02.034.

[166] da Silva RF, Teófilo FA, Parente JE, de Melo AM, de Holanda ÁS. Optimization of composite catenary risers. Mar Struct 2013;33:1–20. doi:10.1016/j.marstruc.2013.04.002.

[167] Gillet A, Francescato P, Saffre P. Single- and multi-objective optimization of composite structures: the influence of design variables. J Compos Mater 2010;44:457–80. doi:10.1177/0021998309344931.

[168] Jing Z, Fan X, Sun Q. Stacking sequence optimization of composite laminates for maximum buckling load using permutation search algorithm. Compos Struct 2015;121:225–36. doi:10.1016/j.compstruct.2014.10.031.

[169] Aymerich F, Serra M. Optimization of laminate stacking sequence for maximum buckling load using the ant colony optimization (ACO) metaheuristic. Compos Part A Appl Sci Manuf 2008;39:262–72. doi:10.1016/j.compositesa.2007.10.011.

[170] Lopez RH, Luersen MA, Cursi ES. Optimization of laminated composites considering different failure criteria. Compos Part B Eng 2009;40:731–40. doi:10.1016/j.compositesb.2009.05.007.

[171] Rao ARM, Lakshmi K. Optimal design of stiffened laminate composite cylinder using a hybrid SFL algorithm. J Compos Mater 2012;46:3031–55. doi:10.1177/0021998311435674.

[172] Ghiasi H, Pasini D, Lessard L. Constrained globalized Nelder-Mead method for simultaneous structural and manufacturing optimization of a composite bracket. J Compos Mater 2008;42:717–36. doi:10.1177/0021998307088592.

[173] Danzi F, Frulla G, Cestino E. Constrained combinatorial optimization of multi-layered composite structures by means of Stud GA with proportionate selection and extinction. Struct Multidiscip Optim 2017;55:2239–57. doi:10.1007/s00158-016-1638-4.

[174] An H, Chen S, Huang H. Laminate stacking sequence optimization with strength constraints using two-level approximations and adaptive genetic algorithm. Struct Multidiscip Optim 2015;51:903–18. doi:10.1007/s00158-014-1181-0.

[175] Rao ARM, Lakshmi K. Multi-objective optimal design of hybrid laminate composite structures using scatter search. J Compos Mater 2009;43:2157–82. doi:10.1177/0021998309339221.

[176] Kunasol N, Suwannik W, Chongstitvatana P. Solving one-million-bit problems using LZWGA. 2006 Int. Symp. Commun. Inf. Technol. Isc., 2006, p. 32–6. doi:10.1109/ISCIT.2006.339882.

[177] Sastry K, Goldberg DE, Llor X. Towards Billion Bit Optimization via Efficient Genetic Algorithms. llliGAL Rep., 2007.

[178] Goldberg DE, Sastry K, Llor X. Toward Routine Billion-Variable Optimization Using Genetic Algorithms. Complexity 2007;12:27–9. doi:10.1002/cplx.

[179] Iturriaga S, Nesmachnow S. Solving very large optimization problems (up to one billion variables) with a parallel evolutionary algorithm in CPU and GPU. 7th Int. Conf. P2P, Parallel, Grid, Cloud Internet Comput., 2012, p. 267–72. doi:10.1109/3PGCIC.2012.63.

[180] Deb K, Myburgh C. Breaking the Billion-Variable Barrier in real-world optimization using a customized evolutionary algorithm. Genet. Evol. Comput. Conf., 2016, p. 653–60. doi:10.1145/2908812.2908952.

[181] Pareto V. Manuale di Economia Politica. Soc. Ed. Libr., 1906.

[182] Irisarri FX, Peeters DMJ, Abdalla MM. Optimisation of ply drop order in variable stiffness laminates. Compos Struct 2016;152:791–9. doi:10.1016/j.compstruct.2016.05.076.

[183] Velea MN, Wennhage P, Zenkert D. Multi-objective optimisation of vehicle bodies made of FRP sandwich structures. Compos Struct 2014;111:75–84. doi:10.1016/j.compstruct.2013.12.030.

[184] Kalhor R, Akbarshahi H, Case SW. Numerical modeling of the effects of FRP thickness and stacking sequence on energy absorption of metal-FRP square tubes. Compos Struct 2016;147:231–46. doi:10.1016/j.compstruct.2016.03.038.

[185] Dal Monte A, Castelli MR, Benini E. Multi-objective structural optimization of a HAWT composite blade. Compos Struct 2013;106:362–73. doi:10.1016/j.compstruct.2013.05.038.

[186] Visweswaraiah SB, Ghiasi H, Pasini D, Lessard L. Multi-objective optimization of a composite rotor blade cross-section. Compos Struct 2013;96:75–81. doi:10.1016/j.compstruct.2012.09.031.

[187] Aumjaud P, Fieldsend JE, Boucher MA, Evans KE, Smith CW. Multi-objective optimisation of viscoelastic damping inserts in honeycomb sandwich structures. Compos Struct 2015;132:451–63. doi:10.1016/j.compstruct.2015.05.061.

[188] Lee DS, Morillo C, Bugeda G, Oller S, Onate E. Multilayered composite structure design optimisation using distributed/parallel multi-objective evolutionary algorithms. Compos Struct 2012;94:1087–96. doi:10.1016/j.compstruct.2011.10.009.

[189] Kalantari M, Dong C, Davies IJ. Effect of matrix voids, fibre misalignment and thickness variation on multi-objective robust optimization of carbon/glass fibre-reinforced hybrid composites under flexural loading. Compos Part B Eng 2017;123:136–47. doi:10.1016/j.compositesb.2017.05.022.

[190] Kalantari M, Dong C, Davies IJ. Multi-objective robust optimization of multi-directional carbon/glass fibre-reinforced hybrid composites with manufacture related uncertainties under flexural loading. Compos Struct 2017;182:132–42. doi:10.1016/j.compstruct.2017.09.019.

[191] De Munck M, De Sutter S, Verbruggen S, Tysmans T, Coelho RF. Multi-objective weight and cost optimization of hybrid composite-concrete beams. Compos Struct 2015;134:369–77. doi:10.1016/j.compstruct.2015.08.089.

[192] Vo-Duy T, Duong-Gia D, Ho-Huu V, Vu-Do HC, Nguyen-Thoi T. Multi-objective optimization of laminated composite beam structures using NSGA-II algorithm. Compos Struct 2017;168:498–509. doi:10.1016/j.compstruct.2017.02.038.

[193] Woods BKS, Hill I, Friswell MI. Ultra-efficient wound composite truss structures. Compos Part A Appl Sci Manuf 2016;90:111–24. doi:10.1016/j.compositesa.2016.06.022.

[194] Rouhi M, Ghayoor H, Hoa SV, Hojjati M. Multi-objective design optimization of variable stiffness composite cylinders. Compos Part B Eng 2015;69:249–55. doi:10.1016/j.compositesb.2014.10.011.

[195] Joglekar S, Von Hagel K, Pankow M, Ferguson S. Exploring how optimal composite design is influenced by model fidelity and multiple objectives. Compos Struct 2017;160:964–75. doi:10.1016/j.compstruct.2016.10.089.

[196] Shaw AD, Dayyani I, Friswell MI. Optimisation of composite corrugated skins for buckling in morphing aircraft. Compos Struct 2015;119:227–37. doi:10.1016/j.compstruct.2014.09.001.

[197] Choi SW, Kim Y, Park HS. Multi-objective seismic retrofit method for using FRP jackets in shear-critical reinforced concrete frames. Compos Part B Eng 2014;56:207–16. doi:10.1016/j.compositesb.2013.08.049.

[198] Qi C, Yang S, Yang LJ, Wei ZY, Lu ZH. Blast resistance and multi-objective optimization of aluminum foam-cored sandwich panels. Compos Struct 2013;105:45–

57. doi:10.1016/j.compstruct.2013.04.043.

[199] Honda S, Igarashi T, Narita Y. Multi-objective optimization of curvilinear fiber shapes for laminated composite plates by using NSGA-II. Compos Part B Eng 2013;45:1071–8. doi:10.1016/j.compositesb.2012.07.056.

[200] Stanford BK, Jutte C., Wu KC. Aeroelastic benefits of tow steering for composite plates. Compos Struct 2014;118:416–22. doi:10.1016/j.compstruct.2014.08.007.

[201] António CC, Hoffbauer LN. Bi-level dominance GA for minimum weight and maximum feasibility robustness of composite structures. Compos Struct 2016;135:83–95. doi:10.1016/j.compstruct.2015.09.019.

[202] Fayazbakhsh K, Nik MA, Pasini D, Lessard L. Defect layer method to capture effect of gaps and overlaps in variable stiffness laminates made by Automated Fiber Placement. Compos Struct 2013;97:245–51. doi:10.1016/j.compstruct.2012.10.031.

[203] Okabe T, Oya Y, Yamamoto G, Sato J, Matsumiya T, Matsuzaki R, et al. Multi-objective optimization for resin transfer molding process. Compos Part A Appl Sci Manuf 2017;92:1–9. doi:10.1016/j.compositesa.2016.09.023.

[204] Akbarzadeh AH, Nik MA, Pasini D. Vibration responses and suppression of variable stiffness laminates with optimally steered fibers and magnetostrictive layers. Compos Part B Eng 2016;91:315–26. doi:10.1016/j.compositesb.2016.02.003.

[205] Dal Monte A, De Betta S, Castelli MR, Benini E. Proposal for a coupled aerodynamic–structural wind turbine blade optimization. Compos Struct 2017;159:144–56. doi:10.1016/j.compstruct.2016.09.042.

[206] Gupta A, Kelly PA, Ehrgott M, Bickerton S. A surrogate model based evolutionary game-theoretic approach for optimizing non-isothermal compression RTM processes. Compos Sci Technol 2013;84:92–100. doi:10.1016/j.compscitech.2013.05.012.

[207] Struzziero G, Skordos AA. Multi-objective optimisation of the cure of thick components. Compos Part A Appl Sci Manuf 2017;93:126–36. doi:10.1016/j.compositesa.2016.11.014.

[208] Lee DS, Morillo C, Oller S, Bugeda G, Oñate E. Robust design optimisation of advance hybrid (fiber-metal) composite structures. Compos Struct 2013;99:181–92. doi:10.1016/j.compstruct.2012.11.033.

[209] Yarasca J, Mantari JL, Petrolo M, Carrera E. Multiobjective Best Theory Diagrams for cross-ply composite plates employing polynomial, zig-zag, trigonometric and exponential thickness expansions. Compos Struct 2017;176:860–76. doi:10.1016/j.compstruct.2017.05.055.

[210] Rocha IBCM, Parente E, Melo AMC. A hybrid shared/distributed memory parallel genetic algorithm for optimization of laminate composites. Compos Struct 2014;107:288–97. doi:10.1016/j.compstruct.2013.07.049.

[211] Yarasca J, Mantari JL, Petrolo M, Carrera E. Best Theory Diagrams for cross-ply composite plates using polynomial, trigonometric and exponential thickness expansions. Compos Struct 2017;161:362–83. doi:10.1016/j.compstruct.2017.05.055.

[212] Choi SW. Investigation on the seismic retrofit positions of FRP jackets for RC frames using multi-objective optimization. Compos Part B Eng 2017;123:34–44.

doi:10.1016/j.compositesb.2017.05.026.

[213] Caccese V, Ferguson JR, Edgecomb MA. Optimal design of honeycomb material used to mitigate head impact. Compos Struct 2013;100:404–12. doi:10.1016/j.compstruct.2012.12.034.

[214] Paz J, Díaz J, Romera L, Costas M. Size and shape optimization of aluminum tubes with GFRP honeycomb reinforcements for crashworthy aircraft structures. Compos Struct 2015;133:499–507. doi:10.1016/j.compstruct.2015.07.077.

[215] Murugan S, Friswell MI. Morphing wing flexible skins with curvilinear fiber composites. Compos Struct 2013;99:69–75. doi:10.1016/j.compstruct.2012.11.026.

[216] Elham A, van Tooren MJL. Weight indexing for wing-shape multi-objective optimization. AIAA J 2014;52:320–37. doi:10.2514/1.J052406.

[217] Todoroki A, Sekishiro M. Modified efficient global optimization for a hat-stiffened composite panel with buckling constraint. AIAA J 2008;46:2257–64. doi:10.2514/1.34548.

[218] Soury E, Behravesh AH, Esfahani ER, Zolfaghari A. Design, optimization and manufacturing of wood-plastic composite pallet. Mater Des 2009;30:4183–91. doi:10.1016/j.matdes.2009.04.035.

[219] Cui X, Wang S, Hu SJ. A method for optimal design of automotive body assembly using multi-material construction. Mater Des 2008;29:381–7. doi:10.1016/j.matdes.2007.01.024.

[220] Ahmadian MR, Vincenti A, Vannucci P. A general strategy for the optimal design of composite laminates by the polar-genetic method. Mater Des 2011;32:2317–27. doi:10.1016/j.matdes.2010.08.036.

[221] Johnson KL, Chowdhury S, Lawrimore WB, Mao Y, Mehmani A, Prabhu R, et al. Constrained topological optimization of a football helmet facemask based on brain response. Mater Des 2016;111:108–18. doi:10.1016/j.matdes.2016.08.064.

[222] Qi C, Sun Y, Hu HT, Wang DZ, Cao GJ, Yang S. On design of hybrid material double-hat thin-walled beams under lateral impact. Int J Mech Sci 2016;118:21–35. doi:10.1016/j.ijmecsci.2016.09.009.

[223] Tran T, Hou S, Han X, Tan W, Nguyen N. Theoretical prediction and crashworthiness optimization of multi-cell triangular tubes. Thin-Walled Struct 2014;82:183–95. doi:10.1016/j.tws.2014.03.019.

[224] Studzinski R. Optimal design of sandwich panels with hybrid core. J Sandw Struct Mater 2017;0:1–13. doi:10.1177/1099636217742574.

[225] Sheyka MP, Altunc AB, Taha MR. Multi-objective genetic topological optimization for design of blast resistant composites. Appl Compos Mater 2012;19:785–98. doi:10.1007/s10443-011-9244-5.

[226] Airoldi A, Bertoli S, Lanzi L, Sirna M, Sala G. Design of a motorcycle composite swing-arm by means of multi-objective optimisation. Appl Compos Mater 2012;19:599–618. doi:10.1007/s10443-011-9227-6.

[227] Asgari M. Material optimization of functionally graded heterogeneous cylinder for

wave propagation. J Compos Mater 2016;50:3525–38. doi:10.1177/0021998315622051.

[228] Vosoughi AR, Nikoo MR. Maximum fundamental frequency and thermal buckling temperature of laminated composite plates by a new hybrid multi-objective optimization technique. Thin-Walled Struct 2015;95:408–15. doi:10.1016/j.tws.2015.07.014.

[229] Baier H, Huber M, Langer H. Design optimization of hybrid material structures. Struct Multidiscip Optim 2008;36:203–13. doi:10.1007/s00158-007-0204-5.

[230] Arikoglu A. Multi-objective optimal design of hybrid viscoelastic/composite sandwich beams by using the generalized differential quadrature method and the non-dominated sorting genetic algorithm II. Struct Multidiscip Optim 2017;56:885–901. doi:10.1007/s00158-017-1695-3.

[231] Dayyani I, Friswell MI. Multi-objective optimization for the geometry of trapezoidal corrugated morphing skins. Struct Multidiscip Optim 2017;55:331–45. doi:10.1007/s00158-016-1476-4.

[232] Zhou Y, Saitou K. Topology optimization of composite structures with data-driven resin filling time manufacturing constraint. Struct Multidiscip Optim 2017;55:2073–86. doi:10.1007/s00158-016-1628-6.

[233] Ghiasi H, Pasini D, Lessard L. Pareto frontier for simultaneous structural and manufacturing optimization of a composite part. Struct Multidiscip Optim 2010;40:497–511. doi:10.1007/s00158-009-0366-4.

[234] Schatz ME, Hermanutz A, Baier HJ. Multi-criteria optimization of an aircraft propeller considering manufacturing: Structural design optimization simultaneously considering a knowledge-based manufacturing and a structural model. Struct Multidiscip Optim 2017;55:899–911. doi:10.1007/s00158-016-1541-z.

[235] Antonio CAC. Local and global Pareto dominance applied to optimal design and material selection of composite structures. Struct Multidiscip Optim 2013;48:73–94. doi:10.1007/s00158-012-0878-1.

[236] Ghasemi AR, Hajmohammad MH. Multi-objective optimization of laminated composite shells for minimum mass/cost and maximum buckling pressure with failure criteria under external hydrostatic pressure. Struct Multidiscip Optim 2017;55:1051–62. doi:10.1007/s00158-016-1559-2.

[237] Araújo AL, Martins P, Soares CMM, Soares CAM, Herskovits J. Damping optimization of viscoelastic laminated sandwich composite structures. Struct Multidiscip Optim 2009;39:569–79. doi:10.1007/s00158-009-0390-4.

[238] Zitzler E, Deb K, Thiele L. Comparison of multiobjective evolutionary algorithms: empirical results. Evol Comput 2000;8:173–95. doi:10.1162/106365600568202.

[239] Wang Z, Sobey AJ. Optimal design of triaxial weave fabric composites for specific strength and stiffness under tension. 18th Eur. Conf. Compos. Mater., Athens: 2018.

[240] Auger A, Bader J, Brockhoff D, Zitzler E. Theory of the hypervolume indicator: Optimal μ-Distributions and the Choice of the Reference Point. Found. Genet. Algorithms - FOGA '09, Orlando, Florida, United States: 2009. doi:10.1145/1527125.1527138.

[241] While L, Bradstreet L, Barone L. A fast way of calculating exact hypervolumes. IEEE Trans Evol Comput 2012;16:86–95. doi:10.1109/TEVC.2010.2077298.

[242] Nguyen HX, Lee J, Vo TP, Lanc D. Vibration and lateral buckling optimisation of thin-walled laminated composite channel-section beams. Compos Struct 2016;143:84–92. doi:10.1016/j.compstruct.2016.02.011.

[243] Şen I, Alderliesten RC, Benedictus R. Design optimisation procedure for fibre metal laminates based on fatigue crack initiation. Compos Struct 2015;120:275–84. doi:10.1016/j.compstruct.2014.10.010.

[244] Shi S, Sun Z, Ren M, Chen H, Hu X. Buckling resistance of grid-stiffened carbon-fiber thin-shell structures. Compos Part B Eng 2013;45:888–96. doi:10.1016/j.compositesb.2012.09.052.

[245] Lemaire E, Zein S, Bruyneel M. Optimization of composite structures with curved fiber trajectories. Compos Struct 2015;131:895–904. doi:10.1016/j.compstruct.2015.06.040.

[246] Nguyen XH, Kim NI, Lee J. Optimum design of thin-walled composite beams for flexural-torsional buckling problem. Compos Struct 2015;132:1065–74. doi:10.1016/j.compstruct.2015.06.036.

[247] Montemurro M, Koutsawa Y, Belouettar S, Vincenti A, Vannucci P. Design of damping properties of hybrid laminates through a global optimisation strategy. Compos Struct 2012;94:3309–20. doi:10.1016/j.compstruct.2012.05.003.

[248] Akoussan K, Hamdaoui M, Daya EM. Improved layer-wise optimization algorithm for the design of viscoelastic composite structures. Compos Struct 2017;176:342–58. doi:10.1016/j.compstruct.2017.05.047.

[249] Mazloomi MS, Ranjbar M, Boldrin L, Scarpa F, Patsias S, Ozada N. Vibroacoustics of 2D gradient auxetic hexagonal honeycomb sandwich panels. Compos Struct 2017;187:593–603. doi:10.1016/j.compstruct.2017.10.077.

[250] Do DTT, Lee S, Lee J. A modified differential evolution algorithm for tensegrity structures. Compos Struct 2016;158:11–9. doi:10.1016/j.compstruct.2016.08.039.

[251] Wang J, Simacek P, Advani SG. Use of Centroidal Voronoi Diagram to find optimal gate locations to minimize mold filling time in resin transfer molding. Compos Part A Appl Sci Manuf 2016;87:243–55. doi:10.1016/j.compositesa.2016.04.026.

[252] Aumjaud P, Smith CW, Evans KE. A novel viscoelastic damping treatment for honeycomb sandwich structures. Compos Struct 2015;119:322–32. doi:10.1016/j.compstruct.2014.09.005.

[253] Badalló P, Trias D, Lindgaard E. Damage tolerance optimization of composite stringer run-out under tensile load. Compos Struct 2015;133:98–104. doi:10.1016/j.compstruct.2015.07.025.

[254] Le-Anh L, Nguyen-Thoi T, Ho-Huu V, Dang-Trung H, Bui-Xuan T. Static and frequency optimization of folded laminated composite plates using an adjusted Differential Evolution algorithm and a smoothed triangular plate element. Compos Struct 2015;127:382–94. doi:10.1016/j.compstruct.2015.02.069.

[255] Vosoughi AR, Gerist S. New hybrid FE-PSO-CGAs sensitivity base technique for

damage detection of laminated composite beams. Compos Struct 2014;118:68–73. doi:10.1016/j.compstruct.2014.07.012.

[256] António CC. A study on synergy of multiple crossover operators in a hierarchical genetic algorithm applied to structural optimisation. Struct Multidiscip Optim 2009;38:117–35. doi:10.1007/s00158-008-0268-x.

[257] Karakaya Ş, Soykasap Ö. Buckling optimization of laminated composite plates using genetic algorithm and generalized pattern search algorithm. Struct Multidiscip Optim 2009;39:477–86. doi:10.1007/s00158-008-0344-2.

[258] Moussavian H, Jafari M. Optimum design of laminated composite plates containing a quasi-square cutout. Struct Multidiscip Optim 2017;55:141–54. doi:10.1007/s00158-016-1481-7.

[259] Zeng F, Xie H, Liu Q, Li F, Tan W. Design and optimization of a new composite bumper beam in high-speed frontal crashes. Struct Multidiscip Optim 2016;53:115–22. doi:10.1007/s00158-015-1312-2.

[260] Wang W, Guo S, Chang N, Zhao F, Yang W. A modified ant colony algorithm for the stacking sequence optimisation of a rectangular laminate. Struct Multidiscip Optim 2010;41:711–20. doi:10.1007/s00158-009-0447-4.

[261] Abachizadeh M, Tahani M. An ant colony optimization approach to multi-objective optimal design of symmetric hybrid laminates for maximum fundamental frequency and minimum cost. Struct Multidiscip Optim 2009;37:367–76. doi:10.1007/s00158-008-0235-6.

[262] Vincenti A, Ahmadian M, Vannucci P. BIANCA : a genetic algorithm to solve hard combinatorial optimisation problems in engineering. J Glob Optim 2010;48:399–421. doi:10.1007/s10898-009-9503-2.

[263] Tseng LY, Chen C. Multiple Trajectory Search for Multiobjective Optimization. 2007 IEEE Congr. Evol. Comput., 2007, p. 3609–16. doi:10.1109/CEC.2007.4424940.

[264] Huband S, Barone L, While L, Hingston P. A Scalable Multi-objective Test Problem Toolkit. Int. Conf. Evol. Multi-Criterion Optim., 2005, p. 280–95. doi:10.1007/978-3-540-31880-4_20.

[265] Liu HL, Chen L, Deb K, Goodman ED. Investigating the effect of imbalance between convergence and diversity in evolutionary multiobjective algorithms. IEEE Trans Evol Comput 2017;21:408–25. doi:10.1109/TEVC.2016.2606577.

[266] Li X, Engelbrecht A, Epitropakis MG. Results of the 2013 IEEE CEC Competition on Niching Methods for Multimodal Optimization. IEEE Congr. Evol. Comput., 2013.

[267] Li X, Engelbrecht A, Epitropakis MG. Results of the 2015 IEEE CEC Competition on Niching Methods for Multimodal Optimization. IEEE Congr. Evol. Comput., 2015.

[268] Cheng R, Li M, Tian Y, Zhang X, Yang S, Jin Y, et al. Final report of the CEC 2017 Competition. IEEE CEC Compet. Evol. Many-Objective Optim., 2017.

[269] Michalewicz Z. Genetic Algorithms + Data Structures = Evolution Programs. New York: Springer-Verlag; 1994.

[270] Haftka RT. Requirements for papers focusing on new or improved global optimization

algorithms. Struct Multidiscip Optim 2016;54:1. doi:10.1007/s00158-016-1491-5.

[271] Nguyen TT, Yao X. Benchmarking and solving dynamic constrained problems. 2009 IEEE Congr Evol Comput CEC 2009 2009:690–7. doi:10.1109/CEC.2009.4983012.

[272] Chaouachi F, Rahali Y, Ganghoffer JF. A micromechanical model of woven structures accounting for yarn-yarn contact based on Hertz theory and energy minimization. Compos Part B Eng 2014;66:368–80. doi:10.1016/j.compositesb.2014.05.027.

[273] Cai D, Tang J, Zhou G, Wang X, Li C, Silberschmidt V V. Failure analysis of plain woven glass/epoxy laminates: Comparison of off-axis and biaxial tension loadings. Polym Test 2017;60:307–20. doi:10.1016/j.polymertesting.2017.04.010.

[274] Lin Q, Chen J, Zhan ZH, Chen WN, Coello CAC, Yin Y, et al. A Hybrid Evolutionary Immune Algorithm for Multiobjective Optimization Problems. IEEE Trans Evol Comput 2015;20:711–29. doi:10.1109/TEVC.2015.2512930.

[275] Li M, Yang S, Liu X. Pareto or Non-Pareto : Bi-Criterion Evolution in Multiobjective Optimization. IEEE Trans Evol Comput 2015;20:645–65.

[276] Tseng L-Y, Chen C. Multiple trajectory search for multi-objective optimization. IEEE Congr. Evol. Comput., 2007, p. 3609–16.

[277] Grudniewski PA, Sobey AJ. cMLSGA : Co-evolutionary Multi-Level Selection Genetic Algorithm (Under Review). Swarm Evol Comput 2019.

[278] Auger A, Bader J, Brockhoff D, Zitzler E. Theory of the hypervolume indicator: Optimal μ-Distributions and the choice of the reference point. InProceedings tenth ACM SIGEVO Work. Found. Genet. algorithms, Orlando, Florida, United States: 2009. doi:10.1145/1527125.1527138.

[279] While L, Bradstreet L, Barone L. A fast way of calculating exact hypervolumes. IEEE Trans Evol Comput 2011;16:86–95. doi:10.1109/TEVC.2010.2077298.

[280] Xiong JJ, Shenoi RA. General aspects on structural integrity. Chinese J Aeronaut 2019;32:114–32. doi:10.1016/j.cja.2018.07.018.

[281] Bai J, Xiong J, Cheng X. Tear Resistance of orthogonal Kevlar-PWF-reinforced TPU film. Chinese J Aeronaut 2011;24:113–8. doi:10.1016/S1000-9361(11)60014-9.

[282] Quaglini V, Corazza C, Poggi C. Experimental characterization of orthotropic technical textiles under uniaxial and biaxial loading. Compos Part A Appl Sci Manuf 2008;39:1331–42. doi:10.1016/j.compositesa.2007.07.008.

[283] Ambroziak A, Kłosowski P. Polyester sail technical woven fabric behaviour under uniaxial and biaxial tensile tests. J Theor Appl Mech 2018:227. doi:10.15632/jtam-pl.56.1.227.

[284] Qiu Z, Chen W, Gao C, Hu Y. Experimental and numerical study on nonlinear mechanical properties of laminated woven fabrics. Constr Build Mater 2018;164:672–81. doi:10.1016/j.conbuildmat.2018.01.004.

[285] Shi T, Chen W, Gao C, Hu J, Zhao B, Wang P, et al. Biaxial strength determination of woven fabric composite for airship structural envelope based on novel specimens. Compos Struct 2018;184:1126–36. doi:10.1016/j.compstruct.2017.10.067.

[286] Gasser A, Boisse P, Hanklar S. Mechanical behaviour of dry fabric reinforcements. 3D

simulations versus biaxial tests. Comput Mater Sci 2000;17:7–20. doi:10.1016/S0927-0256(99)00086-5.

[287] Boisse P, Gasser A, Hivet G. Analyses of fabric tensile behaviour: Determination of the biaxial tension-strain surfaces and their use in forming simulations. Compos - Part A Appl Sci Manuf 2001;32:1395–414. doi:10.1016/S1359-835X(01)00039-2.

[288] De Carvalho N V., Pinho ST, Robinson P. Numerical modelling of woven composites: Biaxial loading. Compos Part A Appl Sci Manuf 2012;43:1326–37. doi:10.1016/j.compositesa.2012.03.017.

[289] Boubaker B Ben, Haussy B, Ganghoffer JF. Consideration of the yarn-yarn interactions in meso/macro discrete model of fabric. Part II: Woven fabric under uniaxial and biaxial extension. Mech Res Commun 2007;34:371–8. doi:10.1016/j.mechrescom.2007.02.002.

[290] Boubaker B Ben, Haussy B, Ganghoffer JF. Mesoscopic fabric models using a discrete mass-spring approach: Yarn-yarn interactions analysis. J Mater Sci 2005;40:5925–32. doi:10.1007/s10853-005-5056-z.

[291] Boubaker B Ben, Haussy B, Ganghoffer JF. Discrete models of fabric accounting for yarn interactions: Simulations of uniaxial and biaxial behaviour. Rev Eur Des Elem 2005;14:653–75. doi:10.3166/reef.14.653-675.

[292] Boubaker B Ben, Haussy B, Ganghoffer JF. Consideration of the yarn-yarn interactions in meso/macro discrete model of fabric. Part I: Single yarn behaviour. Mech Res Commun 2007;34:359–70. doi:10.1016/j.mechrescom.2007.02.003.

[293] Hivet G, Boisse P. Consistent mesoscopic mechanical behaviour model for woven composite reinforcements in biaxial tension. Compos Part B Eng 2008;39:345–61. doi:10.1016/j.compositesb.2007.01.011.

[294] Xu J, Cox BN, McGlockton MA, Carter WC. A binary model of textile composites-II. The elastic regime. Acta Metall Mater 1995;43:3511–24. doi:10.1016/0956-7151(95)00057-3.

[295] McGlockton MA, Cox BN, McMeeking RM. A Binary Model of textile composites: III high failure strain and work of fracture in 3D weaves. J Mech Phys Solids 2003;51:1573–600. doi:10.1016/S0022-5096(03)00038-3.

[296] Yang Q, Cox B. Spatially Averaged Local Strains in Textile Composites Via the Binary Model Formulation. J Eng Mater Technol 2003;125:418. doi:10.1115/1.1605117.

[297] Escárpita DAA. Experimental Investigation of Textile Composites Strength Subject to Biaxial Tensile Loads. Instituto Tecnologico y de Estudios Superiores de Monterrey, 2011.

[298] Bai JB, Xiong JJ, Shenoi RA, Zhu YT. Analytical solutions for predicting tensile and in-plane shear strengths of triaxial weave fabric composites. Int J Solids Struct 2017;120:1339–51. doi:10.1016/j.ijsolstr.2017.05.002.

[299] Bai J, Wang Z, Sobey AJ, Xiong J, Shenoi RA. Micromechanical model for fast prediction of plain weave fabric composite strengths under biaxial tension (Accepted subject to corrections). Compos Part B Eng 2019.

[300] Gross D, Hauger W, Schröder J, Wall WA, Bonet J. Bending and Tension/Compression. Eng. Mech. 2 - Mech. Mater., Springer Berlin Heidelberg; 2011, p. 171.

[301] Daniel IM, Ishai O. Longitudinal Tension - Failure Mechanisms and Strength. Eng. Mech. Compos. Mater. Second, New York: Oxford University Press; 2006, p. 98–9.

[302] Yetman JE, Sobey AJ, Blake JIR, Shenoi RA. Mechanical and fracture properties of glass vinylester interfaces. Compos Part B Eng 2017;130:38–45. doi:10.1016/j.compositesb.2017.07.011.

[303] Ansari R, Hassanzadeh-Aghdam MK, Darvizeh A. On elastic modulus and biaxial initial yield surface of carbon nanotube-reinforced aluminum nanocomposites. Mech Mater 2016;101:14–26. doi:10.1016/j.mechmat.2016.07.008.

[304] Hasanzadeh M, Ansari R, Hassanzadeh-Aghdam MK. Micromechanical elastoplastic analysis of randomly oriented nonstraight carbon nanotube-reinforced polymer nanocomposites. Mech Adv Mater Struct 2018:1–11. doi:10.1080/15376494.2018.1444227.

[305] Tsai SW, Wu EM. A general theory of strength for anisotropic materials. J Compos Mater 1971;5:58–80.

[306] Kollegal MG, Sridharan S. A simplified model for plain woven fabrics. J Compos Mater 2000;34:1756–86.

[307] Liu Z, Zhu C, Zhu P, Chen W. Reliability-based design optimization of composite battery box based on modified particle swarm optimization algorithm. Compos Struct 2018. doi:10.1016/j.compstruct.2018.07.053.

[308] Naik NK, Kavala VR. High strain rate behavior of woven fabric composites under compressive loading. Mater Sci Eng A 2008;474:301–11. doi:10.1016/j.msea.2007.05.032.

[309] Zako M, Uetsuji Y, Kurashiki T. Finite element analysis of damaged woven fabric composite materials. Compos Sci Technol 2003;63:507–16. doi:10.1016/S0266-3538(02)00211-7.

[310] Boisse P, Zouari B, Daniel JL. Importance of in-plane shear rigidity in finite element analyses of woven fabric composite preforming. Compos Part A Appl Sci Manuf 2006;37:2201–12. doi:10.1016/j.compositesa.2005.09.018.

[311] Lin H, Clifford MJ, Long AC, Sherburn M. Finite element modelling of fabric shear. Model Simul Mater Sci Eng 2009;17:0–16. doi:10.1088/0965-0393/17/1/015008.

[312] Jeong HK, Shenoi RA. Probabilistic strength analysis of rectangular FRP plates using Monte Carlo simulation. Comput Struct 2000;76:219–35. doi:10.1016/S0045-7949(99)00171-6.

[313] Sobey AJ, Blake JIR, Shenoi RA. Monte Carlo reliability analysis of tophat stiffened composite plate structures under out of plane loading. Reliab Eng Syst Saf 2013;110:41–9. doi:10.1016/j.ress.2012.08.011.

[314] ASTM D3518M-1994(R01). Standard Test Method for In-Plane Shear Response of Polymer Matrix Composite Materials by Tensile Test of a ±45° Laminate. ASTM; 2001. doi:10.1520/D 3518/D_3518M – 94.

[315] Beer FP, E. Russell Johnston J, Dewolf JT, Mazurek DF. Mechanics of Materials. 2012.

[316] Naik NK, Kuchibhotla R. Analytical study of strength and failure behaviour of plain weave fabric composites made of twisted yarns. Compos - Part A Appl Sci Manuf 2002;33:697–708. doi:10.1016/S1359-835X(02)00012-X.

[317] Shah DU. Characterisation and optimisation of the mechanical performance of plant fibre composites for structural applications (Doctoral dissertation, University of Nottingham). 2013.

[318] Liu Y, Yang JP, Xiao HM, Qu CB, Feng QP, Fu SY, et al. Role of matrix modification on interlaminar shear strength of glass fibre/epoxy composites. Compos Part B Eng 2012;43:95–8. doi:10.1016/j.compositesb.2011.04.037.

[319] Rao RMVGK, Rao S, Sridhara BK. Studies on tensile and interlaminar shear strength properties of thermally cured and microwave cured glass-epoxy composites. J Reinf Plast Compos 2006;25:783–95. doi:10.1177/0731684406063542.

[320] Fan Z, Santare MH, Advani SG. Interlaminar shear strength of glass fiber reinforced epoxy composites enhanced with multi-walled carbon nanotubes. Compos Part A Appl Sci Manuf 2008;39:540–54. doi:10.1016/j.compositesa.2007.11.013.

[321] Harding J, Li YL. Determination of interlaminar shear strength for glass/epoxy and carbon/epoxy laminates at impact rates of strain. Compos Sci Technol 1992;45:161–71. doi:10.1016/0266-3538(92)90038-5.

[322] Kollegal MG, Sridharan S. A simplified model for plain woven fabrics. J Compos Mater 2000;34:1756–86. doi:10.1106/01KC-GJDP-H7TW-9M1H.

[323] Mutlu U, Grudniewski PA, Sobey AJ, Blake JIR. Selecting an optimisation methodology in the context of structural design for leisure boats. Des. Constr. Super Mega Yachts, 2017.

[324] Arian Nik M, Fayazbakhsh K, Pasini D, Lessard L. Surrogate-based multi-objective optimization of a composite laminate with curvilinear fibers. Compos Struct 2012;94:2306–13. doi:10.1016/j.compstruct.2012.03.021.

[325] Kueh ABH, Pellegrino S. Triaxial weave fabric composites. University of Cambridge, 2007.

[326] Aoki T, Yoshida K. Mechanical and thermal behaviours of triaxially-woven carbon/epoxy fabric composite. 47th AIAA/ASME/ASCE/AHS/ASC Struct. Struct. Dyn. Mater. Conf., Rhode Island, Newport: 2006.

[327] Aoki T, Yoshida K. Feasibility study of triaxially-woven fabric composite for deployable structures. 48th AIAA/ASME/ASCE/AHS/ASC Struct. Struct. Dyn. Mater. Conf., Hawaii, Honolulu: 2007.

[328] Zhao Q, Hoa S V., Ouellette P. Progressive failure of triaxial woven fabric (TWF) composites with open holes. Compos Struct 2004;65:419–31. doi:10.1016/j.compstruct.2003.12.004.

[329] Grudniewski PA, Sobey AJ. Multi-level selection genetic algorithm applied to CEC ' 09 test instances. Evol. Comput., 2017, p. 1613–20.

[330] Xu D, Ganesan R, Hoa S V. Buckling analysis of tri-axial woven fabric composite structures subjected to bi-axial loading. Compos Struct 2007;78:140–52.

APPENDIX I: Transformation variables in the micromechanical model for the prediction of biaxial tensile strengths

Appendix A: Definitions for transformation variables C_i

$$C_1 = \frac{1}{EI_1}\int_0^{L_1}\sqrt{1+\left(\frac{\pi h_1}{4L_1}\cos\frac{\pi x}{2L_1}\right)^2}\,dx \tag{A-1}$$

$$C_2 = \frac{1}{EI_1}\int_0^{L_1}\left(\frac{h_1}{2}\sin\frac{\pi x}{2L_1}\right)^2\sqrt{1+\left(\frac{\pi h_1}{4L_1}\cos\frac{\pi x}{2L_1}\right)^2}\,dx \tag{A-2}$$

$$C_3 = \frac{1}{4EI_1}\int_0^{L_1} x^2\sqrt{1+\left(\frac{\pi h_1}{4L_1}\cos\frac{\pi x}{2L_1}\right)^2}\,dx \tag{A-3}$$

$$C_4 = \frac{1}{EI_1}\int_0^{L_1}\left(h_1\sin\frac{\pi x}{2L_1}\right)\sqrt{1+\left(\frac{\pi h_1}{4L_1}\cos\frac{\pi x}{2L_1}\right)^2}\,dx \tag{A-4}$$

$$C_5 = \frac{-1}{2EI_1}\int_0^{L_1} x\left(h_1\sin\frac{\pi x}{2L_1}\right)\sqrt{1+\left(\frac{\pi h_1}{4L_1}\cos\frac{\pi x}{2L_1}\right)^2}\,dx \tag{A-5}$$

$$C_6 = \frac{-1}{EI_1}\int_0^{L_1} x\sqrt{1+\left(\frac{\pi h_1}{4L_1}\cos\frac{\pi x}{2L_1}\right)^2}\,dx \tag{A-6}$$

$$C_7 = \frac{1}{EA_1}\int_0^{L_1}\left[\sqrt{1+\left(\frac{\pi h_1}{4L_1}\cos\frac{\pi x}{2L_1}\right)^2}\right]^{-1}\,dx \tag{A-7}$$

$$C_8 = \frac{1}{4EA_1}\int_0^{L_1}\left(\frac{\pi h_1}{4L_1}\cos\frac{\pi x}{2L_1}\right)^2\left[\sqrt{1+\left(\frac{\pi h_1}{4L_1}\cos\frac{\pi x}{2L_1}\right)^2}\right]^{-1}\,dx \tag{A-8}$$

$$C_9 = \frac{1}{EA_1}\int_0^{L_1}\left(\frac{\pi h_1}{4L_1}\cos\frac{\pi x}{2L_1}\right)\left[\sqrt{1+\left(\frac{\pi h_1}{4L_1}\cos\frac{\pi x}{2L_1}\right)^2}\right]^{-1}\,dx \tag{A-9}$$

$$C_{10} = \frac{1}{EI_2}\int_0^{L_2}\sqrt{1+\left(\frac{\pi h_2}{4L_2}\cos\frac{\pi x}{2L_2}\right)^2}\,dx \tag{A-10}$$

$$C_{11} = \frac{1}{EI_2}\int_0^{L_2}\left(\frac{h_2}{2}\sin\frac{\pi x}{2L_2}\right)^2\sqrt{1+\left(\frac{\pi h_2}{4L_2}\cos\frac{\pi x}{2L_2}\right)^2}\,dx \tag{A-11}$$

$$C_{12} = \frac{1}{4EI_2}\int_0^{L_2} x^2\sqrt{1+\left(\frac{\pi h_2}{4L_2}\cos\frac{\pi x}{2L_2}\right)^2}\,dx \tag{A-12}$$

$$C_{13} = \frac{1}{EI_2}\int_0^{L_2}\left(h_2\sin\frac{\pi x}{2L_2}\right)\sqrt{1+\left(\frac{\pi h_2}{4L_2}\cos\frac{\pi x}{2L_2}\right)^2}\,dx \tag{A-13}$$

$$C_{14} = \frac{-1}{2EI_2}\int_0^{L_2} x\left(h_2\sin\frac{\pi x}{2L_2}\right)\sqrt{1+\left(\frac{\pi h_2}{4L_2}\cos\frac{\pi x}{2L_2}\right)^2}\,dx \tag{A-14}$$

$$C_{15} = \frac{-1}{EI_2}\int_0^{L_2} x\sqrt{1+\left(\frac{\pi h_2}{4L_2}\cos\frac{\pi x}{2L_2}\right)^2}\,dx \tag{A-15}$$

$$C_{16} = \frac{1}{EA_2}\int_0^{L_2}\left[\sqrt{1+\left(\frac{\pi h_2}{4L_2}\cos\frac{\pi x}{2L_2}\right)^2}\right]^{-1}dx \tag{A-16}$$

$$C_{17} = \frac{1}{4EA_2}\int_0^{L_2}\left(\frac{\pi h_2}{4L_2}\cos\frac{\pi x}{2L_2}\right)^2\left[\sqrt{1+\left(\frac{\pi h_2}{4L_2}\cos\frac{\pi x}{2L_2}\right)^2}\right]^{-1}dx \tag{A-17}$$

$$C_{18} = \frac{1}{EA_2}\int_0^{L_2}\left(\frac{\pi h_2}{4L_2}\cos\frac{\pi x}{2L_2}\right)\left[\sqrt{1+\left(\frac{\pi h_2}{4L_2}\cos\frac{\pi x}{2L_2}\right)^2}\right]^{-1}dx \tag{A-18}$$

Appendix B: Definitions for Transformation Variables D_i

$$D_1 = \frac{\begin{vmatrix} -C_4 & 0 & C_6 \\ -\frac{C_{13}}{\lambda} & 2C_{10} & C_{15} \\ -\left[\left(C_5 + C_9\right) + \frac{1}{\lambda}\left(C_{14} + C_{18}\right)\right] & C_{15} & 2\left(C_3 + C_8 + C_{12} + C_{17}\right) \end{vmatrix}}{\begin{vmatrix} 2C_1 & 0 & C_6 \\ 0 & 2C_{10} & C_{15} \\ C_6 & C_{15} & 2\left(C_3 + C_8 + C_{12} + C_{17}\right) \end{vmatrix}} \tag{B-1}$$

$$D_2 = \frac{\begin{vmatrix} 2C_1 & -C_4 & C_6 \\ 0 & -\frac{C_{13}}{\lambda} & C_{15} \\ C_6 & -\left[\left(C_5 + C_9\right) + \frac{1}{\lambda}\left(C_{14} + C_{18}\right)\right] & 2\left(C_3 + C_8 + C_{12} + C_{17}\right) \end{vmatrix}}{\begin{vmatrix} 2C_1 & 0 & C_6 \\ 0 & 2C_{10} & C_{15} \\ C_6 & C_{15} & 2\left(C_3 + C_8 + C_{12} + C_{17}\right) \end{vmatrix}} \tag{B-2}$$

$$D_3 = \frac{\begin{vmatrix} 2C_1 & 0 & -C_4 \\ 0 & 2C_{10} & -\frac{C_{13}}{\lambda} \\ C_6 & C_{15} & -\left[\left(C_5 + C_9\right) + \frac{1}{\lambda}\left(C_{14} + C_{18}\right)\right] \end{vmatrix}}{\begin{vmatrix} 2C_1 & 0 & C_6 \\ 0 & 2C_{10} & C_{15} \\ C_6 & C_{15} & 2\left(C_3 + C_8 + C_{12} + C_{17}\right) \end{vmatrix}} \tag{B-3}$$

APPENDIX II: Transformation variables in the micromechanical model for the prediction of shear moduli and strengths

Appendix A: The transformation variables $Q_n\left(n=1,2,3,.....,58\right)$

$$Q_1 = J_2K_1 + J_3K_2 \tag{A-1}$$

$$Q_2 = Q_1 \tag{A-2}$$

$$Q_3 = J_1K_3 + J_4K_4 \tag{A-3}$$

$$Q_4 = J_1K_5 \tag{A-4}$$

$$Q_5 = J_2K_5 \tag{A-5}$$

$$Q_6 = J_3K_9 \tag{A-6}$$

$$Q_7 = J_2\left(K_{10} + K_{41} + K_{42} + K_{43} - K_{44} - K_{45}\right) + J_3\left(K_{11} + K_{46} - K_{47}\right) \tag{A-7}$$

$$Q_8 = J_2K_9 \tag{A-8}$$

$$Q_9 = J_3K_5 \tag{A-9}$$

$$Q_{10} = -2\left(J_2K_1 + J_3K_2\right) \tag{A-10}$$

$$Q_{11} = -J_2K_6 \tag{A-11}$$

$$Q_{12} = J_3K_{12} \tag{A-12}$$

$$Q_{13} = J_2\left(K_{13} + K_{48} - K_{49}\right) + J_3\left(K_{14} - K_{50}\right) \tag{A-13}$$

$$Q_{14} = J_2K_{15} \tag{A-14}$$

$$Q_{15} = -J_3K_7 \tag{A-15}$$

$$Q_{16} = -Q_{11} \tag{A-16}$$

$$Q_{17} = -Q_{12} \tag{A-17}$$

$$Q_{18} = -Q_{13} \tag{A-18}$$

$$Q_{19} = -Q_{14} \tag{A-19}$$

$$Q_{20} = -Q_{15} \tag{A-20}$$

$$Q_{21} = J_1 K_8 \tag{A-21}$$

$$Q_{22} = -J_2 \left(K_{16} + K_{51} - K_{52} \right) \tag{A-22}$$

$$Q_{23} = -J_2 K_{17} \tag{A-23}$$

$$Q_{24} = J_3 \left(K_{18} - K_{53} \right) \tag{A-24}$$

$$Q_{25} = -J_3 K_{17} \tag{A-25}$$

$$Q_{26} = J_2 \left(K_{19} + K_{54} - K_{55} \right) \tag{A-26}$$

$$Q_{27} = -J_3 \left(K_{20} - K_{56} \right) \tag{A-27}$$

$$Q_{28} = J_5 K_{21} + J_6 K_{22} + J_7 K_{23} + J_8 K_{24} \tag{A-28}$$

$$Q_{29} = Q_{28} \tag{A-29}$$

$$Q_{30} = 2\left(J_5 K_{21} + J_8 K_{24} \right) \tag{A-30}$$

$$Q_{31} = J_5 K_{25} \tag{A-31}$$

$$Q_{32} = J_6 K_{25} \tag{A-32}$$

$$Q_{33} = J_7 K_{29} \tag{A-33}$$

$$Q_{34} = J_6 K_{29} \tag{A-34}$$

$$Q_{35} = J_6 \left(K_{30} + K_{57} + K_{59} + K_{60} - K_{58} - K_{61} \right) + J_7 \left(K_{31} + K_{62} - K_{63} \right) \tag{A-35}$$

$$Q_{36} = J_7 K_{25} \tag{A-36}$$

$$Q_{37} = 2\left(J_5 K_{21} - J_6 K_{22} - J_7 K_{23} + J_8 K_{24} \right) \tag{A-37}$$

$$Q_{38} = -2\sqrt{2}\left(J_5 K_{21} + J_8 K_{24} \right) \tag{A-38}$$

$$Q_{39} = J_5 K_{26} \tag{A-39}$$

$$Q_{40} = -J_6 K_{27} \tag{A-40}$$

$$Q_{41} = J_7 K_{32} \tag{A-41}$$

$$Q_{42} = J_6 K_{33} \tag{A-42}$$

$$Q_{43} = J_6 \left(K_{34} + K_{64} - K_{65} \right) + J_7 \left(K_{35} - K_{66} \right) \tag{A-43}$$

$$Q_{44} = -J_7 K_{28} \tag{A-44}$$

$$Q_{45} = Q_{38} \tag{A-45}$$

$$Q_{46} = Q_{39} \tag{A-46}$$

$$Q_{47} = -Q_{40} \tag{A-47}$$

$$Q_{48} = -Q_{41} \tag{A-48}$$

$$Q_{49} = -Q_{42} \tag{A-49}$$

$$Q_{50} = -Q_{43} \tag{A-50}$$

$$Q_{51} = -Q_{44} \tag{A-51}$$

$$Q_{52} = -\sqrt{2} J_5 K_{26} \tag{A-52}$$

$$Q_{53} = -J_6 K_{36} \tag{A-53}$$

$$Q_{54} = -J_6 \left(K_{37} + K_{67} - K_{68} \right) \tag{A-54}$$

$$Q_{55} = J_7 \left(K_{38} - K_{69} \right) \tag{A-55}$$

$$Q_{56} = -J_7 K_{36} \tag{A-56}$$

$$Q_{57} = J_6 \left(K_{39} + K_{70} - K_{71} \right) \tag{A-57}$$

$$Q_{58} = -J_7 \left(K_{40} - K_{72} \right) \tag{A-58}$$

where $J_n \left(n = 1, 2, 3, ..., 8\right)$ are the coefficients that defined as,

$$J_1 = \frac{1}{EI_{y1}} \tag{A-59}$$

$$J_2 = \frac{1}{EI_{z1}} \tag{A-60}$$

$$J_3 = \frac{1}{GI_{p1}} \tag{A-61}$$

$$J_4 = \frac{1}{EA_1} \tag{A-62}$$

$$J_5 = \frac{1}{EI_{y2}} \tag{A-63}$$

$$J_6 = \frac{1}{EI_{z2}} \tag{A-64}$$

$$J_7 = \frac{1}{GI_{p2}} \tag{A-65}$$

$$J_8 = \frac{1}{EA_2} \tag{A-66}$$

Appendix B: The transformation variables $K_n\left(n=1,2,3,.....,72\right)$

$$K_1=\int_0^{L_1}\frac{\gamma^2x^2}{2\left(1+\gamma\right)^2}\sqrt{1+\left(\frac{\pi h_1}{4L_1}\cos\frac{\pi x}{2L_1}\right)^2}\,dx \tag{B-1}$$

$$K_2=\int_0^{L_1}\frac{\gamma^2\left(h_1\sin\frac{\pi x}{2L_1}\right)^2}{8\left(1+\gamma\right)^2}\sqrt{1+\left(\frac{\pi h_1}{4L_1}\cos\frac{\pi x}{2L_1}\right)^2}\,dx \tag{B-2}$$

$$K_3=\int_0^{L_1}\left(\frac{h_1}{2}\sin\frac{\pi x}{2L_1}\right)^2\sqrt{1+\left(\frac{\pi h_1}{4L_1}\cos\frac{\pi x}{2L_1}\right)^2}\,dx \tag{B-3}$$

$$K_4=\int_0^{L_1}\left(\sqrt{1+\left(\frac{\pi h_1}{4L_1}\cos\frac{\pi x}{2L_1}\right)^2}\right)^{-1}dx \tag{B-4}$$

$$K_5=\int_0^{L_1}\sqrt{1+\left(\frac{\pi h_1}{4L_1}\cos\frac{\pi x}{2L_1}\right)^2}\,dx \tag{B-5}$$

$$K_6=\int_0^{L_1}\frac{\sqrt{2}\gamma x}{1+\gamma}\sqrt{1+\left(\frac{\pi h_1}{4L_1}\cos\frac{\pi x}{2L_1}\right)^2}\,dx \tag{B-6}$$

$$K_7=\int_0^{L_1}\frac{\gamma\left(h_1\sin\frac{\pi x}{2L_1}\right)}{\sqrt{2}\left(1+\gamma\right)}\sqrt{1+\left(\frac{\pi h_1}{4L_1}\cos\frac{\pi x}{2L_1}\right)^2}\,dx \tag{B-7}$$

$$K_8=\int_0^{L_1}\left(h_1\sin\frac{\pi x}{2L_1}\right)\sqrt{1+\left(\frac{\pi h_1}{4L_1}\cos\frac{\pi x}{2L_1}\right)^2}\,dx \tag{B-8}$$

$$K_9=\int_{L_1-\frac{w_2}{2}}^{L_1}w_1^2\sqrt{1+\left(\frac{\pi h_1}{4L_1}\cos\frac{\pi x}{2L_1}\right)^2}\,dx \tag{B-9}$$

$$K_{10}=\int_{L_1-\frac{w_2}{2}}^{L_1}4x^2\sqrt{1+\left(\frac{\pi h_1}{4L_1}\cos\frac{\pi x}{2L_1}\right)^2}\,dx \tag{B-10}$$

$$K_{11}=\int_{L_1-\frac{w_2}{2}}^{L_1}\left(h_1\sin\frac{\pi x}{2L_1}\right)^2\sqrt{1+\left(\frac{\pi h_1}{4L_1}\cos\frac{\pi x}{2L_1}\right)^2}\,dx \tag{B-11}$$

$$K_{12}=\int_{L_1-\frac{w_2}{2}}^{L_1}\frac{\gamma w_1\left(h_1\sin\frac{\pi x}{2L_1}\right)}{\sqrt{2}\left(1+\gamma\right)}\sqrt{1+\left(\frac{\pi h_1}{4L_1}\cos\frac{\pi x}{2L_1}\right)^2}\,dx \tag{B-12}$$

$$K_{13}=\int_{L_1-\frac{w_2}{2}}^{L_1}\frac{2\sqrt{2}\gamma x^2}{1+\gamma}\sqrt{1+\left(\frac{\pi h_1}{4L_1}\cos\frac{\pi x}{2L_1}\right)^2}\,dx \tag{B-13}$$

$$K_{14}=\int_{L_1-\frac{w_2}{2}}^{L_1}\frac{\gamma\left(h_1\sin\frac{\pi x}{2L_1}\right)^2}{\sqrt{2}\left(1+\gamma\right)}\sqrt{1+\left(\frac{\pi h_1}{4L_1}\cos\frac{\pi x}{2L_1}\right)^2}\,dx \tag{B-14}$$

$$K_{15}=\int_{L_1-\frac{w_2}{2}}^{L_1}\frac{\sqrt{2}\gamma w_1 x}{1+\gamma}\sqrt{1+\left(\frac{\pi h_1}{4L_1}\cos\frac{\pi x}{2L_1}\right)^2}\,dx \tag{B-15}$$

$$K_{16}=\int_{L_1-\frac{w_2}{2}}^{L_1}4x\sqrt{1+\left(\frac{\pi h_1}{4L_1}\cos\frac{\pi x}{2L_1}\right)^2}\,dx \tag{B-16}$$

$$K_{17}=\int_{L_1-\frac{w_2}{2}}^{L_1}2w_1\sqrt{1+\left(\frac{\pi h_1}{4L_1}\cos\frac{\pi x}{2L_1}\right)^2}\,dx \tag{B-17}$$

$$K_{18}=\int_{L_1-\frac{w_2}{2}}^{L_1}2w_1\left(h_1\sin\frac{\pi x}{2L_1}\right)\sqrt{1+\left(\frac{\pi h_1}{4L_1}\cos\frac{\pi x}{2L_1}\right)^2}\,dx \tag{B-18}$$

$$K_{19}=\int_{L_1-\frac{w_2}{2}}^{L_1}4w_1 x\sqrt{1+\left(\frac{\pi h_1}{4L_1}\cos\frac{\pi x}{2L_1}\right)^2}\,dx \tag{B-19}$$

$$K_{20}=\int_{L_1-\frac{w_2}{2}}^{L_1}2\left(h_1\sin\frac{\pi x}{2L_1}\right)\sqrt{1+\left(\frac{\pi h_1}{4L_1}\cos\frac{\pi x}{2L_1}\right)^2}\,dx \tag{B-20}$$

$$K_{21}=\int_{0}^{L_2}\left(\frac{h_2}{2\sqrt{2}}\sin\frac{\pi x}{2L_2}\right)^2\sqrt{1+\left(\frac{\pi h_2}{4L_2}\cos\frac{\pi x}{2L_2}\right)^2}\,dx \tag{B-21}$$

$$K_{22}=\int_{0}^{L_2}\frac{x^2}{2\left(1+\gamma\right)^2}\sqrt{1+\left(\frac{\pi h_2}{4L_2}\cos\frac{\pi x}{2L_2}\right)^2}\,dx \tag{B-22}$$

$$K_{23}=\int_0^{L_2}\frac{\left(h_2\sin\frac{\pi x}{2L_2}\right)^2}{8\left(1+\gamma\right)^2}\sqrt{1+\left(\frac{\pi h_2}{4L_2}\cos\frac{\pi x}{2L_2}\right)^2}\,dx \tag{B-23}$$

$$K_{24}=\int_0^{L_2}\frac{1}{2}\left(\sqrt{1+\left(\frac{\pi h_2}{4L_2}\cos\frac{\pi x}{2L_2}\right)^2}\right)^{-1}dx \tag{B-24}$$

$$K_{25}=\int_0^{L_2}\sqrt{1+\left(\frac{\pi h_2}{4L_2}\cos\frac{\pi x}{2L_2}\right)^2}\,dx \tag{B-25}$$

$$K_{26}=\int_0^{L_2}\frac{\left(h_2\sin\frac{\pi x}{2L_2}\right)}{\sqrt{2}}\sqrt{1+\left(\frac{\pi h_2}{4L_2}\cos\frac{\pi x}{2L_2}\right)^2}\,dx \tag{B-26}$$

$$K_{27}=\int_0^{L_2}\frac{\sqrt{2}x}{1+\gamma}\sqrt{1+\left(\frac{\pi h_2}{4L_2}\cos\frac{\pi x}{2L_2}\right)^2}\,dx \tag{B-27}$$

$$K_{28}=\int_0^{L_2}\frac{\left(h_2\sin\frac{\pi x}{2L_2}\right)}{\sqrt{2}\left(1+\gamma\right)}\sqrt{1+\left(\frac{\pi h_2}{4L_2}\cos\frac{\pi x}{2L_2}\right)^2}\,dx \tag{B-28}$$

$$K_{29}=\int_{L_2-\frac{w_1}{2}}^{L_2}w_2^2\sqrt{1+\left(\frac{\pi h_2}{4L_2}\cos\frac{\pi x}{2L_2}\right)^2}\,dx \tag{B-29}$$

$$K_{30}=\int_{L_2-\frac{w_1}{2}}^{L_2}4x^2\sqrt{1+\left(\frac{\pi h_2}{4L_2}\cos\frac{\pi x}{2L_2}\right)^2}\,dx \tag{B-30}$$

$$K_{31}=\int_{L_2-\frac{w_1}{2}}^{L_2}\left(h_2\sin\frac{\pi x}{2L_2}\right)^2\sqrt{1+\left(\frac{\pi h_2}{4L_2}\cos\frac{\pi x}{2L_2}\right)^2}\,dx \tag{B-31}$$

$$K_{32}=\int_{L_2-\frac{w_1}{2}}^{L_2}\frac{w_2\left(h_2\sin\frac{\pi x}{2L_2}\right)}{\sqrt{2}\left(1+\gamma\right)}\sqrt{1+\left(\frac{\pi h_2}{4L_2}\cos\frac{\pi x}{2L_2}\right)^2}\,dx \tag{B-32}$$

$$K_{33}=\int_{L_2-\frac{w_1}{2}}^{L_2}\frac{\sqrt{2}w_2x}{1+\gamma}\sqrt{1+\left(\frac{\pi h_2}{4L_2}\cos\frac{\pi x}{2L_2}\right)^2}\,dx \tag{B-33}$$

$$K_{34}=\int_{L_2-\frac{w_1}{2}}^{L_2}\frac{2\sqrt{2}x^2}{1+\gamma}\sqrt{1+\left(\frac{\pi h_2}{4L_2}\cos\frac{\pi x}{2L_2}\right)^2}\,dx \tag{B-34}$$

$$K_{35}=\int_{L_2-\frac{w_1}{2}}^{L_2}\frac{\left(h_2\sin\frac{\pi x}{2L_2}\right)^2}{\sqrt{2}\left(1+\gamma\right)}\sqrt{1+\left(\frac{\pi h_2}{4L_2}\cos\frac{\pi x}{2L_2}\right)^2}\,dx \tag{B-35}$$

$$K_{36}=\int_{L_2-\frac{w_1}{2}}^{L_2}2w_2\sqrt{1+\left(\frac{\pi h_2}{4L_2}\cos\frac{\pi x}{2L_2}\right)^2}\,dx \tag{B-36}$$

$$K_{37}=\int_{L_2-\frac{w_1}{2}}^{L_2}4x\sqrt{1+\left(\frac{\pi h_2}{4L_2}\cos\frac{\pi x}{2L_2}\right)^2}\,dx \tag{B-37}$$

$$K_{38}=\int_{L_2-\frac{w_1}{2}}^{L_2}2w_2\left(h_2\sin\frac{\pi x}{2L_2}\right)\sqrt{1+\left(\frac{\pi h_2}{4L_2}\cos\frac{\pi x}{2L_2}\right)^2}\,dx \tag{B-38}$$

$$K_{39}=\int_{L_2-\frac{w_1}{2}}^{L_2}4w_2x\sqrt{1+\left(\frac{\pi h_2}{4L_2}\cos\frac{\pi x}{2L_2}\right)^2}\,dx \tag{B-39}$$

$$K_{40}=\int_{L_2-\frac{w_1}{2}}^{L_2}2\left(h_2\sin\frac{\pi x}{2L_2}\right)\sqrt{1+\left(\frac{\pi h_2}{4L_2}\cos\frac{\pi x}{2L_2}\right)^2}\,dx \tag{B-40}$$

$$K_{41}=\int_{L_1-\frac{w_2}{2}}^{L_1}4w_2x\sqrt{1+\left(\frac{\pi h_1}{4L_1}\cos\frac{\pi x}{2L_1}\right)^2}\,dx \tag{B-41}$$

$$K_{42}=\int_{L_1-\frac{w_2}{2}}^{L_1}w_2^2\sqrt{1+\left(\frac{\pi h_1}{4L_1}\cos\frac{\pi x}{2L_1}\right)^2}\,dx \tag{B-42}$$

$$K_{43}=\int_{L_1-\frac{w_2}{2}}^{L_1}4L_1^2\sqrt{1+\left(\frac{\pi h_1}{4L_1}\cos\frac{\pi x}{2L_1}\right)^2}\,dx \tag{B-43}$$

$$K_{44}=\int_{L_1-\frac{w_2}{2}}^{L_1}4L_1w_2\sqrt{1+\left(\frac{\pi h_1}{4L_1}\cos\frac{\pi x}{2L_1}\right)^2}\,dx \tag{B-44}$$

$$K_{45}=\int_{L_1-\frac{w_2}{2}}^{L_1}8L_1x\sqrt{1+\left(\frac{\pi h_1}{4L_1}\cos\frac{\pi x}{2L_1}\right)^2}\,dx \tag{B-45}$$

$$K_{46}=\int_{L_1-\frac{w_2}{2}}^{L_1}\left(h_1\sin\frac{\pi\left(L_1-\frac{w_2}{2}\right)}{2L_1}\right)^2\sqrt{1+\left(\frac{\pi h_1}{4L_1}\cos\frac{\pi x}{2L_1}\right)^2}\,dx \tag{B-46}$$

$$K_{47}=\int_{L_1-\frac{w_2}{2}}^{L_1}2h_1^2\sin\frac{\pi x}{2L_1}\sin\frac{\pi\left(L_1-\frac{w_2}{2}\right)}{2L_1}\sqrt{1+\left(\frac{\pi h_1}{4L_1}\cos\frac{\pi x}{2L_1}\right)^2}\,dx \tag{B-47}$$

$$K_{48}=\int_{L_1-\frac{w_2}{2}}^{L_1}\frac{\sqrt{2}\gamma w_2 x}{1+\gamma}\sqrt{1+\left(\frac{\pi h_1}{4L_1}\cos\frac{\pi x}{2L_1}\right)^2}\,dx \tag{B-48}$$

$$K_{49}=\int_{L_1-\frac{w_2}{2}}^{L_1}\frac{2\sqrt{2}\gamma L_1 x}{1+\gamma}\sqrt{1+\left(\frac{\pi h_1}{4L_1}\cos\frac{\pi x}{2L_1}\right)^2}\,dx \tag{B-49}$$

$$K_{50}=\int_{L_1-\frac{w_2}{2}}^{L_1}\frac{\gamma h_1^2\sin\frac{\pi x}{2L_1}\sin\frac{\pi\left(L_1-\frac{w_2}{2}\right)}{2L_1}}{\sqrt{2}\left(1+\gamma\right)}\sqrt{1+\left(\frac{\pi h_1}{4L_1}\cos\frac{\pi x}{2L_1}\right)^2}\,dx \tag{B-50}$$

$$K_{51}=\int_{L_1-\frac{w_2}{2}}^{L_1}2w_2\sqrt{1+\left(\frac{\pi h_1}{4L_1}\cos\frac{\pi x}{2L_1}\right)^2}\,dx \tag{B-51}$$

$$K_{52}=\int_{L_1-\frac{w_2}{2}}^{L_1}4L_1\sqrt{1+\left(\frac{\pi h_1}{4L_1}\cos\frac{\pi x}{2L_1}\right)^2}\,dx \tag{B-52}$$

$$K_{53}=\int_{L_1-\frac{w_2}{2}}^{L_1}2w_1h_1\sin\frac{\pi\left(L_1-\frac{w_2}{2}\right)}{2L_1}\sqrt{1+\left(\frac{\pi h_1}{4L_1}\cos\frac{\pi x}{2L_1}\right)^2}\,dx \tag{B-53}$$

$$K_{54}=\int_{L_1-\frac{w_2}{2}}^{L_1}2w_1w_2\sqrt{1+\left(\frac{\pi h_1}{4L_1}\cos\frac{\pi x}{2L_1}\right)^2}\,dx \tag{B-54}$$

$$K_{55}=\int_{L_1-\frac{w_2}{2}}^{L_1}4L_1w_1\sqrt{1+\left(\frac{\pi h_1}{4L_1}\cos\frac{\pi x}{2L_1}\right)^2}\,dx \tag{B-55}$$

$$K_{56}=\int_{L_1-\frac{w_2}{2}}^{L_1}2h_1\sin\frac{\pi\left(L_1-\frac{w_2}{2}\right)}{2L_1}\sqrt{1+\left(\frac{\pi h_1}{4L_1}\cos\frac{\pi x}{2L_1}\right)^2}\,dx \tag{B-56}$$

$$K_{57}=\int_{L_2-\frac{w_1}{2}}^{L_2}4L_2^2\sqrt{1+\left(\frac{\pi h_2}{4L_2}\cos\frac{\pi x}{2L_2}\right)^2}\,dx \tag{B-57}$$

$$K_{58}=\int_{L_2-\frac{w_1}{2}}^{L_2}4L_2w_1\sqrt{1+\left(\frac{\pi h_2}{4L_2}\cos\frac{\pi x}{2L_2}\right)^2}\,dx \tag{B-58}$$

$$K_{59}=\int_{L_2-\frac{w_1}{2}}^{L_2}w_1^2\sqrt{1+\left(\frac{\pi h_2}{4L_2}\cos\frac{\pi x}{2L_2}\right)^2}\,dx \tag{B-59}$$

$$K_{60}=\int_{L_2-\frac{w_1}{2}}^{L_2}4w_1x\sqrt{1+\left(\frac{\pi h_2}{4L_2}\cos\frac{\pi x}{2L_2}\right)^2}\,dx \tag{B-60}$$

$$K_{61}=\int_{L_2-\frac{w_1}{2}}^{L_2}8L_2x\sqrt{1+\left(\frac{\pi h_2}{4L_2}\cos\frac{\pi x}{2L_2}\right)^2}\,dx \tag{B-61}$$

$$K_{62}=\int_{L_2-\frac{w_1}{2}}^{L_2}\left(h_2\sin\frac{\pi\left(L_2-\frac{w_1}{2}\right)}{2L_2}\right)^2\sqrt{1+\left(\frac{\pi h_2}{4L_2}\cos\frac{\pi x}{2L_2}\right)^2}\,dx \tag{B-62}$$

$$K_{63}=\int_{L_2-\frac{w_1}{2}}^{L_2}2h_2^2\sin\frac{\pi x}{2L_2}\sin\frac{\pi\left(L_2-\frac{w_1}{2}\right)}{2L_2}\sqrt{1+\left(\frac{\pi h_2}{4L_2}\cos\frac{\pi x}{2L_2}\right)^2}\,dx \tag{B-63}$$

$$K_{64}=\int_{L_2-\frac{w_1}{2}}^{L_2}\frac{\sqrt{2}w_1x}{1+\gamma}\sqrt{1+\left(\frac{\pi h_2}{4L_2}\cos\frac{\pi x}{2L_2}\right)^2}\,dx \tag{B-64}$$

$$K_{65}=\int_{L_2-\frac{w_1}{2}}^{L_2}\frac{2\sqrt{2}L_2x}{1+\gamma}\sqrt{1+\left(\frac{\pi h_2}{4L_2}\cos\frac{\pi x}{2L_2}\right)^2}\,dx \tag{B-65}$$

$$K_{66}=\int_{L_2-\frac{w_1}{2}}^{L_2}\frac{h_2^2\sin\frac{\pi x}{2L_2}\sin\frac{\pi\left(L_2-\frac{w_1}{2}\right)}{2L_2}}{\sqrt{2}\left(1+\gamma\right)}\sqrt{1+\left(\frac{\pi h_2}{4L_2}\cos\frac{\pi x}{2L_2}\right)^2}\,dx \tag{B-66}$$

$$K_{67}=\int_{L_2-\frac{w_1}{2}}^{L_2}2w_1\sqrt{1+\left(\frac{\pi h_2}{4L_2}\cos\frac{\pi x}{2L_2}\right)^2}\,dx \tag{B-67}$$

$$K_{68} = \int_{L_2 - \frac{w_1}{2}}^{L_2} 4L_2 \sqrt{1 + \left(\frac{\pi h_2}{4L_2} \cos \frac{\pi x}{2L_2} \right)^2}\, dx \tag{B-68}$$

$$K_{69} = \int_{L_2 - \frac{w_1}{2}}^{L_2} 2w_2 h_2 \sin \frac{\pi \left(L_2 - \frac{w_1}{2} \right)}{2L_2} \sqrt{1 + \left(\frac{\pi h_2}{4L_2} \cos \frac{\pi x}{2L_2} \right)^2}\, dx \tag{B-69}$$

$$K_{70} = \int_{L_2 - \frac{w_1}{2}}^{L_2} 2w_1 w_2 \sqrt{1 + \left(\frac{\pi h_2}{4L_2} \cos \frac{\pi x}{2L_2} \right)^2}\, dx \tag{B-70}$$

$$K_{71} = \int_{L_2 - \frac{w_1}{2}}^{L_2} 4L_2 w_2 \sqrt{1 + \left(\frac{\pi h_2}{4L_2} \cos \frac{\pi x}{2L_2} \right)^2}\, dx \tag{B-71}$$

$$K_{72} = \int_{L_2 - \frac{w_1}{2}}^{L_2} 2h_2 \sin \frac{\pi \left(L_2 - \frac{w_1}{2} \right)}{2L_2} \sqrt{1 + \left(\frac{\pi h_2}{4L_2} \cos \frac{\pi x}{2L_2} \right)^2}\, dx \tag{B-72}$$

APPENDIX III: Samples of optimal designs for triaxial weave fabric composite optimisation

Table III- 1 Samples of optimal designs of triaxial weave fabric composites

	Tensile Modulus (GPa)	Tensile Strength (MPa)	L (mm)	w (mm)	h (mm)
1	4.36	423	0.59	0.34	0.66
2	4.63	417	0.60	0.35	0.54
3	5.20	388	0.65	0.37	0.41
4	6.02	332	0.75	0.43	0.47
5	6.60	311	0.85	0.49	0.78
6	7.05	298	0.94	0.54	1.14
7	7.73	283	0.96	0.55	0.84
8	8.12	274	1.00	0.58	1.04
9	8.91	252	1.08	0.62	1.58
10	9.52	245	1.08	0.62	1.06
11	9.77	240	1.09	0.63	1.04
12	10.0	236	1.10	0.64	0.98
13	10.4	230	1.13	0.65	1.22
14	10.8	222	1.14	0.65	0.94
15	11.1	219	1.16	0.67	1.25
16	11.6	213	1.18	0.68	0.98
17	11.8	210	1.19	0.69	1.13
18	12.1	207	1.20	0.70	0.94
19	38.4	199	17.32	10.00	1.33

APPENDIX IV: League table of benchmarking for the optimal designs of plain weave fabric composites under tension and shear

Appendix A: mHV and mIGD results of the 10 solvers on solving the five-objective, three-objective and bi-objective optimisation problems

Table IV-A- 1. The five-objective optimisation benchmarking results of the 10 solvers at 200 generations

5 Obj. Tensile Strength, Tensile Modulus, Shear Strength, Shear Modulus & Areal Density									
	mHV min	mHV mean	mHV max	mHV rank	mIGD min	mIGD mean	mIGD max	mIGD rank	Total Rank
cMLSGA	0.0952	0.0966	0.0968	1	0.0104	0.0123	0.0234	1	1
MTS	0.0960	0.0965	0.0968	2	0.0168	0.0184	0.0204	3	2
BCE	0.0868	0.0960	0.0974	3	0.0122	0.0164	0.0588	2	2
U-NSGA-III	0.0933	0.0956	0.0952	4	0.0200	0.0281	0.0688	5	4
IBEA	0.0859	0.0942	0.0960	6	0.0161	0.0220	0.0619	4	5
HEIA	0.0929	0.0951	0.0967	5	0.0218	0.0310	0.0420	6	6
MOEA/DPSF	0.0889	0.0937	0.0952	7	0.0384	0.0597	0.1105	7	7
MOEA/DMSF	0.0813	0.0847	0.0968	9	0.0209	0.0604	0.0876	8	8
MOEA/D	0.0847	0.0874	0.0892	8	0.0459	0.0651	0.1293	9	8

Table IV-A- 2. The three-objective moduli optimisation benchmarking results of the 10 solvers at 200 generations

3 Obj. Tensile Modulus, Shear Modulus & Areal Density									
	mHV min	mHV mean	mHV max	mHV rank	mIGD min	mIGD mean	mIGD max	mIGD rank	Total Rank
HEIA	0.2982	0.3011	0.3021	1	0.0082	0.0122	0.0208	2	1
cMLSGA	0.2973	0.3004	0.3016	3	0.0054	0.0115	0.0185	1	2
U-NSGA-III	0.2945	0.3007	0.3020	2	0.0099	0.0132	0.0242	3	3
MTS	0.2984	0.2989	0.2996	4	0.0160	0.0189	0.0210	4	4
IBEA	0.2923	0.2989	0.3011	5	0.0127	0.0201	0.0260	5	5
BCE	0.2608	0.2939	0.3021	6	0.0102	0.0238	0.0551	6	6
MOEA/DPSF	0.2159	0.2566	0.2893	7	0.0334	0.0770	0.1132	8	7
MOEA/D	0.2271	0.2519	0.2729	8	0.0466	0.0698	0.0985	7	7
MOEA/DMSF	0.2308	0.2470	0.2735	9	0.0675	0.0938	0.1197	9	9

Table IV-A- 3. The three-objective strengths optimisation benchmarking results of the 10 solvers at 200 generations

3 Obj. Tensile Strength, Shear Strength & Areal Density									
	mHV min	mHV mean	mHV max	mHV rank	mIGD min	mIGD mean	mIGD max	mIGD rank	Total Rank
HEIA	0.1319	0.1319	0.1320	2	0.0030	0.0064	0.0231	1	1
cMLSGA	0.1315	0.1319	0.1320	2	0.0024	0.0064	0.0280	1	1
U-NSGA-III	0.1319	0.1320	0.1320	1	0.0021	0.0101	0.0308	3	1
IBEA	0.1298	0.1316	0.1320	4	0.0034	0.0136	0.0404	4	4
BCE	0.1138	0.1303	0.1320	6	0.0033	0.0208	0.0721	5	5
MTS	0.1304	0.1308	0.1313	5	0.0128	0.0264	0.0349	6	5
MOEA/DMSF	0.1068	0.1179	0.1320	7	0.0284	0.0668	0.0986	7	7
MOEA/D	0.0898	0.1086	0.1319	8	0.0052	0.1160	0.1881	8	8
MOEA/DPSF	0.0638	0.1018	0.1319	9	0.0311	0.1380	0.2595	9	9

Table IV-A- 4. The bi-objective specific shear strength to stiffness ratio optimisation benchmarking results of the 10 solvers at 200 generations

2 Obj. Specific Shear Strength & Specific Shear Modulus									
	mHV min	mHV mean	mHV max	mHV rank	mIGD min	mIGD mean	mIGD max	mIGD rank	Total Rank
NSGA-II	0.008256	0.008264	0.0083	1	1.11E-07	6.30E-05	0.0011	1	1
MOEA/DPSF	0	0.0075	0.0083	2	1.04E-06	0.0090	0.1256	2	2
MOEA/DMSF	0	0.0063	0.0083	5	1.04E-06	0.0149	0.1261	3	4
MOEA/D	0	0.0068	0.0083	3	1.04E-06	0.0195	0.1249	4	3
IBEA	0	0.0064	0.0083	4	3.81E-07	0.0263	0.1269	6	5
cMLSGA	0	0.0062	0.0083	6	1.61E-07	0.0216	0.1258	5	6
MTS	0	0.0033	0.0074	7	0.0080	0.0461	0.0903	7	7
BCE	0	0.0027	0.0083	8	1.04E-06	0.0833	0.1716	8	8
HEIA	0	0.0010	0.0083	9	6.06E-07	0.1211	0.1964	9	9

Table IV-A- 5. The bi-objective specific tensile strength to stiffness ratio optimisation benchmarking results of the 10 solvers at 200 generations

2 Obj. Specific Tensile Strength & Specific Tensile Modulus									
	mHV min	mHV mean	mHV max	mHV rank	mIGD min	mIGD mean	mIGD max	mIGD rank	Total Rank
cMLSGA	0.0418	0.0532	0.0618	1	0.0047	0.0187	0.0308	1	1
NSGA-II	0.0503	0.0526	0.0541	2	0.0179	0.0202	0.0214	2	2
MOEA/D	0.0443	0.0496	0.0612	4	0.0059	0.0221	0.0286	3	3
MOEA/DMSF	0.0421	0.0487	0.0557	5	0.0164	0.0236	0.0312	4	4
IBEA	0.0021	0.0501	0.0544	3	0.0184	0.0263	0.1787	6	4
MOEA/DPSF	0.0386	0.0459	0.0604	6	0.0090	0.0261	0.0385	5	6
MTS	0.0381	0.0437	0.0489	7	0.0249	0.0314	0.0374	7	7
BCE	0	0.0200	0.0543	8	0.0144	0.0992	0.2319	8	8
HEIA	0	0.0024	0.0185	9	0.0635	0.1694	0.2880	9	9

Appendix B: Samples of optimal designs of plain weave fabric composites

Table IV-B- 1. Samples of optimal designs of plain weave fabric composites

Mechanical Properties & Density					Geometric Parameters					
Shear Strength (MPa)	Shear Modulus (GPa)	Tensile Strength (MPa)	Tensile Modulus (GPa)	Areal Density (g/m^2)	L_1 (mm)	L_2 (mm)	w_1 (mm)	w_2 (mm)	h_1 (mm)	h_2 (mm)
81.23	4.27	317.70	16.39	153.69	0.32	0.67	1.23	0.44	0.040	0.040
156.16	5.44	391.70	17.91	161.18	0.60	0.91	1.79	0.66	0.043	0.040
120.35	6.35	336.74	18.18	171.41	0.36	0.94	1.86	0.49	0.043	0.041
144.38	4.39	620.88	22.85	188.20	0.75	0.55	1.09	0.70	0.058	0.041
117.55	5.45	552.37	23.12	196.29	0.61	0.59	1.16	0.54	0.062	0.042
186.38	5.91	487.00	23.66	204.25	0.42	0.54	1.08	0.50	0.061	0.040
143.75	6.20	630.59	24.72	211.58	0.73	0.54	1.08	0.54	0.070	0.040
95.45	6.56	604.41	25.45	217.85	0.96	0.99	1.96	0.70	0.073	0.042
124.67	5.30	656.06	26.10	223.77	1.20	0.90	1.80	0.83	0.077	0.040
140.80	6.11	709.26	27.21	239.27	0.88	0.54	1.08	0.57	0.085	0.052
134.65	6.99	723.21	27.09	241.22	0.93	0.54	1.08	0.53	0.086	0.046
136.91	6.80	728.96	27.93	252.43	0.92	0.54	1.07	0.56	0.090	0.055
41.09	4.94	678.88	28.57	264.51	0.40	0.33	0.66	0.33	0.095	0.041
127.84	7.33	735.12	28.92	276.03	0.88	0.54	1.08	0.55	0.100	0.043
73.52	6.59	739.80	29.22	282.93	0.92	0.59	1.17	0.55	0.110	0.049
39.72	6.99	720.68	29.77	296.19	0.72	0.81	1.62	0.47	0.110	0.044
183.49	6.89	742.12	29.41	305.95	1.60	1.00	2.00	1.03	0.110	0.040
162.34	7.85	740.20	28.88	315.60	1.31	0.90	1.79	0.89	0.110	0.040
196.75	6.99	585.01	28.59	343.19	0.47	0.90	1.80	0.73	0.110	0.044

APPENDIX V: Published papers

Paper 1: Published in *Composite Structures* in 2018

Composite Structures 201 (2018) 616–624

Contents lists available at ScienceDirect

Composite Structures

journal homepage: www.elsevier.com/locate/compstruct

Optimal design of triaxial weave fabric composites under tension

Zhenzhou Wang[a], Jiangbo Bai[b,*], Adam Sobey[a], Junjiang Xiong[b], Ajit Shenoi[c]

[a] Fluid Structure Interactions Group, University of Southampton, Southampton, UK
[b] School of Transportation Science and Engineering, Beihang University, Beijing 100191, China
[c] Southampton Marine and Maritime Institute, University of Southampton, Southampton, UK

ARTICLE INFO

Keywords:
Triaxial weave fabric (TWF)
Multi-objective optimisation
Tensile mechanical properties
Genetic Algorithms

ABSTRACT

Triaxial weave fabrics are increasingly used in ultralight structures, such as the wings of unmanned aerial vehicles (UAVs) and deployable antenna on spacecraft. The tensile strength to stiffness ratio for these applications is important, requiring an optimal weave pattern; in this paper Genetic Algorithms are used to improve these designs. The mechanical response is obtained using the minimum total complementary potential energy principle where the yarns are approximated as curved beams in a micromechanical unit cell. Leading Genetic Algorithms are benchmarked to determine which perform best. The results form a disconnected Pareto front where the left hand part can be used for flexible structures but is difficult to find. An overall improvement in strength to stiffness ratio of 1191% is made with 643 designs found better than a current example. The selection of the Genetic Algorithm is shown to be crucial with only MLSGA-NSGAII regularly finding the entire Pareto front.

1. Introduction

Novel ultralight applications are creating a demand for new materials. These new materials need to have good mechanical properties despite the low mass requirement. Triaxial weave fabrics (TWF), illustrated in Fig. 1, are an example of materials finding growing usage in these structures. They are composites with longitudinal fibres in three directions, 0° and ± 60°, which provide mechanically quasi-isotropic properties, are lightweight due to the high degree of porosity and reduce the impact from air loads. It is also possible to design these structures with a small number of layers, as low as 1. The tensile strength to stiffness ratio is the most important mechanical property in many applications of triaxial weave fabric composites, especially for deployable antenna on spacecraft and ultra-thin wing skins of unmanned aerial vehicles (UAVs) as these properties provide flexible structures that are damage resistant. The crimp, or undulation, of the yarns significantly influences the mechanical properties and requires an optimal weave pattern to maximise the strength to stiffness ratio. However, it is not fully known how close the currently available fibre design schemes are to optimal, since these materials are relatively new.

Genetic Algorithms (GAs) are popular tools for finding optimal composite designs. A review of Composite Structures, Composites Part A, Composites Part B and Composites Science and Technology shows 214 papers utilising Genetic Algorithms to optimise composite structures and materials since 2008. The optimisation problems can be classified into single objective, weighted multi-objective, reducing a multiple objectives problem down to one objective, and multi-objective problems. Multi-objective problems represent the most interesting set as they provide an engineer with a greater understanding of the design space; 39 of the papers found focus on these problems by generating Pareto fronts. Single objective or weighted average problems tend to be easier to solve so a wider range of Genetic Algorithms are capable of solving the problems especially if combined with variable spaces that are small and/or simple.

It is essential to utilise a suitable algorithm for solving an optimisation problem. The 'no free lunch' theorem states that an algorithm that improves its performance on a category of problems inevitably degrades its performance on other types; optimisation algorithms are designed to be specialist to a problem type or have lower performance across all problems. Therefore, a variety of Genetic Algorithms have been developed to solve multi-objective problems categorised by their performance on different types of problems. As an example to demonstrate the importance of selecting the correct algorithm, Mutlu et al. [1] benchmark the performance of a number of popular algorithms on a composite grillage optimisation problem. The problem has limited input variables but even this simple problem demonstrates the need for state-of-the-art algorithms to evolve the entire Pareto front, and that these should be specialist algorithms reflecting the problem type. Reviewing the multi-objective optimisation papers, where a Pareto front is developed, the most popular Genetic Algorithm was NSGA-II but a

* Corresponding author.
E-mail address: baijiangbo@buaa.edu.cn (J. Bai).

https://doi.org/10.1016/j.compstruct.2018.06.090
Received 6 December 2017; Received in revised form 10 May 2018; Accepted 22 June 2018
Available online 27 June 2018

Paper 2: Presented and submitted in *18th European Conference on Composite Materials* in 2018

Optimal design of triaxial weave fabric composites for specific strength and stiffness under tension

ZhenZhou Wang[1*] and Adam Sobey[1]

[1]Fluid Structure Interactions Group, University of Southampton, Southampton, UK (*, corresponding author: zw9e14@soton.ac.uk)

Keywords: Triaxial weave fabric (TWF), Multi-objective optimisation, Tensile mechanical properties and surface density, Genetic Algorithms

Abstract

Triaxial weave fabric (TWF) composites are increasingly used in ultralight flexible structures, such as deployable antenna on spacecraft and wing skins of unmanned aerial vehicles (UAVs). High specific strength to stiffness ratios are important to avoid damage under large deflections and during folding and unfolding, whilst ensuring that they remain light weight. Genetic Algorithms (GAs) are widely used in the composite optimisation literature to find weaves that give optimal properties. Previously MLSGA-NSGAII and NSGA-II were shown to have the best performance in finding optimal schema for triaxial weave fabric composites and are used to generate Pareto Fronts of stiffness and strength. In this study the density of the material is also considered. 500 Pareto front points are achieved with 15 designs that are potentially capable of being designed for ultralight structures. A potential increase of 228.05% in the strength to stiffness ratio with increase of 149.49% in the strength is made with the same surface density as a current example. These allow selection of designs with high specific strength to stiffness ratios, ensuring practical designs that can be used for ultra-lightweight applications.

1. Introduction

Ultralight composite materials can be utilised to create the wing skins of unmanned aerial vehicles (UAVs) and deployable antenna on spacecraft. These applications require materials with a high strength to stiffness ratios despite the low mass requirement. Triaxial weave fabric (TWF) composites are constructed with 0° and ± 60° triaxial yarns, illustrated in Figure 1, providing mechanically quasi-isotropic properties. These materials are lightweight due to the high degree of porosity and have good fire and weather resistance. Optimal weave patterns are required to maximise the strength and stiffness while minimising the surface density of the material.

Genetic Algorithms (GAs) are popularly utilised to solve optimisation problems in the composite literature. Mutlu et al. [2] benchmarked the performance of a number of popular algorithms on a composite grillage optimisation problem. The problem has limited input variables but even this simple problem demonstrates the need for state-of-the-art algorithms to evolve the entire Pareto front, and that these should be specialist algorithms reflecting the problem type. Genetic Algorithms are considered to be an excellent tool for providing optimal weave patterns for TWF composites but this is a complex problem, with a complicated landscape in the search space, and requires the correct Genetic Algorithm to be used. Wang et al. [1] developed a methodology for optimisation of TWF composites, benchmarking a range of modern Genetic Algorithms to maximise the strength and stiffness. The results show 643 schema that improve the strength to stiffness ratio from 28.80% to 1191%, but these weaves don't account for density, meaning that a number of these solutions might be inappropriate for ultra-

lightweight applications. This paper therefore extends that study by including density to determine how this might constrain the final results. The best performing Genetic Algorithms from the previous study, NSGA-II and MLSGA-NSGAII are used, with the same analytical method developed by Bai et al. [3].

2. Analytical TWF model for tensile strength, tensile modulus and surface density

Bai et al. [3] developed an analytical model to predict the tensile modulus and strength of TWF composites. The idealised geometry parameters of a unit cell of a TWF composite and the corresponding micrograph of an actual TWF composite are shown in Figure 1. The neutral axis of the undulated triaxial yarns is assumed to follow a sinusoidal function. The internal forces and bending moments are illustrated in Figure 2 under the tensile loading along the 0 degree yarn direction.

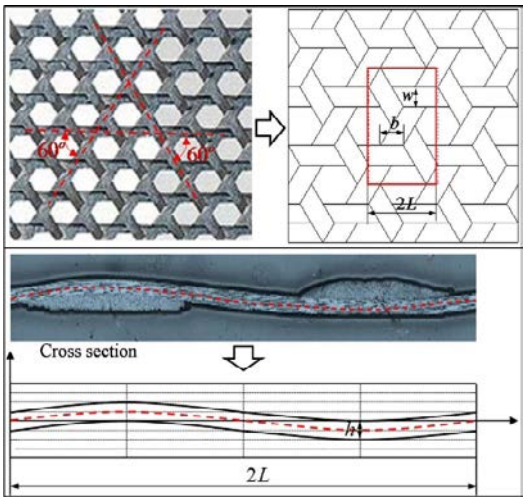

Fig. 1. Unit cell and micrograph of TWF composites [1]

We refer to Bai et al. [3] for a detailed introduction to the analytical model where this analytical model is verified in Wang et al. [1]. In brief the tensile stiffness, S_T, is expressed in equation 1 as,

$$S_T = \frac{P_T}{\sqrt{3}\Delta_{P_T}}, \tag{1}$$

where P_T is external tensile force and Δ_{P_T} is the displacement of the unit cell in the direction of external force. Strength per unit length, X_t, can be calculated using equation 2,

$$X_t = \frac{min(P_{tf1}, P_{tf2})}{2\sqrt{3}L}. \tag{2}$$

The internal tensile loading along the 0 degree and $\pm$ 60 degrees yarns are defined as P_{tf1} and P_{tf2}, where the internal tensile loading along $\pm$ 60 degrees yarns are the same, and L is the undulation length shown in Figure 1. The extension of Equation 1 and 2 contain a series of transformation variables derived by means of the minimum total complementary potential energy principle, representing the integration of micromechanical properties along the undulated 0 degree and $\pm$ 60 degrees yarns.

This model is extended to include the surface density of TWF composites which is evaluated according to the geometry parameters and idealised undulation shape. The fibre volume fraction is 0.65, which is the same as the experimental sample in the Kueh and Pellegrino technical report [4]. The density of the T300/Hexcel 8552 fibre tow, ρ_c, is expressed in equation 3,

$$\rho_c = \rho_f \times v_f + \rho_m \times v_m, \tag{3}$$

where the ρ_f is the density of the fibre 1760 kg/m^3, v_f is the volume fraction of the fibre, ρ_m is the density of the matrix 1301 kg/m^3 and v_m is the volume fraction of the matrix.

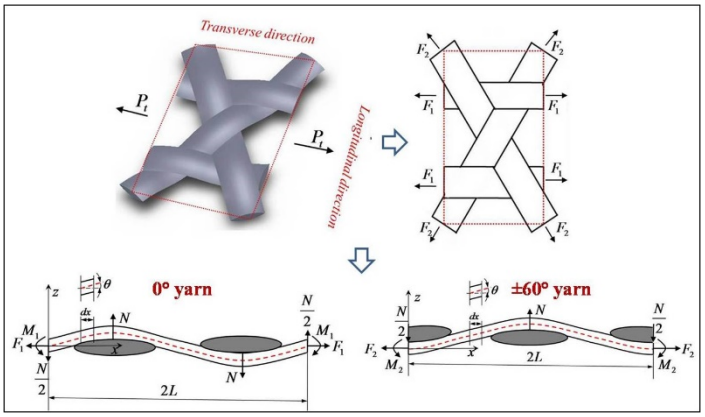

Fig. 2. Internal forces and bending moments on a unit cell [1]

The surface density of the TWF composites can then be expressed in equation 4 as,

$$\rho = 2\rho_c wh * 4\left[\int_0^{\frac{L}{2}} \sqrt{1 + \left(\frac{\pi h}{2L}\cos\frac{\pi x}{L}\right)^2}\, dx + \int_0^{L} \sqrt{1 + \left(\frac{\pi h}{2L}\sin\frac{\pi x}{L}\right)^2}\, dx\right] * \frac{1000000}{4\sqrt{3}L^2}, \tag{4}$$

w here is the width and h is the thickness of the fibre tows. The surface density from Equation 4 is utilised with strength and stiffness to evaluate the fitness of a given weave. In order to validate the surface density calculation the predictions are compared to the surface density taken from measurements performed by Kueh and Pellegrino [4]. An undulation length of 1.56mm, a width of 0.803mm and a thickness of 0.078mm is used. The comparison between the measurements of TWF composites and the analytical method are shown in Table 2.

Table 2. Verification of surface density predictions from analytical model

		Density [g/m^2]
Measurements[4]	Specimen 1	104.62
	Specimen 2	112.35
	Specimen 3	112.31
	Specimen 4	114.20
	Specimen 5	115.08
	Mean	111.71
Prediction		111.36
Error between prediction and mean		0.31%

3. Multi-objective design methodology

MLSGA-NSGAII and NSGA-II are utilised to optimise the weave pattern. In order to perform a fair test between the two Genetic Algorithms the same genetic operator types and operator rate as documented in Wang et al. [1] are used. The population size and generation number are also kept the

same so that the number of total fitness function evaluations is consistent. For further details on the mechanisms of the Genetic Algorithms Deb et al. [5] provides a detailed introduction to NSGA-II and Grudniewski and Sobey [6] for details of MLSGA.

3.1. Formulation of multi-objective optimisation problem

It is demonstrated that the two Genetic Algorithms achieve better optimisation results when the problem is unconstrained [1]. Therefore, the multi-objective optimisation problems are formulated as unconstrained for the TWF composite material in Equations 5 to provide materials with a maximum strength and minimum surface density under tension and a second simulation where the maximum stiffness and minimum surface density are required.

$$\begin{cases} Minimise\ \{1/Tensile\ Strength(n,w,h), Surface\ Density(n,w,h)\}, \\ or \\ Minimise\ \{1/Tensile\ Stiffness(n,w,h), Surface\ Density(n,w,h)\}, \\ L = n * \left(50 - \sqrt{3} * w\right) + \sqrt{3} * w, \\ The\ range\ of\ variables: \quad n \in [0,1], \\ 0mm < w \leq 10mm, \\ 0mm < h \leq 2mm. \end{cases} \tag{5}$$

T300/Hexel8552 is selected as the fibre and matrix combination to be optimised as the most mature TWF composite. The yarn undulation length, L, yarn width, w, and height, h, are the parameters influencing the strength, stiffness and density in the analytical model. The ranges of these variables are selected to ensure suitability for a range of existing applications for TWF composites. The interval between variables has been selected to be at 10^{-10} millimetres, substantially beyond the capability of current manufacturing demonstrated in [1], because the optimisation procedure seeks to fully document the objective space.

4. Optimisation of TWF composites and benchmarking of Genetic Algorithms

Two optimisations are performed on strength-density and stiffness-density problems respectively to investigate the relationship between strength, stiffness and density. In order to avoid the influences caused by the stochastic characteristics of the solvers 30 independent runs are performed for each study. To determine the quality of the Pareto front, a numerical comparison is performed between NSGA-II and MLSGA-NSGAII at a population size of 1500. Since the real Pareto front is unknown for these cases a mimicked inverted generational distance (mIGD) [1] is derived by generating the best Pareto front from all of the available data, defined in equation 6,

$$mIGD(O, M^*) = \frac{\sum_{v \in M^*} d(v, O)}{|M^*|}, \tag{6}$$

where M^* is a set of points along the mimicked Pareto front, O is a set of points on the currently obtained Pareto front, v represents each point in the set M^* and $d(v, O)$ is the minimum Euclidean distance between v and the points in O; lower mIGD values reflect a better quality and diversity of the obtained Pareto front. The mIGD values at each generation are illustrated in Figure 3 for the best and worst cases as well as the average from the 30 simulations of strength-density optimisation. The results are not included for the simpler stiffness-density problem as both algorithms easily resolve this front. Figure 3 shows that MLSGA-NSGAII converges faster than NSGA-II, except in the worst case where MLSGA-NSGAII takes 200 generations to converge. MLSGA-NSGAII achieves the best result in the case of 1500 population size and 200 generation and obtains better results after running the first 50 generations. This indicates that the advantage of MLSGA-NSGAII over NSGA-II is reduced in these cases compared

to the previous study [1]. Additionally, it is illustrated that both algorithms obtain large differences in convergence between the best and worst results among the 30 independent simulations.

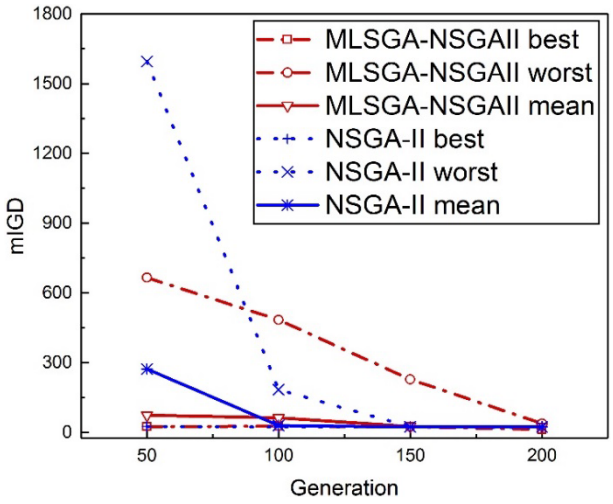

Fig. 3. Convergence of NSGA-II and MLSGA-NSGAII on the strength-density optimisation

According to the mIGD results the runs generating the best Pareto front from the 30 simulations for strength-density problem are illustrated in Figure 4 for each of the two algorithms. When optimising for strength and density, MLSGA-NSGAII and NSGA-II both find a disconnected Pareto front with a good spread of results, covering a similar range; the discontinuities are highlighted in Figure 4. NSGA-II achieves a lower density of Pareto front points on the bottom left part of the front relative to MLSGA-NSGAII. It is found that MLSGA-NSGAII and NSGA-II both capture the entire disconnected Pareto front in all the 30 independent runs with 500 points across the entire Pareto front each run, making this Pareto front easier to capture than the results from Wang et al. [1]. This is because the discontinuities are smaller than the Pareto front achieved in the previous study and the diversity mechanism of NSGA-II, crowding distance, maintains a higher diversity in its population and across the gaps. The advantages of the collective evolutionary mechanism in MLSGA-NSGAII are smaller in this case, as diversity of the population is less important.

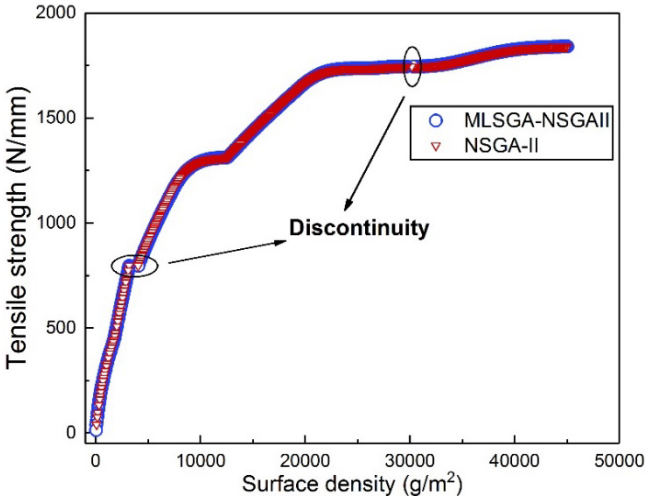

Fig. 4. Strength-density Pareto fronts for strength vs density

The designs at the extreme points of the Pareto front are L = 0.67 mm, w = 0.39 mm and h = 0.02 mm for the extreme bottom left point and L = 0.39 mm, w = 0.22 mm and h = 2 mm for the extreme top right point. The point at the extreme top right is more dense with a 100 times greater thickness and is about two times more compact. The extreme top right design has a high strength per unit length value, 1839.92 N/mm, but the two extreme point designs achieve similar strength per unit cross-sectional area values, 459.98 MPa at extreme top right design and 457.37 MPa at extreme bottom left design, which are high among all the optimal designs. The two points on either side of the right hand discontinuity have the same strength per unit length, 1744.56 N/mm, and same thickness, 2 mm, but one is much denser than the other, 29599.3 g/m^2 and 30326.9 g/m^2, again the denser design is more compact. The lower left discontinuity has similar designs to the discontinuity in a previous study [1], the point to the left of the disconnection has a large undulation length and yarn width, similar to the weave pattern shown in Figure 6d of Wang et al. [1]. However the point to the right has a significantly more compact weave pattern with slightly smaller thickness, which looks similarly to the weave pattern illustrated in Figure 6c of [1]. This shows that compact weave patterns increase the strength per unit cross-sectional area and thick yarns tend to decrease this value.

For the stiffness-density optimisation, the relationship between the stiffness and surface density is linear in the Pareto front. Both solvers achieved the same density of points on the Pareto front, covering the same range of designs. However, all of the designs on the Pareto front have large fibre tow undulation lengths, meaning that the woven fibre tows are as straight as possible to increase the stiffness but that all of the optimal designs are distributed on one side of the variable space. Since they have a linear relationship and are less interesting for real applications, the stiffness-density problem is not discussed further.

The results for the MLSGA-NSGAII algorithm are chosen to demonstrate the implications for the TWF composite designs, as they have the best performance. The optimal designs from a previous study [1] are compared with the Pareto front of current study which include the surface density. It is shown that the Pareto front of the previous study covers the same range of points as the bottom left front in the current study up until the first discontinuity, which is shown in Figure 5a. This demonstrates that the optimal designs from the previous study are also useful for real applications. In order to compare the optimal designs with the experimental samples, the unit of tensile strength is transferred from N/mm to MPa by dividing by the thickness of the TWF composites, 2h, since each interlacing point has two yarns stacked together; the new Pareto front is shown in Figure 5b. The designs on the lower left front in Figure 5b illustrate high stiffness despite having the lowest strengths. The right side front contains designs having similar strengths with lower stiffness compared to the designs from the upper left front. They achieve slightly higher strength to stiffness ratios than Wang et al. [1] but are significantly denser. The designs in the top left hand front are therefore judged to have properties most useful for ultra-lightweight applications. TWF composites usually consist of 3-5 layers in applications [4]. If a material is made from five layers of the experimental sample this gives a surface density of around 550 g/m^2. The top left hand front contains 15 designs having a surface density lower than 550 g/m^2 which having a larger tensile strength, from 370 MPa to 467.5 MPa, and lower stiffness, from 6.6 GPa to 12 GPa, than the experimental specimen [4].

Of these samples three designs have a surface density lower than the experimental sample and a higher strength to stiffness ratio. The extreme strength to stiffness ratio of the current study is 1230%, which is larger than the experimental sample but the density is 40216% denser than the experimental sample, where the previous study achieved a highest improvement of strength to stiffness ratio by 1191% [1]. However, the previous specific design with highest strength to stiffness ratio has larger density, 303.86 g/m^2, and thicker than the experimental sample, 111.75 g/m^2. A point with a surface density closer to the experimental sample but thinner [4], 110.86 g/m^2, is shown to have a tensile strength of 413.43 MPa, showing an increase of 149.49% in strength compared to the experimental sample. Furthermore, the stiffness is decreased by 15.94% from 13.53 GPa in the experiment to 10.30 GPa for the optimal design, meaning that the strength to stiffness ratio increases by 228.05% compared with the experimental sample. The previous study illustrated one design with similar surface density as the specific design in the current study and the experimental sample, 129.98 g/m^2, showing an increased strength to stiffness

ratio of 896.29% with a tensile strength of 441.66 MPa and stiffness of 3.62 GPa. The specific design in the previous study achieves significantly improvement of strength to stiffness ratio with an acceptable increase of density. It is demonstrated that the optimal designs from the two studies extend the selection of TWF composite designs for engineers and that if a material with a similar density to those currently available was required, that there is are still a number of design available that can increase the strength to stiffness ratio.

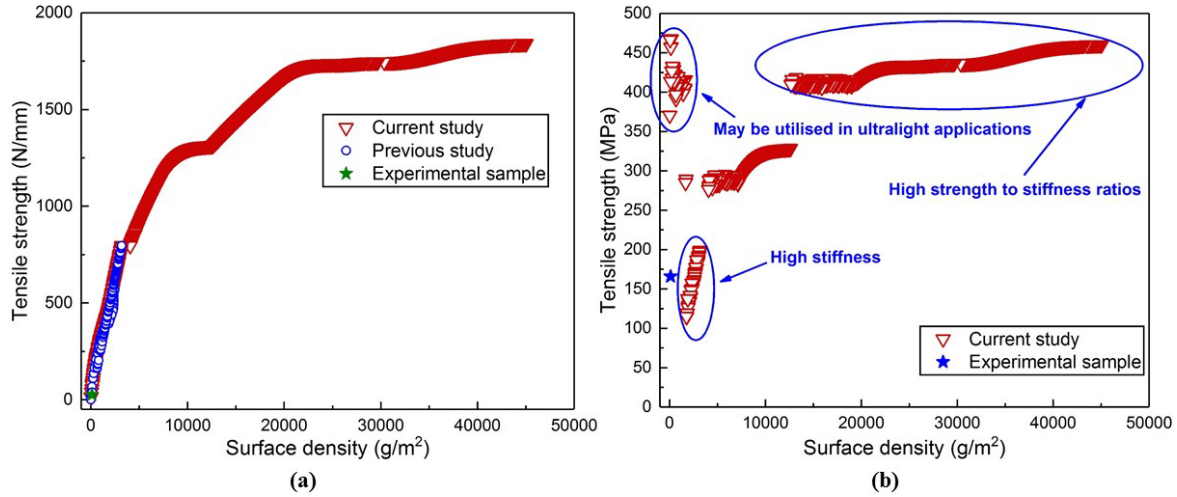

Fig. 5. Implication of TWF composite designs: (a) Comparison between current study and previous study; (b) Pareto front of tensile strength from current study after unit transfer

5. Discussion and limitations

Wang et al. [1] shows that MLSGA-NSGAII and NSGA-II are the two best algorithms for solving the TWF composite optimisation problem, where MLSGA-NSGAII achieves better results, converges faster and has better robustness than NSGA-II. This study confirms these results showing that MLSGA-NSGAII achieves the best results and converges faster on average. Both Genetic Algorithms find the entire Pareto front on every run when solving the strength-density optimisation problem, since the disconnected Pareto front has significantly smaller gaps compared with the previous study. Both algorithms achieve better robust performance with increased numbers of fitness evaluations, where the differences between the best and worst results are significantly reduced. The addition of the surface density makes the search space smaller and the problem easier to solve, and more useful. However, the previous results still demonstrate some solutions that a designer might be interested in, that are not available in this set of results. The advantages of MLSGA-NSGAII in maintaining a more diverse population through collective evolutionary mechanisms and crowding distance are smaller when solving the strength-density optimisation problem. However, it is worth solving this as a many-objective optimisation problem and to perform further benchmarking to evaluate the dominant characteristics of the problem helping to determine the selection of solvers for further exploration of these problems in the future.

The designs in the bottom left part of the front in Figure 4 demonstrate similar strength per unit cross-sectional area compared to those on the right side part of the front but are much lighter. This is because the right side front designs have more compact weave patterns and are much thicker than the bottom left part front designs, making the cross-sectional area much larger. The previous study [1] concluded that compact weave patterns provide high strength but it is found in the current study that compact weave patterns and high thicknesses significantly increase the surface density, which conflicts with the purpose of producing ultralight weight structures. Therefore, it is essential to select suitable weave patterns of TWF composites. The previous study found 643 designs that achieve higher strength to

stiffness ratios than the experimental sample. However, after accounting for the density of the TWF composites, only three designs achieve higher strength to stiffness ratios with lower density than the experimental sample in the current study. However, there are also 17 optimal designs in the previous study which have slightly higher densities than the experimental sample whilst having higher strength to stiffness ratios. This is because the current study achieved the Pareto front providing optimal designs for a wide range of density, which inevitably reduce the density of Pareto front points at the most interesting areas. Therefore, it is worth searching for optimal designs at the most interesting area by restricting the TWF composite density range. The focus of the current study is tensile properties and density, but due to the diversity of points, designers should be able to find a suitable weave pattern matching their required secondary characteristics, such as buckling performance.

6. Conclusions

Triaxial weave fabrics (TWF) are increasingly used in novel ultralight applications and there is a requirement to improve material properties. The material properties are dependent on the weave pattern, so optimising the designs can lead to improved TWFs. In this paper the best two Genetic Algorithms, selected as being the best performing based on a previous study [1], are used to find optimal weave patterns of TWF composites in tension. The benchmarking demonstrates that for this problem MLSGA-NSGAII achieves the best results and converges faster, similar to the results in the previous paper. Of the proposed strength-density Pareto front results there are 3 designs which have a lower density, higher strength and stiffness than the experiment. One design matching the surface density of a current experimental sample [4] gives an increase in the strength of 149.49% and an increase in the strength to stiffness ratio of 228.05%. Additionally, since TWF composites are usually layup for 3-5 layers in the applications, there are 15 of designs having a surface density lower than the five layers of experimental sample, 550 g/m^2, with tensile strength larger than 370 MPa and strength to stiffness ratios higher than the experimental sample [4], which may be capable of being designed for flexible ultralight structures. From the Wang et al. [1] one design with similar surface density as the specific design in the current study and the experimental sample, 129.98 g/m^2, shows an increased strength to stiffness ratio of 896.29% with a tensile strength of 441.66 MPa and stiffness of 3.62 GPa. Showing that the addition of density as a selection criterion only slightly limits the selection from the previous study that the majority of points are still feasible.

Acknowledgements

This project was supported by the Lloyds Register Foundation and Chinese Scholarship Council.

References

[1] Wang ZZ, Bai JB, Sobey AJ, Xiong JJ, Shenoi RA. Optimal design of triaxial weave fabric composites under tension. Composite Structures. 2018. (Under Review)

[2] Mutlu U, Grudniewski PA, Sobey AJ, Blake JIR. Selecting an optimisation methodology in the context of structural design for leisure boats, Design & Construction of Super & Mega Yachts, Genoa, Italy, May 2017.

[3] Bai JB, Xiong JJ, Shenoi RA, Zhu YT. Analytical Solutions for Predicting Tensile and In-plane Shear Strengths of Triaxial Weave Fabric Composites. International Journal of Solids and Structures, 2017; 120: 199-212.

[4] Kueh ABH, Pellegrino S. Triaxial weave fabric composites. Department of Engineering, University of Cambridge, June 30, 2007.

[5] Deb K, Pratap A, Agarwal S, Meyarivan TA. A fast and elitist multi-objective genetic algorithm: NSGA-II. IEEE transactions on evolutionary computation, 2002; 6(2):182-97.

[6] Grudniewski PA, Sobey AJ. Multi-Level Selection Genetic Algorithm applied to CEC'09 test instances. In Evolutionary Computation (CEC), 2017 IEEE Congress on 2017 (pp. 1613-1620). IEEE.

Paper 3: Published in *Composite Structures* in 2019

Composite Structures 233 (2020) 111739

Contents lists available at ScienceDirect

Composite Structures

journal homepage: www.elsevier.com/locate/compstruct

A comparative review between Genetic Algorithm use in composite optimisation and the state-of-the-art in evolutionary computation

ZhenZhou Wang*, Adam Sobey

Fluid Structure Interactions Group, Boldrewood Innovation Campus, University of Southampton, Burgess Road, Southampton SO16 7QF, UK

ARTICLE INFO

Keywords:
Genetic Algorithms (GAs)
Evolutionary computation
Composite structures
Literature review
Multi-objective optimisation
Many-objective optimisation

ABSTRACT

The task of providing optimal composite structures is increasingly difficult. New analysis approaches seek to model the material at the fibre/matrix scale and increasingly more control is sought over the material, for example optimising individual tows, and the structure, where new manufacturing techniques are proposed that will allow revolutionary new topologies. This additional complexity will stretch design engineers and as such it is important that state-of-the-art design methods are implemented to help take advantage of these exciting new opportunities, including computational optimisation methods. To determine best practice and the current limitations of the techniques a review of Genetic Algorithms in optimisation of composite materials and structures is performed over the last 10 years. This is compared to a technical review of the developments of Genetic Algorithms in the evolutionary computation literature. By better understanding how Genetic Algorithms are used in composite structures and comparing to evolutionary computational literature, recommendations are provided to help increase the use of Genetic Algorithms in solving composite optimisation problems in the future.

1. The importance of Genetic Algorithms to optimisation of composites

Optimisation techniques are widely used across many different disciplines. They are best used to provide innovative solutions or to gain insights into complex problems. Evolutionary algorithms are one of the most popular categories of optimisation techniques, especially in engineering design, as they are capable of finding solutions in large and complex search spaces. A database of applications of evolutionary algorithms, Coello Coello [1], shows 4983 papers utilising evolutionary algorithms to solve multi-objective optimisation problems from 1988 to 2017. The proportion of different evolutionary algorithms from this database are summarised in Fig. 1, where the papers with titles containing 'evolutionary algorithm' are not counted since it is hard to distinguish and summarise which evolutionary algorithm is used in each of those papers. The main evolutionary algorithms used are: Genetic Algorithms (GAs), Particle Swarm Optimisations (PSOs), Ant Colony (AC), Simulated Annealing (SA), Differential Evolution (DE), Immune Algorithms (IA), Artificial Bee Colony (ABC) and Firefly Algorithm (FA). The largest proportion of algorithms being used are Genetic Algorithms which occupy 56% of applications, showing the continued popularity of this type of optimisation algorithm despite the increasing competition from other methods.

The publications from this database, related to Genetic Algorithms, fall into 23 research broad fields. These fields, and the number of publications in each field, are shown in Fig. 2 where the composite structures optimisation theme is ranked in the lower half, indicating that there might be room for greater uptake of these methods to help understand the behaviour of these materials. As a field optimisation algorithms are used less in composite structures and materials than in similar engineering themes such as Aeronautics & Astronautics and Material Manufacturing, though there might be some overlap between them. Whilst Composite Structures might be considered to be a small field, its complexity and importance require consideration for how optimisation techniques can be better utilised to help future research and industrial applications.

Due to the importance of optimisation to the future of composite structures, and the significance of Genetic Algorithms within the field of optimisation, the use of Genetic Algorithms in Composite Structures/Materials is reviewed in this paper. In order to cover all relevant papers on this topic, allowing a more critical review of the state-of-the-art, the publications related to composite material/structure optimisation in 17 journals are reviewed: *Composites Science and Technology (CST), Composites Part A: Applied Science and Manufacturing (CPA), Composites Part B: Engineering (CPB), Composite Structures (CS), Applied Composite Materials (AppCM), International Journal of Solids and Structures (IJSS),*

* Corresponding author.
E-mail address: zw9e14@soton.ac.uk (Z. Wang).

https://doi.org/10.1016/j.compstruct.2019.111739
Received 29 July 2019; Received in revised form 18 October 2019; Accepted 26 November 2019
Available online 30 November 2019